

THE MECHANISMS OF SULFUR-CONTAINING METAL COMPLEXES
AS UV-STABILISERS

by

SAHAR NADHUM AL-MALAIKA

A Thesis Submitted for the Degree of
Doctor of Philosophy
of the University of Aston in Birmingham

February 1981

SUMMARY

THE UNIVERSITY OF ASTON IN BIRMINGHAM

THE MECHANISMS OF SULFUR-CONTAINING METAL COMPLEXES

AS UV-STABILISERS

Sahar Nadhum Al-Malaika

Submitted for the Degree of PhD

February 1981

The antioxidant activities of some sulfur-containing compounds have been studied in polyolefins (polyethylene and polypropylene) and in model systems initiated by alkoxy radical generators (hydroperoxides).

The chemical reactions involved in the antioxidant behaviour of nickel complexes of dithiophosphoric and xanthic acids were investigated both by kinetic methods and product analysis. Two mechanisms were identified: the first is a radical trapping process involving the metal complex itself and the second is a Lewis acid catalysed destruction of hydroperoxides by a transformation product(s) of the metal complex and not by the complex itself. The extent of the participation of each of these processes was found to be a function of the hydroperoxide/antioxidant ratio: at low molar ratios, the first process predominates.

Disulfides derived from the above complexes were found to be the initial oxidative products of the metal dithiolates and these were also investigated. The main mechanism of their antioxidant action involves the decomposition of hydroperoxides through their oxidation products, by a catalytic ionic process. Their efficiency depends very much on the availability of oxygen. The catalytic function is enhanced under conditions of severe (excess oxygen) processing of disulfides in the polymer.

Extensive photo- and thermo-oxidative stabilisation of polyethylene and polypropylene was achieved when the sulfur-containing metal complexes, and their corresponding disulfides, were incorporated in the polymer. Furthermore, synergistic combinations with the commercial UV-stabiliser, 2-hydroxy-4-octyloxybenzophenone, has led to a superior performance when compared to commercially available UV-stabilisers.

KEY WORDS

Mechanisms of stabilisation
Thermal stabilisers
UV-stabilisers
Antioxidants
Dithiolates for polyolefin stabilisation

ACKNOWLEDGEMENTS

I am deeply indebted to Professor G Scott for his invaluable supervision and guidance and for his unabated interest in this work.

I wish to record my sincere thanks to the Head of the Department, Professor W R McWhinnie, for his continued interest and encouragement. My thanks are also due to my colleagues in the Polymer Group who have tried in every way to shoulder some of my duties during the writing-up of this work.

My thanks are due to the many technical staff, without whose help and co-operation much of this work would have been impossible.

I wish to acknowledge the University of Aston for the award of a postgraduate scholarship (1976-1979) and for the support during the continuation period.

I am truly thankful to my husband for his encouragement and interest.

The perseverance of Mrs S Baker is gratefully acknowledged. Her typing skills survived through her commendable tolerance.

DECLARATION

The work described herein was carried out at the University of Aston in Birmingham between October 1976 and October 1979.

It has been done independently and submitted for no other degree.

Malaika

Sahar Nadhum Al-Malaika

February 1981

TO MIRAS AND LULA

<u>CONTENTS</u>	<u>PAGE</u>
Summary	ii
Acknowledgements	iii
List of Figures	xiv
List of Tables	xvi
List of Abbreviations	xvii
<u>CHAPTER 1</u> <u>INTRODUCTION</u>	1
1.1 Auto-Oxidation of Polyolefins	2
1.2 Oxidative Degradation: Effects of Environ- ment and Processing Factors	5
1.3 Polymer Stabilisation	11
1.4 Mechanisms of Photostabilisation in Polyolefins	14
1.4.1 UV-Screening and Absorption	15
1.4.2 Excited State Quenching	16
1.4.3 Radical Scavenging	17
1.4.4 Peroxide Decomposition	18
1.5 Synergism	21
1.6 Technological Applications of Dithio- phosphates and Xanthates	22
1.7 Aim and Scope of Project	24
<u>CHAPTER 2A</u> <u>EXPERIMENTAL</u>	
2A.1 Materials	25
2A.1.1 Polymers	25

<u>CONTENTS</u>	<u>PAGE</u>	
2A.1.2	Stabilisers	25
2A.1.3	Solvents	25
2A.1.4	Purification of Hydroperoxides	27
2A.1.5	Preparations	28
2A.1.5.1	Potassium Ethyl and Butyl Xanthate	28
2A.1.5.2	Nickel(II) Ethyl and Butyl Xanthate	28
2A.1.5.3	Cuprous(I) Ethyl and Butyl Xanthate	28
2A.1.5.4	Zinc Ethyl Xanthate	30
2A.1.5.5	Nickel Dialkyl Dithiophosphate	30
2A.1.5.6	Zinc Di-isopropyl Dithiophosphate	31
2A.1.5.7	Dialkyl Thiophosphoryl Disulfide and O,O'- Dibutyl Dithiophosphoroate	31
2A.1.5.8	Di-2-Hydroxybenzophenone Dithiophosphoric Acid	32
2A.1.6	Solubility of Stabilisers	32
2A.2	Handling of Polymer Test-Samples	33
2A.2.1	Processing of Polymers	33
2A.2.2	Film Preparation	34
2A.2.3	Extraction of Polymer Films	35
2A.3	Accelerated Testing Devices	35
2A.3.1	Ultra-Violet. Exposure Cabinet	35
2A.3.2	Heat Ageing Oven	37
2A.4	Monitoring of Oxidation Degradation and Additives in Films and Solutions	38
2A.4.1	Functional Group Measurements and IR Absorption of Stabilisers	38
2A.4.2	Stabiliser Disappearance and Spectral Measurements	39
2A.4.3	Flexural Test	39

<u>CONTENTS</u>	<u>PAGE</u>	
2A.4.4	Melt Flow Index	39
2A.5	Thermal Decomposition of CHP	40
2A.5.1	Reaction Cell and Experimental Procedure	40
2A.5.2	Hydroperoxide Determination	42
2A.6	Kinetics of Disappearance of the Additive	43
2A.7	Methods Used in Product Analysis	44
2A.7.1	Gas-Liquid Chromatography	44
2A.7.2	Thin Layer Chromatography	46
2A.7.3	Infra-Red Spectrophotometry	46
2A.7.4	UV-Spectrophotometry	46
2A.8	Thermogravimetry	48
<u>CHAPTER 2B</u> <u>PHYSICAL CHARACTERISTICS OF DITHIOPHOSPHATES</u> <u>AND XANTHATES</u>		
2B.1	General Reactions and Characteristics of Dithiophosphates and Xanthates	49
2B.2	Optical Characteristics of Metal Dithio- phosphates and Related Compounds	53
2B.2.1	UV-Spectra	53
2B.2.2	IR-Spectra	55
2B.3	Thermal Characteristics of MDRP and Related Compounds	58
2B.4	Optical Characteristics of MRX and Related Compounds	61
2B.4.1	UV-Spectra	61
2B.4.2	IR-Spectra	63
2B.5	Thermal Characteristics of MRX and Related Compounds	64

<u>CONTENTS</u>		<u>PAGE</u>
2B.6	Solubility of Metal Dithiophosphate and Xanthate in Inert Hydrocarbon Solvents	65
<u>CHAPTER 3</u>	<u>PHOTO- AND HYDROPEROXIDE-INDUCED DECOMPOSITION OF METAL COMPLEXES AND DISULFIDES IN SOLUTION</u>	
3.1	Object	75
3.2	Results	76
3.2.1	Effect of UV-Light on MRX and RX	76
3.2.1.1	NiRX and RX	76
3.2.1.2	ZnRX	77
3.2.2	Reactions of TBH with NiRX and RX at Room Temperature in the Presence and Absence of UV-Light	77
3.2.3	Effects of UV-Light and TBH on NiDRP, ZnDIP and DiPDiS	79
3.3	Discussion	81
3.3.1	Effect of Light and Hydroperoxide on NiRX and RX	81
3.3.2	Effects of Solvents on Photostability of NiRX and ZnRX	85
3.3.3	Effect of Solvents, Light and Hydroperoxide on MDRP and DiPDiS	88
3.3.4	Comparison Between NiDRP and NiRX	89

CHAPTER 4 STABILISATION OF LDPE

4A	<u>THE INFLUENCE OF METAL DITHIOLATES AND CORRESPONDING DISULFIDES ON THE THERMAL OXIDATIVE STABILITY OF LDPE</u>	
4A.1	Object	104
4A.2	Results	105
4A.2.1	Thermo-Oxidative Stability of Unstabilised PE	105
4A.2.2	Thermogravimetry of Metal Dithiolates and Corresponding Disulfides	106
4A.2.3	Thermal Antioxidant Behaviour of MRX and RX	108
4A.2.4	Thermal Antioxidant Behaviour of MDPB and DiPDiS	110
4A.3	Discussion	112
4A.3.1	Thermal Stability of Metal Dithiolates and Their Corresponding Disulfides	112
4A.3.2	Thermal Antioxidant Behaviour of Metal Dithiolates and Corresponding Disulfide	113
4B	<u>THE INFLUENCE OF METAL DITHIOLATES AND CORRESPONDING DISULFIDES ON THE PHOTO- OXIDATIVE STABILITY OF LDPE</u>	
4B.1	Object	125
4B.2	Results	126
4B.2.1	Photo-Oxidative Stability of Unstabilised LDPE	126

<u>CONTENTS</u>	<u>PAGE</u>	
4B.2.2	Photo-Oxidative Stability of PE in the Presence of MDRP and DiPDiS	126
4B.2.3	Photo-Oxidative Stability of PE in the Presence of MRX and RX	128
4B.2.4	Evaluation of the Photo-Oxidative Stability of PE in the Presence of Synergistic Mixtures of HOBP with Metal Dithiolates and Corresponding Disulfides	130
4B.3	Discussion	135
4B.3.1	Photo-Oxidative Stability of Unstabilised LDPE135	
4B.3.2	Photo-Oxidative Stability of PE in the Presence of Nickel Dithiolates and Corresponding Disulfides	136
4B.3.3	Photo-Oxidative Stability of PE in the Presence of Zinc and Copper Dithiolates	144
4B.3.4	Photo-Oxidative Stability of Synergistic Combination of Dithiolates with HOBP	146
<u>CHAPTER 5</u>	<u>STABILISATION OF LDPE MASTERBATCHES</u>	
5.1	Object	164
5.2	Results	165
5.2.1	Spectral Characteristics of MB Films	165
5.2.2	Photo-Oxidation of Stabilised LDPE in Masterbatch Preparation	170
5.2.3	Thermal Oxidation of Stabilised PE in Masterbatch Preparation	171
5.3	Discussion	174

<u>CONTENTS</u>	<u>PAGE</u>	
5.3.1	Photo-Oxidative Stabilisation of Masterbatch Preparation	174
5.3.2	Thermo-Oxidative Stabilisation of PE MB Preparations	177
5.3.3	Mechanisms of Stabilisation of PE in MB Preparation Using Different Antioxidants	179
5.3.3.1	DiPDiS	179
5.3.3.2	NiDIP	183
5.3.3.3	Synergistic Combinations of NiDIP and DiPDiS with HOBP	188
 <u>CHAPTER 6</u> <u>STABILISATION OF PP</u>		
6.1	Object	203
6.2	Results	204
6.2.1	Photo- and Thermo-Oxidation of PP	204
6.2.2	Photostabilisation of PP by NiDBP, NiBX, and DiPDiS and their Combination with HOBP and IRGANOX 1076	205
6.2.3	Effect of Nickel Dithiolates and their Corresponding Disulfides on Thermo- Oxidative Stability of PP in the Presence and Absence of IRGANOX 1076	209
6.3	Discussion	211
6.3.1	Thermo- and Photo-Oxidative Stability of PP	211
6.3.2	Effect of NiDBP, NiBX, and DiPDiS on Oxidative Stability of PP	212

<u>CONTENTS</u>	<u>PAGE</u>
<u>CHAPTER 7</u>	<u>DECOMPOSITION OF HYDROPEROXIDES IN MODEL COMPOUNDS</u>
7.1	Object 226
7.2	Results 227
7.2.1	Thermal Decomposition of CHP in the Presence and Absence of Nickel Dithiolates in Chlorobenzene at 110 ^o 227
7.2.2	Auto-Oxidation of Dodecane in the Presence and Absence of NiDBP and DiPDiS at 150 ^o 230
7.2.3	Photodecomposition of CHP in the Presence of NiDBP and DiPDiS 231
7.2.4	Kinetics of Disappearance of Additives 233
7.2.5	Product Analysis 233
1.	By Gas Liquid Chromatography 233
2.	By Infrared Spectrophotometry 235
3.	By Thin-Layer Chromatography 236
4.	By UV-Analysis 238
7.3	Discussion 239
7.3.1	Thermal Decomposition of CHP in the Presence and Absence of Nickel Dithiolates in Chlorobenzene at 110 ^o 239
7.3.2	Auto-Oxidation of Dodecane in the Presence and Absence of NiDBP and DiPDiS at 150 ^o 246
Conclusion	272
Suggestions for Further Work	276
Appendix	Published Work
1.	Europ. Polym. J. <u>16</u> , 503 (1980)
2.	Europ. Polym. J. <u>16</u> , 709 (1980)
References	280

LIST OF FIGURES

<u>Figure</u>	<u>Page</u>	<u>Figure</u>	<u>Page</u>
2A.1	36	3.15	101
2A.2	37	3.16	102
2A.3	41	3.17	102
2A.4	45	3.18	103
2A.5	47	4A.1	118-119
2B.1	67-68	4A.2	120
2B.2	69	4A.3	121
2B.3	70	4A.4	122
2B.4	71-72	4A.5	122
2B.5	73	4A.6	123
2B.6	74	4A.7	124
3.1	92	4A.8	124
3.2	93	4B.1	151
3.3	93	4B.2	152
3.4	94	4B.3	152
3.5	94	4B.4	153
3.6	95	4B.5	154
3.7	95	4B.6	155
3.8	96	4B.7	155
3.9	97	4B.8	156
3.10	98	4B.9	156
3.11	98	4B.10	157
3.12	99	4B.11	157
3.13	100	4B.12	158
3.14	99	4B.13	158

<u>Figure</u>	<u>Page</u>	<u>Figure</u>	<u>Page</u>
4B.14	159	6.9	225
4B.15	160	6.10	225
4B.16	161	7.1	251
4B.17	162	7.2	252
4B.18	163	7.3	253
5.1	192	7.4	254
5.2	193	7.5	255-256
5.3	194	7.6	256
5.4	194	7.7	257
5.5	195	7.8	258
5.6	196	7.9	259
5.7	196-198	7.10	260
5.8	199	7.11	261
5.9	199	7.12	262
5.10	200	7.13	263
5.11	201	7.14	264
5.12	202	7.15	265
6.1	220	7.16	266
6.2	221	7.17	267
6.3	221	7.18	268
6.4	222	7.19	269
6.5	223	7.20	269
6.6	223	7.21	270
6.7	224	7.22	270
6.8	224	7.23	271

LIST OF TABLES

<u>Table</u>	<u>Page</u>
2A.1	26
2A.2	29
2A.3	29
2B.1	54
2B.2	57
2B.3	62
2B.4	64
2B.5	65
3.1	81
4A.1	106
4A.2	107
4A.3	108
4A.4	109
4A.5	110
4A.6	111
4A.7	114
4B.1	127
4B.2	131
4B.4	143
5.1	165
6.1	206
6.2	210
7.1	229

LIST OF ABBREVIATIONS

CM	Closed mixer
OM	Open mixer
[5,CM]	5 min. processing in open mixer
PIP	Photo-oxidative induction period
TIP	Thermo-oxidative induction period
EMT	Embrittlement time
MB	Masterbatch [containing 2.5% additive]
DMB	Diluted Masterbatch [contains 0.1%, or 0.25%, prepared from MB and unstabilised polymer]
NS	Normally processed sample [contains 0.1% additive]
PE	Polyethylene
LDPE	Low density polyethylene
PP	Polypropylene
IR	Infrared
UV	Ultra-Violet
TG	Thermogravimetry
TLC	Thin layer chromatography
GLC	Gas liquid chromatography
DRDiSO	Thiophosphoryl disulfide-based oxidation products, R=isopropyl [ip] or butyl [B].

Abbreviations for additives used are given in table 2A.1 [p.26].

CHAPTER ONE

I N T R O D U C T I O N

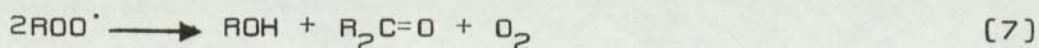
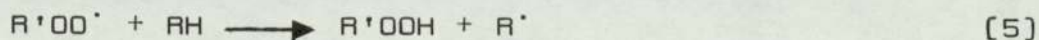
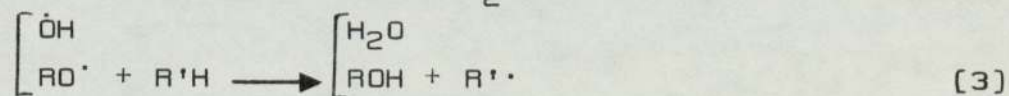
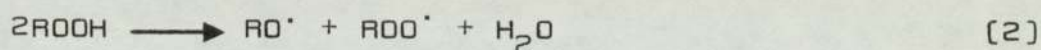
The need to prolong the useful-lifetime and durability of polymer articles coupled with an increased awareness of the rewards in terms of energy conservation and long-term labour/cost economies has transformed the study of polymer stabilisation from a mere academic pre-occupation to a practical objective. In terms of energy savings alone, doubling the 'usable' lifetime of an article, for instance, can easily mean a saving of 100% in real cost when materials, fuel, machine wear, time and labour are taken into account.

Although polyolefins are generally regarded as intrinsically stable polymers, many of the apparent shortcomings of the in-service articles are inherited from the various manufacturing stages and processing history, both of which affect drastically the ultimate stability, hence usability, of polymer articles. The need to combat the deleterious effects of processing of polymers at elevated temperatures cannot be exaggerated. Incorporation of anti-oxidants during processing of polymers has been widely used to minimise the oxidative conditions of processing. An efficient antioxidant system can be successfully designed through a proper understanding of the mechanism of action by which available stabilisers exert their stabilising effect on the host polymer matrix under different thermo- and photo-oxidative environments.

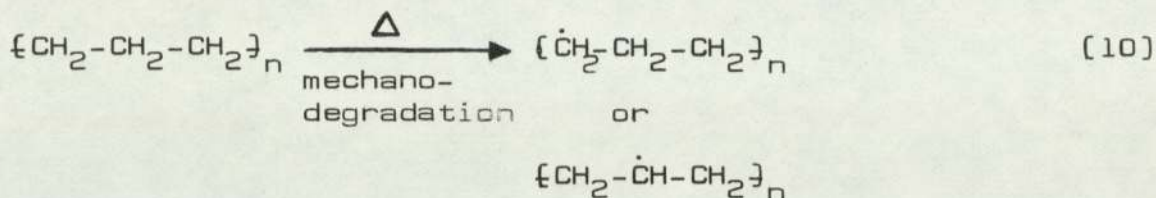
1.1 Auto-Oxidation of Polyolefins

Oxidation of polyolefins is, in many respects, similar to that of low molecular weight hydrocarbons^[1a]. In particular, polyethylene (PE) and polypropylene (PP) exhibit no induction period and undergo radical-chain auto-oxidation^[2] [Scheme 1.1] normally associated with hydrocarbon oxidation^[3]. In the presence of oxygen, alkyl and peroxy radicals are the key propagating species in the mechanism shown [Scheme 1.1]. A pre-requisite for equations 1 and 2 to occur is the formation of alkyl radicals in the auto-oxidising hydrocarbon substrate.

Apart from the direct formation of alkoxy, peroxy, and alkyl radicals [eqs. 1-3] through the action of environmental factors, e.g. light and heat, alkyl radicals are produced additionally [eq. 10] upon shearing of polymer chains during high temperature processing. The high reactivity of these radicals towards oxygen results in a preponderance of peroxy radicals in polyolefins [eq. 4 in Scheme 1.1].



Scheme 1.1 Hydrocarbon auto-oxidation

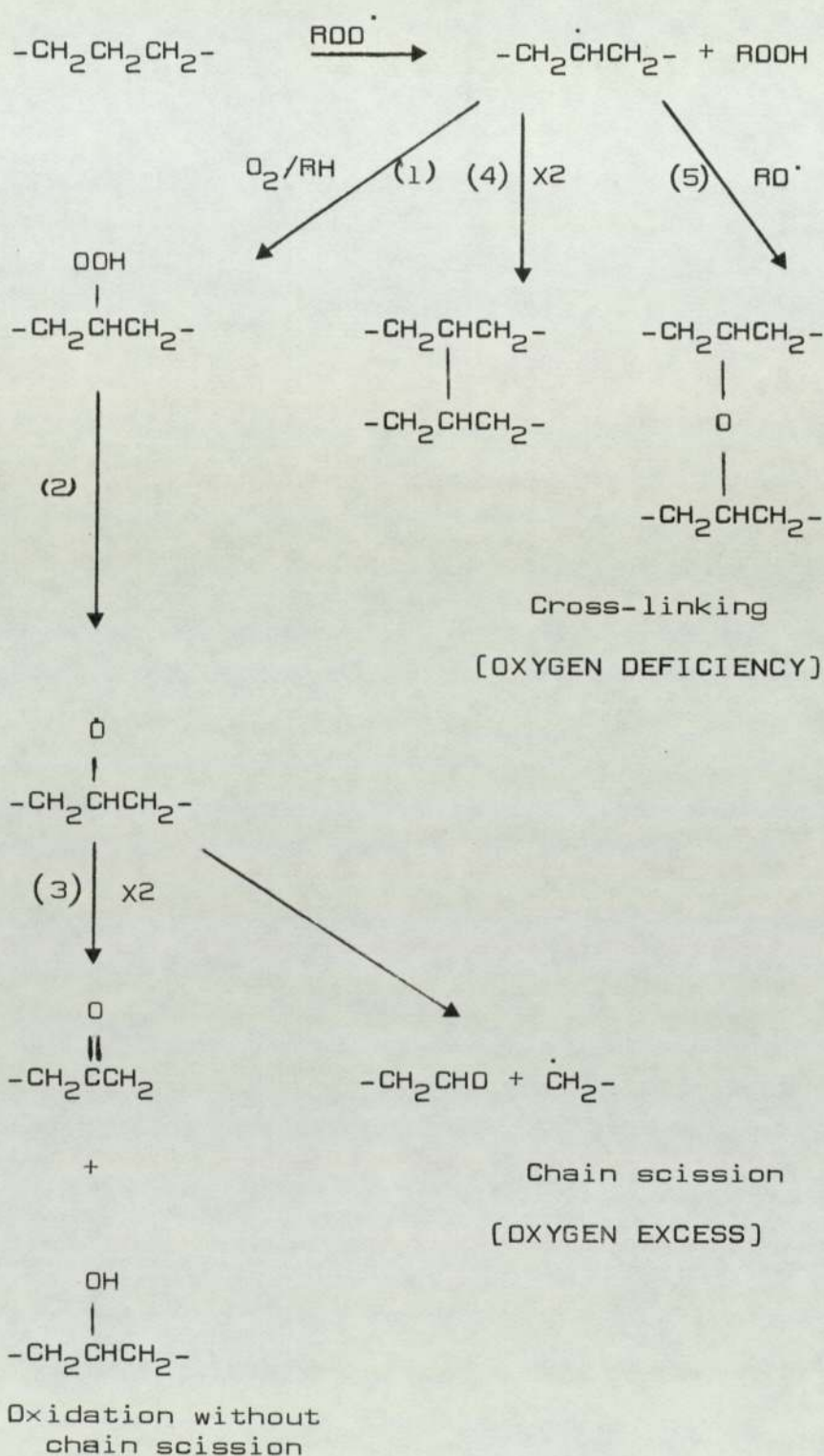


The absorption of oxygen by polyolefins is marked by an initial rapid auto-acceleration followed by auto-retardation^[2]. Thin films are usually employed in the study of oxidation of polymers in order to minimize the effect of oxygen diffusion^[4]. A consequence of all this is that hydroperoxide moieties [eq. 5] assume even greater importance under the conditions of high temperature processing. Processing of PE and PP at 150° and 180°, respectively, leads therefore to the formation and accumulation of polymer hydroperoxides. Decomposition of these hydroperoxides^[4,5] give rise to carbonyl products [eq. 1 in Scheme 1.2] in the presence of excess oxygen, or to cross-linked products [eqs. 4 and 5 in Scheme 1.2] in an oxygen-deficient environment^[5,6].

Gradual deterioration in the chemical and physical attributes of polyolefins occurs^[7,8] therefore at a rate which is pre-determined by the thermal history of the polymer [see Scheme 1.2]. Environmental factors, and adventitious groups or impurities, which are present initially, exert additional deleterious effects^[7,8].

The theme of this chapter is to review current knowledge of the detrimental effects of the various environmental agents and processing conditions [Sec. 1.2], and to show how these may be combated, to minimize their effects, thereby extending the service life of polyolefins [Sec. 1.3].

Scheme 1.2 Cross-linking and chain scission during oxidation of polyethylene (after scheme 1, reference 6)



Ultraviolet light absorbed by polymers affects several competing or consecutive radical and molecular reactions. A consequence of these reactions is the rapid build-up of oxidation products with concomitant changes in chemical, physical and mechanical properties, e.g. chain scission and cross-linking, reduction in molecular weight and increased brittleness^[9].

Commercially produced polyolefins show a continuous UV-absorption. Effectively, therefore, exposed polymer articles absorb energetic solar radiation (300-400 nm) which is capable of bond photocleavage with, in some cases, initiation of photochemical changes^[10].

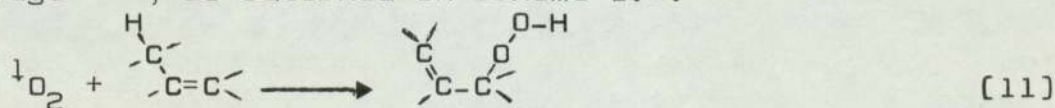
Chromophoric groups, present as impurities introduced deliberately or adventitiously during processing and manufacture as oxidation products are chiefly responsible for the 'photoactivity' of the polymer, giving rise to sensitised degradation of polyolefins^[8,11,12]. Catalyst residues [e.g. in PP and HDPE] and unsaturation [e.g. vinylidene in low density polyethylene, LDPE] are the usual impurities obtained as a result of polymerisation process^[12].

Polycyclic aromatic hydrocarbons, e.g. alkyl derivatives of naphthalene, phenanthrene and anthracene may also be absorbed by polymers exposed to polluted atmospheres^[13], although these hydrocarbons were not found^[14] in newly fabricated polymers.

Primary pollutants, such as ozone, sulfur dioxide, and nitrogen dioxide, may react directly with the polymer, or under the influence of light, may give rise to secondary 'pollutants' formed in situ in the polymer, e.g. atomic and singlet oxygen, which may sensitize the oxidation of the substrate^[15a]. The relevance of singlet oxygen sensitized oxidation of polymers has been the subject of some controversy^[5].

Singlet oxygen [¹O₂] can be formed^[16] via decomposition of an ozone complex, self-termination of primary and secondary peroxy radicals during auto-oxidation of hydrocarbon, or through photosensitized formation via energy transfer from excited polymer carbonyls [formed during processing or by photolysis]^[16]. However, it is readily deactivated by several of the gaseous 'contaminants' and other chemicals, e.g. H₂O, O₂, N₂, CO₂, which are adsorbed on the polymer surface or, present in large excess in the gas phase with which the polymer surface is in contact^[15]. Consequently, its importance should not be exaggerated.

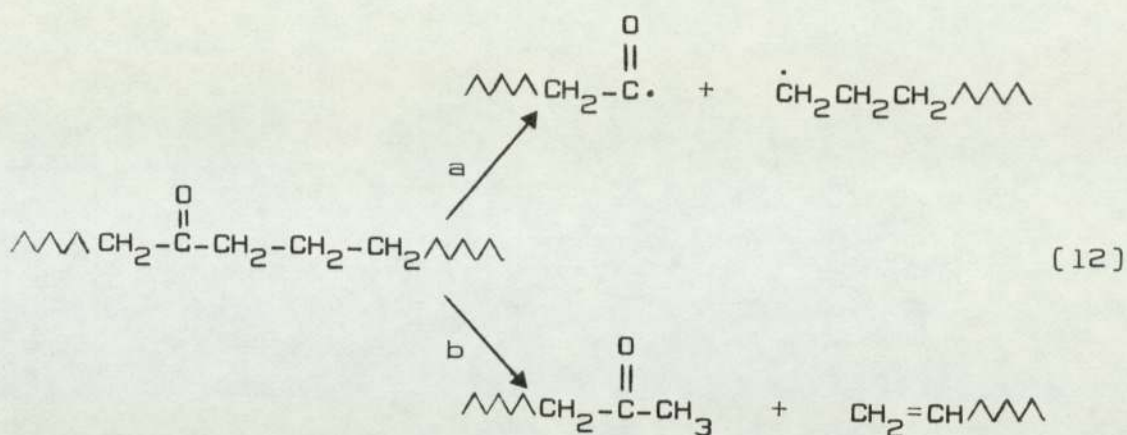
Singlet oxygen may add to unsaturation [eq. 11] to give hydroperoxides^[16] which in turn may undergo thermal or photolytic cleavage to macro-alkoxyl radicals, and subsequent β-scission which leads to polymer backbone cleavage^[16], as outlined in Scheme 1.2.



The relatively low reactivity^[14] of vinyl and vinylidene groups present in PE toward 1O_2 also suggests that singlet oxygen may play an insignificant role as an initiator of oxidation. However, the fact that hydroperoxides are formed during thermal oxidation of polyolefins^[17], and that these act^[11,17] as photoinitiators during the early stages of photo-oxidation, adds further weight to the conclusion^[16] that if 1O_2 is important it can only be important in the very early stages of UV-exposure.

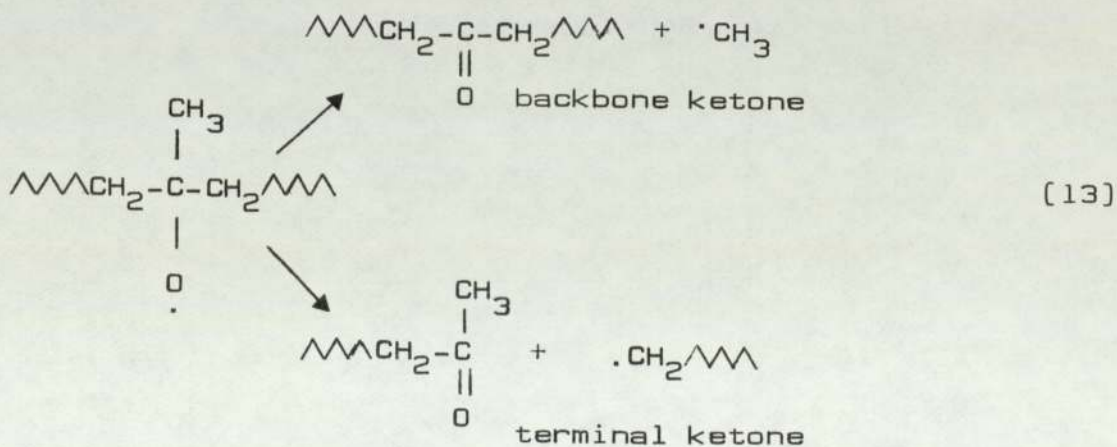
Polymer hydroperoxides, and their decomposition products [see Scheme 1.2] are the most important of all sensitising chromophores formed in polyolefins during thermal processing and during environmental exposure^[8,11,12,17]. These are the precursors of in-chain ketones and end-chain [methyl ketones] polymer carbonyls, which play a more significant role in sensitising degradation at later stages of thermal- and photo-oxidation of polyolefins^[18].

Photolysis of polymer carbonyl gives rise to polymer radicals and unsaturation as intermediate products by Norrish-type reactions [eqs. 12a and b]. Clearly carbonyl groups can photo-initiate oxidation in a radical generating process [eq. 12a] causing chain scission or rearrange in a non-radical process [eq. 12b] to give molecular products with backbone scission^[15b].



It has been found^[19,20] that the extent of hydroperoxide formation during thermal processing operations determines the rate of photo-oxidation during the initial stages of UV-exposure of the polymer. Accordingly, the prior thermal history of polymers will, to a major extent, determine their behaviour during photo-oxidation^[8,12].

In the radical-chain mechanism for the decomposition of polymer hydroperoxide [Scheme 1.1], the rate of the photo-initiation step [eq. 1] is much faster than the rate of a thermal initiation step [eq. 2]^[21,22]. Alkoxy radicals formed from either step [eqs. 1 and 2] or, additionally, from self-termination [eq. 6] of peroxy radicals formed during thermolysis [eq. 2] undergo β -scission [eq. 13] or hydrogen abstraction [eq. 14]^[22,23].



Both polymer hydroperoxides and carbonyls formed during processing of polyolefins are sensitive to UV-light^[12,25]. UV-absorption by polymer hydroperoxides, e.g. in PE, can give rise to ketones and alcohols as well as cross-linked products. At normal oxygen pressures, e.g. during processing of polymers in an open mixer of a torque-rheometer, a high concentration of alkyl peroxy radicals^[6] prevails (see Sec. 1.1). Disproportionation of these radicals predominates giving ketone and alcohol (eq. 7 in Scheme 1.1 and steps 1-3 in Scheme 1.2).

Processing of polymers in an oxygen deficient^[6] atmosphere, e.g. in closed mixer of a torque-rheometer, in a barrel of a screw extruder, or during UV-initiated oxidation (where the rate of initiation is high compared to the rate of oxygen diffusion into the polymer), results in higher yield of alkyl radicals. Termination of these radicals (eqs. 8&9 in Scheme 1.1) is responsible for cross-linking reactions (steps 4 and 5 in Scheme 1.2) which become less competitive with oxidative chain scission at higher oxygen concentration^[19].

1.3 Polymer Stabilisation

Polymer stabilisation can, in principle, be effected economically when a relatively low concentration of stabiliser (antioxidant) which can interfere with the auto-oxidative sequence [Scheme 1.1] of polymer degradation is added, singly, or in combination with others.

The antioxidant function of the stabiliser may therefore be classified^[26,27] according as to whether it intercepts radicals formed during chain propagation [eqs. 4 and 5], or chain initiation [eqs. 1, 2 and 10]. That is the antioxidant either breaks chains [CB], or removes or stabilises potential radical generators [preventive antioxidants].

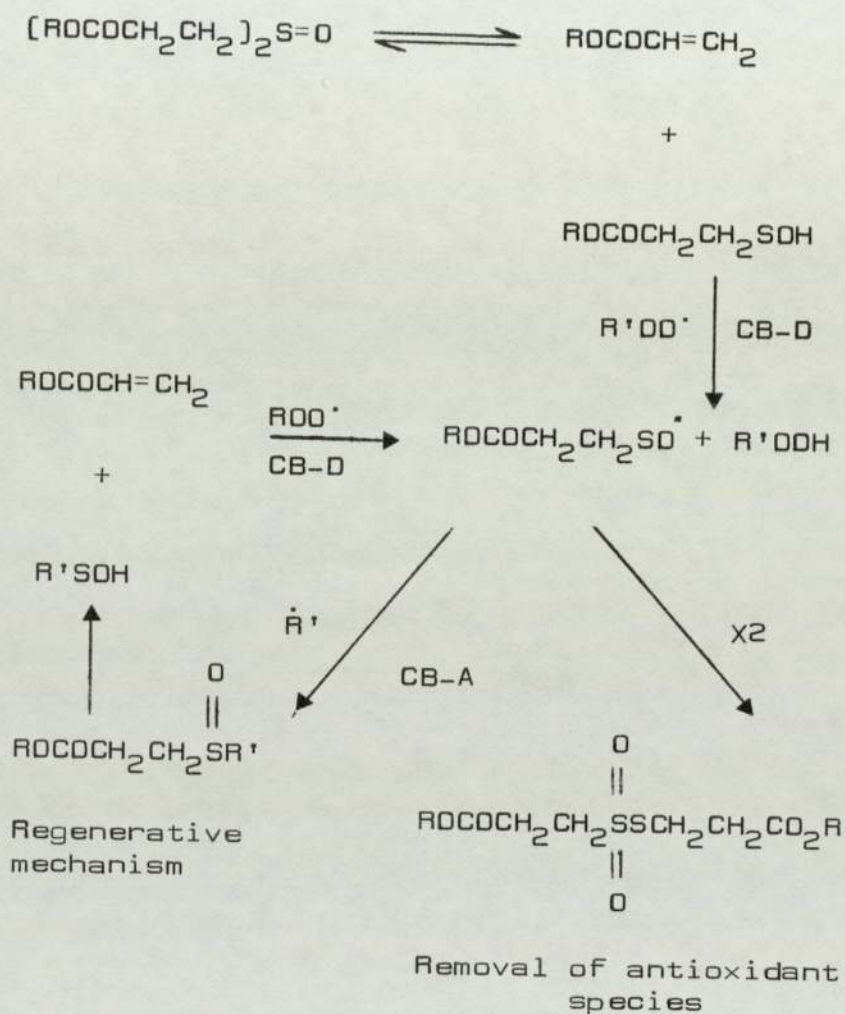
(i) Kinetic Chain Breaking [CB] Antioxidants^[5,6]

Alkyl radicals formed during hydrocarbon oxidation are readily oxidised to alkyl peroxy radicals at normal pressures. The ratio of these two radicals in an auto-oxidising system is a function of oxygen concentration. Processing of polyolefins in a normal oxygen atmosphere, e.g. in an open mixer of a torque-rheometer, favours alkyl peroxy radicals ($ROO\cdot$) formation, whereas processing in an oxygen deficient atmosphere, e.g. in a closed mixer, favours alkyl radicals ($R\cdot$). In practice, therefore, the ratio $ROO\cdot : R\cdot$ dictates the choice of a particular antioxidant.

Electron donor chain breaking [CB-D] antioxidants, e.g. hindered phenols and aromatic amines, are effective at high ($ROO\cdot : R\cdot$) ratios, whereas electron acceptor [CB-A] antioxidants, e.g. quinones, nitrocompounds, nitrones, and

phenoxy and nitroxyl radicals, are effective at low $[ROO^\bullet : R^\bullet]$ ratio. Thus reducing agents (CB-D antioxidants) interfere with ROO^\bullet while oxidising agents (CB-A antioxidants) intercept R^\bullet much more efficiently.

Scheme 1.3 Regeneration behaviour of antioxidant species
[after scheme 5, reference 6]



Chain breaking antioxidants which can act, during the course of its stabilising function, both as reductants and oxidants for ROO^\bullet and R^\bullet , respectively, may exhibit regenerative behaviour [Scheme 1.3] under conditions where both radicals are important. For example dilaurylsulphinyl-dipropionate, an effective melt stabiliser for PP^[6].

(ii) Preventive Antioxidants, [PA]

These act to reduce the rate of chain initiation. Their function is therefore to suppress degradation rate by physical processes (absorbing, quenching, screening), or by chemical reactions (decomposing peroxides). The destruction of hydroperoxides by a non-radical process is the key role in the preventive action of these antioxidants.

Catalytic peroxide decomposers [PD-C] are exemplified by sulfur-containing compounds. The active species^[28] (SO_3 or H_2SO_4) formed from these compounds are the antioxidants responsible for the removal of hydroperoxides in a non-radical generating process. Examples within this class include thiodipropionates^[29], metal complexes of mercaptobenzthiazole^[30], of dithiocarbamic acid^[31,32] and of dithiophosphoric acid^[32-34]. Phosphite esters on the other hand, have been shown^[5] to behave primarily as stoichiometric peroxide decomposers [PD-S].

The extent of cross-linking and chain scission in PE and PP depend on oxygen concentration [see Sec.1.1]. Thus, for example, PP is much more sensitive to chain scission than is PE^[5]. Both cross-linking and chain scission are effectively inhibited, however, by CB-A, PD-C, and CB-D antioxidants^[5].

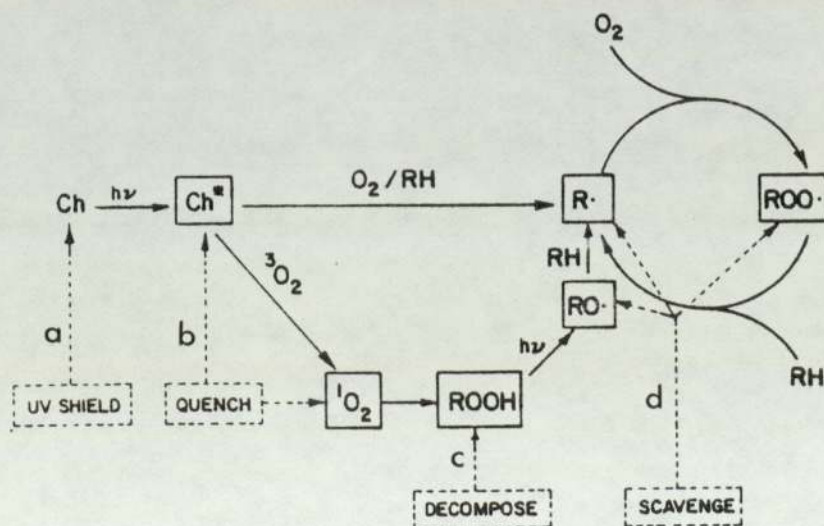
A typical chain breaking [CB-D] phenolic antioxidant, Irganox 1076 [see Table 2A.1, Sec. 2A.1] was shown^[5] to be an effective melt stabiliser. Catalytic peroxide decomposers, e.g. zinc and nickel dithiocarbamate [ZnDEC and NiDEC] were also found^[5] to be effective melt stabilisers. The typical UV-absorber, 2-hydroxy-4-octyloxybenzophenone [HOBP], however, was found^[5] to have only a minor chain breaking effect on both peroxide and carbonyl formation in PE and PP.

In general, the amorphous phase in polyolefins is more sensitive to oxidation than the crystalline phase^[35]. Moreover, additives or stabilisers have a tendency to accumulate in the amorphous phase^[35], which is an advantage. A general understanding of the mode(s) of stabilising action of a prospective stabiliser is paramount in the quest for suitable compounds which can impart optimized stabilising performance during the service-life of a host polymer.

The photodegradative route shown [Scheme 1.4] can be interrupted, halted, or diverted by one or more of the following mechanistically feasible processes^[25].

- Prevention of UV-excitation,
- Deactivation of excited molecules,
- Decomposition of impurity chromophores, and
- Scavenging of reactive radicals.

Scheme 1.4 Key steps of polyolefin photo-oxidation
[after scheme 1, reference 25]



1.4.1 UV-Screening and Absorption

The preferential absorption of harmful radiation by UV-absorbers may provide adequate protection against photo-initiated oxidation of polyolefins^[26]. Compounds which have intense UV-absorption in the region 300 to 400 nm can be considered as UV-absorbers, provided^[36a] they have available some energy-dissipating non-radiative (photo-physical) processes which allow them to protect themselves without sensitising the host polymer (or its chromophoric impurities). For example, 2-hydroxybenzophenone contains intramolecularly hydrogen bonded phenolic -OH groups which has a sacrificial stabilising effect in addition to deactivation of the excited molecule by radiationless transitions^[25].

Since photo-oxidation is a surface phenomenon, reflective or opaque pigment particles^[25] can shield a polymer surface from harmful radiation. Protection offered by a UV-screen is usually undermined by mechanical abrasion^[35]. However, most UV screens act by additional stabilising mechanisms as in the case of carbon black^[25]. Nickel dithiocarbamate^[31] and dithiophosphate^[22], on the other hand, were shown to exert a greater UV-stabilising action than could be accounted for by UV-screening action. The effectiveness of colourless UV stabilisers (commercially sought after for polyolefin films) is limited^[25] by their finite upper limit of molar extinction coefficients (ca. $10^5 \text{ M}^{-1} \text{ cm}^{-1}$), so that large concentrations (2-0.5 Wt%) are needed to protect thin (ca. 25 μm) substrates.

1.4.2 Excited State Quenching

In the absence of perfect light shields (UV-screens and absorbers), chromophoric impurities in polyolefin can be excited by UV light. Moreover, in the absence of suitable deactivators, excited chromophoric groups can photo-initiate oxidative degradation^[25].

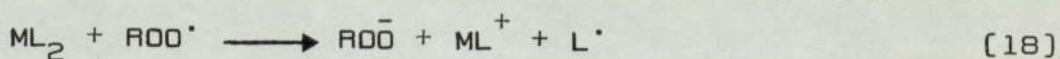
Energy transfer from a photoexcited species (S^*) to a quencher (Q) molecule can provide an efficient stabilising route for excited states of a chromophore provided that the excited quencher molecule can dissipate its acquired [excess] energy harmlessly^[25]. Efficient energy transfer, however, can only occur if the triplet energy (E_T) of the quencher (stabiliser) lies below that of the chromophore^[36b]. In principle, therefore, the commercial UV-stabiliser, UV1084 [Ni(II) n-butylamino (2-2' thio bis (tertiary octyl phenolate)) ($E_T = 27000 \text{ cm}^{-1}$)] is expected to quench triplet states of α , β -unsaturated carbonyls ($E_T = 29500 \text{ cm}^{-1}$) more efficiently than HOBP with $E_T = 25000 \text{ cm}^{-1}$ on account of better energy matching. Similar arguments suggest^[37] that tetraethyl thiuram disulfide, nickel and iron dithiocarbamates can deactivate triplet states of carbonyls to some extent. It has been suggested that nickel dithiocarbamate may deactivate the triplet carbonyl of benzophenone^[38]. Quenching of excited states of hydroperoxides is, in principle, an attractive alternative to carbonyl quenching. The dissociative nature of these states, however, makes it difficult to achieve^[25].

Long range energy transfer ($S^* \longrightarrow Q$) may take place when the emission spectrum of S^* and the absorption spectrum of Q overlap significantly. This can be an efficient route for the transfer of energy at low quencher concentrations^[25]. Energy transfer by the collisional mechanism can only become important at high quencher concentration.

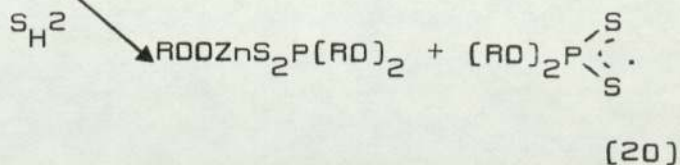
1.4.3 Radical Scavenging

The removal of chain propagating species is a well-known function of CB antioxidants [see Sec. 1.3.1]. Reactive radicals, e.g. ROO^* , RO^* and R^* , can be trapped by suitable scavengers. In addition to a CB antioxidant function, metal chelates of dithiophosphates have been found^[39-41] to scavenge alkylperoxyl radicals [two radicals can be scavenged by one metal chelate molecule]. Products of this oxidative process are the disulfides; these were found^[40] to be unreactive toward alkylperoxyl radicals.

Although radical-trapping mechanism (eq. 18) has been proposed^[42] for



a number of metal chelates of dithiophosphoric^[43], dithiocarbamic, salicylic acids, oximes^[31,44], etc., there is still uncertainty as to the actual mechanism involved^[43]: electron transfer from the metal ion to form an intermediate complex (eq. 19) or displacement of a ligand radical by the alkylperoxyl radical in an S_H2 process (eq. 20).



1.4.4 Peroxide Decomposition (PD)

Removal [or decomposition] of hydroperoxides in non-radical generating processes [to give stable molecular products] or their protection against decomposition, represent a preventive form of oxidation inhibition^[5]. In both cases, the hydroperoxide radical initiation mechanism^[5], under both thermal and photo-oxidative conditions [eqs. 1 and 2 in Scheme 1.1] are interrupted.

Both PD-C and PD-S antioxidants [see Sec. 1.3.2] inhibit hydroperoxide and carbonyl formation during the processing of polyolefins^[5]. In this respect, they are similar to CB-D antioxidants [see Sec. 1.3.1]. Several sulfur-containing metal complexes are known to operate chiefly by this mechanism, e.g. nickel and zinc dithiocarbamates^[31, 44-46] and zinc mercaptobenzthiazole^[47].

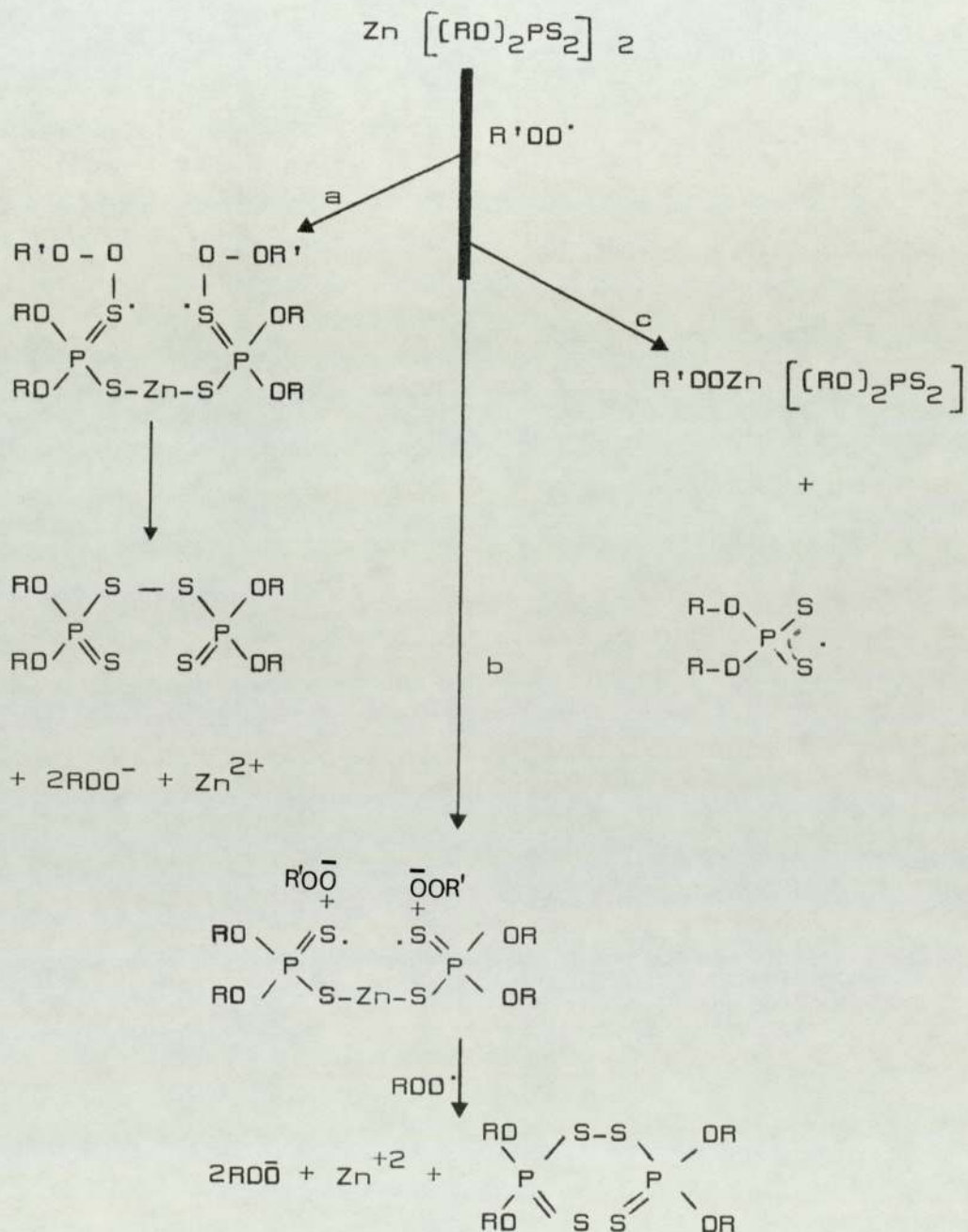
Decomposition of hydroperoxides has been generally attributed^[26] to the generation of several progressively higher sulfur-oxidation states, with concomitant reduction of the hydroperoxide to its derived alcohol. SO_3 [or H_2SO_4]^[47] have been proposed as the effective ionic catalysts for hydroperoxide decomposition.

Metal dithiolates have been found^[5] to display two kinds of antioxidant activity: (i) initially they assume the role of CB-D antioxidant, and this is followed by, (ii) peroxide decomposing activity during later stages of oxidation and particularly at high hydroperoxide : metal complex ratio. Under these conditions their action involves the catalytic non-radical [PD-C] decomposition of hydroperoxides by the acid formed by oxidative disruption of the sulfur containint complex.

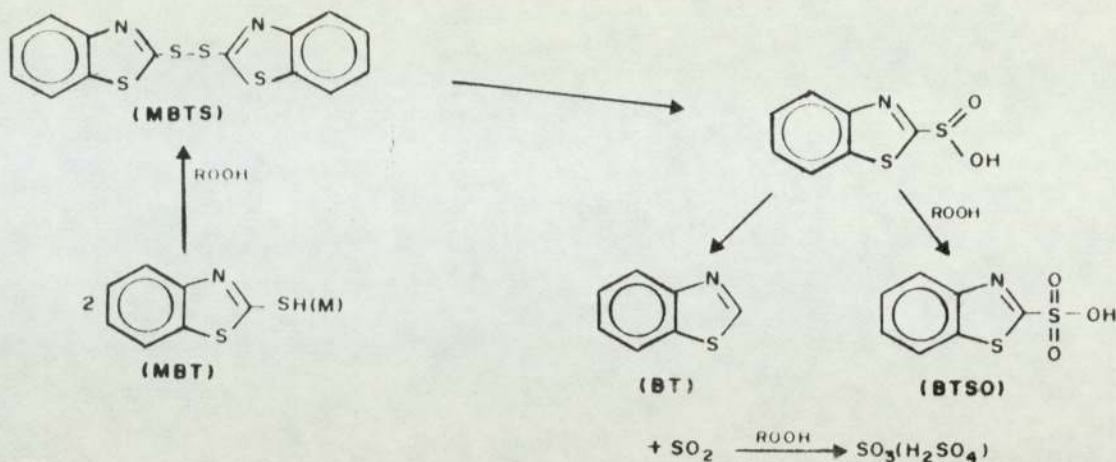
Zinc di-isopropyl dithiophosphate [ZnDIP] is given here as an example for this class of antioxidants to illustrate the CB-D and PD antioxidant function. Three mechanisms have been proposed^[42,48] for the initial CB-D antioxidant function of ZnDIP. An initial process involving an electron transfer from the metal complex to alkylperoxyl radical which is followed by the formation of the disulfide directly [according to Schemes 1.5a and 1.5b] or indirectly [Scheme 1.5c] via the dimerisation of thiyl radicals. Disulfides or thiyl radicals formed from the reaction of ZnDIP with hydroperoxides^[49,50] during the CB-D activity of the antioxidant are further oxidised; these oxidation products can efficiently decompose hydroperoxides by catalytic non-radical mechanism, via the formation of SO_3 or H_2SO_4 . This process is entirely analogous to the formation of an ionic catalyst for hydroperoxide decomposition from mercaptobenzthiazole and its metal complexes through the intermediate disulfide^[47], Scheme 1.6.

Scheme 1.5 Mechanisms for the initial CB-D antioxidant Function of ZnDIP

- addition to sulfur bond and disulfide formation [48]
- disulfide formation [48]
- ligand displacement [42]



Scheme 1.6 Antioxidant mechanism of MBT and ZMBT
[after scheme 9, reference 6]



1.5 Synergism

Two or more antioxidants exhibit synergism, or otherwise, depending on whether their overall protective effect is greater than the sum of their individual effects^[16]. Homosynergism results^[16] when two or more antioxidants which operate by the same mechanism have unequal reactivities. Heterosynergism arises^[16] from the co-operative effect of antioxidants which function by different mechanisms. Synergistic combination of CB-D and PD-C antioxidants offer therefore maximum protection to the polymer^[16]. For example, UV-absorber, HOBP, can synergise effectively with both CB and PD antioxidants; this has been established^[45,46] for both PE and PP.

An autosynergistic behaviour is obtained^[16] when the same antioxidant functions by more than a single mode of action. For example, amine antioxidants are more effective than the phenolic antioxidants due to their additional ability to complex metal ions.

Dialkyl dithiophosphates are long established additives in the oil industries^[51]. Many oil-soluble, neutral derivatives of the higher molecular weight dialkyl and diaryl dithiophosphates are claimed^[51,52] to improve extreme pressure properties, decrease corrosion, serve as antioxidant and antisludging agents in detergents and in lubricating oil. Barium and zinc dialkyl dithiophosphates are notable examples; alkyl groups containing 6-8 carbon atoms afford maximum oil stability.

Thiophosphoryl disulfides are said^[52] to be useful in oils, for high pressure lubricants, for stabilisers, or as flotation agents. Polysulfides of diaryldithiophosphate have been used^[52] as vulcanization accelerators and additives for lubricating oils. Dithiophosphates have also been recommended^[53] for use as antiozonants for rubber. For example, amides of dithiophosphoric acid^[53] show antioxidant, antiozonant, thermal and light stabilising properties. Nickel dialkyl dithiophosphates have also been recommended^[54] as antiozonants. Nickel dialkyl dithiophosphates are effective light stabilisers for poly- α -olefins^[18,22], whereas barium diaryldithiophosphate and other salts of dithiophosphoric acid have been recommended^[55] for stabilisation of halogen-containing polymers, e.g. polyvinyl chloride.

Xanthates have been put to a wide variety of industrial uses and applications. Apart from their renowned use as

flotation agents^[56], a number of xanthic salts have been used^[56] as vulcanization accelerators. Zinc isopropyl- and butyl-xanthate were found^[56] to be among the most efficient salts. Nickel amyl, potassium tridecyl, and zinc isopropyl xanthate have been recommended^[56] as additives for lubricating oils to reduce oxidation and corrosion. Nickel xanthate has been reported to act as ozone protective agent when used in combination with a conventional chain-breaking antioxidant, e.g. phenyl β -naphthylamine,^[1c].

Alkyl xanthic disulfides (dixanthogens) have been used as regulating agents in butadiene polymerisation^[56]. Dixanthogens with alkyl group containing three carbon atoms are said^[56] to increase the film strength of lubricating oil. Butyl dixanthogen has been claimed^[56a] as vulcanisation accelerator, while isopropyl dixanthogen was used^[56a] as a modifier in polymerisation and stabilisation of polysulfone resins.

1.7 Aim and Scope of Project

Extensive literature on polymer stabilisation has accumulated over the past few years [5-7,9,18,22,23,26]. Considerable progress has been achieved in our understanding of the mechanism of antioxidant action of several classes of sulfur-containing compounds [29,38,45-47]. Oxidative degradation during processing of polymers, and subsequent heat ageing or UV exposure, has been linked to the activity of hydroperoxides [8,17,19]. Removal or decomposition of these species is the key to polymer stabilisation by additives. The mechanism by which these additives decompose polymer hydroperoxides has remained an open question.

The aim of the present study is three-fold:

1. To explore the suitability of metal dithiophosphates and xanthates for polymer stabilisation when used alone, or in combination with other known stabilisers, with due consideration to existing knowledge on dithiocarbamates.
2. To investigate the modes of action of these stabilisers by conducting studies on model and polyolefin systems.
3. To re-examine the peroxide decomposing activity of 1,1-dithiolates by a systematic comparative study in model compounds at elevated temperatures, and to establish the mechanism of their antioxidant action.

CHAPTER TWO

A. E X P E R I M E N T A L

2A.1 MATERIALS

2A.1.1 Polymers

Commercial grade unstabilised low density polyethylene (alkathene WJG47; MFI=2) and polypropylene (HF20/CV170) were supplied by ICI and were normally stored in the dark inside a deep freezer.

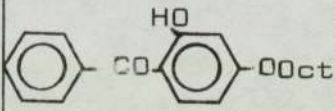
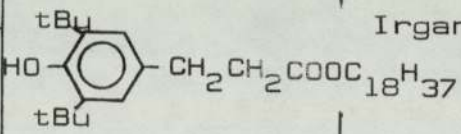
2A.1.2 Stabilisers

Ethyl and isopropyl dixanthogen and zinc isopropylxanthate were used as supplied by Robinson Brothers. Sodium salts (ex Albright and Wilson commercial grade, ca. 70%) of dialkyl dithiophosphates [ethyl, isopropyl, and butyl] were purified and used for the preparation of heavy metal dithiophosphates. 2-hydroxy-4-octyloxybenzophenone (Cyanamide UV531) and Irganox 1076 (Ciba-Geigy) were used as received. A list of additives, and their code names, is given in Table 2A.1. Apart from the additives mentioned above, the other additives were prepared by standard methods [see Sec. 2A.1.5].

2A.1.3 Solvents

Technical grade solvents were used for all the preparations, and were distilled when required for recrystallisation and extraction (of films). Analar and spectroscopic grades were used for all operations involving spectral studies of solutions, i.e. recrystallisation, irradiation, optical spectra, etc. Puriss grade chlorobenzene and dodecane (Koch-Light) were used as received in studies of the kinetics of hydroperoxides and additives by iodometric and spectroscopic methods.

Table 2A.1 Stabilisers and their code name

Compound	Structure	Code Name
Nickel (II) Dialkyl Dithiophosphate	$[(OR)_2PSS]_2Ni$	NiDRP R=E, I, B ^[a]
Zinc (II) Di-isopropyl Dithiophosphate	$[(DiPr)_2PSS]_2Zn$	ZnDIP
Cupric (II) Di-isopropyl Dithiophosphate	$[(DiPr)_2PSS]_2Cu$	CuDIP
Di-Alkyl Thiophosphoryl Disulfide	$[(OR)_2PSS]_2$	DRDiS R=iP ^[b] , B
Nickel (II) Alkyl Xanthate	$[DRCSS]_2Ni$	NiRX R=E, B
Zinc (II) Alkyl Xanthate	$[DRCSS]_2Zn$	ZnRX; R=E, I
Cuprous (I) Alkyl Xanthate	$[DRCSS] Cu$	CuRX R=E, B
Alkyl Dixanthogen	$[DRCSS]_2$	RX R=E, I
2-Hydroxy-4-Octyloxy Benzophenone		HOBP ^[c]
n-Octadecyl-3-(3',5'-di-ter. butyl-4' hydroxy-) Phenyl Propionate		Irganox 1076 ^[d]

[a] E = Ethyl, I = Isopropyl, B = Butyl

[b] iP = isopropyl [used only with thiophosphoryl disulfide]

[c,d] Commercial antioxidants

2A.1.4 Purification of Hydroperoxides

Koch-Light technical grades of cumene hydroperoxide (stabilised by 6% of 15% w/w slurry of sodium carbonate) and of tertiary butyl hydroperoxide were purified by a modified version of Kharasch method^[57], as described below.

(i) Cumene Hydroperoxide (CHP)

50g [1.25 mole] of sodium hydroxide in 100 ml of water was added to 152 g [1.0 mole] of CHP at 0°. The sodium salt was filtered, washed with 25% sodium hydroxide solution, and suspended in 500 ml of distilled water. A stream of carbon dioxide was bubbled through the suspension and when all the hydroperoxide has been reliberated the solution became opaque and separated into two layers. The upper layer was washed three times with distilled water. The product was finally distilled under vacuum, 52-55 / 0.01 torr, as a colourless liquid; purity by iodometric titration was better than 98%.

(ii) Tertiary Butyl Hydroperoxide (TBH)

To a cooled [ca. 10°] solution of 200 g of technical grade TBH in 200 ml hexane, 160 ml of a cooled 25% aqueous solution of sodium hydroxide was added. The sodium salt which separated was washed with 100 ml sodium hydroxide solution followed by hexane. The salt was then suspended in hexane and the TBH was liberated by a treatment with acetic acid. The hexane layer was thoroughly washed with water and was then fractionally distilled. The fraction boiling at 60°/12 torr was collected.

2A.1.5 Preparations

2A.1.5.1 Potassium-Ethyl [KEX] and Butyl-Xanthate [KBX]

This was prepared according to literature^[58]. Potassium hydroxide and absolute ethyl alcohol were refluxed for one hour. Carbon disulfide was added slowly to the cool decantate, and the precipitate was washed with ether and dried in vacuum desiccator over silica gel. The yellow powder obtained [58% yield] was identified by its melting point, Table 2A.3, elemental analysis [Table 2A.2] and IR spectrum.

2A.1.5.2 Nickel(II) Ethyl- [NiEX] and Butyl- [NiBX] Xanthate

This was prepared by the slow addition of a methanol solution of acetate [53%] to KEX, or KBX^[59]. The solid was washed with water and dried in a vacuum desiccator. An orangish-brown solid [53% yield] was obtained which was identified by its melting point [Table 2A.3], elemental analysis, Table 2A.2, IR spectrum [Fig. 2B.5 and 6, Sec. 2B.3.2] and UV spectrum [Fig. 2B.4, Sec. 2B.3.1].

2A.1.5.3 Cuprous(I) Ethyl-[CuEX] and Butyl- [CuBX] Xanthate

The reaction of cupric sulfate with the appropriate potassium salt [KEX and KBX] in aqueous medium gave an impure orangish-yellow precipitate^[60]. The precipitate was repeatedly digested with ether until all co-precipitated dixanthogen was removed [4 digestions]. Complete removal of dixanthogens was ascertained by following the characteristic

Table 2A.2 Elemental analysis

Compound	% Found			% Calculated		
	C	H	S	C	H	S
KEX	22.48	3.14	40.01	22.64	3.22	38.0
CuEX	19.8	2.9	30.14	19.5	2.9	29.81
NiEX	24.48	3.63	50.9	23.92	3.35	52.8
ZnEX	15.1	3.0	38.0	15.6	3.2	35.0
ZnDIP	34.0	5.1	26.8	34.2	5.9	25.5
NiDEP	22.1	4.9	30.4	22.4	4.7	29.9

Table 2A.3 Additives used, their colours and melting points

Additives	Colour of Crystals	Colour of solution ($1 \times 10^{-4}M$)	Melting point ($^{\circ}C$)		
			Found	Lit.	Ref.
NiDBP	dark purple	colourless	66- 67	-	-
NiDIP	dark purple	colourless	137-139	-	-
NiDEP	dark purple	colourless	108-110	105	63
DiPDiS	creamy	colourless	90- 91	90-91	64
ZnDIP	creamy	colourless	140-142	147-148	64
Cu DIP	lemon yellow	colourless	-	-	-
KBX	lemon yellow	colourless	200	-	-
NiBX	brown	yellow	87- 89	89	56e
NiEX	brown	yellow	136-138	137	56e
EX	creamy-yellow	colourless	30- 32	32.5	56e
KEX	lemon yellow	colourless	230	-	-
IX	creamy	colourless	55- 57	57	56e
ZnEX	creamy	colourless	136-138	138	61
ZnIX	creamy	colourless	156-158	-	-
CuBX	dark yellow	insoluble	$d > 190$	-	-
CuEX	dark yellow	insoluble	$d > 190$	$d > 190$	60

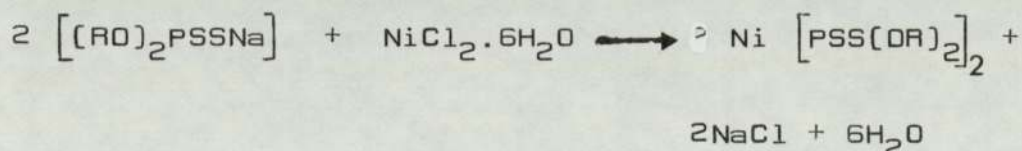
bands of dixanthogen [$1200-1300 \text{ cm}^{-1}$ and $1000-1024 \text{ cm}^{-1}$]. The final product [47% yield] which was insoluble, at room temperature, in most solvents showed a decomposition temperature on melting [see Table 2A.3].

2A.1.5.4 Zinc(II) Ethyl Xanthate [ZnEX]

This was prepared by dropwise addition of aqueous solution of KEX to aqueous zinc sulphate solution^[61]. The precipitate was washed with water and dried in vacuum desiccator. The white solid was obtained in 65% yield, and was characterised by its melting point [Table 2A.3], IR spectrum [Fig. 2B.5, Sec. 2B.3.2], UV-spectrum [Fig. 2B.4, Sec. 2B.3.1], and elemental analysis [Table 2A.2].

2A.1.5.5 Nickel(II) Dialkyl Dithiophosphates [NiDRP]

Nickel complexes of diethyl [E], di-isopropyl [I] and dibutyl [B] dithiophosphate were prepared^[62] by the dropwise addition of an alcoholic solution of nickel chloride to an alcoholic solution of the corresponding sodium salt according to the stoichiometry of the reaction.



The product was filtered, washed with ethanol, and dried in vacuum oven at room temperature. The nickel complexes were identified by their dark purple colour, melting point [Table 2A.3], IR spectra [Fig. 2B.2 and 3, Sec. 2B.2.2], UV-spectra [Fig. 2B.1, Sec. 2B.2.1] and elemental analysis [Table 2A.2].

Nickel (II) dibutyl dithiophosphate [NiDBP] was also prepared directly from dibutyl dithiophosphoric acid. The latter was prepared^[63] by refluxing phosphorous pentasulfide and butanol under nitrogen until the solution became clear yellow. The acid solution was identified by its IR spectrum [Fig. 2B.2a, Sec. 2B.2.2] and UV spectrum [Fig. 2B.1c, Sec. 2B.2.1]. This acid was used immediately for preparation of the nickel complex by addition of nickel salt.

2A.1.5.6 Zinc (II) di-isopropyl dithiophosphate [ZnDIP]

This was prepared^[64] by the reaction of zinc sulphate with sodium di-isopropyl dithiophosphate in aqueous solution under nitrogen and continuous stirring. The white precipitate [75% yield] was recrystallised from chloroform to give almost clear crystals with sharp melting point [Table 2A.3]. The product was identified by elemental analysis [Table 2A.2] and by its IR spectrum [Fig. 2B.3, Sec. 2B.2.2].

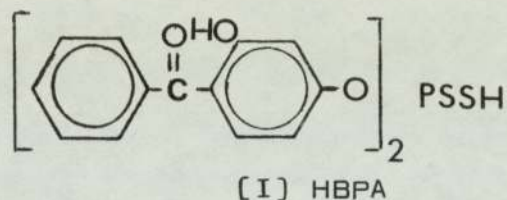
2A.1.5.7 Di-alkyl Thiophosphoryl Disulfide [DRDiS] and 0,0'-Dibutyl Dithiophosphoroate

Di-isopropyl- [DiPDiS] and dibutyl- [DBDiS] thiophosphoryl disulphide were prepared according to literature method^[65] by oxidation of the corresponding acid or its sodium salt. DiPDiS was prepared by addition of excess sodium hypochlorite to the sodium salt of di-isopropyl dithiophosphoric acid at 10^o^[65]. The disulfides were identified by their IR [Fig. 2B.2 and 3, Sec. 2B.2.2] and UV [Fig. 2B.1, Sec. 2B.2.1] spectra. DiPDiS has a melting point of 90-91^o [Table 2A.3].

Dibutyl dithiophosphate ester was prepared according to literature method^[66] and was supplied by Mr P Yick. The IR spectrum of the ester is shown in Fig. 2B.1d, Sec. 2B.2.2.

2A.1.5.8 Di-2-Hydroxybenzophenone Dithiophosphoric Acid
[HBPA]

The observation made in the masterbatch preparation [Sections 5.2.2 and 5.3.3.3] of the possible formation of a stable acid [I] prompted this preparation.



Phosphorous pentasulfide was slowly added with nitrogen bubbling to a vigorously stirred solution of 2-4-dihydroxybenzophenone in toluene. The mixture was refluxed until the solution became clear dark red. The UV-spectrum of the acid is shown in Fig. 5.7c, Sec. 5.2.1.

2A.1.6 Solubility of Stabilisers

Saturated solutions of zinc and nickel complexes [stabilisers] were prepared in different low molecular weight saturated hydrocarbons. The solubility of the complexes were deduced from the absorption spectra of the supernatant liquid [assuming the validity of Lambert Beers' Law].

2A.2 Handling of Polymer Test-Samples

2A.2.1 Processing of Polymers

LDPE and PP were processed in a prototype RAPRA torque-rheometer^[67], which is essentially a small mixing chamber [cavity volume 39 cc], with mixing screws contra-rotating at two different speeds; the high speed [60 r.p.m.] was used for processing.

The mixing chamber was operated either open to the atmosphere [open mixer], or sealed by a pneumatically-operated ram [ram pressure ca. $2.7 \times 10^{-5} \text{ Nm}^{-2}$, i.e. 2.7 atm.] to ensure processing under oxygen deficient conditions [closed mixer]. The polymer charge was calculated using the density values of the polymer. 35 g and 20 g of polymer was used to charge the mixing chamber for processing in a closed and open mixer, respectively. Calculated weights of additives were mixed with the polymer charge to obtain the percentage or concentrations required in the final polymer test film.

(i) Normal Samples [NS]

These contained 2.5×10^{-4} M/100 g [ca. 0.1% of the additive.

(ii) Masterbatch [MB]

These contained 2.5% w/w additive in the appropriate polymer charge. The stabilised polymer was generally processed for 30 minutes in an open mixer [30, OM].

(iii) Diluted Masterbatches (DMB)

Masterbatch preparations were diluted to a final concentration of 0.125%, or occasionally 0.25%, by mixing calculated amounts of stabilised MB polymer sample with the appropriate polymer charge of unstabilised PE in open or closed mixer.

A normal working procedure was adopted to minimize systematic error. The additive/polymer mixture was introduced into the preheated chamber at 150^o and 180^o for LDPE and PP, respectively, with the ram operated in the case of closed mixer operation. At the end of the set processing time, the chamber was opened, and a sample of the polymer melt was collected within the first 20 seconds. This was quenched immediately in cold water. Finally, the stabilised polymer mass was dried, chopped, placed in polyethylene (unstabilised) bag and was kept inside the freezer for subsequent film preparation.

2A.2.2 Film Preparation

Film thickness of approximately 200 μm (ca. 0.008 inch) was compression moulded using a Daniel press with electrically heated plattens. The processed polymer (6 g) was wrapped in layers of cellophane and flattened on a cold press (at room temperature) for 30 s. at (25 ton. in^{-2}). The resulting disc was placed between cellophane sheets (used as mould release agent) and was compression moulded using stainless steel glazing plates. The plattens of the press were maintained at 150^o and 180^o for PE and PP, respectively. Before applying the full pressure, the polymer disc was

preheated for one minute (at zero pressure) to allow for the material to flow and then pressed for 2 minutes at full pressure (35 ton. in⁻²). Immediately thereafter the plattens were cooled to ca. 40° by running cold water while maintaining full pressure. Sections of uniform thickness were selected as test films for ageing and UV-exposure. The remaining sections were stored in the dark inside a deep freezer.

2A.2.3 Extraction of Polymer Films

Test films were normally extracted with toluene (at 55°) or with hexane (at room temperature). The extractability of additives was assessed by UV-spectrophotometry. Complete removal of extractable additives was normally achieved in few hours, after which time the intensity of the characteristic UV absorption of the stabiliser was reduced to zero. Extracted films were subsequently dried in a vacuum oven overnight at room temperature.

2A.3 Accelerated Testing Devices

2A.3.1 Ultra-Violet Exposure Cabinet

The UV-exposure cabinet, Fig. 2A.1 [supplied by Laboratory Thermal Equipments] comprises two concentric cylinders. The outer cylinder (diameter 1.1 m) houses 32 fluorescent tubes: 24 tubes type C (Philips actinic blue 20W/05), and 8 tubes type A1 (20W Westinghouse sunlamp FS20). The tubes are symmetrically arranged on a 3:1 basis. The spectral output of this combination of fluorescent tubes is shown in Fig. 2A.2. The combined light envelope approximates to the solar energy distribution especially in the 280-340 nm region^[68]. Based on previous studies^[69] the intensity of light reaching the sample surface was



Fig.2A.1 UV-exposure cabinet

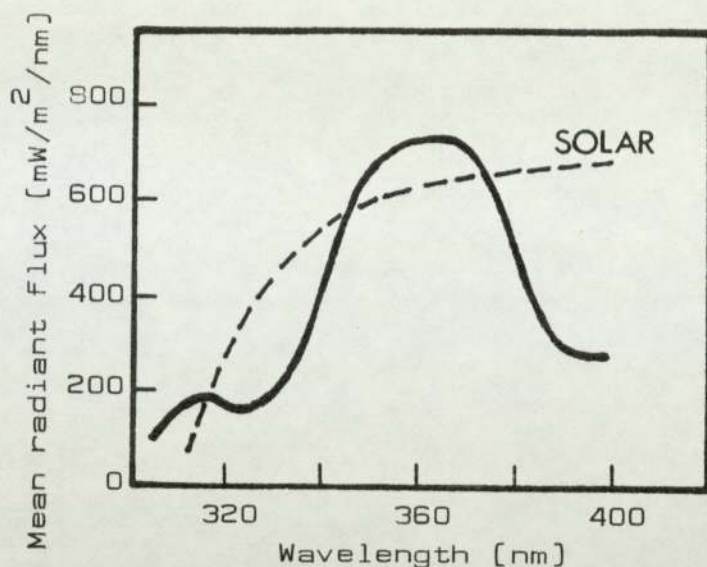


Fig.2A.2 Spectral distribution of 8 'sun lamps' with 24 'Actinic' lamps arranged symmetrically [—] and solar radiation, maximum mid-summer clear sky radiation [----].

assumed to be about 44.3 W.m^{-2} . To maintain a long-term uniform spectral distribution inside the UV-cabinet, fluorescent tubes are replaced sequentially every 200 hours of operation. Exposure times are indicated on a counter clock to the nearest 3.6 seconds.

The inner cylinder is a rotating drum. Samples placed on this drum are 15 cm from the fluorescent tubes. Temperature inside the cabinet is about 30° .

2A.3.2 Heat-Ageing Oven

The heat ageing oven [Wallace] conforms to the British Standards for thermal testing of polymer films. The oven consists of six separate identical compartments, fitted with a temperature control [$\pm 2^{\circ}$]. A constant air flow (in

this case 2.5 cuft. h⁻¹) is maintained in each compartment and is controlled by a universal pressure valve. Test films are inserted in the centre of these compartments which have been maintained at appropriate temperatures (LDPE 110^o, PP 140^o).

2A.4 Monitoring of Oxidation Degradation and Additives in Films and Solutions

2A.4.1 Functional Group Measurements and Infrared (IR) Absorptions of Stabilisers

In general IR absorption regions of oxygen-containing functional groups were routinely followed for light and heat aged films at intervals. Perkin-Elmer grating spectrophotometer model 457 was used for following changes in the polymer films. Perkin-Elmer model 599 was used for kinetics of reactions of CHP and product analysis in chlorobenzene and dodecane.

Evaluation of the degree of degradation (or stabilisation) is based on the extent of carbonyl groups build-up during the course of the reaction. To account for variations in film thicknesses and instrumental errors in intensity measurements, use is made of internal reference bands in LDPE (1895 cm⁻¹) and in PP (905 cm⁻¹) which are unaffected by oxidation. A carbonyl index is, therefore, defined as the ratio of the carbonyl absorption at 1710 cm⁻¹ to the appropriate reference band. The carbonyl absorption at 1710 cm⁻¹, as well as other functional group absorptions, were determined using the base line method^[70].

2A.4.2 Stabiliser Disappearance and Spectral Measurements

UV- and visible absorption spectra of stabilisers in solution or in polymer films were recorded on Unicam SP800 spectrophotometer. The disappearance of different stabilisers under photo-oxidative (in films and in solution) and thermo-oxidative (in films) conditions was followed by monitoring the UV characteristic absorption bands of the stabiliser. Similarly, reactions between hydroperoxides [CHP and TBH] with different metal complexes and their corresponding disulfides, were monitored by spectrophotometry both at fixed wavelengths and continuous scanning over the UV-range.

2A.4.3 Flexural Test

Embrittlement times (EMT) were estimated for UV-exposed and heat-aged films by noting the time required for the film to break when flexed once through 180° by hand. This test can serve as a qualitative guide for the durability of the films; it is a more reliable test for PP than for PE because of the sharp embrittlement times obtained in the case of the former. These tests are useful for comparative purposes within the same set of films and experimental conditions.

2A.4.4 Melt Flow Index (MFI)

Thermal-oxidative stability of unstabilised polymer during processing is markedly effected by the use of suitable melt stabilisers. MFI is inversely proportional to the molecular weight of the polymer. By comparison with the value of the unstabilised polymer (control), a constant MFI value suggests good melt stabilisation.

PP was extruded on a Davenport melt indexer (serial no 985) at 230^o under a load of 2.16 kg and the manufacturer's recommended procedure^[71] was followed, except that a disc with an internal diameter of 0.0465 inch was used instead. The polymer was allowed to extrude for one minute before samples were collected. Samples extruded in 30 seconds were collected and weighed when cold. The average weight of 5 consecutive samples was obtained. MFI values quoted in Sec. 6.2.2 refer to the weight in grammes of polymer collected in 10 minutes.

2A.5 Thermal Decomposition of Cumene Hydroperoxide (CHP)

2A.5.1 Reaction Cell and Experimental Procedure

A specially designed cell (Fig. 2A.3) was used in the study of thermal decomposition reactions of CHP. A slow steady stream of nitrogen was normally allowed to purge the solvent and reactants before and during the course of the reaction. 1 ml samples were normally withdrawn at 5 minutes intervals.

To ensure the complete absence of oxygen in certain experiments (for example, to simulate a closed mixer conditions for processing of polymer samples) several identical reactions were carried out simultaneously under exactly identical conditions. Each of these reactions were sampled only once and thus furnished a single point on the kinetic plot [see for example, curve 2 in Fig. 7.7], Sec. 7.2.2].

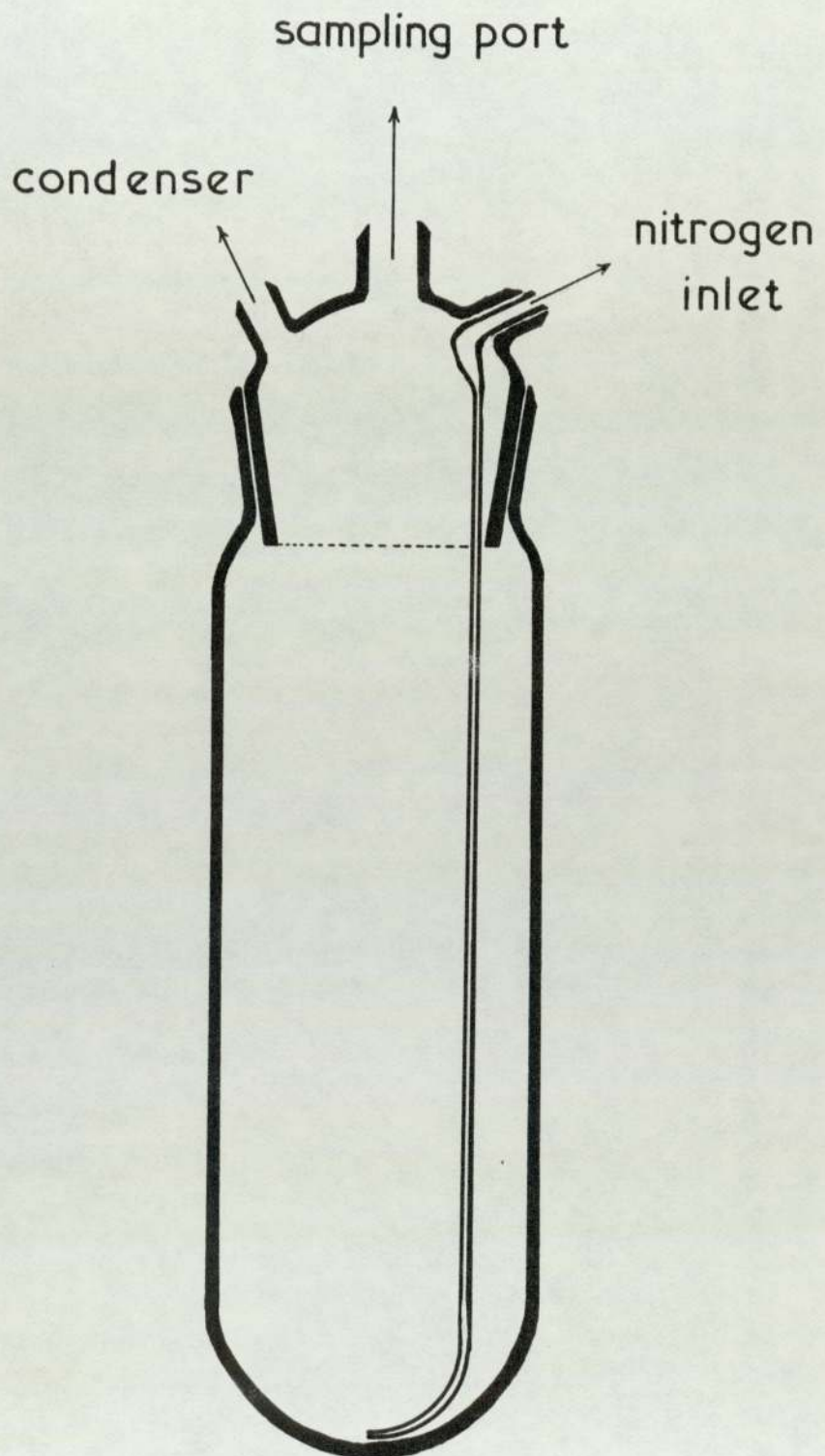


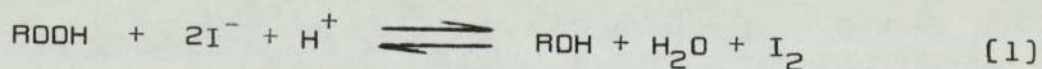
Fig.2A.3 Apparatus for decomposition studies of CHP

In a typical experiment, the reaction cell was placed in a thermostated oil bath ($\pm 0.5^\circ$) for an initial period of 5 minutes. The exact amount of solvents was introduced and allowed a further 5 minutes to attain the bath temperature. A calculated amount of CHP stock solution (prepared in the same solvent) was added and was then followed (after 5 minutes) by the addition of the required amount of the additive stock (prepared in the same solvent) solution. A further 5 minutes was allowed to ensure better mixing before the commencement of the kinetic run.

2A.5.2 Hydroperoxide Determination

Iodometric titration and IR spectrophotometry were used for the determination of hydroperoxides during thermal decomposition in the absence and presence of additives.

The iodometric method^[72,73] is based on the quantitative conversion of iodide ions to iodine by oxidants. Thus, for example, hydroperoxides oxidise [eq. 1] the iodide ions



in an acidic medium, and the amount of iodine liberated is determined by titration with sodium thiosulfate. Dialkyl peroxides interfere with this reaction. However, the rate of conversion of iodide to iodine is slow, and therefore the amount of liberated iodine is assumed to be directly proportional to the hydroperoxide concentration^[72,73].

The following reagents were used for the titration,
20% w/v sodium iodide in isopropanol,
10% v/v acetic acid in isopropanol, and
0.01 N sodium thiosulfate [AR grade].

The thiosulfate solution was prepared in boiled distilled water and stabilised with a few drops of chloroform, and stored in the dark. The titer was determined by titration with a standard 0.1 N iodine solution. The following procedure was used for titration.

To a 25 ml of 10% acetic acid in isopropanol and 10 ml of 20% sodium iodide in isopropanol was added 1 ml of the solution under test. This was refluxed for 5 minutes and allowed to cool for 3 minutes. 10 ml of distilled water was then added and the liberated iodine was titrated against 0.01 N sodium thiosulfate.

Decomposition of CHP was also followed by monitoring the disappearance of the IR-absorption at 3520 cm^{-1} . A variable path liquid cell was used for solvent compensation. A satisfactory correlation was established between the chemical and spectrophotometric methods of analysis for hydroperoxides.

2A.6 Kinetics of Disappearance of the Additive

Rates of disappearance of additives, during their reaction with CHP, were followed by UV-spectrophotometry at 30° and 70° . Typically, a 0.1 cm quartz cuvette was allowed to attain the required temperature (using thermostated cell

block accessory on Unicam SP800] prior to the introduction of 0.3 ml of the appropriate CHP/hexane stock solution. A calculated amount [in microlitres] of an additive stock solution [prepared in the same spectral grade solvent] was then forcibly injected and thoroughly mixed. Changes in the metal-ligand charge-transfer band of the different nickel complexes were monitored at fixed wavelengths: 316 nm [NiDRP and NiRX] and 325 nm [NiDRC]. Except for the case of extremely fast reactions, the initial time of addition and mixing [ca.15 s] was not unacceptable in this study.

In addition to the fixed-wavelength kinetic runs, repetitive scans over the spectral range 450-200 nm were also recorded; the scan time [2 minutes] places an upper limit on the corresponding spectral features of reactants and products within a single scan.

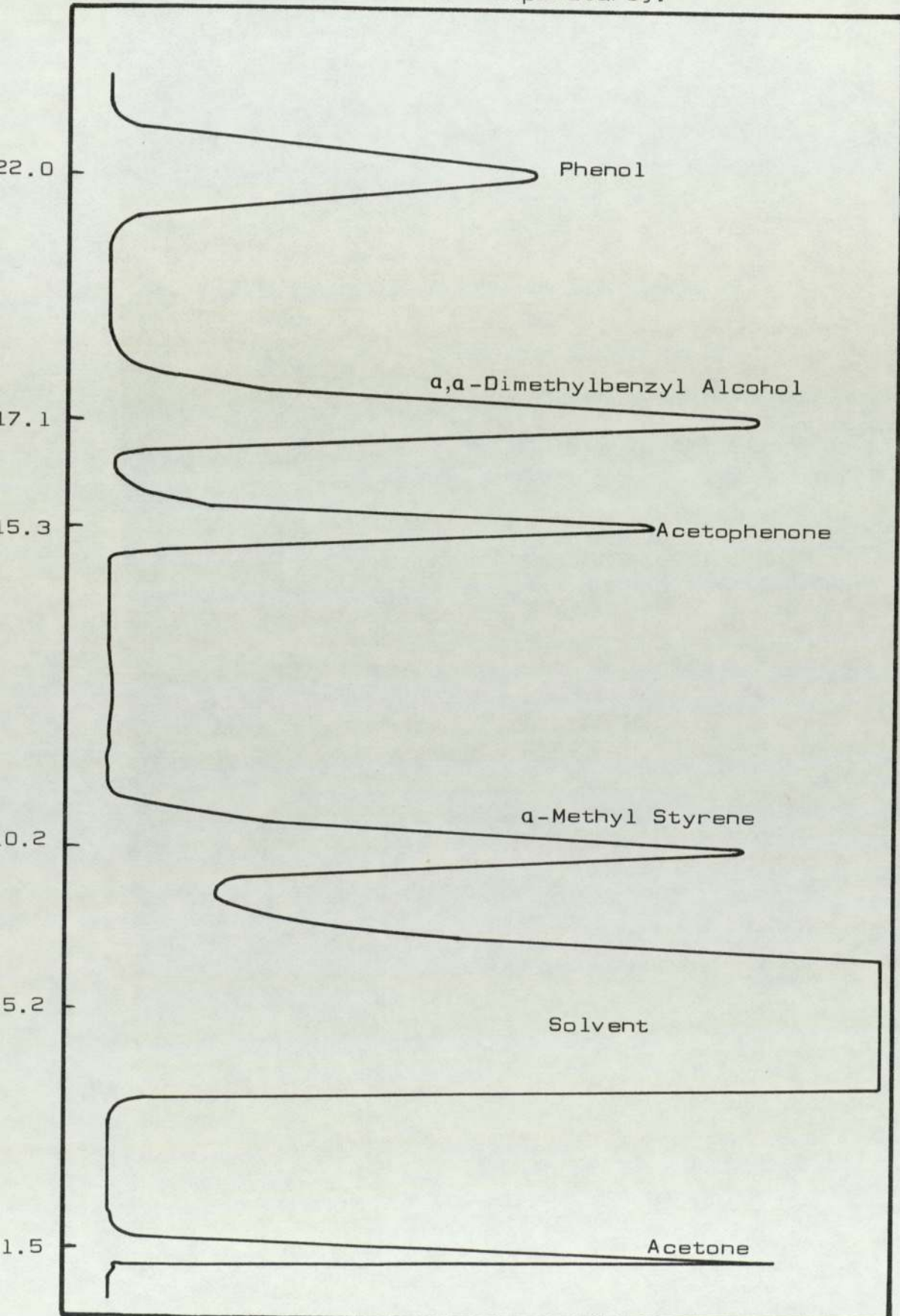
2A.7 Methods used in Product Analysis

2A.7.1 Gas-Liquid Chromatography [GLC]

Products of thermal decomposition of CHP, in the presence and absence of additives, were examined on a Perkin-Elmer chromatograph model F30 using a temperature programme and a flame ionisation detector [FID]. Good separation of the products was achieved on a 2 metre stainless steel column packed with 10% polyethyleneglycol adipate on chromosorb W.

A typical chromatogram is given in Fig.2A.4. In cases where decomposition of hydroperoxides was not complete, or when analysis of the reaction mixture during the induction period was required, the undecomposed hydroperoxide was reduced to α -cumyl alcohol by the addition of excess triphenyl phosphine^[74] to the sample before GLC analysis.

Fig.2A.4 Typical GLC chromatogram of decomposition products of CHP. Products resolved on a stainless steel polyethylene glycol adipate (20% W/W) on chromosorb W, at an initial temperature of 85° (8°/min, and 150° final temperature).



A blank reaction between triphenyl phosphine and CHP was used to generate a calibration curve [Fig.2A.5] and a second curve was obtained to correlate the concentration with the band area for α -cumyl alcohol. In this way any α -cumyl alcohol which is formed via the reduction of triphenyl phosphine can be deducted.

2A.7.2 Thin Layer Chromatography [TLC]

Products of decomposition of CHP in chlorobenzene, in the presence of additives, were detected by TLC. Kiesel gel plates with binder and fluorescein [No F₂₅₄] were used. Separation was effected using benzene as a developer. Products were detected under UV-light [254 nm].

2A.7.3 Infra-Red Spectrophotometry

The formation of phenol, acetone, and acetophenone were confirmed by monitoring absorptions at 3570 cm^{-1} , 1710 cm^{-1} , and 1670 cm^{-1} , respectively. The reaction of CHP in chlorobenzene, in the presence of additives was sampled at intervals. The samples were quenched immediately in liquid nitrogen and were later analysed by IR using a variable-path cell.

2A.7.4 UV-Spectrophotometry

The formation of phenol was followed by UV-spectrophotometry, both at a fixed wavelength [$\lambda = 278\text{ nm}$] and by a continuous scanning, during the course of reaction of CHP with the additives. Because of overlapping absorptions of products, it was difficult to aim at a quantitative assessment of the products of interest.

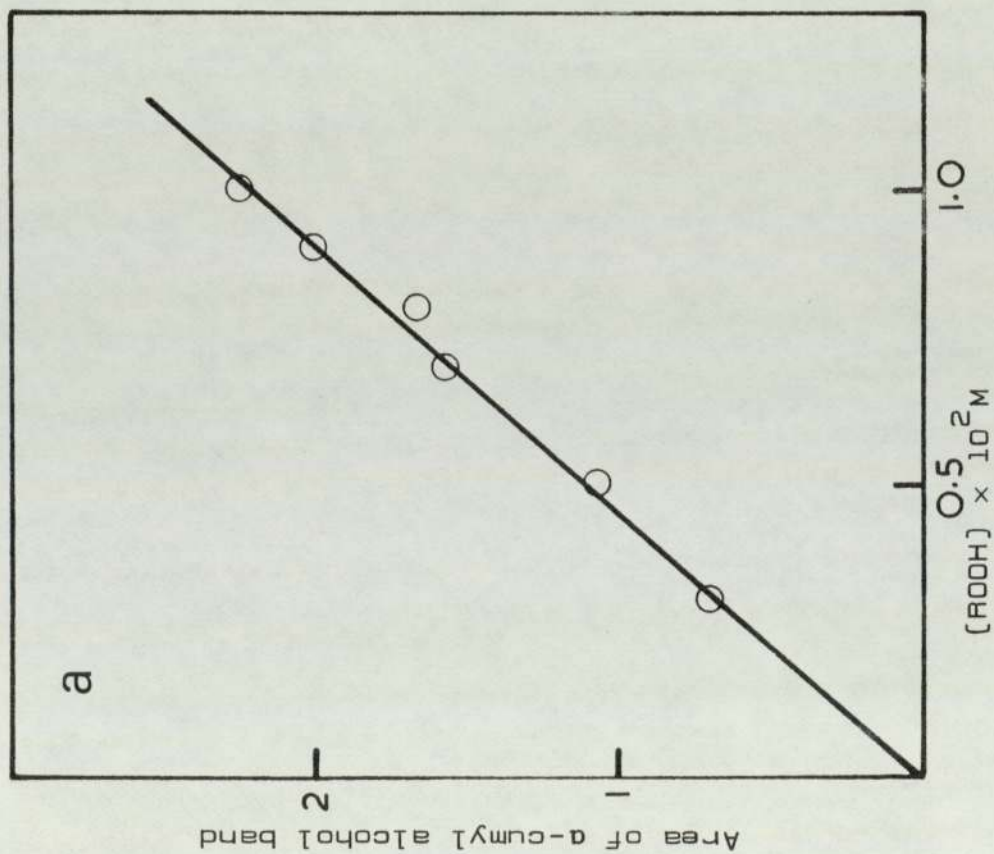
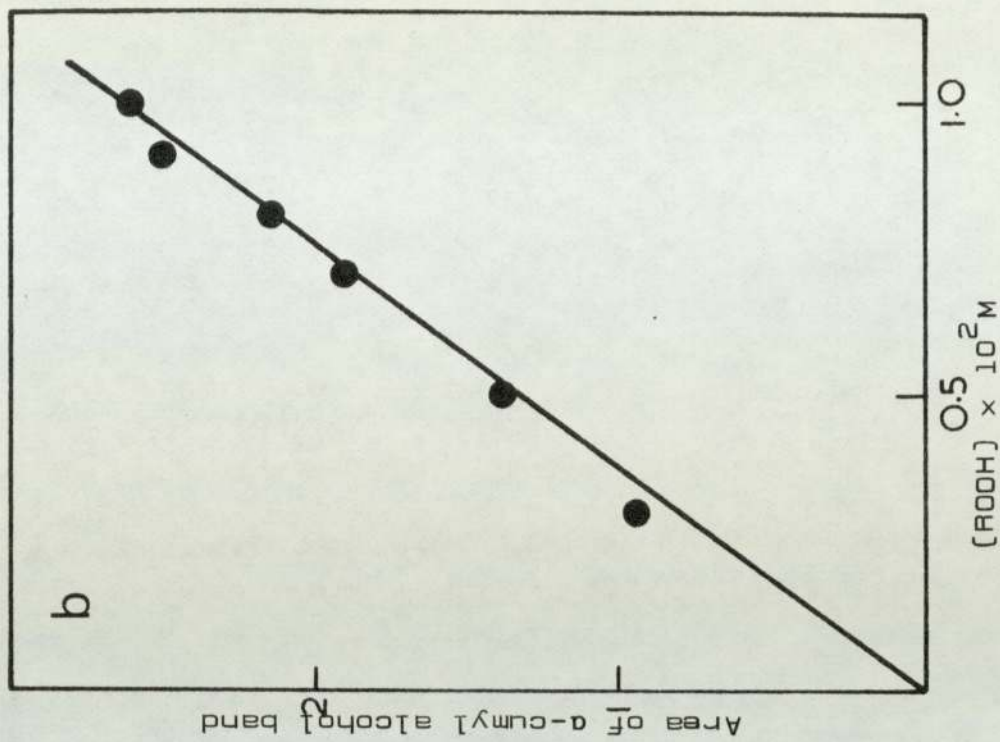


Fig.2A.5 (a) Calibration curve for the yield of α -cumyl alcohol during decomposition of CHP on GLC column.



(b) Calibration curve for the quantitative conversion of CHP to α -cumyl alcohol affected by triphenyl phosphine prior to GLC analysis.

Weight loss measurements were carried out on a Stanton Thermobalance using a fixed temperature program [$8^{\circ}.\text{min}^{-1}$]. Typically, 35mg sample was accurately weighed in a silica crucible and was placed in the furnace. The empty crucible was calibrated under the same conditions used for the samples.

CHAPTER TWO

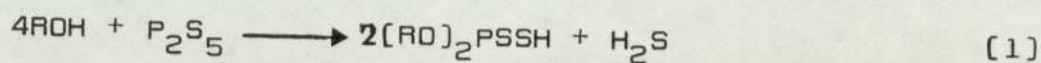
B. PHYSICAL CHARACTERISTICS

OF

DITHIOPHOSPHATES AND XANTHATES

2B.1 General Reactions and Characteristics of
Dithiophosphates and Xanthates

Metal dialkyl dithiophosphates are normally prepared directly by the reaction [reaction 1] of P_2S_5 with the appropriate alcohol via dialkyl dithiophosphoric acid [I], which is rather unstable under the oxidative-hydrolytic action of aqueous reagents on exposure to the atmosphere^[75].



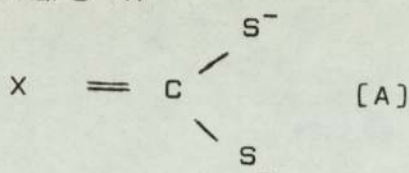
[I]

Scheme 2B.1 shows some of the more important reactions^[76] of dithiophosphoric acid [I]. They suggest that [I] is a highly acidic 'mercaptan'^[77]. Thus it is readily oxidised to disulfides [II], and adds with ease to olefins (irrespective of the presence or absence of peroxides in the olefin). For example, addition of [I], R=ethyl, to 1-octene in the presence of CHP^[77] yields the ester [VII]. The ester [IV] is formed by reaction of the acid [I] with alcohol. Further, transesterification of [I] by a higher boiling alcohol, R'OH, yields^[78] an acid [V] which contains the alkoxy group of the homologous alcohol R'OH (see also Sec. 5.3.3.3). [I] reacts with alkylperoxyl radicals giving rise to a less reactive dithiophosphoryl radical $[RO]_2PSS\cdot$ [VI].^[43] Dithiophosphoric acid [I] is, therefore, an effective inhibitor of hydrocarbon oxidation^[43].

The neutral inner nickel complexes [III] prepared from [I] are more stable than the analogous nickel complexes derived from dithiocarbamic acid $[R_2NCSSH]$, which, in turn,

are more stable than that of xanthic acid [ROCSSH]^[79,80]. This is explained on the basis of the higher acidity of [I], hence the stability of the derived nickel complexes toward acids and toward spontaneous decomposition to sulfides fall in the order^[79], NiDRP > NiDRC > NiRX. The higher stability of MDRP has been associated with the greater extent of S → M π-bonding^[79]. The P-S bond in MDRP ligand is essentially a σ-bond.

Lewis basicity of the sulfur atoms in metal dithiocarbamates has been thoroughly investigated. Resonance structure A



was found^[81a] to be unimportant when X=RO when compared with its contribution for the case X=R₂N. This kind of resonance stabilisation favours, therefore, a greater Lewis basicity in dithiocarbamates. Conversely the acidity of the 1,1-dithio acids is highest in dithiophosphoric acid [I] and least in xanthic acid^[79,81c]

Free xanthic acids [ROCSSH] react readily with metal ions to form water-soluble [alkali-metals] or water-insoluble, strongly coloured complexes of heavy metal xanthates. The latter can be prepared from the former which are themselves the product of the xanthation reaction between carbon disulfide and the appropriate alkoxide^[56b].

Whereas dithiolate ligands appear to stabilise the higher oxidation states of metal ions (e.g. Fe (III) and Co (III) rather than Fe (II) and Co (II), respectively), univalent copper ion is stabilised by xanthates^[56b] and, to a lesser extent, disubstituted dithiocarbamates^[81b]. Cu (I) alkyl xanthate was presumed to be polymeric^[81b] and extremely insoluble in organic solvent in the presence of the lower alkyl homologues (see Sec.2B.6). The reducing action of the xanthate ligand was found to favour, on thermodynamic grounds, the formation of Cu (I) xanthate in both aqueous and non-aqueous media^[82].

2B.2 Optical Characteristics of Metal Dithiophosphates and Related Compounds

2B.2.1 UV-Spectra

Nickel complexes of dialkyl dithiophosphoric acid are highly coloured. The monomeric nature of these complexes has been suggested^[79]. These complexes show^[79] similar spectral characteristics in a wide variety of organic solvents. Solutions containing the dithiophosphate ligand, however, appear^[79] colourless when compared with the yellowish colour noted for the xanthate. The colour of some typical dithiophosphate complexes are given in Table 2A.3 [see Sec. 2A.1.5].

In addition to the d-d and ligand internal transition absorptions, the spectra of nickel dithiophosphates contain intense absorptions which are not found in the spectrum of the free ligand. These have been assigned as charge transfer [$L \rightarrow M$ ^[62], or $M \rightarrow L$ ^[83]] bands. A typical spectrum is shown in Fig. 2B.1. Because of their high extinction coefficient, these bands dominate the UV-absorption spectrum of metal complexes of dithiophosphates and are, therefore, associated with the effectiveness of these complexes as UV stabilisers [see Sec. 4B.2.2]. Relevant spectral data for the various MDRP complexes are given in Table 2B.1.

The charge-transfer band at 316 nm [assigned^[62] as a 3P-3S excitation of sulfur] was used in this study for estimating the post-processing level of the nickel complex, its extractability, and rates of disappearance [see Sec. 4B.2.2]. Because of the lack of UV-absorption for ZnDIP,

Table 2B.1 Spectral Data for NiDRP (R=E,I,B): wavelength maxima (λ_{\max}) and molar extinction coefficient (ϵ). Numbers in parenthesis refer to shoulder.

NiDEP			NiDIP			NiDBP		DiPDIs		
[nm]	[ϵ]	Literature[62]	[nm]	[ϵ]	Literature[66]		[nm]	[ϵ]	[nm]	[ϵ]
		[nm]			[ϵ]	[nm]				
670	-	689 75	670	64	682	62	670	-		
514	-	524 90	514	80	520	80	515	-		
376	-	383 800	379	450	385	700	385	-		
316	18,000	317 16,400	316	19,900	-	-	316	23,780		
[280]	-	[280] 4,000	[280]	3,000	-	-	[280]	-	250	2,700
228	-	228 10,000	230	-	-	-	230	-		

this additive was not investigated to the same extent as the nickel complex. However, the absence of a UV-spectrum was used to advantage by following the disulfide formation during photo-induced decomposition of hydroperoxides by ZnDIP [see Sec. 3.2.3].

Thiophosphoryl disulfides [R=I,B] exhibit weaker UV-absorption [Table 2B.1] compared to the metal complexes, and shows [Fig. 2B.1b] a broad and continuous absorption.

UV-spectra of dibutyl dithiophosphoric acid [I,R=butyl] and dibutyl dithiophosphate ester [IV, R=R'=butyl] are also shown in Fig. 2B.1c and 1d. As mentioned earlier the ligand internal transition appear rather weak and occur roughly in the same region for the acid, ester, and disulfide.

2B.2.2 IR-Spectra

Figures 2B.2 and 2B.3 show KBr-disc IR spectra for dithiophosphoric acid [I], its sodium, nickel, copper and zinc salts, and of dithiophosphoryl disulfide. Throughout these spectra two strong characteristic bands emerge: a P=S stretch [$630-700\text{ cm}^{-1}$] and P-O-C stretch [$970-1020\text{ cm}^{-1}$].

The P=S band was found^[84] to shift its position to higher frequency on going from the acid and transition metal complexes [$630-670\text{ cm}^{-1}$] to the sodium or potassium salts [$690-702\text{ cm}^{-1}$]. This was attributed^[84] to the fact that P=S stretching vibration absorbs at higher frequency in the highly ionic salts than it does in salts having covalent sulfur to metal bond as in the acid and transition metal complexes.

The P-O-C [alkyl] absorption was also used in the identification of these compounds. Furthermore, both P=S and P-O-C stretching vibrations were used to follow changes in the additive polymer during thermal- or photo-oxidation of stabilised polymer films, and following solvent extraction of the stabilised films [see Sec. 4 and 5].

The IR absorption region $970-1020\text{ cm}^{-1}$ was also used successfully in establishing the nature of the alkyl group in the metal complex^[85]. Thus, for example, normal butyl (n-Bu) shows two bands of equal intensity at 972 cm^{-1} and 1012 cm^{-1} due to P-O in P-O-n-Bu stretch [compare these bands with those of the other dithiophosphates, cf. Fig. 2B.2d with 2B.3a; see also Table 2B.2. For normal alkyls, R=hexyl and higher groups, 'attached' to the phosphorous atom, the P-O-C absorption was shown^[85] to occur between 985 cm^{-1} and 997 cm^{-1} . In branched alkyl groups, e.g. R=isopropyl (i-Pr), this absorption occurs at a lower frequency (ca. 970 cm^{-1}); see Fig. 2B.3. Furthermore, in the presence of R=i-Pr, a triplet R-O-P absorption is found in the region of $1100-1200\text{ cm}^{-1}$. The triplet and doublet features of the P-O-C stretch serve, therefore, to distinguish between dithiophosphates derived from primary and secondary alcohols, respectively^[85].

IR absorptions in the region $510-575\text{ cm}^{-1}$ arise from P-S-M stretching vibrations^[85]. The strong absorption around $350-360\text{ cm}^{-1}$, found in the IR spectrum of NiDRP [Figs. 2B.2 and 2B.3], is attributed^[63] to Ni-S stretching vibration.

IR absorptions due to P-S stretch in the case of the disulfides (e.g. DiPDiS, Fig. 2B.3d) occur^[33] at 500 cm^{-1} [strong] and 455 cm^{-1} [medium]. The corresponding positions of the absorptions in the case of the acid^[86] are 541-546 cm^{-1} and 510-530 cm^{-1} , respectively, cf. values in Table 2B.2 for dibutyl dithiophosphoric acid (555 cm^{-1} and 535 cm^{-1}). The observed shift may be due to internal hydrogen bonding^[76].

Table 2B.2 Frequencies of IR vibrations of some dithiophosphates

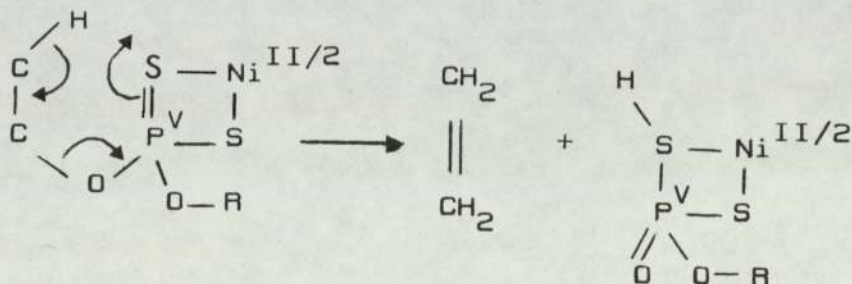
Compound	P-O-C(alkyl) [cm^{-1}]	P=S [cm^{-1}]	P-S-(M,H,S) [cm^{-1}]	Ni-S [cm^{-1}]
Dibutyl Di-thio-phosphoric acid	970, 1020	665	535, 555	-
NaDBP	970, 1020	690	565	-
NiDBP	970, 1020	635	540	360
NiDEP	970	640	540	360
NiDIP	970	635	540	360
ZnDIP	970	650	540	-
CuDIP	970	635	530	-
DiPDiS	970	635	500(S) 455(M)	-

2B.3 Thermal Characteristics of MDRP and Related Compounds

In general, the thermal stability of MDRP is influenced by the chemical properties of the central ion M, the ligand DRP, and their possible interactions. On heating, the crystalline metal complexes may melt, sublime, decompose, or undergo a solid phase transition.

The rate of decomposition of MDRP was found to increase with increasing number of hydrogens on the β -carbon atoms in the alkyl groups, and with decreasing metal cation size^[86] for a series of divalent metals (M=Ni, Cu, Zn). Thermal decomposition at 155^o was proposed^[86] to involve isomerisation and intramolecular [cis] elimination of olefin from the thio-ether isomer (Scheme 2B.2). Olefin elimination may also occur^[63] by transfer of a proton to the sulfur atom in a six-membered cyclic mechanism (Scheme 2B.3).

Scheme 2B.3 Olefin elimination from Ni DIP



In the case of NiDRP, the presence of bulkier R group effects the stability of the Ni-S bond. As a result of crowding about the phosphorus atom, branched chain alkyl groups forces the P-S-Ni angle to increase and thereby induce a strain in the 4-membered P-S-Ni-S ring. For a cyclohexyl substituent group the steric effects appear to be minimum^[63,86,87] and a stable nickel complex is obtained.

Thermogravimetric studies [see Sec. 4A.2.2] on MDRP [M=Ni,Zn] and DiPDiS has indicated that decomposition occurs with no apparent stepwise loss in weight. The relative thermal stabilities of the different metal complexes under atmospheric oxygen will be discussed later [Secs. 4A.2.2 and 4A.3.1]. In general, all the metal complexes of the type MRDP have low melting points, see Sec. 2A.1.5, Table 2A.3.

Solid phase transitions have a special place when dealing with polymers. Heating [during processing] and cooling [after processing, quenching] of a polymer may involve changes in the morphology and crystallisation pattern of the polymer. Of more interest to us here is the effect of cooling the hot stabilised melt [stabilised by a metal complex which is normally crystalline at room temperature]. As polymer crystallization proceeds, the additive will be gradually rejected from the crystalline phases of the polymer and may go to the amorphous phase or may migrate to the surface. This phenomenon is known to be central to all oxidation processes in polymers^[88]. Accumulation of the stabiliser in the amorphous, photo-oxidation sensitive zones will, therefore, render it more protected against oxidation^[22].

2B.4 Optical Characteristics of MRX and Related Compounds

2B.4.1 UV-Spectra

Alkyl xanthates are known to stabilise several oxidation states of metal ions^[81]. Of interest in the present study are complexes of Ni (II), Zn (II) and Cu (I). Apart from the zinc complex, the other complexes are strongly coloured [see Table 2A.3, Sec. 2A.1.5]. Fig. 2B.4a shows the UV-absorption spectrum of nickel xanthate. The spectrum is dominated by an intense charge-transfer band ca. 316 nm, with intra-ligand absorptions occurring at shorter wavelengths [250 nm and 215 nm]. Less intense absorptions (by an order of magnitude) are seen in the visible spectrum of nickel xanthate [Fig. 2B.4a], ZnRX show a charge transfer band ca. 300 nm [Fig. 2B.4b]. Spectral characteristics of the metal complexes of interest are listed in Table 2B.3.

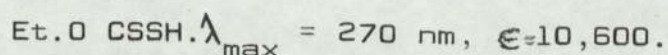
UV-absorption of mildly processed [5,CM] PE film containing NiEX shows an identical absorption spectrum to that in hexane solution. Because of the insoluble nature of Cu(I)RX, no solution absorption spectrum is available for this complex; its spectrum was recorded, however, in Cu(I)EX-stabilised PE-film (intense yellow coloured) and showed 'low-intensity' bands around 400 and 255 nm. Inspection of the film showed no exudation or rejection of the complex from PE during processing and UV-exposure.

Dixanthogens display a continuous absorption spectrum [Fig. 2B.4c and Table 2B.3]. Three bands^[89] are discernable in the spectrum of isopropyl dixanthogen: 365 nm ($n \rightarrow \pi^*$), 285 nm ($\pi - \pi^*$), and 243 nm ($n \rightarrow \sigma^*$).

Table 2B.3 Spectral Data for MAX and IX: wavelength maxima (λ_{max}) and molar extinction coefficients (ϵ)

NiEX			NiBX		ZnEX		ZnIX		IX			
[nm]	[ϵ]	Literature(62)	[nm]	[ϵ]	Literature(89)							
		[nm]									[ϵ]	[nm]
650	-	642 50	650	-	-	-	-	-	-	-	-	-
480	1,450	480 1,500	480	-	-	-	-	-	-	-	-	-
416	2,450	390 1,300	416	-	-	-	-	-	-	-	-	-
316	28,150	316 25,000	316	30,000	300	17,000	300	14,170	365	-	365	11
250	18,770	-	250	-	242	15,000	240	12,720	285	17,400	285	16,218
215	29,000	-	215	-	217	-	-	-	243	25,100	243	23,988

Studies on xanthate decomposition^[90] have been aided by examination of changes in the UV-spectra of alkyl xanthic acid and its salts. Acidification of a xanthate salt ($\lambda_{\text{max}} = 301 \text{ nm}$) results in the formation of free xanthic acid: for example,



The spectrum of the neutral ester, EtOCSSEt , ($\lambda_{\text{max}} = 278 \text{ nm}$, $\epsilon = 11,200$), is almost identical to the analogous acid.

2B.4.2 IR-Spectra

Figures 2B.5 and 2B.6 show KBr disc IR spectra for MRX ($M = \text{Ni, Cu, Zn}$; $R = \text{E, B, I}$). Characteristic absorptions^[91] occur in the regions $1020\text{-}1070 \text{ cm}^{-1}$ [assigned to C=S stretch] and at 1200 cm^{-1} and $1110\text{-}1140 \text{ cm}^{-1}$ [assigned to C-O-C stretch, symmetric and asymmetric, respectively], see also Table 2B.4. It was found^[91] that the weaker absorption in the $1110\text{-}1140 \text{ cm}^{-1}$ region appeared to have variable intensity and is sensitive to the length of the hydrocarbon chain and the nature of the metal centre.

The stronger IR absorption which occurs at 1200 cm^{-1} [in ZnRX] appears to shift^[91] to 1250 cm^{-1} and 1270 cm^{-1} for EX and IX, respectively. This shift is accompanied by a lowering of intensity of the 1110 cm^{-1} band in dixanthogen compared to ZnRX (cf. Figs. 2B.5 and 6). IR-absorptions due to C-S stretch in MRX occurs in the $800\text{-}950 \text{ cm}^{-1}$ region [Figs. 2B.5 and 6, Table 2B.4]. Asymmetric C-S stretch in the C-S-S-C moiety of EX occurs^[89] ca. 850 cm^{-1} [see Fig. 2B.5d].

Table 2B.4 Frequencies of IR vibrations of some xanthates

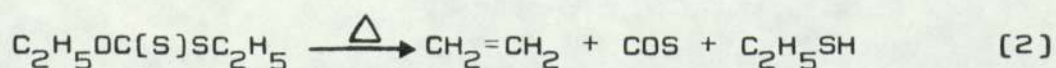
Compound	C-O-C (cm^{-1})	C=S (cm^{-1})	C-S (cm^{-1})
NiEX	1120, 1265	1025	860
CuEX	1120, 1200	1030	870
ZnEX	1120, 1210	1025	865
IX	1150, 1270	1000-1020	900
EX	1120, 1250	1020	850

2B.5 Thermal Characteristics of MRX and Related
Compounds

Free xanthic acids are unstable oils that decompose readily on moderate heating with liberation of carbon disulfide^[90]. Like other dithioacids, they are readily oxidised by air to the corresponding disulfides^[92].

Dixanthogens are characterized^[90] by high boiling points, and low thermal stability. The lower dixanthogens are oils, insoluble in water and are only moderately stable toward heat. Xanthogen monosulfides are^[56c] either low melting point compounds or oils. Pyrolysis of dixanthogens was found^[56d] to yield alkyl carbonate, ROCSOR, and alkyl xanthate esters, ROCSSR.

In general, xanthate esters undergo thermal decomposition which, depending on their structure, occurs in the range 150-250^o^[90]. Olefins and mercaptans were found to be products of pyrolysis^[56d] of xanthate esters [eq. 2].



2B.6 Solubility of Metal Dithiophosphate and Xanthate in Inert Hydrocarbon Solvents

The effect of alkyl group structure on the solubility of metal complexes was found to follow the order $n\text{-Bu} \gg i\text{-Pr} > \text{Et}$. Nickel complexes showed higher solubilities than the corresponding zinc analogues (Table 2B.5). Table 2B.5 compares the solubilities of these additives in several inert hydrocarbon solvents [see Sec. 2A.1.6 for experimental details].

Long linear alkyl chains appear to effect higher solubility in the same hydrocarbon solvent. The critical nature of the length of the alkyl group, however, has recently been demonstrated^[93].

Table 2B.5 Solubilities of metal dithiolates in different solvents

Solvent	Soluble concentration of additive in g/35 g solv.					
	NiDBP	NiDIP	NiDEP	NiEX	ZnEX	ZnIX
Hexane	very soluble	0.081	0.086	0.019	0.0015	0.007
Heptane		0.112	0.084	0.022	0.0018	0.005
Dodecane		0.087	0.071	0.024	0.0015	0.003

It was found^[93] that NiRX is much more soluble in hexane and squalane when $R=C_8H_{17}$ than when $R=C_{18}H_{37}$. It was also found^[93] that the solubility of NiDRC in squalene is much higher when $R=C_8H_{17}$ than when $R=n-C_4H_9$.

The importance of the alkyl group in the case of Cu(I) RX has already been discussed. Ethyl cuprous xanthate is insoluble in all organic solvents at room temperature whereas longer linear alkyl chains showed increased solubility [81b].

The solubility of NiDBP in the various solvents appears exceptional. By comparison with NiDIP, NiDBP appears to be 'infinitely' soluble. On this basis alone, NiDBP is obviously the additive of choice since greater solubility in PE and PP would be expected.

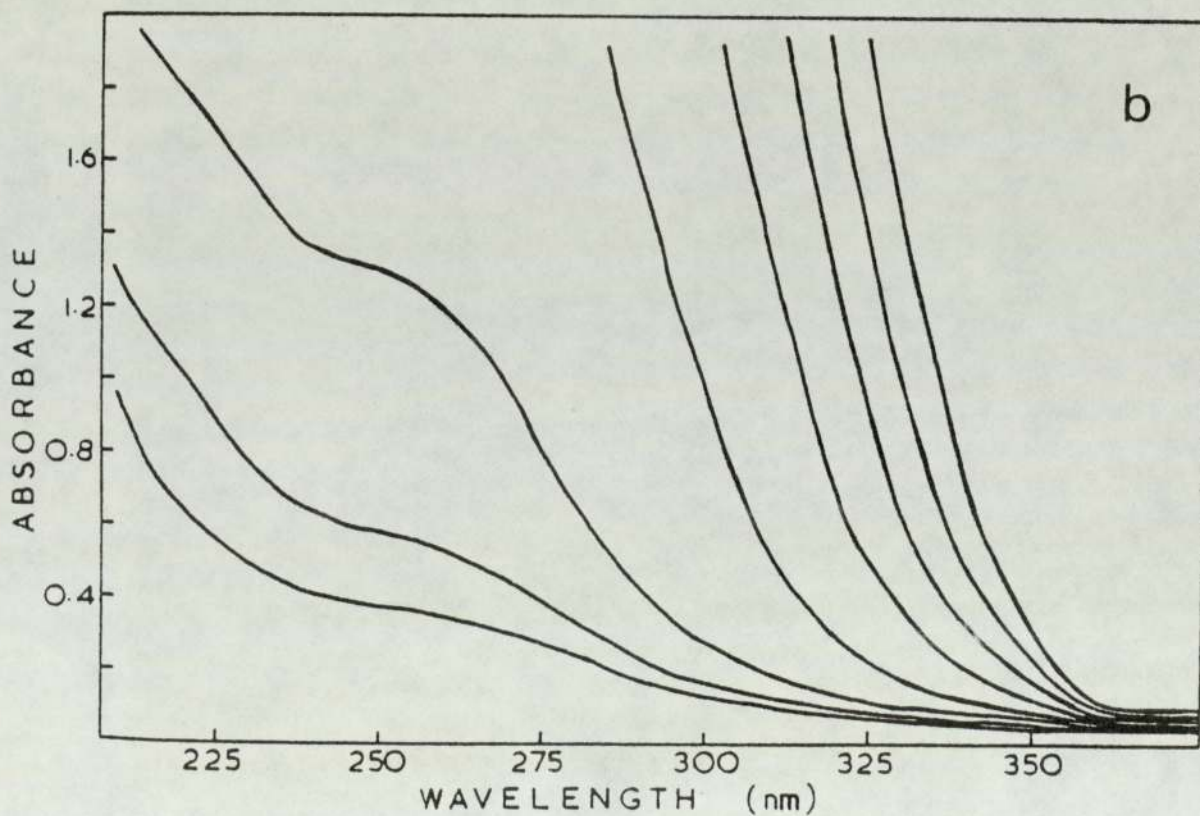
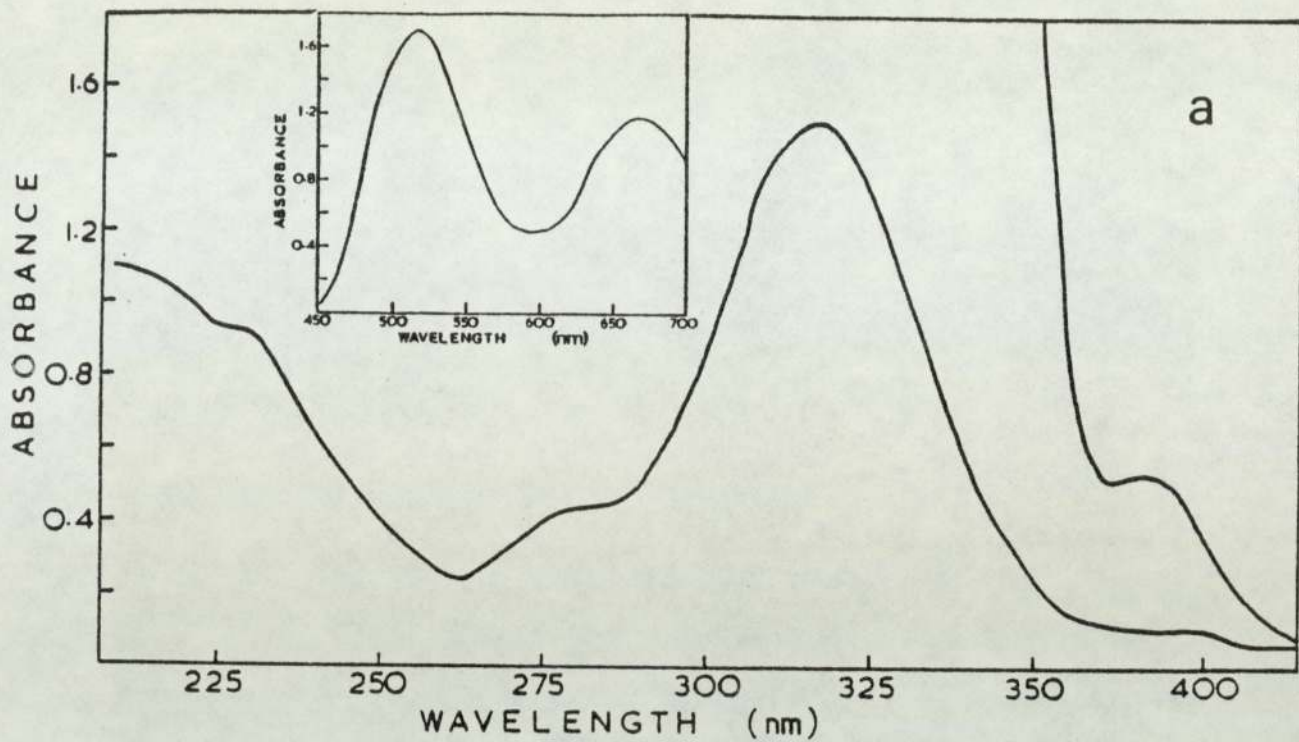


Fig.2B.1 UV-absorption spectra of NiDBP [a] and DiPDiS [b] in hexane and the absorption of NiDBP in the visible region [inset]. Absorptions at higher concentrations are also shown.



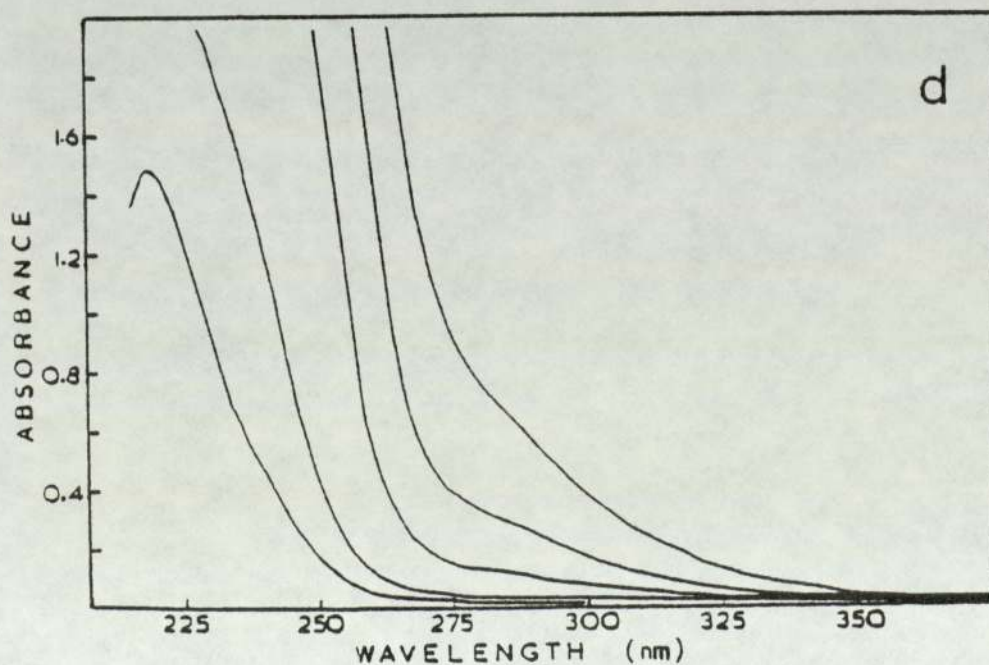
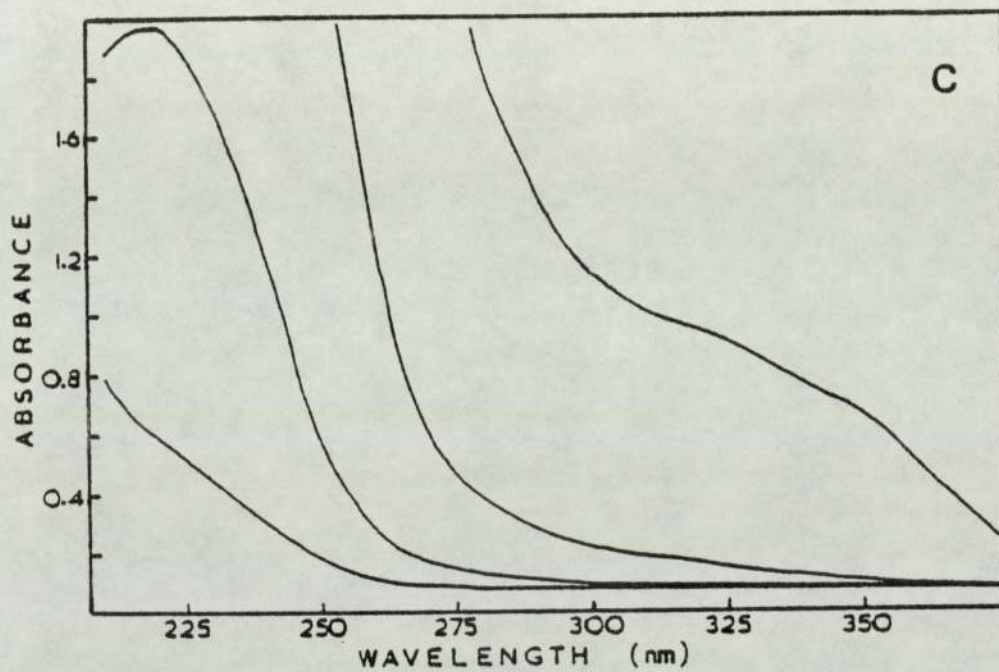
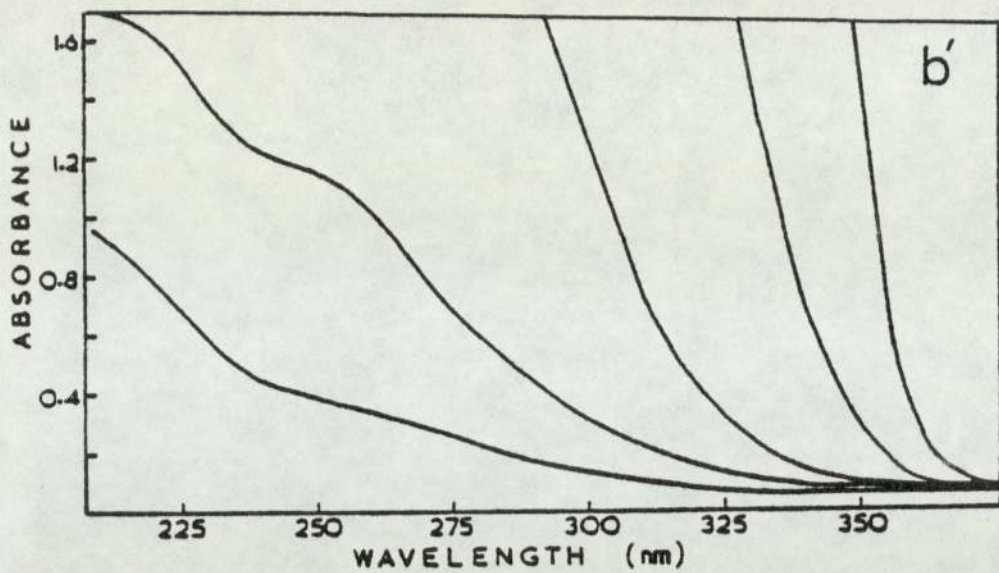


Fig.2B.1(cont)UV-absorption spectra of dibutyl thiophosphoryl disulfide (b'), dibutyl dithiophosphoric acid (c), and dibutyl dithiophosphoroate (d) in hexane. Absorptions at higher concentrations are also shown.

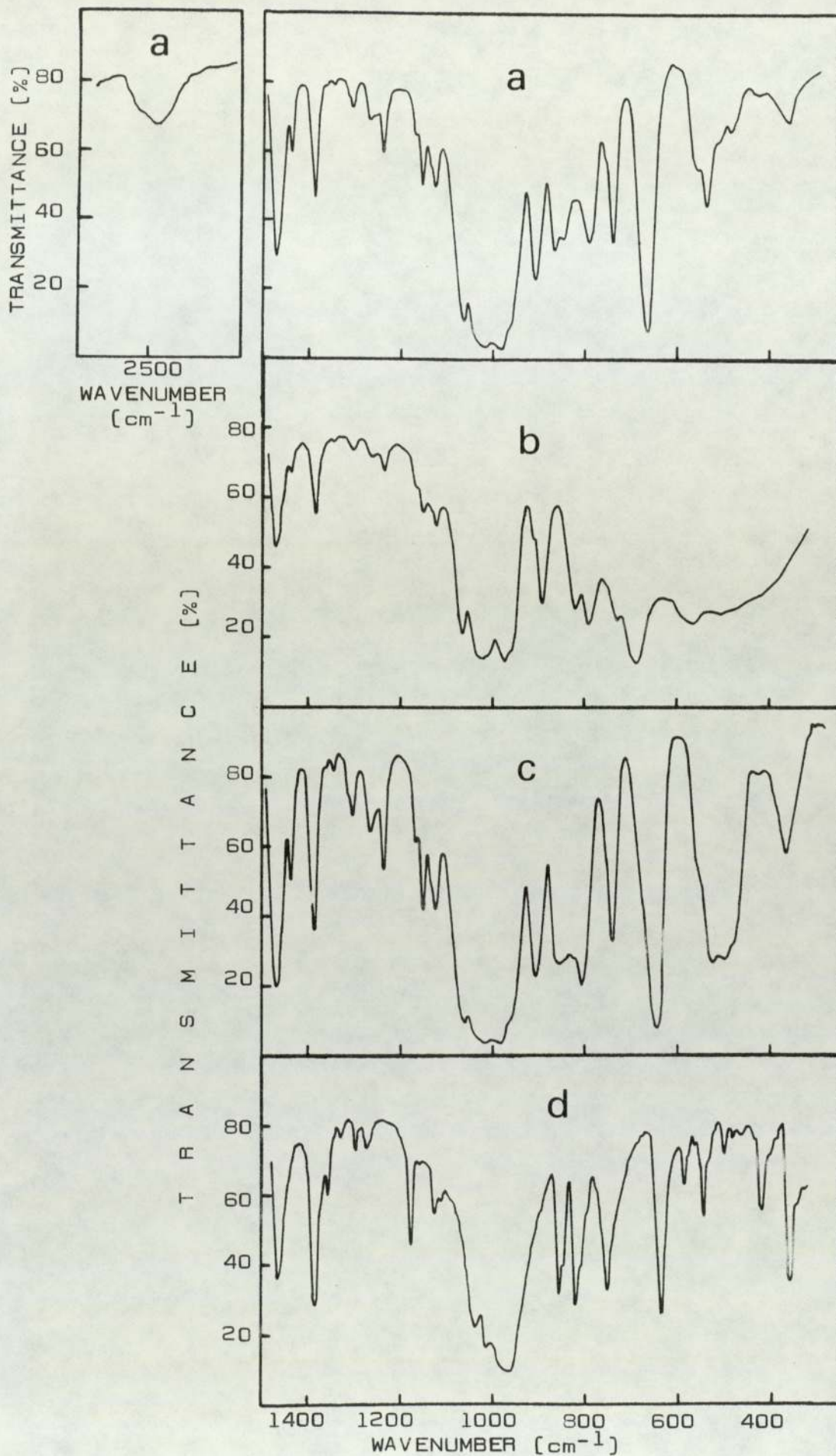


Fig.2B.2 Infrared spectra of dibutyl dithiophosphoric acid (a), its sodium salt (b), its disulfide (c), and its nickel salt (d).

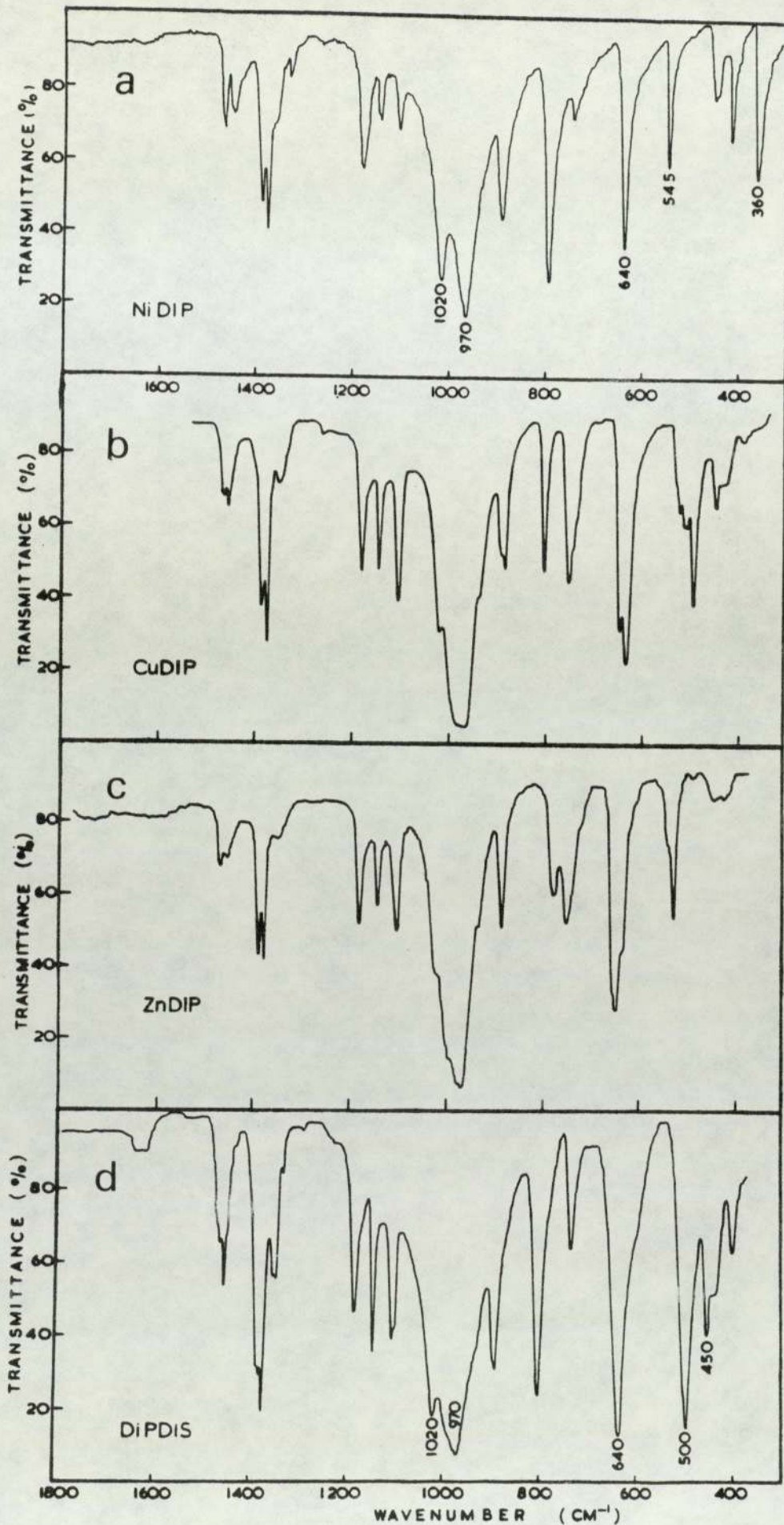


Fig.2B.3 Infrared spectra of metal dithiophosphates and DiPDiS (ca.1%) in a KBr pellet.

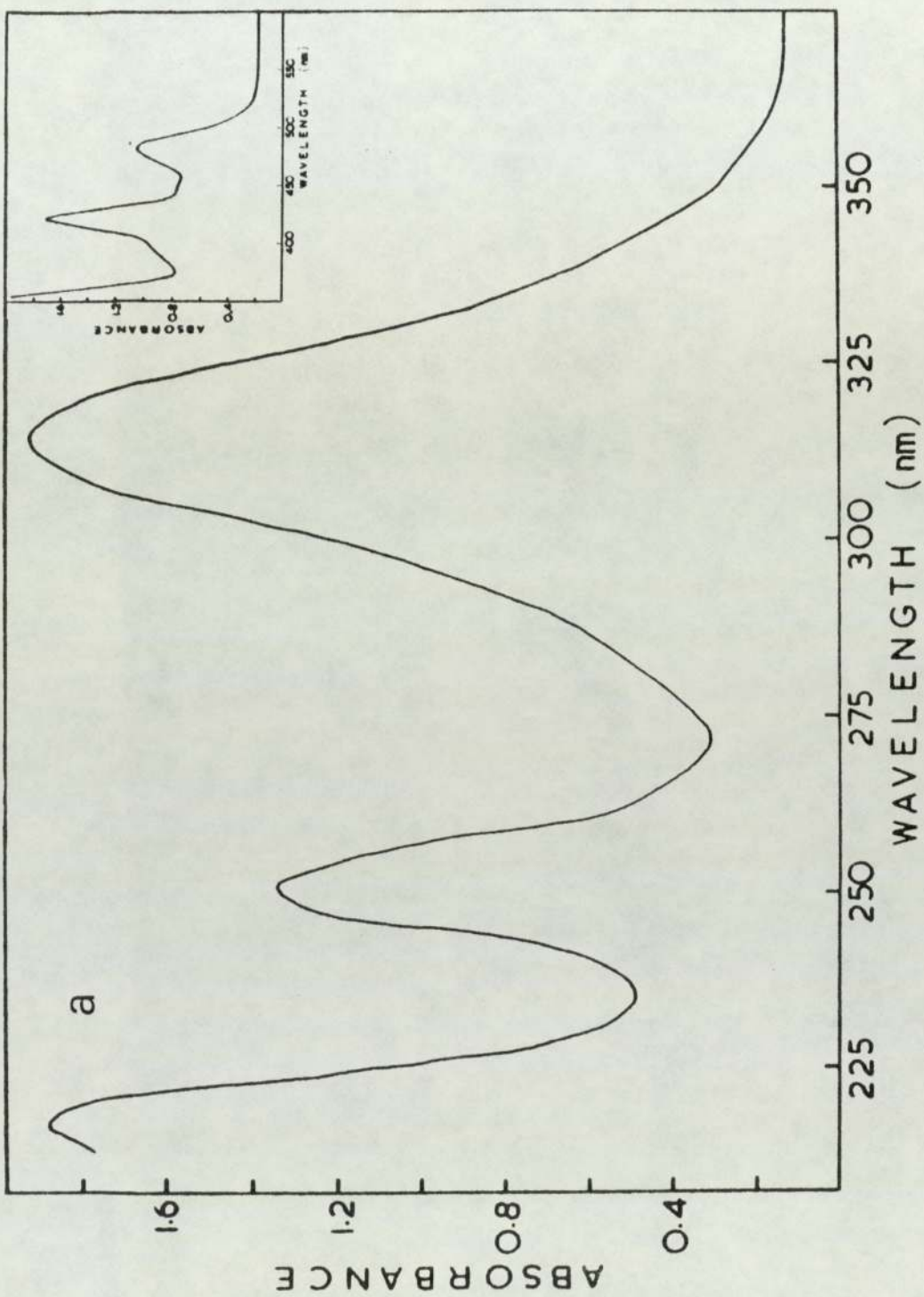


Fig.2B.4a UV- and visible [inset] absorption spectra of NiBX in hexane.

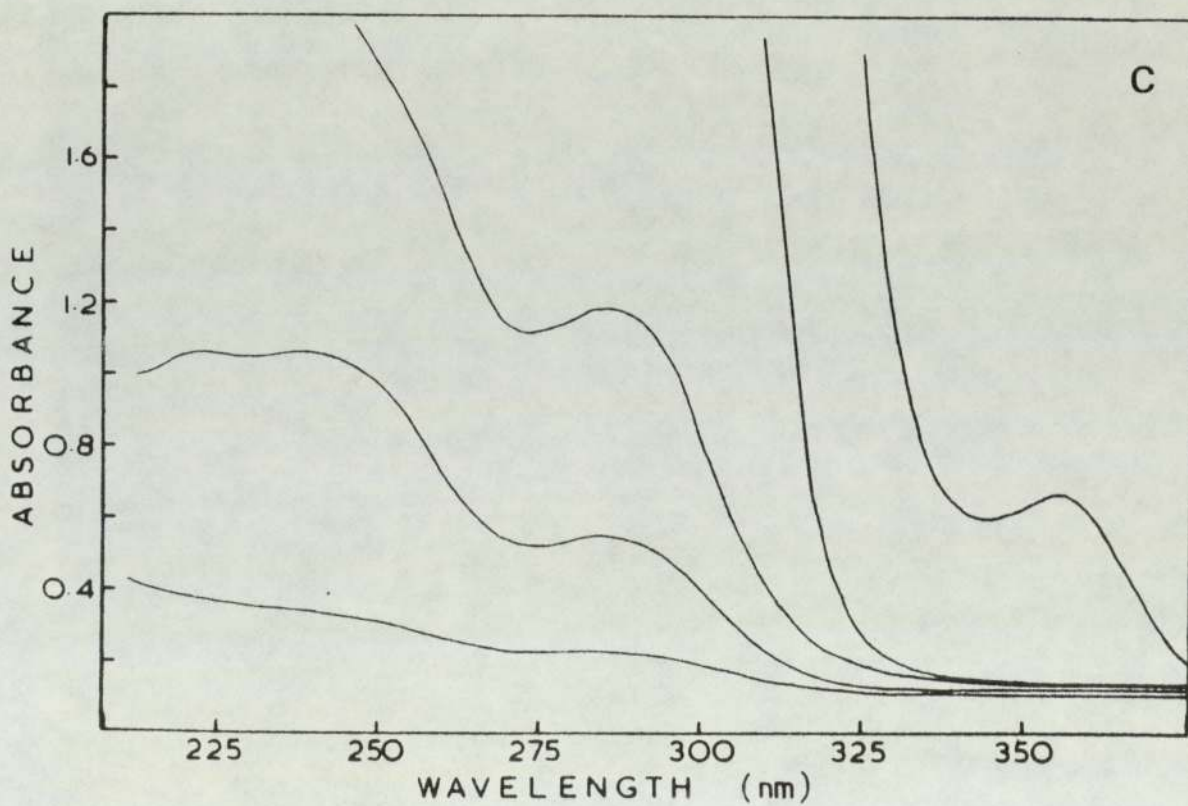
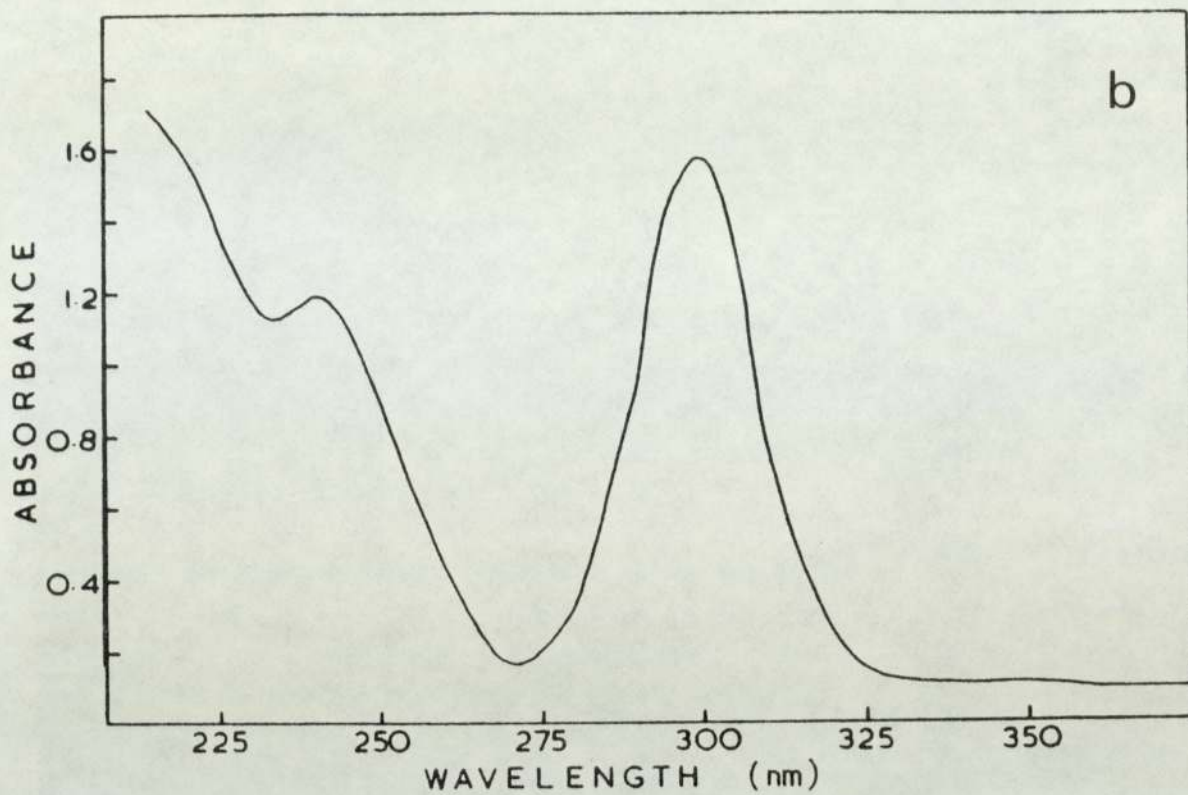


Fig.2B.4 UV-absorption spectra of ZnIX [b] and IX [c] in hexane. Absorptions at higher concentrations of IX are also shown.

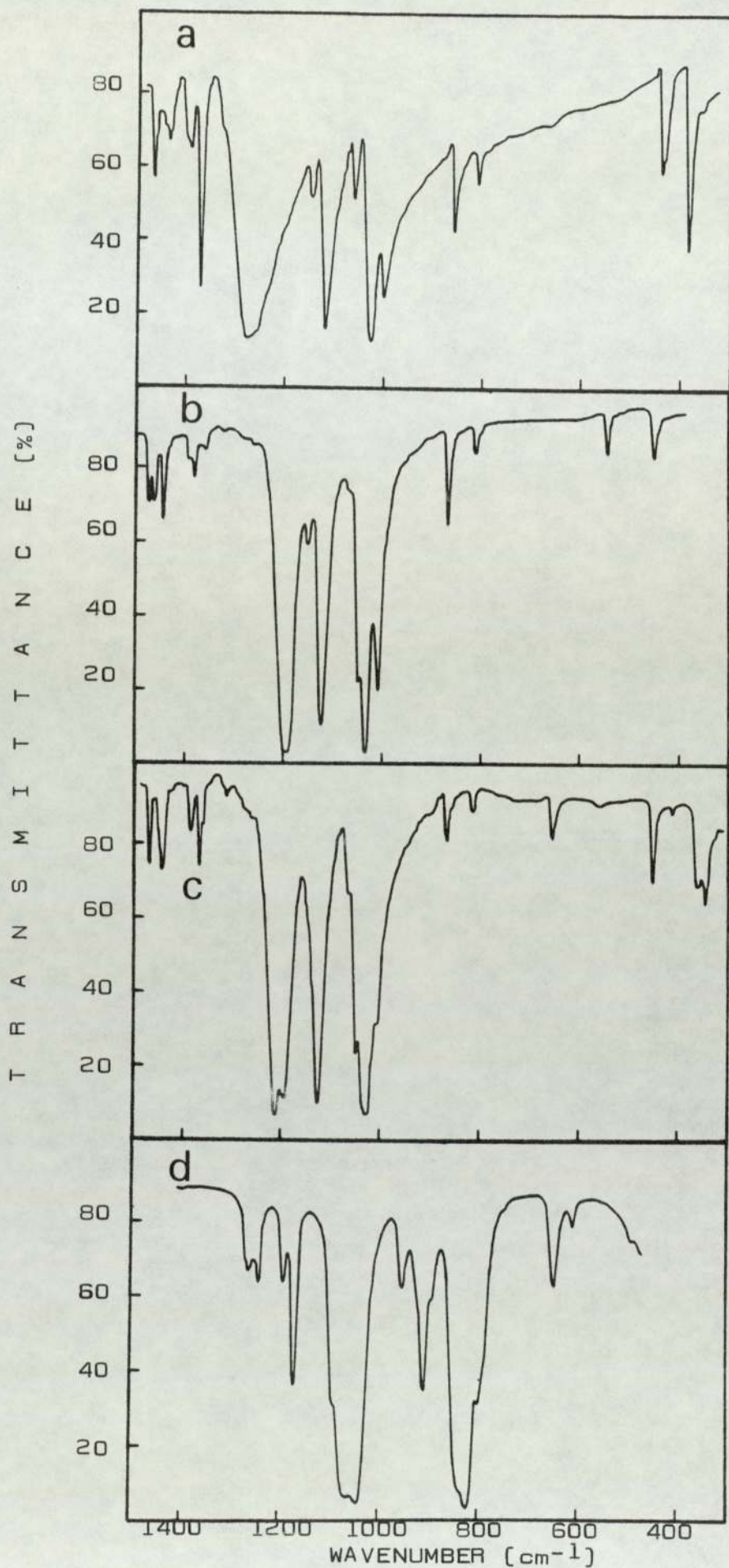


Fig.2B.5 Infrared spectra of [a] NiEX; [b] CuEX; [c] ZnEX; [d] EX. [ca.1%] in KBr pellet.

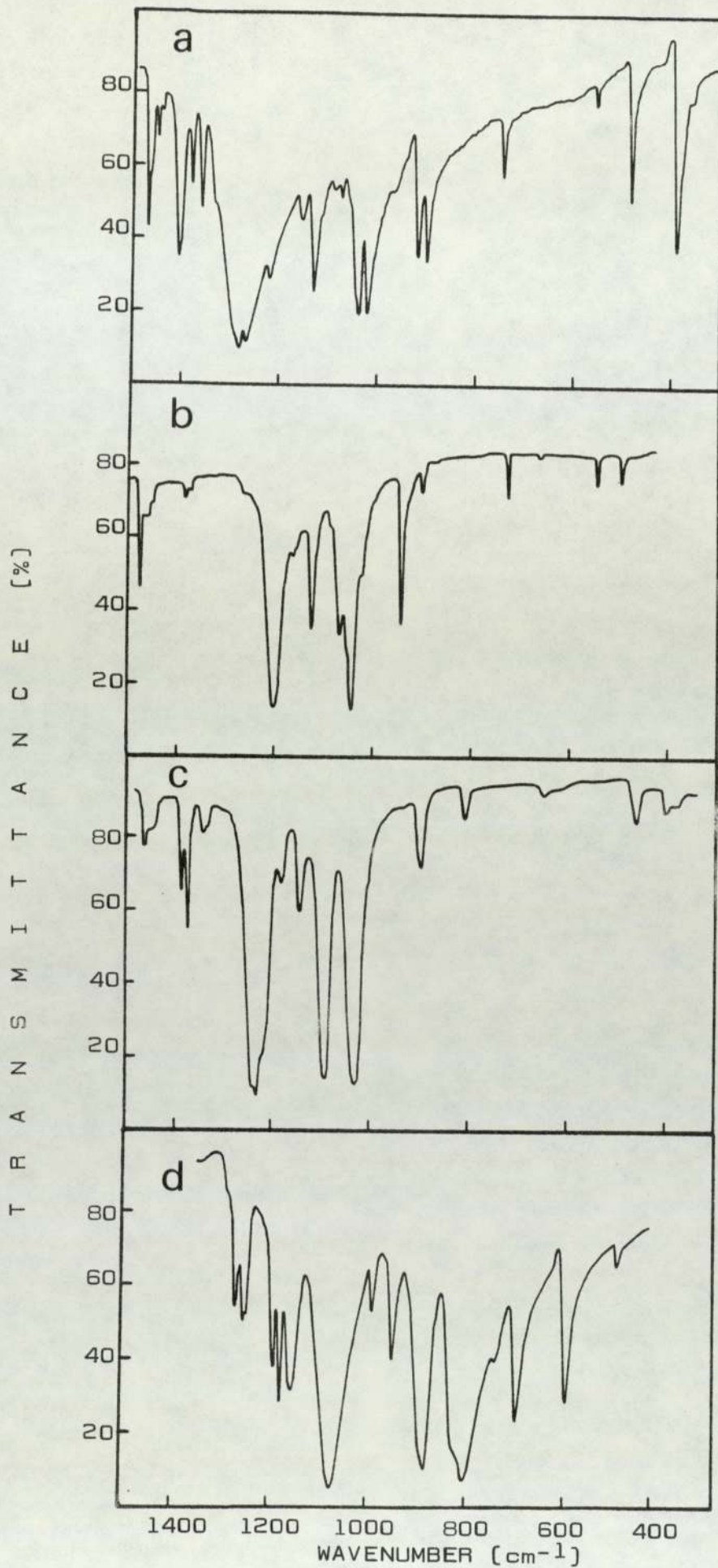


Fig.2B.6 Infrared spectra of (a) NiBX; (b) CuBX; (c) ZnIX; (d) IX. (ca.1%) in KBr pellet.

CHAPTER THREE

PHOTO- AND HYDROPEROXIDE-INDUCED DECOMPOSITION

OF

METAL COMPLEXES AND DISULFIDES

IN SOLUTION

3.1 OBJECT

In this chapter the photolytic stability of metal complexes of xanthic acid, MRX (M= Ni(II), Zn(II); R= E,B), and dithiophosphoric acid, MDRP (M= Ni(II), Zn(II); R= I,B), is examined in different solvents. Dixanthogen, RX (R= E,I), and di-isopropyl thiophosphoryl disulfide DiPDiS, are similarly studied. Solutions prepared from the above compounds are exposed in the UV-cabinet, and UV-spectrophotometry is used to follow changes in the absorption spectra of the photolyzate at specified intervals. The effect of the different solvents on these changes is also investigated. Rates of photolysis of the above metal complexes and their corresponding disulfides are calculated from these measurements at room temperature. Hydroperoxide (TBH) initiated reactions with the different metal complexes, and the corresponding disulfides in the presence and absence of light, are also investigated. Kinetic and spectral information obtained from these reactions are compared with hydroperoxide-free photo-initiated reactions. All photolyses are conducted in the presence of air.

3.2 RESULTS

3.2.1 Effect of UV-Light on MRX and RX

3.2.1.1 NiRX and RX

Time-dependent UV-spectra for the photolysis of NiEX [5.6×10^{-4} M] in hexane showed isobestic behaviour [Fig. 3.1] around 285 nm and 263 nm. New absorption [weak] features were formed with [apparent] maxima ca. 275 nm and 235 nm [Fig. 3.1]. The new bands are similarly effected by UV-light and disappear upon further photolysis. Kinetic plots for the disappearance of the parent complex band at 316 nm and the rate of appearance of the new absorption feature at 275 nm are shown in Fig. 3.2. In hexane, and at the same molar concentration [5.6×10^{-4} M], NiBX displays similar kinetic plots for the 316 nm and 275 nm of NiEX in hexane and cyclohexane [Fig. 3.3] indicate greater photostability in the former solvent. At a molar concentration of 5.8×10^{-5} , the lifetime of the metal complex in hexane and in cyclohexane is 55 h and 30 h, respectively.

UV-photolysis of isopropyl dixanthogen [IX] in hexane effects a systematic reduction in the intensity of the dixanthogen absorption [Fig. 3.4]. Decay of the 285 nm band follow first order kinetics with rate constant $k = 2 \times 10^{-4} \text{ s}^{-1}$ [curve 1 in Fig. 3.5]. Ethyl dixanthogen [EX] is similarly effected by UV-light.

3.2.1.2 ZnRX

Photolysis of ZnEX [5.6×10^{-5} M] in hexane and cyclohexane solutions appeared [see Fig. 3.6] to proceed faster in hexane. [cf. 12 hours in hexane and 17 hours in cyclohexane]. The gradual decrease in the intensity of the UV-absorption spectrum of ZnEX [Fig. 3.7] is accompanied by the emergence of an absorption feature centred around 275 nm. Further photolysis of the solution results in the disappearance of this new absorption.

3.2.2 Reactions of TBH with NiRX and RX at room temperature in the presence and absence of UV-Light

The relatively fast reaction of NiBX in the presence of TBH at room temperature was studied. Figure 3.8 shows a continuous scan for a reaction conducted in hexane in which the ratio NiBX : TBH is 1 : 100 ([TBH] = 0.5×10^{-2} M). The disappearance of the 316 nm band was accompanied by the appearance of new absorptions around 285 nm and 243 nm. Figure 3.8 (inset) shows the spectrum of the final product from this reaction. Fig. 3.9 shows this same reaction at double the concentrations of each reactant while keeping the same molar ratio [TBH at 1×10^{-2} M]. The increase in the intensity of the spectral features which occur in the region of the two windows [ca. 275 and 236 nm] of the parent metal complex is very clear [see Fig. 3.9]. The similarity of these spectral features with those obtained during the photolysis of NiRX [in the absence of TBH, see Fig. 3.1] is striking. Figure 3.9 (inset) shows the UV-spectra of the reaction mixture at the beginning of the reaction [curve 0]

and after the consumption of the nickel complex [curve 48], i.e. UV-absorption of the reaction product. Based on these results the yield of the new product, which is identified as dixanthogen, [see Fig. 3.4 for the spectrum of dixanthogen] is ca. 30%. The product formed from the reaction of NiBX with TBH at room temperature was found to be unaffected by the undecomposed TBH [Fig. 3.8]. The amount of undecomposed TBH can be obtained qualitatively from the intensity of the 215 nm band after complete disappearance of the nickel complex.

The reaction at room temperature between IX and TBH at a molar ratio of 1 : 100 ($[TBH] = 0.5 \times 10^{-2} M$) revealed [Fig. 3.10] an extremely slow reaction. No appreciable spectral change was observed over a period of 12 hours. On the other hand, a photoinduced reaction between IX and TBH at the same molar ratio of 1 : 100 ($[TBH] = 0.5 \times 10^{-2} M$) revealed a fast disappearance of the dixanthogen. The decay of the 285 nm band was found to follow first order kinetics [curve 2 in Fig. 3.5], with rate constant $k = 1.3 \times 10^{-3} s^{-1}$. When the reaction of NiBX with TBH (at a molar ratio of 1 : 100 with $[TBH] = 0.5 \times 10^{-2} M$) was photo-initiated, the metal complex was found to be consumed within 100 minutes. [cf. 720 minutes in the absence of UV-light].

Products obtained from the reaction of NiBX with TBH, in the presence and absence of UV-light, were very similar [Fig. 3.8 is an example]. The kinetics of disappearance of the 316 nm band of NiBX during its reaction with TBH at room temperature and at a 1 : 100 molar ratio ($[TBH] = 0.5 \times 10^{-2} M$), in the absence ($k = 2.0 \times 10^{-5} s^{-1}$) and presence ($k = 1.1 \times 10^{-4} s^{-1}$) of UV-light, is compared in Fig. 3.11. The photo-initiated reaction is about six times faster.

The photolysis of NiDBP was found to proceed faster in more oxidisable solvents. The kinetics of disappearance of NiDBP (7.0×10^{-5} M) in hexane, cyclohexane, and propan-2-ol [Fig. 3.12] which was followed by monitoring the changes in the 316 nm band of the metal complex, agrees with the order of oxidisability of the solvents: propan-2-ol > cyclohexane > hexane^[94]. Following UV-exposure of NiDBP in hexane, an overall intensification of the spectrum was found to occur in the region 275-250 nm. Fig. 3.12 [inset] compares the photostability of NiDBP and NiBX in hexane at the same molar concentration of 4.0×10^{-4} .

The reaction, at room temperature, between NiDIP and TBH in hexane at a molar ratio of 1 : 100 ($[TBH] = 1 \times 10^{-2}$ M) was followed by continuous scan of the UV-absorption spectra of the metal complex [Fig. 3.13]. The decay of the 316 nm band of the metal complex follows first order kinetics with rate constant $k = 1.3 \times 10^{-4} \text{ s}^{-1}$ [curve 1 in Fig. 3.14]. Figure 3.13 [inset] shows UV-spectra of the reactants [curve 0] at the time of mixing [reaction time $t = 0$], and of the products [curve 3.5] when the metal complex was fully consumed, i.e. $t = 3.5$ h [compare with 24 h for NiBX at the same molar concentration] after which time no further change occurred in the UV-spectrum. The new spectral absorption feature of the product obtained from the reaction of NiDIP with TBH was found to be the same whether the reaction was initiated by UV-light or not. In the presence of light, however, the reaction [Fig. 3.15] was found to occur at a much faster rate [$k = 1.03 \times 10^{-3} \text{ s}^{-1}$] [curve 2 in Fig. 3.14];

this is about eight times faster than in the absence of light (curve 1 in Fig. 3.14).

The reaction of DiPDiS with TBH, at room temperature, at molar ratio 1 : 100, $[TBH = 1 \times 10^{-2} \text{ M}]$, was extremely slow; no change in the spectral features of DiPDiS occurred over a period of 10 h. However, in the presence of UV-light, the reaction of DiPDiS with TBH is very fast; a new broad absorption feature emerged (Fig. 3.15) with a band maximum around 260 nm, and a minimum (window) around 250 nm. The position of the window (Fig. 3.16) falls within the wavelength region of the absorption maximum of DiPDiS itself. UV-photolysis of an authentic sample of DiPDiS in hexane effected a similar change in the spectrum of DiPDiS, i.e. gave a new absorption maximum around 260 nm and a window around 250 nm. Further photolysis of the solution led to the disappearance of this new spectral feature. If, however, photolysis is discontinued, in the absence or presence of TBH, this new spectral feature remains unaltered even after 12 hours (see inset of Fig. 3.16). The reaction of NiDIP with TBH, in the presence and absence of UV-light, produced exactly the same spectral feature (maximum at 260 nm and minimum at 250 nm) (Figs. 3.15, 3.13 (inset), and 3.17).

In contrast to the other metal $[M=Ni,Zn]$ dithiolates, ZnDIP does not absorb above 225 nm. The reaction of ZnDIP with TBH at room temperature, therefore, affords a unique system since absorbing reaction products can be examined by following their UV-absorptions.

3.3 DISCUSSION

3.3.1 Effect of Light and Hydroperoxide on NiRX and RX

Nickel xanthates are photolytically more stable than the corresponding dixanthogens. It was shown that during photolysis of hexane solution, the rate of disappearance of both the 316 nm band of NiRX, and the 285 nm band of RX, follow first order kinetics. However, the rate of disappearance of NiEX [$k = 2.9 \times 10^{-6} \text{ s}^{-1}$, see curve 1 in Fig. 3.2] is about 68 times slower than isopropyl dixanthogen [$k = 2 \times 10^{-4} \text{ s}^{-1}$, see curve 1 in Fig. 3.5].

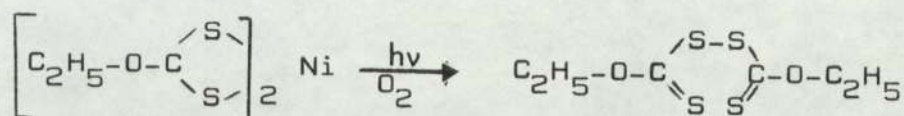
Photolysis of related classes of dithiolates [ZnDIP^[43] and FeDBC^[95]] have indicated the formation of disulfides [i.e. DiPDiS and TBTD, respectively]. By analogy, the new features obtained from the photolysis of NiEX and NiBX examined here were ascribed to diethyl and dibutyl dixanthogen [RX]. The UV-absorption characteristics of RX are shown in Table 3.1.

Table 3.1 Spectral data for dixanthogen RX^[90];
wavelength [nm] and molar extraction coefficient [ϵ]

R	λ_{max} [ϵ]	λ_{max} [ϵ]	λ_{max} [ϵ]
CH ₃	240 [19,950]	278 [7,943]	351 [79]
i-C ₃ H ₇ ^[a]	243 [23,990]	285 [16,220]	365 [10]
n-C ₄ H ₉	244 [23,990]	286 [8,318]	365 [81]

[a] Values calculated from this work are 285 [11,600],
243 [26,000]

Based on these data, the dixanthogen yield from the above photolysis of NiEX [see Figs. 3.1 and 3.2], relative to the initial concentration of the nickel complex was around 7%:

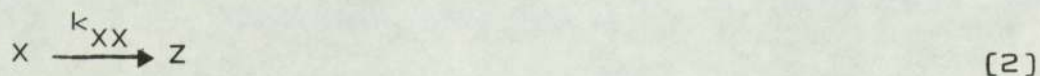
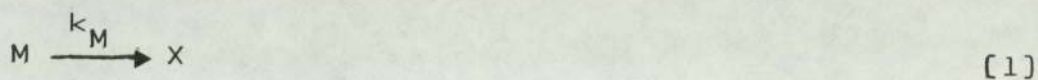


The possibility of the formation of free ethyl xanthic acid and diethyl xanthate $[\text{C}_2\text{H}_5\text{OCSSC}_2\text{H}_5]$ were also considered. Abstraction of a hydrogen to yield the ethyl xanthic acid is feasible. This was not, however, corroborated from the spectral results obtained which indicates the formation of disulfides. Although diethyl xanthate^[90] exhibits UV-absorptions,

$$\lambda_{\text{max}} [\epsilon] : 223 [7,080], 280 [11,200], 354 [52.4],$$

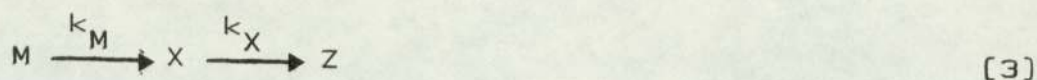
which are apparently similar to the spectrum of dixanthogen, examination of the spectrum [Fig. 3.4] and Table 3.1, however, reveal differences in both the intensity of the bands and their position.

Under the influence of UV-light and oxygen at room temperature photolysis rates of M [eq. 1] and X [eq. 2] shows that k_M is less than k_{XX} [cf. Figs. 3.2 with 3.5].

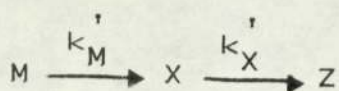


where M is the metal complex disappearing with a rate constant k_M , X is the disulfide disappearing with a rate constant k_{XX} [for an authentic sample of disulphide], or with

a rate constant k_X [for a disulfide intermediate, in the presence of M, eq. 3].



For nickel ethyl xanthate [NiEX], $k_M = 2.9 \times 10^{-6} \text{ s}^{-1}$ [see Fig. 3.2] and for isopropyl dixanthogen [IX] $k_{XX} = 2.0 \times 10^{-4} \text{ s}^{-1}$ [see curve 1 in Fig. 3.5]. The smaller rate of disappearance of the nickel complex is reflected in its greater photostability compared to that of the corresponding disulfide [see Figs. 3.2 and 3.5]. Photolysis of the metal complex takes place in a consecutive reaction [eq. 3]. In this case, only when the extinction coefficient, multiplied by the concentration of X, i.e. $\epsilon_X C_X$, becomes comparable to $\epsilon_M C_M$ [see Sec. 2B.3.1] will k_X be important. It is clear from this analysis that X tends to accumulate in the system with further photolysis of M, hence the observed increase in the window-regions ca. 275 and 236 nm of the UV-spectra of M [Fig. 3.1]. Upon further UV-exposure, the actual amounts of X remaining in the system will vary subject to the ratio $\epsilon_X C_X : \epsilon_M C_M$. Beyond a critical value of this ratio, the contribution of k_X is substantial, with complete formation of products Z when M and X are exhausted [Fig. 3.2]. The nature of the intermediate product, X, was therefore verified, although the absorption spectrum of M prevents the observation of an unadulterated UV-absorption spectrum of the product which could have been compared with an authentic sample of [X]. Direct spectral evidence, however, does become feasible from the reaction [eq. 4] of metal complexes with TBH at room temperature [compare Figs. 3.8 and 3.9 with Fig. 3.10 for the dixanthogen:



[4]

since $k'_X \ll k'_M$ [see Sec. 3.2.2], an accumulation of product X, shows spectral features which are identical to an authentic sample of the disulfide [see inset of Fig. 3.8 and curve 48 in Fig. 3.9]. Isopropyl-dixanthogen at room temperature did not decompose TBH [Fig. 3.10] and vice versa. The reaction of NiBX with TBH gives rise to a stable product which does not decompose hydroperoxides further at room temperature. No change in the product's spectrum was observed after a period of several hours. This product, therefore, shows an identical behaviour, and UV absorption, to the authentic dixanthogens [compare inset of Fig. 3.8 with Fig. 3.10].

It has been shown in the present study [Chap. 7] that disulfides are formed from nickel dithiolates when the latter are oxidised in model systems, at high temperatures, by hydroperoxides. Under these conditions the disulfides, and their oxidation products, were found to be responsible for the hydroperoxide decomposition. The formation of disulfides from the metal complexes via a photo- or TBH-initiated oxidation at room temperature was similarly verified for a number of these metal complexes: NiRX, [Figs. 3.1 and 3.8], NiDRP [Fig. 3.13, Sec. 3.3.3], and ZnDIP [Fig. 3.18, Sec. 3.3.3]. The formation and identification of the product X as disulfides was therefore concluded on the basis of spectral and kinetic evidence.

Although disulfides appear ineffective in decomposing hydroperoxides at room temperature as was shown for IX (Fig. 3.10), and for the reaction product of NiRX with hydroperoxide (Fig. 3.8), thermally initiated reactions of hydroperoxide with disulfides and with nickel xanthate indicate a fast hydroperoxide decomposition (Sec. 7.2.1). The rate of disappearance of the 285 nm band in the reaction of IX/TBH (at room temperature) and that of the 316 nm band of the NiRX/TBH reaction (under similar conditions) occurs much more quickly when these reactions are initiated by light (see curve 2 in Figs. 3.5 and 3.11). The photo-initiated NiRX/TBH reaction appears to be six times faster than thermally-initiated TBH reaction at room temperature. That it is the oxidation products of disulfides, and not the disulfides themselves which are responsible for the observed efficiency in decomposing hydroperoxides at elevated temperatures (see Sec. 3.2.2), is seen to supplement the above conclusion.

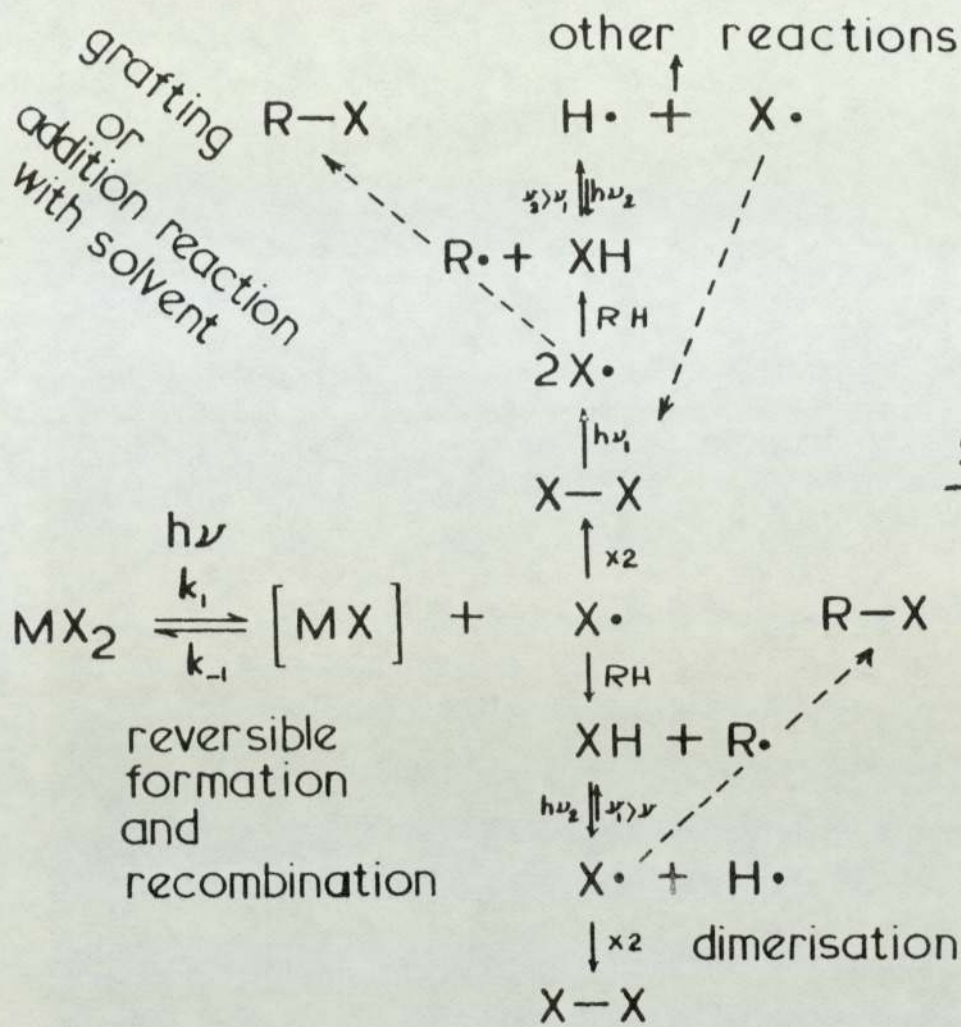
3.3.2 Effects of Solvents on Photostability of NiRX and ZnRX

A comparison between the rates of photolysis of nickel and zinc xanthates in hexane and cyclohexane reveals some notable differences. Photolysis of NiRX follows first order kinetics (Fig. 3.3) with rate constant $k_h = 2.9 \times 10^{-6} \text{ s}^{-1}$ (in hexane) and $k_c = 5 \times 10^{-6} \text{ s}^{-1}$ (in cyclohexane). The photolysis of ZnRX showed the reverse behaviour: $k_h = 2.2 \times 10^{-5} \text{ s}^{-1}$ and $k_c = 1.6 \times 10^{-5} \text{ s}^{-1}$ (Fig. 3.6). It is clear that the photostability of these complexes are greatly influenced by the solvent. The lifetime of NiEX in hexane

and cyclohexane is ca. 80 h and 40h, respectively [Fig. 3.3]. At the same molar concentration, ZnEX has a lifetime of 12 h and 17 h in hexane and cyclohexane, respectively [Fig. 3.7].

The photolysis of metal xanthates in non-polar solvents is greatly influenced by the oxidisability of the medium. Processes in which hydrogen-abstraction are important are influenced by solvents possessing labile hydrogen. Thus, reactions involving radicals (X^{\cdot}) should show increased amounts of XH. Apart from termination reactions, coupling reactions of radicals should be considered. The formation of dixanthogens from both NiEX [Fig. 3.1] and ZnEX [Fig. 3.7] is very important. Although dixanthogens were formed from the photolysis of zinc and nickel xanthates, the actual conversion of the metal complexes, e.g. NiRX, into dixanthogens is more convincing from results of TBH-initiated decomposition of metal xanthates. The lower conversion effected by light [e.g. for NiRX, the dixanthogen yield is ca. 7%] compared to conversions obtained in the presence of TBH [for NiRX the dixanthogen yield is ca. 30%] is a reflection on the efficiency of ligand oxidation by oxygen [oxygen is an indirect source of hydroperoxide] and hence hydroperoxide.

Apart from the interest in the disulfides themselves, their formation is vital to the mechanistic argument of the following scheme.



Since the photolysis of the zinc complex is faster in hexane than in cyclohexane [Fig.3.6], the process of hydrogen abstraction appears to be less competitive than the other two main processes, i.e. recombination and dimerisation. On the other hand, a faster disappearance of nickel xanthate in cyclohexane [Fig.3.3] indicates the importance of hydrogen abstraction in the presence of the more oxidisable solvent (i.e. solvent with a labile hydrogen). A possible explanation which accounts for the decrease in the encounter rate of radicals with themselves, free radicals, $X\cdot$, should be formed to a much lower extent. The lower turn-over of the radicals [in NiRX] suggest a favourable situation

for the regeneration of the parent complex [which is responsible for the observed induction period before decomposition commences], hence the longer lifetime of nickel xanthate in hexane (Fig. 3.3). A faster decay of the zinc analogue [at the same molar concentration and in the same solvent, Fig. 3.6], on the other hand indicates that the reversible formation of the parent complex, i.e. recombination process, is less favoured, hence the photolabile nature of ZnRX.

3.3.3 Effect of Solvent, Light, and Hydroperoxide on MDRP and DiPDiS

The nickel dithiophosphates constitutes yet another group of metal dithiolates which yield disulfides by photo- and hydroperoxide-initiated oxidation. This was concluded on the basis of spectral evidence [inset in Fig. 3.13] which indicates the formation of DiPDiS as an intermediate. Thus, the formation of a product [with $\lambda_{\max} = 260$ nm, λ_{\min} [window] = 250 nm] exactly identical to the product formed during photo- or hydroperoxide-initiated reaction of DiPDiS [Fig. 3.17] confirms this point. Furthermore, in the presence and absence of UV-light, the product of the reaction NiDIP-TBH displays spectral features which are identical to those observed for the product of the photo-initiated reaction of DiPDiS with TBH [Fig. 3.16]. Since these new spectral features underwent no further change when photolysis was discontinued [inset in Fig. 3.16], the products concerned must possess identical behaviour toward UV-light and hydroperoxides. A DiPDiS-based product is, therefore, confirmed for the reaction of nickel

dithiophosphate with hydroperoxide. Since the reaction of DiPDiS with TBH at room temperature in the absence of UV light was found to occur at a negligible rate, the initial step [see Sec. 3.2.3] in the photo-initiated reaction, for example, must involve a homolytic cleavage of the disulfide bond.

The formation of DiPDiS from photo- or hydroperoxide-initiated reaction of NiDIP is, therefore, established. A similar analysis can be used in the case of ZnDIP which clearly produces DiPDiS in its reaction with TBH at room temperature [Fig. 3.18]. Hence the analysis which was previously applied to nickel xanthates [Sec. 3.3.1] can be similarly applied here for the case of nickel and zinc dithiophosphates. Further, in considering the influence of the solvent on the mechanism of photo-initiated oxidation, the earlier scheme [Scheme.3.1, Sec. 3.3.2] which was given for nickel xanthates is equally valid for nickel dithiophosphates.

3.3.4 Comparison between NiDRP and NiRX

In general nickel dithiophosphates and nickel xanthates display similar behaviour toward light and hydroperoxides. The rates at which these photo- and hydroperoxide-initiated oxidations occur, however, are markedly different. These points are discussed in the following outline.

1. NiDBP is somewhat more stable to UV-light than NiBX. Solutions with similar absorbances show NiDBP to be 1.25 times more stable toward UV-light. Inset of Fig. 3.12 reflects this difference when their differences in extinction coefficient are taken into account.

2. The reaction of TBH with nickel dithiophosphate and nickel xanthate at room temperature is quite fast. These reactions are further facilitated by UV-light. At a molar ratio of 1 : 100 [nickel complex : TBH], the rate of disappearance of NiDIP was found to be about seven times faster than NiBX [Fig. 3.8 and 3.13]. Photo-initiated reactions of TBH with NiDIP effects an even faster disappearance of the complexes; hence NiDIP disappears about eight times faster than NiBX [Figs. 3.9 and 3.15].

3. Disulfides arise from both nickel dithiophosphates and nickel xanthates. The intermediate nature of disulfides was evident from the photolysis of these complexes, at room temperature, in the presence and absence of a hydroperoxide [Figs. 3.1, 3.8, 3.9, 3.13].

4. Although disulfides were formed during the photolysis of NiDRP and NiRX, in the presence and absence of hydroperoxides, the nature of the disulfide obtained from NiDRP is 'transitory'. Further reaction of this disulfide with TBH, in the presence or absence of light, [see for example inset of Fig. 3.16] resulted in the formation of a new product which displayed spectral features (λ_{\max} 260 nm, λ_{\min} [window] 250 nm) that are characteristically different from those of the disulfide. This result compares well with the behaviour of DiPDiS itself upon photolysis. Photolysis of an authentic sample of DiPDiS, in the presence and absence of TBH, was found [Fig. 3.16] to generate the same spectral features described above. Disulfides formed from the nickel xanthates were found to give rise to no new spectral feature with further reaction

with TBH [see Fig. 3.8], or when photolysed. Photolysis of an authentic sample of dixanthogen was found to reproduce this observation, i.e. spectral photobleaching, without the formation of any new spectral feature.

5. The reactions of nickel dithiophosphates and xanthates appear to proceed through almost identical processes, in the presence of TBH or under the influence of light. In the absence of TBH, photo-initiated reactions are dependent on the level of oxygen present in the solution; normally oxygen concentration is about 10^{-3} M at room temperature. Thus, photolysis of a solution containing, for example, 1×10^{-5} M NiRX implies that the molar ratio of NiRX : O₂ is about 1 : 100. TBH being a much stronger oxidant than atmospheric oxygen should afford a greater yield of disulfide, i.e. greater conversion of metal complex to the corresponding disulfide. This was demonstrated in several instances: for example, compare 7% 'disulfide' yield from photolysis of NiRX with 30% yield from reaction of NiRX with TBH at room temperature [see Sec. 3.3.1 and 3.2.2].

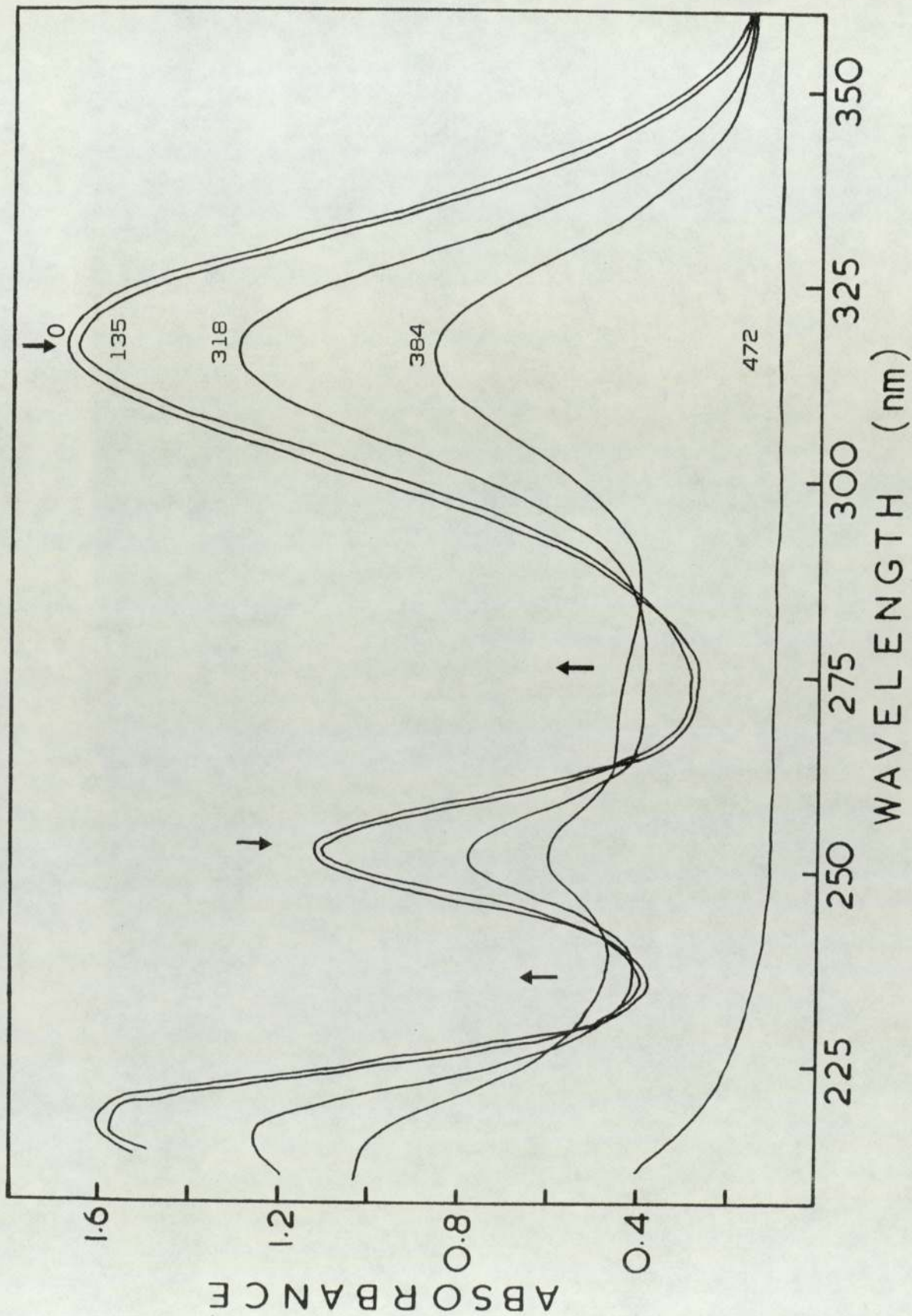


Fig. 3.1 Changes in the UV-absorption spectrum during photolysis of NiEX ($5.6 \times 10^{-4} M$) in hexane solution. Numbers on curves are irradiation time in hours.

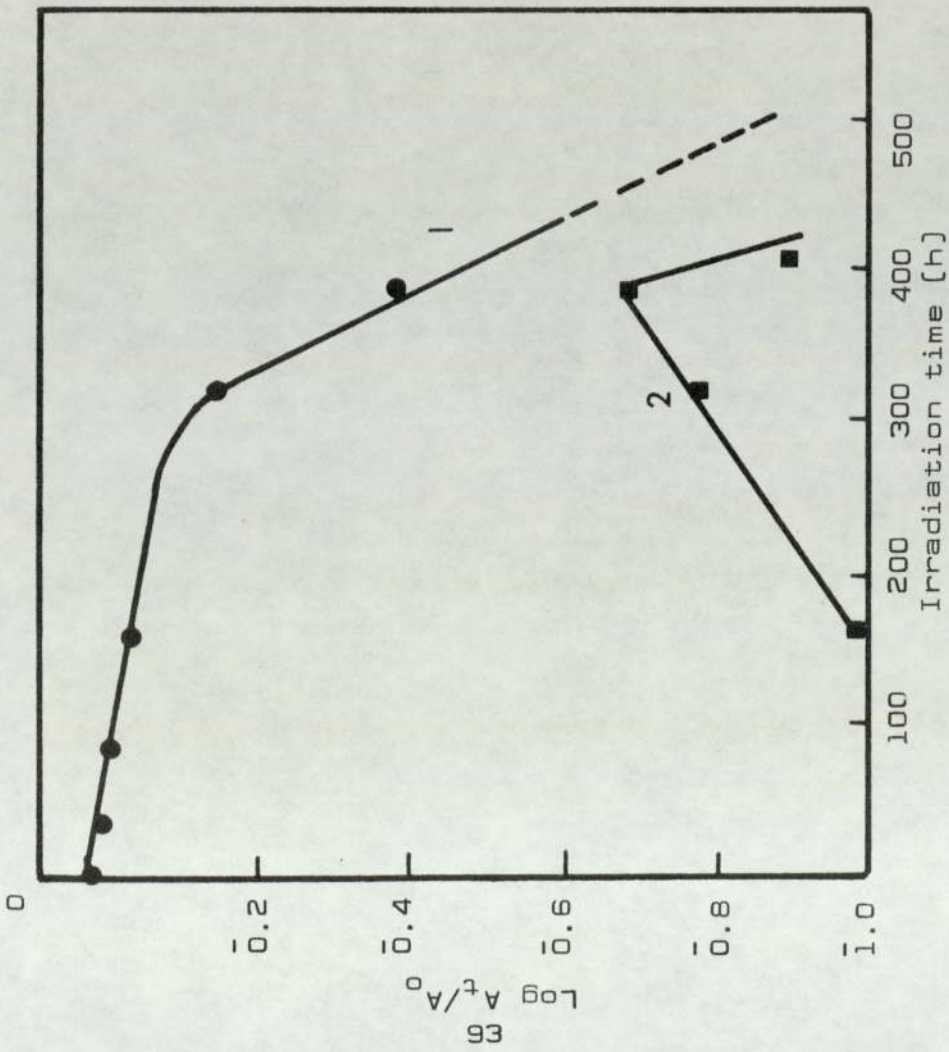


Fig. 3.2 Kinetics of disappearance of the 316 nm band (1) and appearance of the new 275 nm band (2) during photolysis of 5.6×10^{-4} M NiEX in hexane solution.

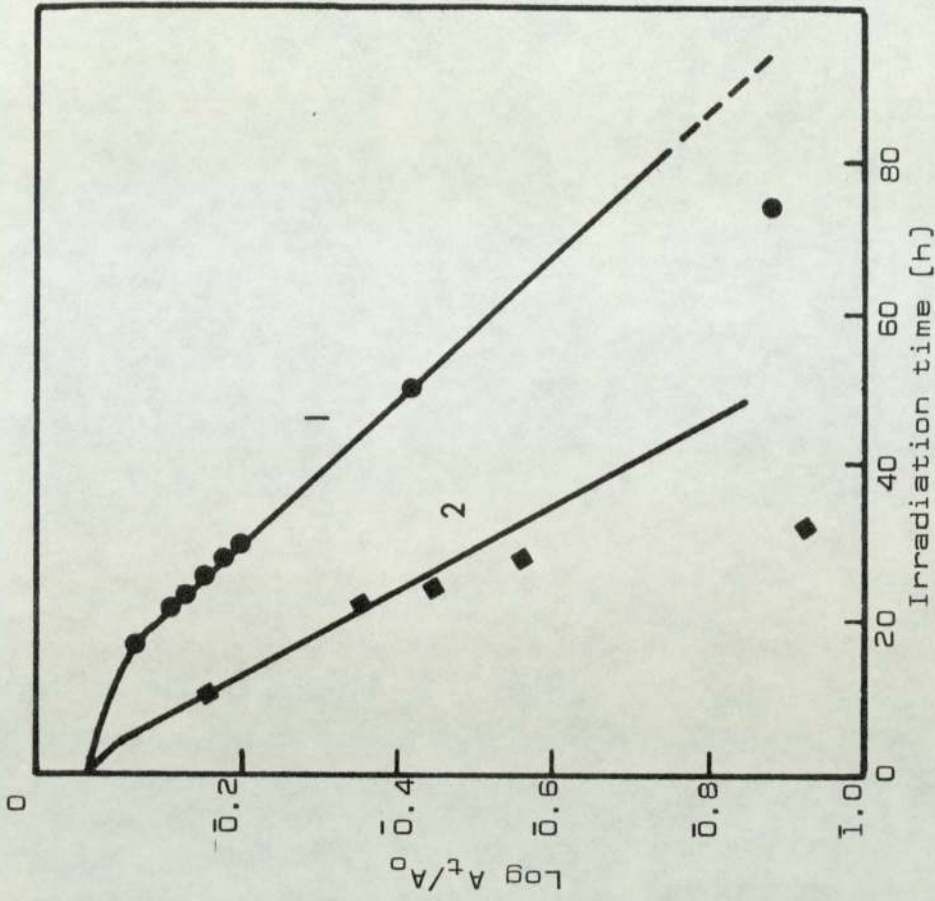


Fig. 3.3 Kinetics of disappearance of the 316 nm band of NiEX (5.8×10^{-5} M) in hexane (1) and cyclohexane (2) solutions during photolysis.

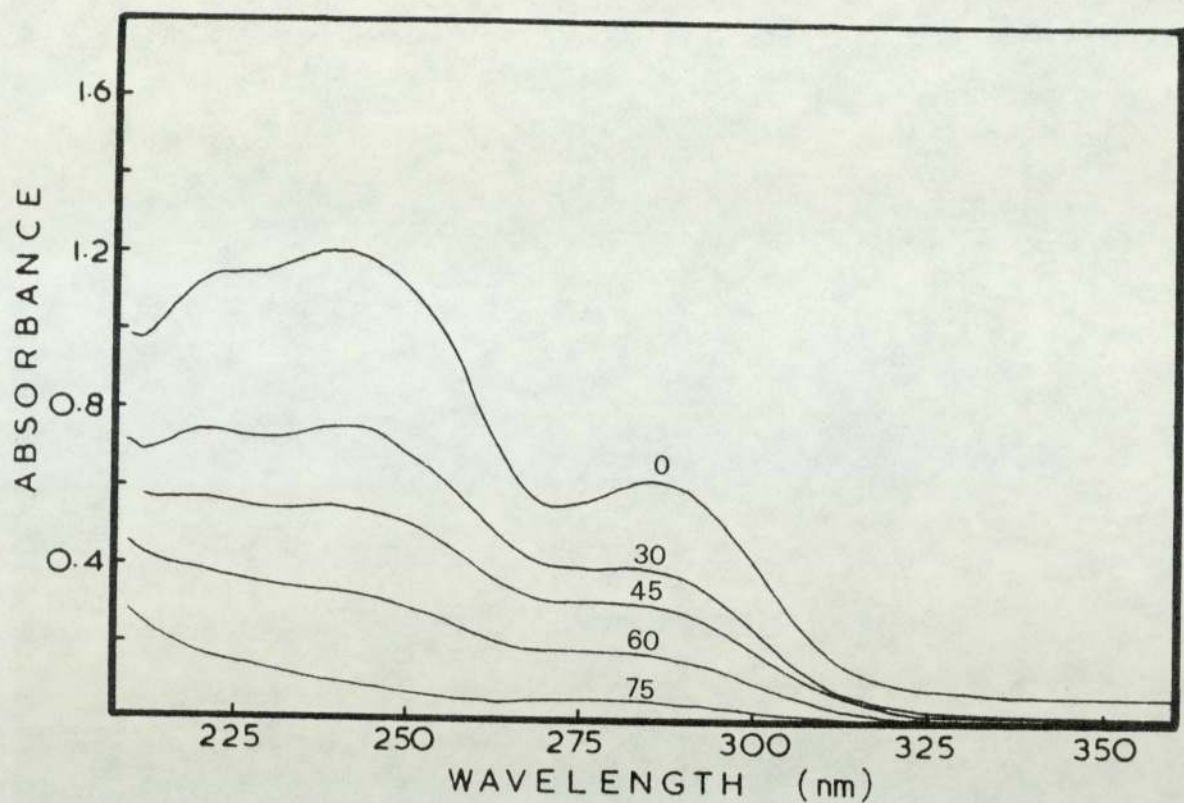


Fig.3.4 Spectral changes during photolysis of $0.5 \times 10^{-4} \text{ M}$ IX in hexane solution. Numbers on curves are exposure times in minutes.

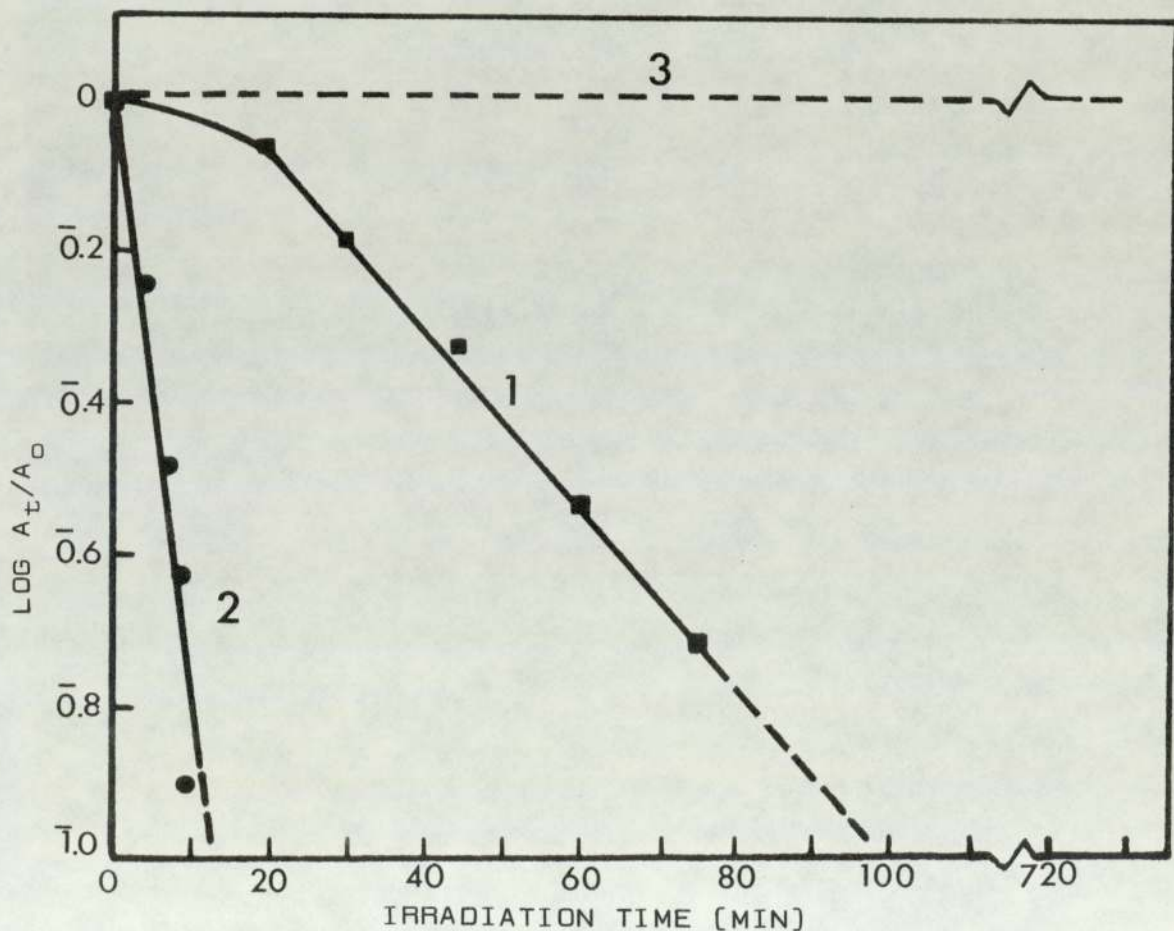


Fig.3.5 Kinetics of disappearance of the 285 nm band of IX ($0.5 \times 10^{-4} \text{ M}$) in hexane in the absence [1] and presence [2] of TBH ($0.5 \times 10^{-4} \text{ M}$) during photolysis. Curve 3 is the reaction of IX with TBH at room temperature.

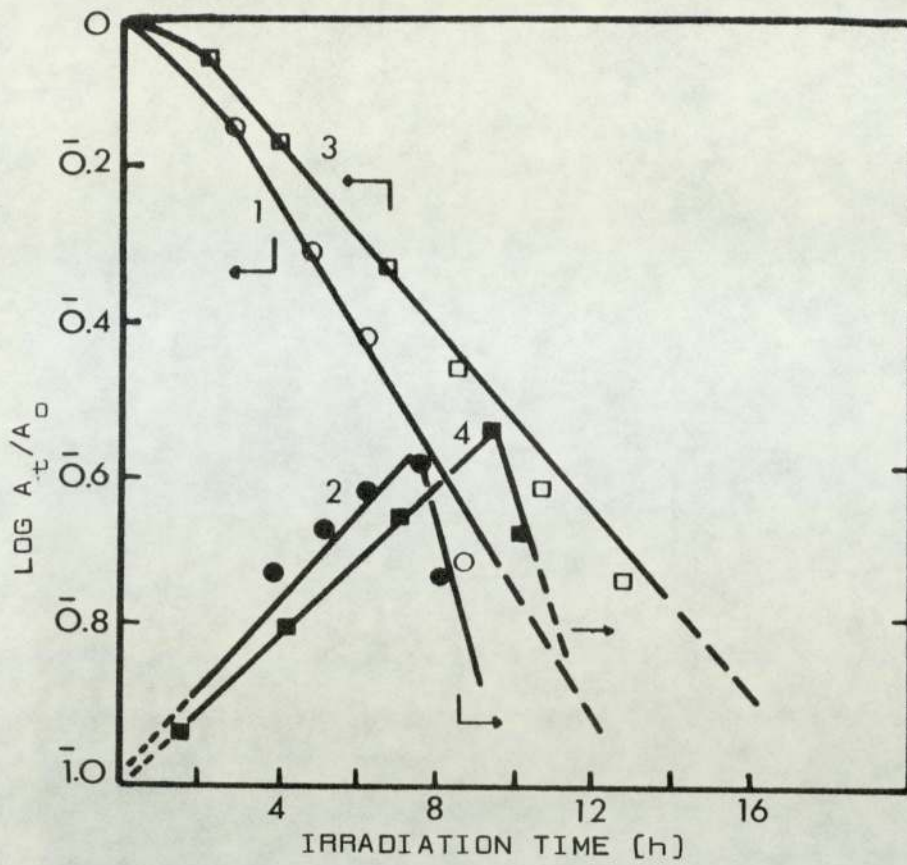


Fig.3.6 Kinetics of disappearance of the 300 nm band of ZnEX ($5.6 \times 10^{-5} \text{M}$) in hexane [1] and cyclohexane [3]. Rate of appearance of new band ca.275 nm in hexane [2] and cyclohexane [4] is also shown.

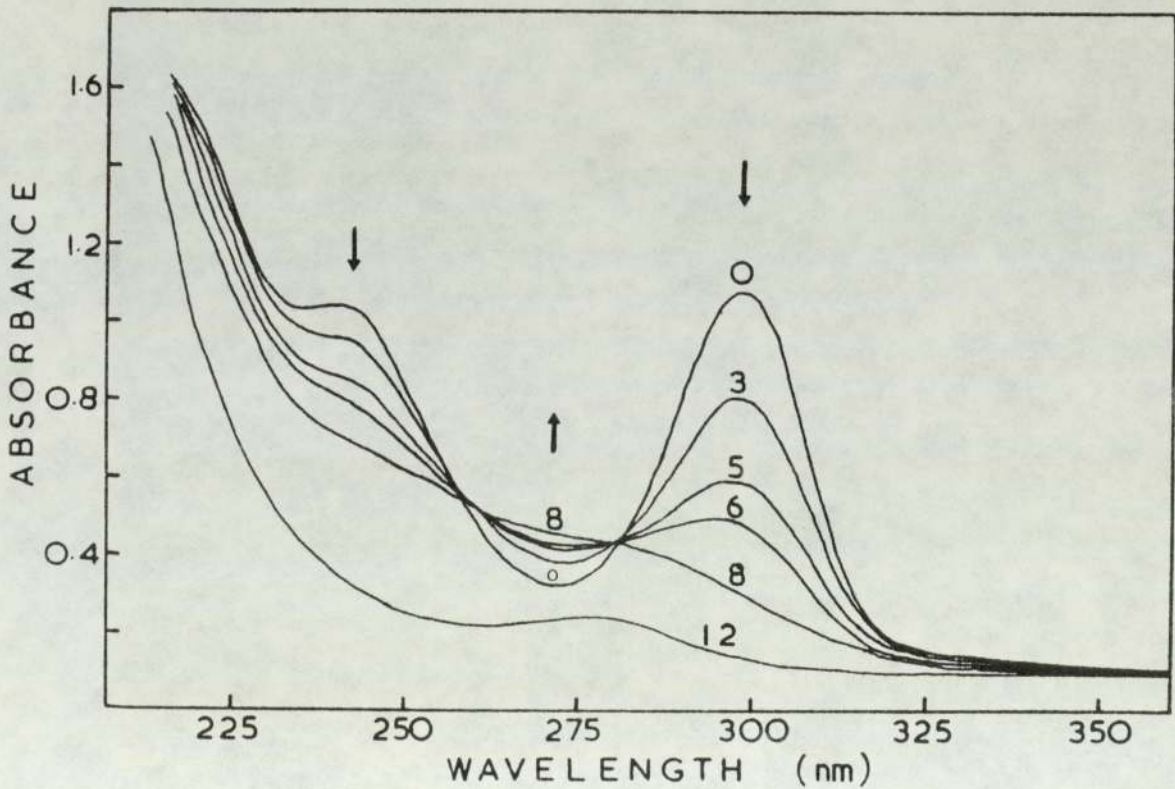


Fig.3.7 Spectral changes during photolysis of $5.6 \times 10^{-5} \text{M}$ ZnEX in hexane solution. Numbers on curves are exposure times in hours.

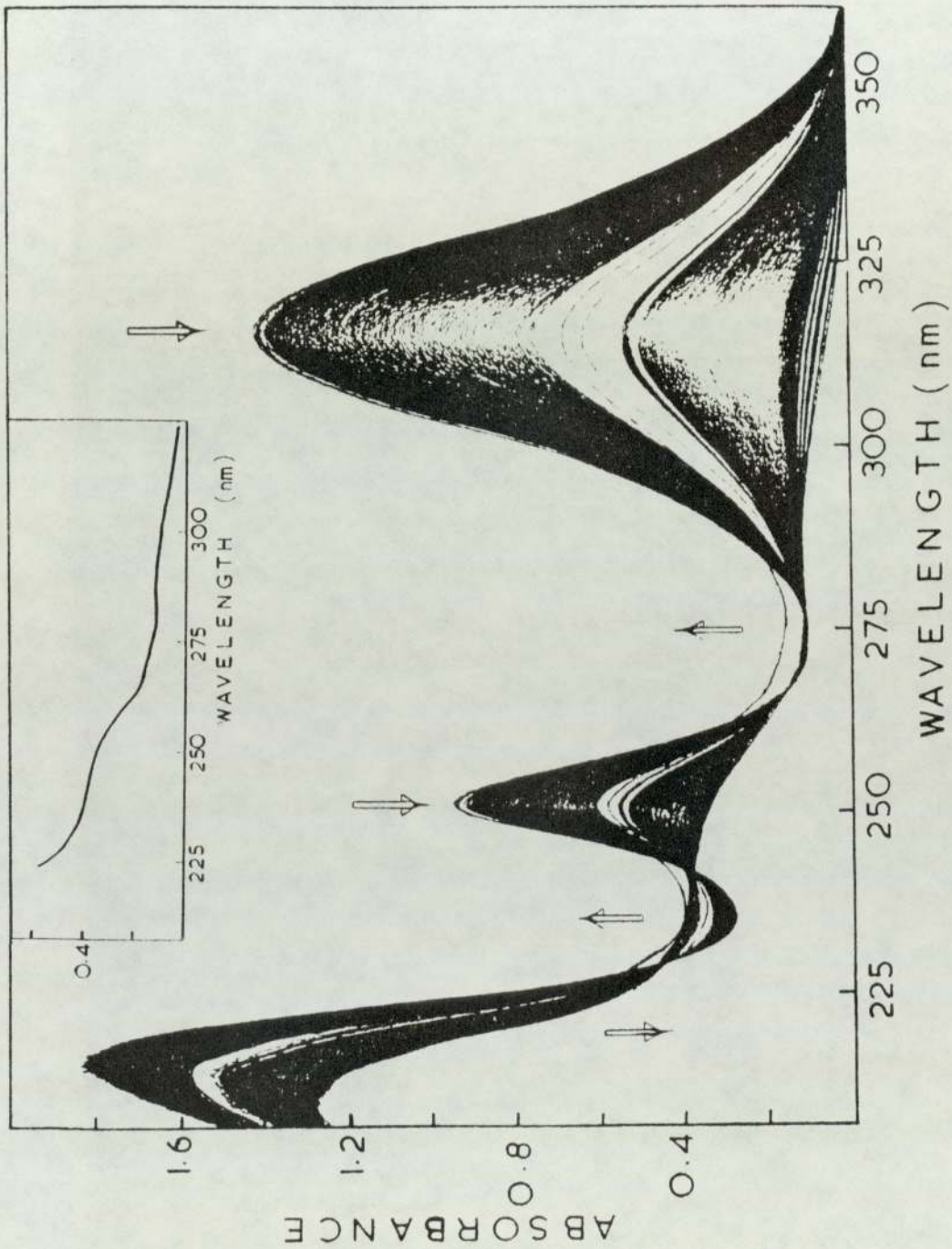


Fig.3.8 Superimposed (continuous run) UV-spectra during the reaction of NiBX ($0.5 \times 10^{-4} \text{M}$) with TBH ($0.5 \times 10^{-2} \text{M}$) at room temperature. Inset shows the UV-absorption spectra at the end of the reaction. (i.e. after 24h).

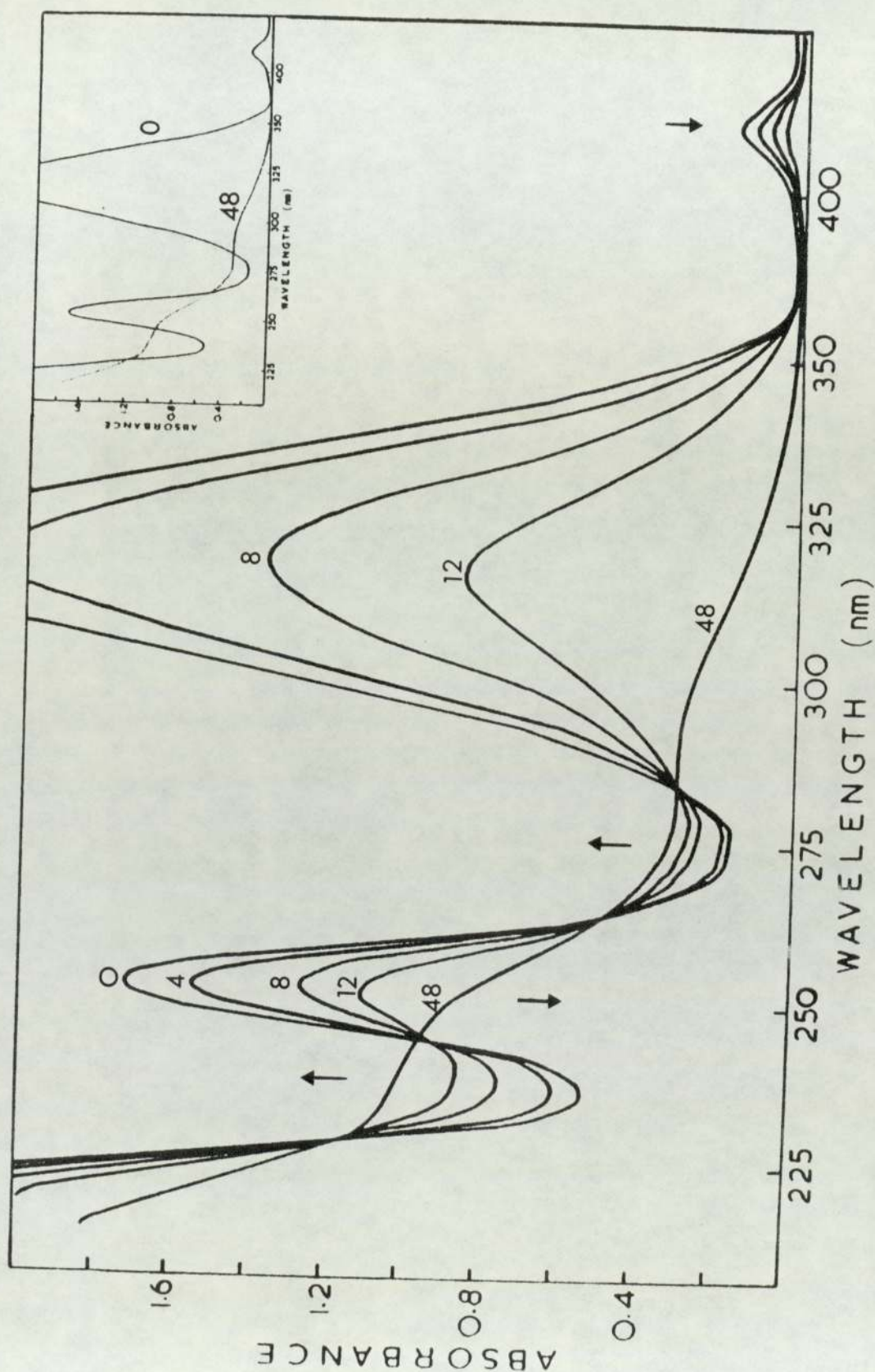


Fig.3.9 Spectral changes during a reaction of NiBX with TBH at a molar ratio of 1:100 $[(TBH)=1 \times 10^{-2}M]$ at room temperature. Reaction time [h] is shown on the curves. Inset shows the UV-absorption spectra at the beginning of the reaction [t=0, curve 0] and that of the product [t=48h, curve 48].

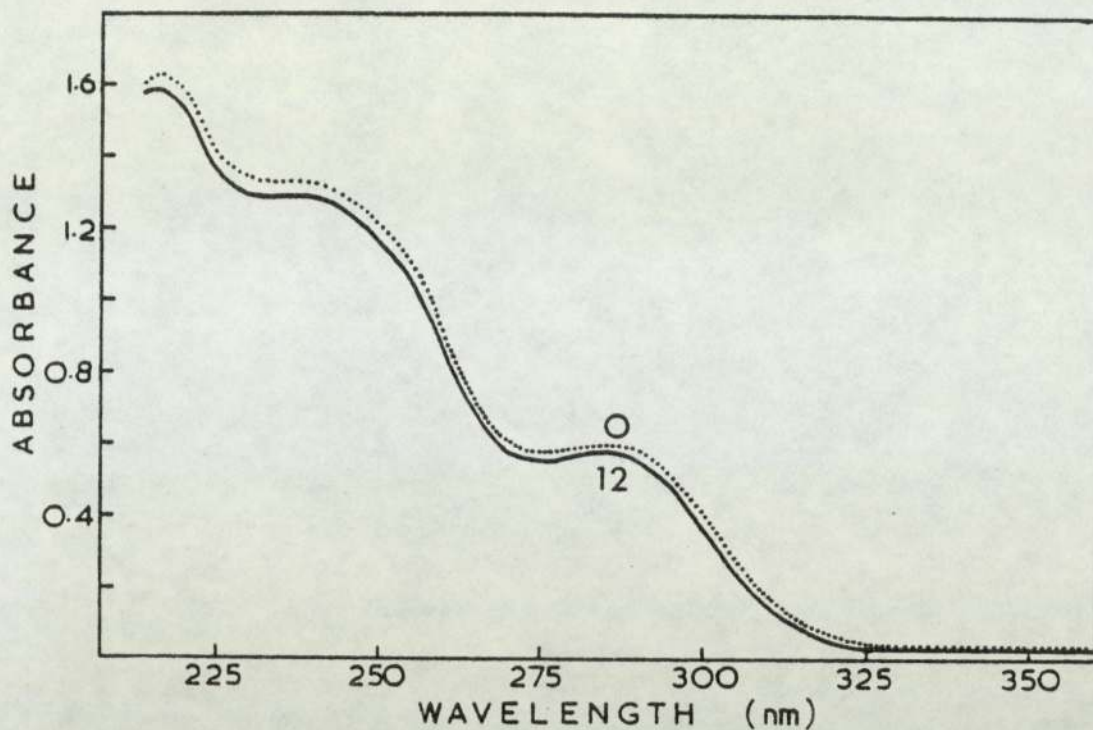


Fig.3.10 Superimposed UV-absorption spectra from a reaction of IX with TBH at a molar ratio of 1:100 $[TBH]=0.5 \times 10^{-2} M$, at room temperature. Scans were monitored continuously for 12 hours; numbers on curves are reaction times in hours.

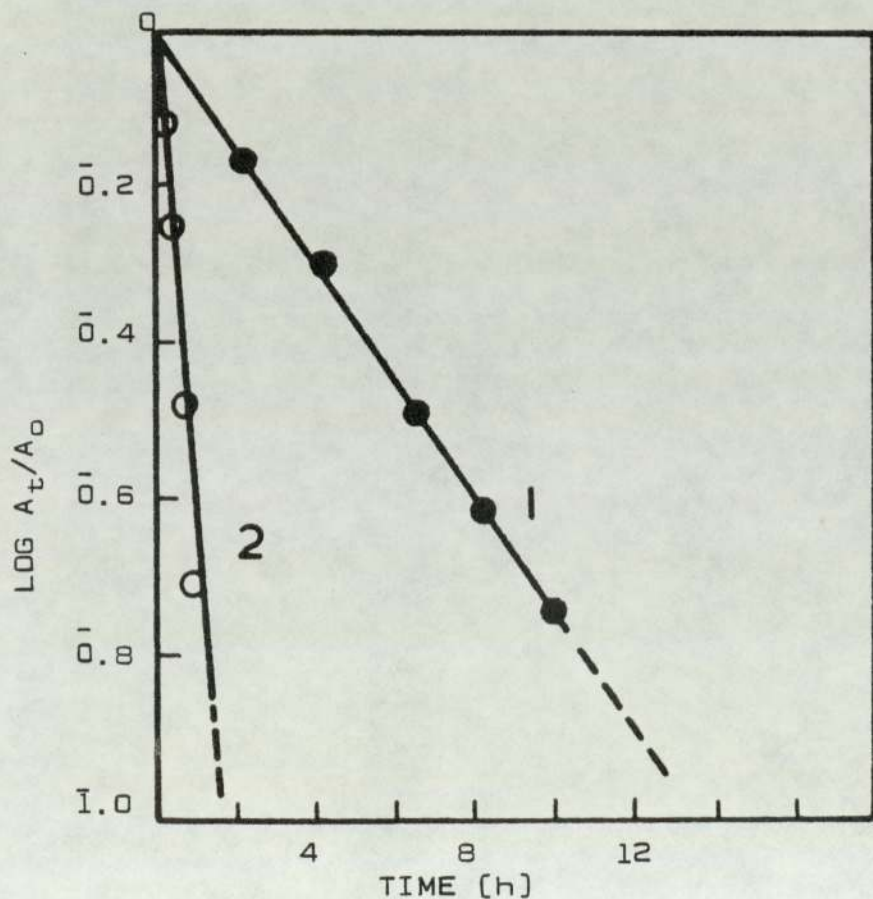


Fig.3.11 First order kinetics for the disappearance of 316 nm band of NiBX during its reaction with TBH at a 1:100 molar ratio $[TBH]=0.5 \times 10^{-2} M$, at room temperature in the absence (1) and presence (2) of light.

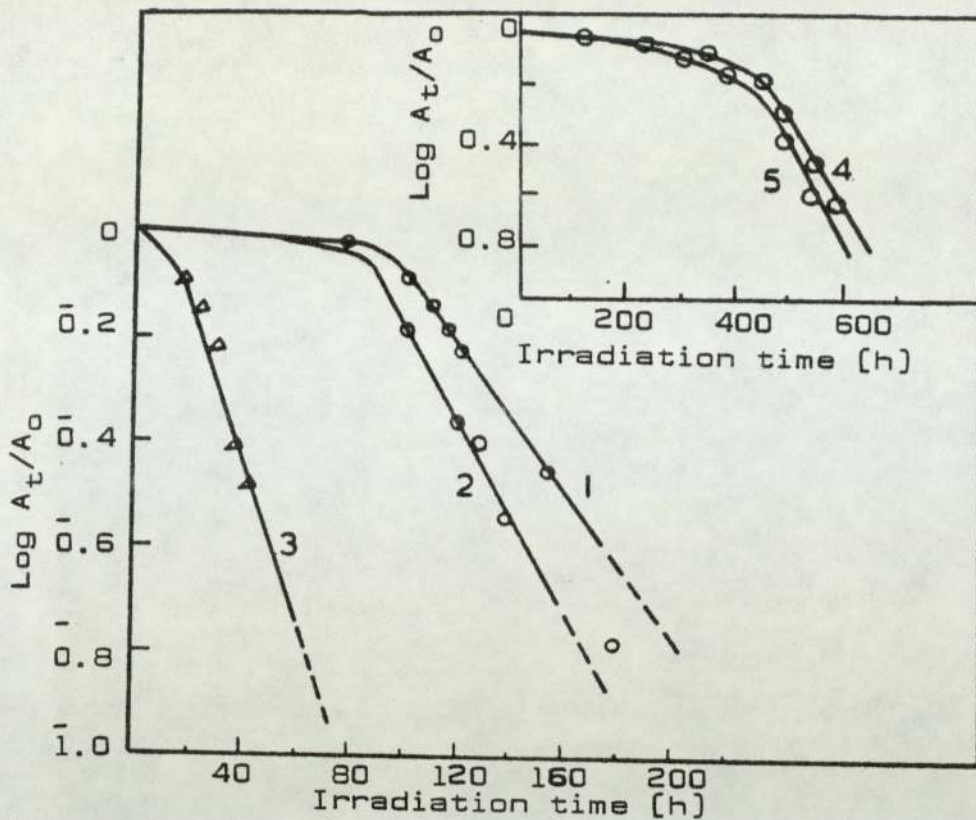


Fig.3.12 Kinetics of disappearance of 316 nm band of NiDBP ($7.0 \times 10^{-5} \text{M}$) during UV-irradiation in hexane [1], cyclohexane [2], and propanol [3]. Inset compares kinetics of disappearance of 316 nm band of NiDBP [4] and NiBX [5] in hexane, both at a concentration of $4.0 \times 10^{-4} \text{M}$.

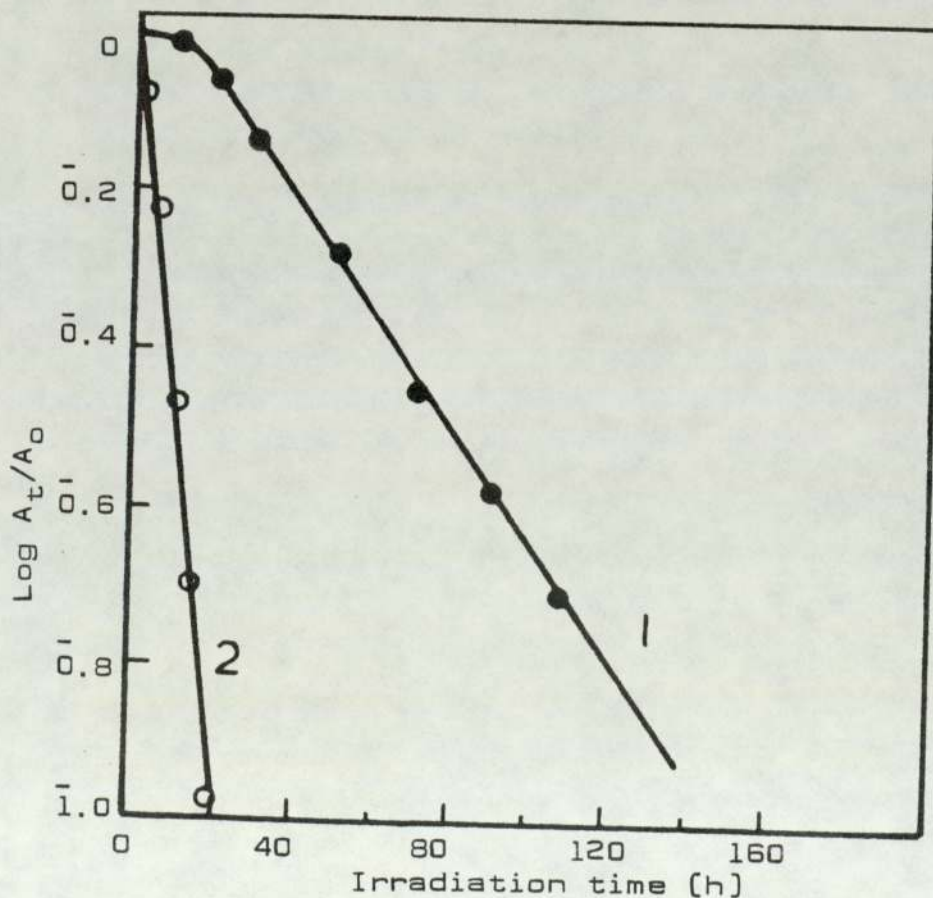


Fig.3.14 First order kinetics of the disappearance of 316 nm band of NiDIP during its reaction with TBH at a molar ratio of 1:100 ($[\text{TBH}] = 1 \times 10^{-2} \text{M}$, in hexane, in the presence (2) and absence (1) of light.

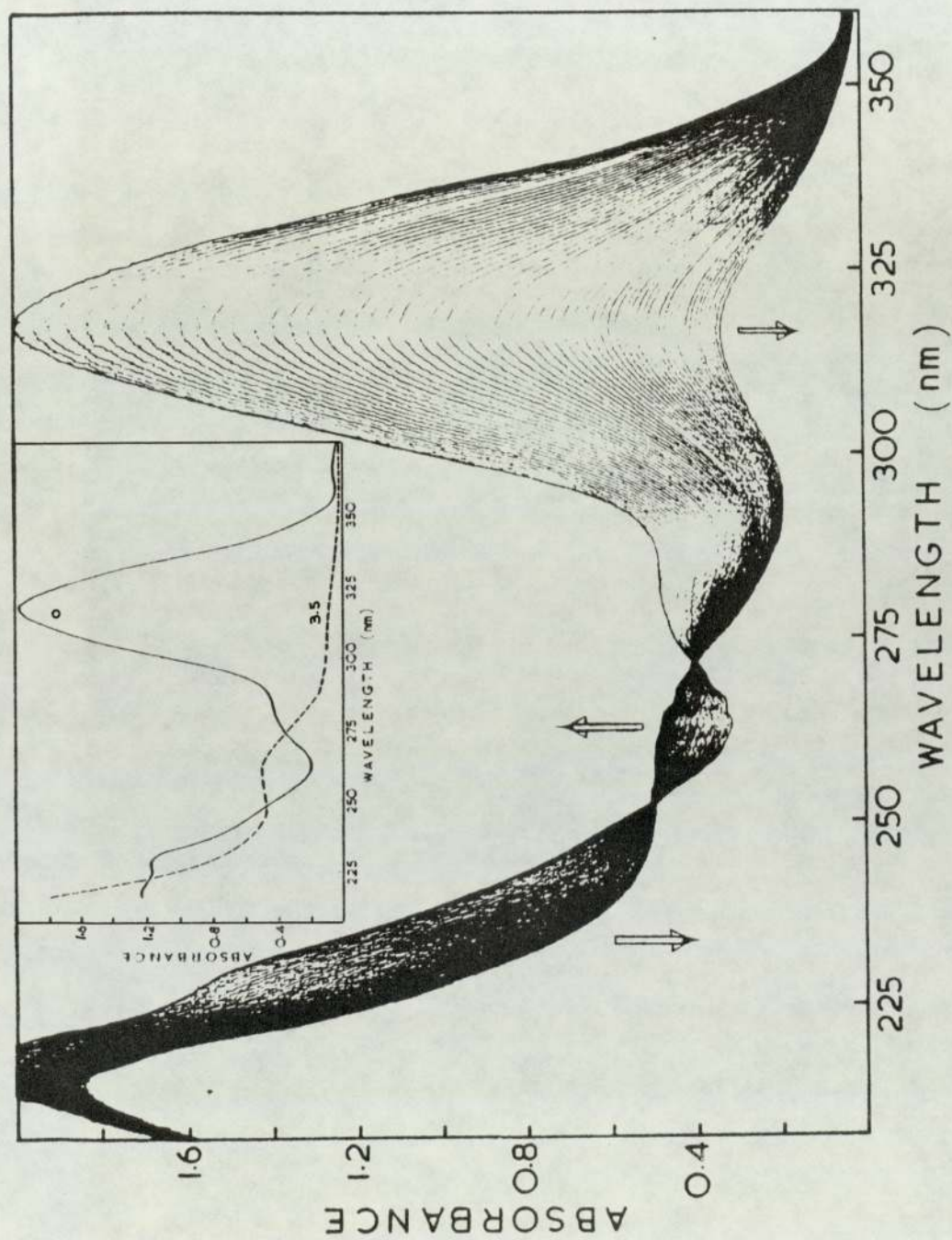


Fig. 3.13 Superimposed (continuous run) UV-spectra during the reaction of NiDIP ($0.5 \times 10^{-4} \text{M}$) with TBH ($0.5 \times 10^{-2} \text{M}$) at room temperature. Inset shows the UV-absorption spectra at the beginning and the end of the reaction.

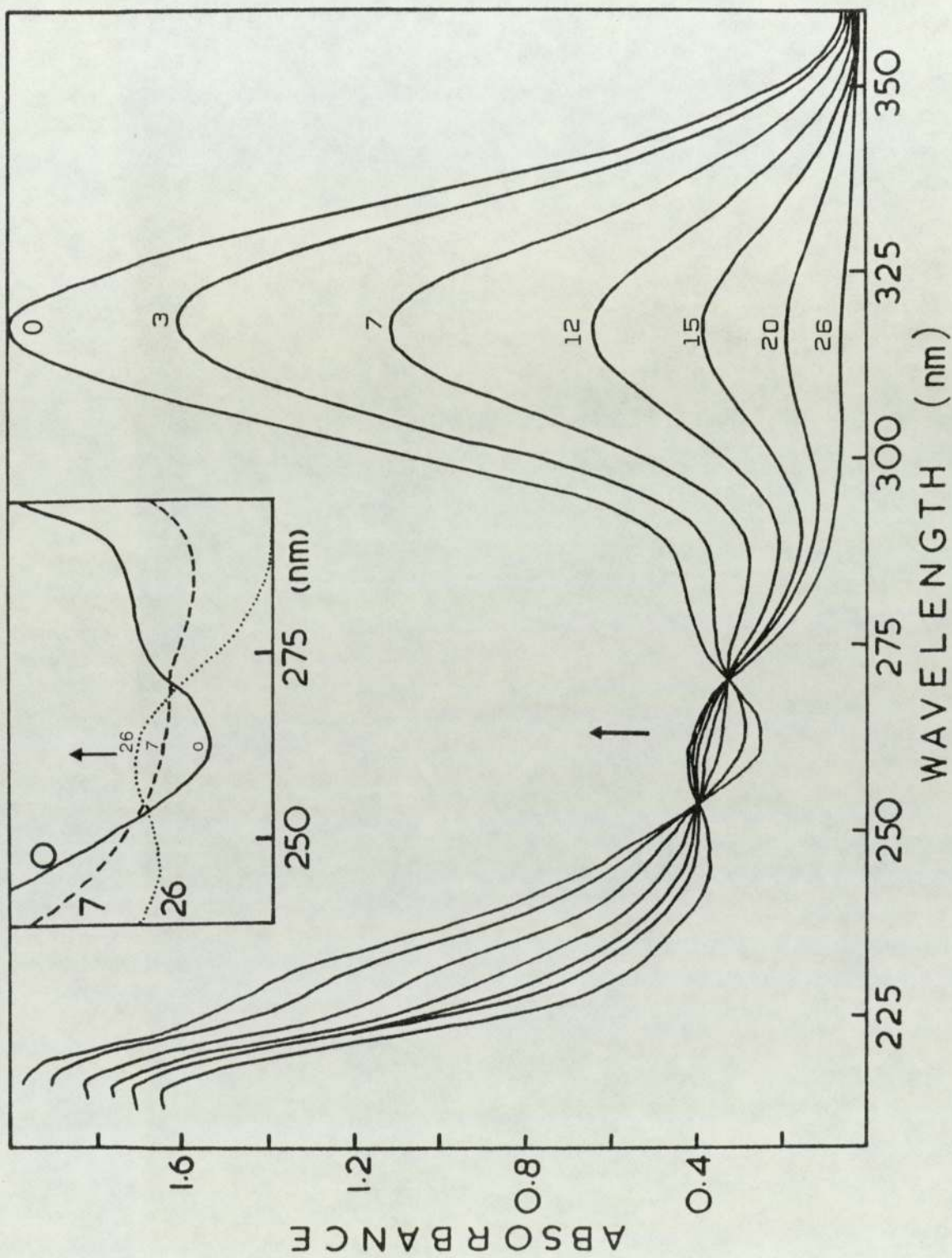


Fig.3.15 Spectral changes during the reaction of NiDIP with TBH in hexane in the presence of light, at a molar ratio of 1:100 $[(\text{TBH})]=1 \times 10^{-2} \text{M}$. Numbers on curves are exposure times (minutes). INSET reproduces the region 250-275 nm of some of the curves showing the intermediate and final product formation.

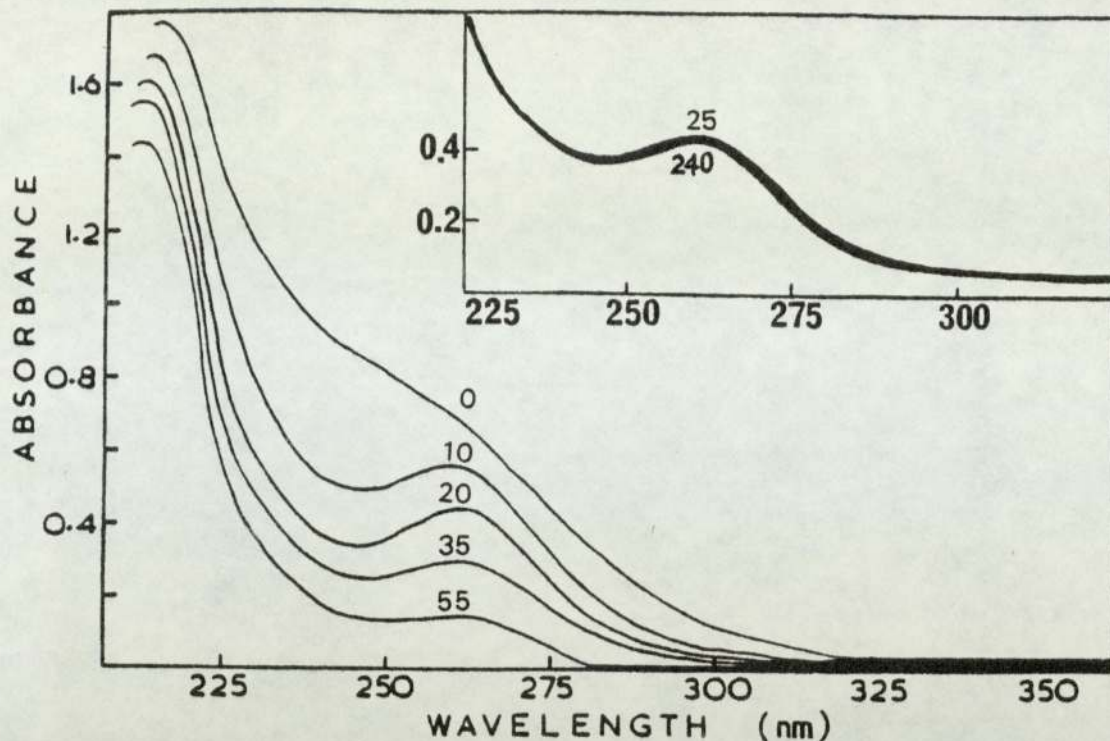


Fig.3.16 Spectral changes during the reaction of DiPDiS ($1 \times 10^{-4} \text{M}$) with TBH ($1 \times 10^{-2} \text{M}$) in hexane at room temperature, in the presence of UV-light. Exposure times (min) are shown on curves. The inset shows this same reaction when initially exposed to UV-light for 25 min and subsequent dark reaction over a period of 4h continuous scanning.

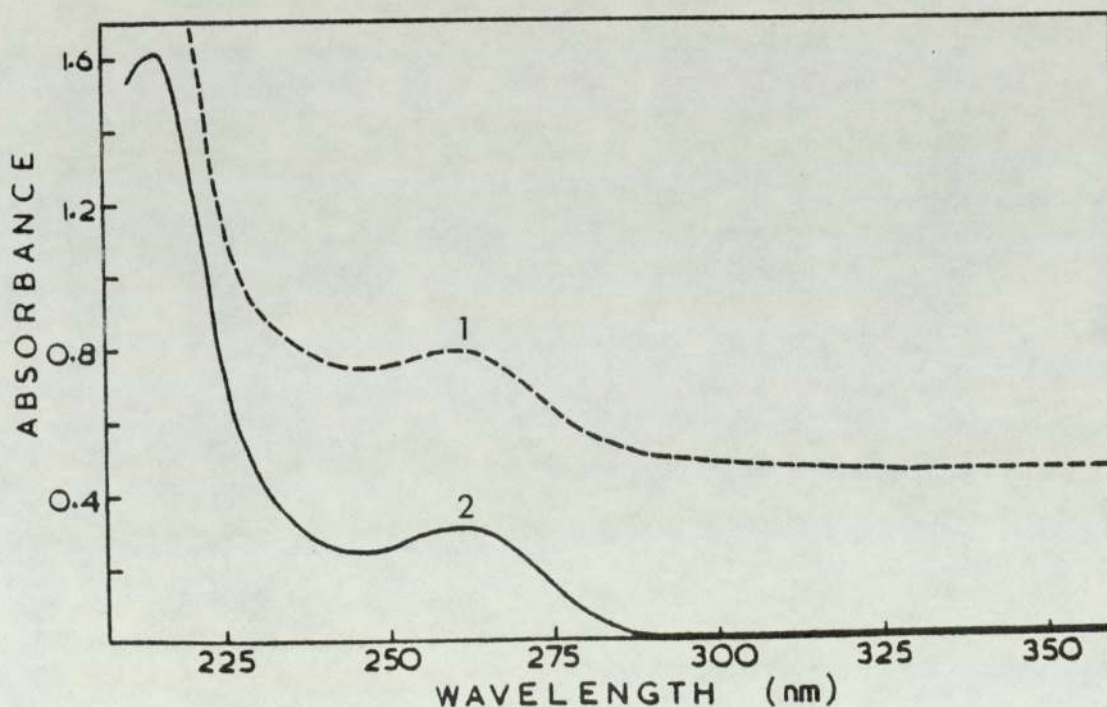


Fig.3.17 Photoproduct of reaction of TBH with NiDIP [1] and DiPDiS [2] at room temperature. On further photolysis these spectral features disappear. Curve 1 is displaced by 0.4 absorbance unit.

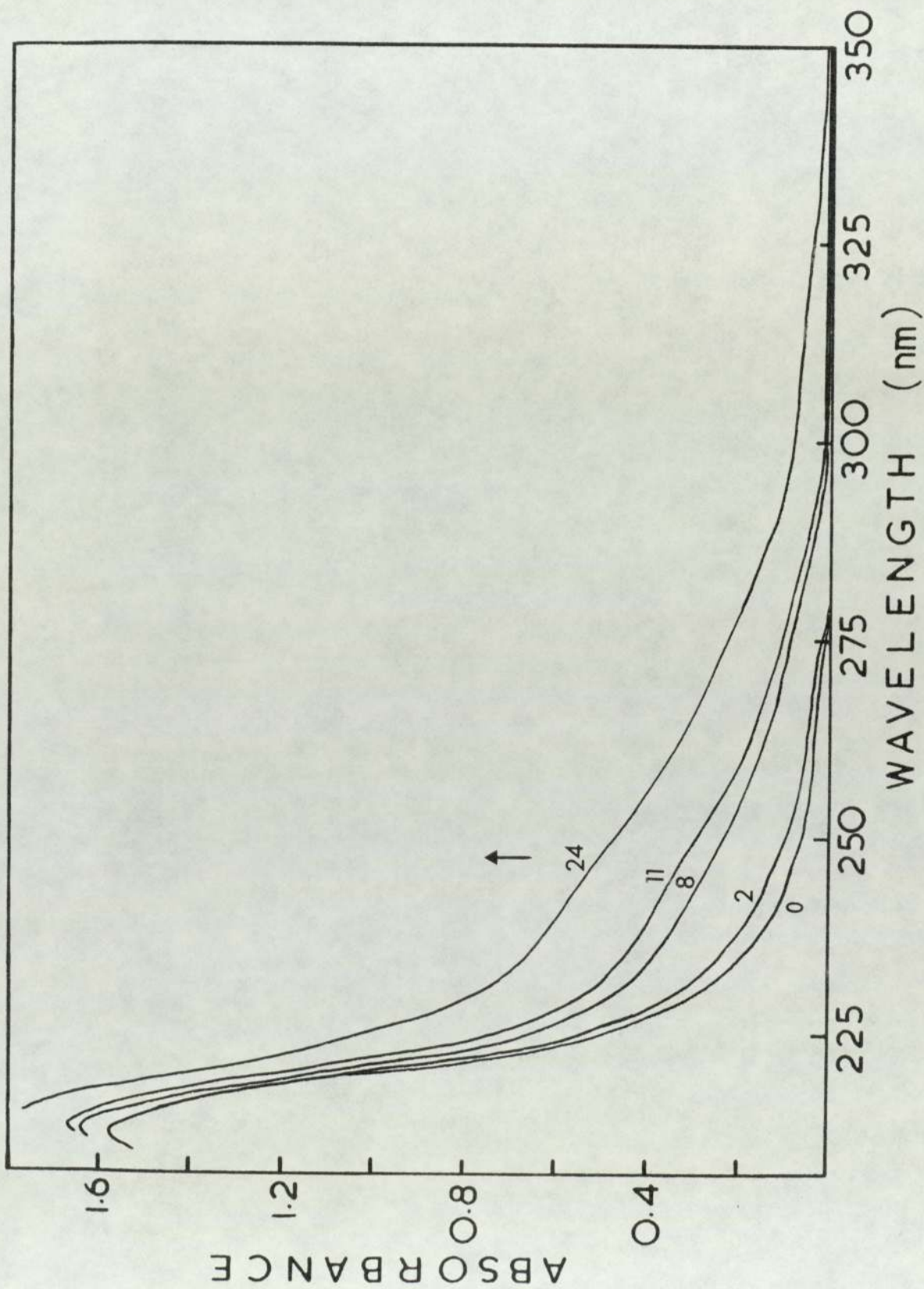


Fig.3.18 UV-spectral changes during reaction of ZnDIP ($1 \times 10^{-4} M$) with TBH ($1 \times 10^{-2} M$) in hexane at room temperature. Numbers on the curves are reaction times in hours.

CHAPTER FOUR

STABILISATION

OF

LOW DENSITY POLYETHYLENE

4A. THE INFLUENCE OF METAL DITHIOLATES AND
CORRESPONDING DISULFIDES ON THE THERMO-
OXIDATIVE STABILITY OF LDPE

4A.1 OBJECT

In this chapter the effects of ethyl, isopropyl, and butyl substituents on the thermal stability of NiRX (R = E, B), ZnEX, NiDRP (R = B, E, I), ZnDIP, and the corresponding disulfides, dixanthogen (RX) and di-isopropyl thiophosphoryl disulfide (DiPDiS), are examined by thermogravimetry, in the presence of air.

Each of the above additives is also compounded (2.5×10^{-4} M/100g) with unstabilised polyethylene and processed at 150^o for 30 minutes in an open mixer (30, OM) unless otherwise specified. Films are prepared from the processed polymer (by compression moulding) and are used in the evaluation of the thermo-oxidative stability of PE during ageing at 110^o, in the presence of air in a Wallace oven (see Sec. 2A.3.2). Toluene extraction (see Sec. 2A.2.3) of the stabilised films is undertaken to examine the extent of bound antioxidants and their effects on thermo-oxidative stability of the polymer.

4A.2 RESULTS

4A.2.1 Thermo-oxidative Stability of Unstabilised PE

The infrared absorption spectra of an unstabilised PE film, before and after thermo-oxidative ageing (Fig. 4A.1), showed a change in absorption at $3600-3000\text{ cm}^{-1}$, $1850-1600\text{ cm}^{-1}$, and $1200-850\text{ cm}^{-1}$ [see Table 4A.1]. This change has been found to correlate directly with the degree of oxidation of the film [24,96]. Formation of hydroperoxides [absorption band at 3555 cm^{-1}] proceeds at a faster rate than the formation of carbonyl during thermal oxidation (Fig. 4A.1a); a significant build-up in the carbonyl chromophore occurs only after the decay of the hydroperoxides.

The $1850-1600\text{ cm}^{-1}$ region shows pronounced changes during the thermal treatment at 110° (Fig. 4A.1). A major contribution to the total carbonyl content in thermally oxidised PE is that of ketone carbonyls [24]. Table 4A.1 lists the various functional groups which suffer changes during thermo-oxidation.

The region of the C-H deformational vibration ($1200-800\text{ cm}^{-1}$) shows two closely related absorptions which arise from vinyl and vinylidene (Table 4A.1). Thermal ageing of LDPE causes a reduction in the vinylidene absorption [curve 2 in Fig. 4A.1a] while the vinyl absorption appears to be almost unaffected [see Fig. 4A.1]. Similarly, the vinylene group, $\text{RHC}=\text{CHR}$, which has a weak absorption in the polymer [at 964 cm^{-1}] show little change during ageing.

Table 4A.1 Functional groups^a which occur in PE before^b and after^c ageing and UV-exposure

Functional group	Structure	[cm ⁻¹]	Ref.
-OOH free ^c	-OOH	3555	96, 98, 99
Polymeric associated -OH ^c	-OH	3380	97
Anhydride ^c	C(O) O C(O)	1820	99
Peracid ^c	C(O) OH	1785	96
Perester ^c	C(O) OOR	1765	96
Ester ^c	C(O) OR	1745	96, 99
Aldehyde ^c	C(O) H	1730	96, 99
Terminal or methyl ketone ^c	R C(O) CH ₃	1725	100
Internal ketone ^c	R C(O) R	1720	96, 99
Carboxylic acid ^c	C(O) OH	1710-15	96, 100
α - β -unsaturated ketone ^c	-CH=CH-C(O)	1685	99, 101
Internal double bond ^b	R-CH=CH-R	1645	99
C-O in carboxylic acid ^c	C-O	1185	102
C-C in long chain (in amorphous region) ^{b, d}	C-C	1080	110
disubstituted trans alkene ^c	RHC=CRH	990	99
disubstituted (cis) alkene ^{b, c} (vinylene)	RHC=CHR	964	99
vinyl group or terminal double bond ^c	RCH=CH ₂	909	99
vinylidene group ^{b, d}	RRC=CH ₂	887	99

a. Absorption bands due to these groups show an increase in intensity after ageing and UV-exposure except (d) which shows a decrease

4A.2.2 Thermogravimetry of Metal Dithiolates and
Corresponding Disulfides

Non-isothermal weight loss experiments for pure crystals of NiDRP (R = E, I, B) in air and DiPDiS (Fig. 4A.2) were found to result in characteristic single stage weight-loss (or thermogravimetric, TG) curves. Using exactly identical procedures [see Sec. 2A.8], all the TG curves exhibit similar shapes, but are displaced relative to one another. Two plateaus are observed: initial, with 'procedural' decomposition temperature, T_i , which marks the end of this plateau, and a final plateau which lies beyond the final decomposition temperature, T_f [see TG curve for DiPDiS, Fig. 4A.2]. Thermal decompositions in an oxidative (air) atmosphere initially show, in the case of NiDRP and DiPDiS (Fig. 4A.2) and NiRX and RX (Fig. 4A.3), a slow weight-loss which is followed by a much faster decomposition step. Table 4A.2 lists the 'decomposition temperatures', T_d , i.e. temperatures at which the rate of cumulative weight change is a maximum; these T_d values are based on figure 4A.2 and 4A.3.

Table 4A.2 Decomposition temperatures, T_d , for xanthates'
and dithiophosphates' antioxidants

Xanthates		Dithiophosphates	
Antioxidant	T_d [$^{\circ}$ C]	Antioxidant	T_d [$^{\circ}$ C]
NiEX	165	NiDEP	180
NiBX	145	NiDBP	145
-	-	NiDIP	170
ZnEX	115	ZnDIP	165
IX	130	DiPDiS	135
EX	145	-	-

4A.2.3 Thermal Antioxidant Behaviour of MRX and RX

Films of LDPE containing MRX (M = Cu(I), Zn(II), Ni(II); R = E, B) were examined under the thermo-oxidative conditions of a Wallace oven at 110^o. Fig. 4A.4 shows changes in the carbonyl index for aged films of LDPE, which were stabilised by the various metal xanthates. Both NiEX [curve 2] and NiBX [curve 1] effect greater stabilisation than copper- [curve 3] and zinc- [curve 4] xanthate, although CuBX imparts greater thermo-oxidative stability to LDPE than does ZnEX. Thermo-oxidative induction periods [TIP] for the various metal xanthate-stabilised LDPE films [see Fig. 4A.4] are given in Table 4A.3.

Table 4A.3 Thermo-oxidative induction periods [TIP] observed during ageing at 110^o of MRX-stabilised PE films [30, OM].
[MRX] = 2.5 × 10⁻⁴ M/100g

MRX	TIP (h)
ZnEX	25
CuBX	50
NiEX	450
NiBX	600

The stabilising effect of NiRX (R = E, B) on the thermo-oxidative stability of LDPE is shown in figure 4A.5. By comparison with nickel butyl xanthate [curve 2'], the ethyl analogue [curve 3'] is almost completely lost overnight

[i.e. 20 h compared to 200 h for NiBX]. TIP for both NiEX [curve 3] and NiBX [curve 2], however, is twice these values. Figure 4A.5 and Table 4A.4 show that the thermo-oxidative stabilisation afforded by both NiEX and NiBX are quite similar. A similar thermo-oxidative stability was observed for a LDPE film stabilised with NiBX, which was extracted prior to thermal ageing [curve 4]; using conditions which were shown to effectively remove NiBX [see Sec. 2A.2.3].

Table 4A.4 Thermo-oxidative induction periods [TIP]
observed during ageing of xanthate-stabilised
PE (30, 0M) films; [antioxidant] = 2.5×10^{-4} M/100g

Antioxidant	TIP [h]	Antioxidant life-time in film ^a [h]
NiBX	600	200
NiBX [ext] ^b	500	0
NiBX [ext] ^c	630	200
NiEX	450	20
IX	510	-

- a. followed by monitoring the disappearance of metal ligand absorption at 316 nm
- b. extracted after processing and before oven ageing
- c. extracted after thermal ageing for 200 h [when NiBX was completely destroyed]

Furthermore, a NiBX-stabilised PE film extracted after 200 h oven ageing [curve 1 in Fig. 4A.5] was found to be slightly more stable than the unextracted film [curve 2 in Fig. 4A.5]. Isopropyl dixanthogen [IX] effects similar thermo-oxidative stability in PE. Fig. 4A.5 reveals only a slight difference between the dixanthogen and the nickel xanthate [both extracted and untreated samples].

The thermo-oxidative stability afforded by NiBX when LDPE was processed for 30 min. at 150^o in the presence of limited [closed mixer] and unlimited [open mixer] supply of air is compared in Fig. 4A.6, curves 1 and 2. These results show that processing in an open mixer leads to better stabilisation.

4A.2.4 Thermal Antioxidant Behaviour of MDRP and DiPDiS

Figure 4A.7 compares the thermo-oxidative behaviour of LDPE in the presence of different metal dithiophosphates. Compared to zinc(II) - [curve 4] and copper(II) - [curve 3] analogues, nickel(II) - di-isopropyl dithiophosphate [curve 2] imparts the highest thermo-oxidative stability to the substrate. Induction periods observed for aged films of stabilised PE [see Fig. 4A.7] are given in Table 4A.5.

Table 4A.5 Thermo-oxidative induction periods [TIP]
observed during ageing [at 110^oC] of MDRP
stabilised PE [30,0M]; [MDRP] = 2.5 × 10⁻⁴M/100g

MDRP	TIP [h]
ZnDIP	250
CuDIP	300
NiDIP	420
NiDBP	450

The effect of NiDRP (R = B, I) and DiPDiS on the thermo-oxidative stability of PE is shown in figure 4A.8. The thermal stability afforded by DiPDiS (curve 3) is slightly less than that of the parent nickel complex (curve 2) and is very similar to that of the extracted films [the nickel complex was effectively removed after extraction, see Sec. 2A.2.3. The disappearance of NiDIP (curve 2') and NiDBP (curve 1') during ageing of stabilised PE films follows first order kinetics. The length of the induction periods afforded by the nickel complexes (see Table 4A.6 and Fig. 4A.8) is almost twice their lifetimes in the film.

Table 4A.6 Thermo-oxidative induction periods [TIP] and lifetime of metal complex observed during ageing of LDPE (30, 0M) stabilised with the anti-oxidants shown; [antioxidant] = 2.5×10^{-4} M/100g

Antioxidants	TIP (h)	Lifetime of metal complex (h) ^a
NiDBP	450	200
NiDIP	420	80
NiDIP (ext) ^b	400	0
DiPDiS	400	-

a. estimated by monitoring the disappearance of metal ligand complex at 316 nm

b. extracted after processing and before oven ageing

4A.3 DISCUSSION

4A.3.1 Thermal Stability of Metal Dithiolates and Their Corresponding Disulfides

The thermal decomposition of MDRP has been investigated by several workers [86,103,104]. Steric and electronic factors were shown to be important when bulky alkyl groups are present [86]. Products of thermal and thermo-oxidative decomposition, and the effect of the alkyl group on these metal complexes have already been discussed (Sec. 2B.3). It is shown in the present work, that thermo-oxidative stability of pure complexes of alkyl xanthates and dialkyl dithiophosphates (Figs. 4A.3 and 4A.2) fall in the following order of increasing stability, $R = B < I < E$. This order coincides with the order of melting point for the linear alkane substituents [see Table 2A.3, Sec. 2A.1.5]. NiDIP appears to behave differently; although it has a higher melting point than the ethyl analogue, its TG curves indicate a lower decomposition temperature [see Table 4A.2]. But, as far as the TG curves (Fig. 4A.2) of the pure crystals of the metal complexes are concerned, all three nickel complexes ($R = E, I, B$) are not quite stable at 150° , the processing temperature used for PE. Examination of Figures 4A.2 and 4A.3 indicates that decomposition of these complexes is well under way at temperatures much below T_d [shown in Table 4A.2]. This is evident from the initial decomposition temperatures shown below:

NiDRP	NiDBP	NiDIP	NiDEP
T_i ($^{\circ}$ C)	125	145	150

DiPDiS starts to decompose at even lower temperatures ($T_i \sim 105^\circ\text{C}$). It is found [see Table 4A.7 later] that some of the nickel dialkyl dithiophosphates are lost during processing in PE but that the greatest loss was obtained for NiDEP. This conflicts with the order of thermal stability, in the presence of air, [from TG measurements]. Figure 4A.2 indicates a stability order of NiDRP for the alkyl substituents, R : E > I > B. However, this may be explained if NiDBP is much more compatible with PE than either ethyl or isopropyl analogues. The fact that NiDBP is 'infinitely' soluble [see Sec. 2B.6] in organic solvents than NiDIP is suggestive of a compatibility order in favour of the butyl analogue.

4A.3.2 Thermal Antioxidant Behaviour of Metal Dithiolates and Corresponding Disulfide

During thermal oxidation of unstabilised PE both hydroperoxides and carbonyl compounds undergo appreciable changes^[24]. Hydroperoxides [3555 cm^{-1}] are known to be formed in the early stages of oxidation [during processing]^[24] and during thermal ageing^[96,98] of PE at 110°C in air. These hydroperoxides were also found to be precursors for other oxygen-containing groups^[96,19]; they are formed rapidly and prior to the formation of carbonyls when the polymer is processed in the presence of excess air^[19]. It has also been shown^[19] that the maximum rate of initial carbonyl formation in PE samples processed at long times in the presence of air [e.g. processed for 30 min. in an open mixer] is associated with a higher initial hydroperoxide concentration, and a higher rate of hydroperoxide formation

during subsequent thermal oxidation. Figure 4A.1a also shows this clearly during thermal ageing of PE at 110°. Further, it was found^[105] that acids and ketones are the main carbonyl products which are formed in unstabilised PE during thermal ageing. It has been suggested^[105] that the ketone is 'in-chain' rather than methyl ketone, whereas acids^[105] are a result of chain scission.

In an oxidative environment, NiDRP and NiRX are found to be effective thermal stabilisers for polyethylene. At the same molar concentration, NiRX is somewhat more effective than NiDRP; compare curves 1 and 2 in figure 4A.8 and curve 2 in figure 4A.5.

The processing severity of the polymer affects the persistence of NiRX and NiDRP in the polymer. Table 4A.7 shows that nickel ethyl xanthate is more susceptible to losses compared to the corresponding nickel dithiophosphate.

Table 4A.7 Persistence of NiRX and NiDRP in LDPE film following processing (30, 0M) and compression moulding. Initial concentration of antioxidant is 2.5×10^{-4} M/100g

Antioxidant	Amount of antioxidant remaining in film	
	Concentration [M/100g]	Percentage
NiBX	1.6×10^{-4}	64
NiEX	0.3×10^{-4}	12
NiDBP	1.59×10^{-4}	64
NiDIP	1.35×10^{-4}	54
NiDEP	1.10×10^{-4}	44

Thus after processing the amount of NiEX remaining in the specimen film was only 12% of the complex originally compounded. This is reflected in the short lifetime [20 h] for the disappearance of NiEX during ageing [see curve 7 in Fig. 4A.5, and Table 4A.4]. By comparison, and under the same set of experimental conditions, NiBX showed only limited loss [Table 4A.7] hence the prolonged lifetime [200 h] during ageing experiments [see curve 6 in Fig. 4A.5]. This difference between NiEX and NiBX, i.e. the amount of the complex remaining in the specimen films, must result from differences in compatibility and volatility since results from the non-isothermal weight-loss experiments [see TG curves in Fig. 4A.3] show no real difference in the chemical stability of these two complexes in the presence of thermo-oxidative environment. Instead, the TG curves [Fig. 4A.3] suggest that under the processing conditions used, thermal decomposition [and hence the loss of the metal complex] should effect NiBX more than NiEX.

The actual amounts of NiBX and NiEX present cannot be fully responsible for the thermo-oxidative stability of polyethylene. Table 4A.4 shows that NiEX is less effective than NiBX under thermo-oxidative conditions. However, Table 4A.7 shows that a substantial part of the NiEX originally present must have been converted [through the disulfide] to the effective thermal antioxidant since only 12% of the original metal complex was still present after processing. Table 4A.4 shows that this disappeared within 20 h of thermal oxidation, compared with TIP of 450 h.

Scott and co-workers^[23,32,44,47] have shown that products formed from metal dithiolates are effective thermal antioxidants rather than the metal complexes themselves. Studies in model systems have demonstrated the formation of disulfides as initial transformation products during the antioxidant function of xanthates and dithio-phosphates. This will be discussed in Chapter 7. Further, disulfides were found to be precursors of a variety of oxyacids of sulfur^[47,29] which are effective catalysts for the ionic decomposition of hydroperoxides. Typical disulfides [DiPDiS and IX] were, therefore, used to examine their effectiveness as thermal stabilisers in the polymer. The behaviour of these disulfides was found to be only slightly inferior to that of the parent nickel complexes [e.g. compare curves 2 and 3 in Fig. 4A.8] and similar to that of the extracted films [e.g. curve 3 in Fig. 4A.8]. Further, the behaviour of both NiDRP and NiRX under processing conditions is quite complex since antioxidant residues formed by thermal oxidative destruction of the initially added complex become chemically bound to the polymer giving rise to powerful thermal antioxidant activity. This antioxidant activity appears to be only slightly influenced by the amount of nickel complex present in the film prior to thermal ageing.

Chemically bound antioxidants^[108,109] do not suffer from the common problem of volatilisation or extraction and have been used to overcome shortcomings of unbound stabilisers. The failure to affect a reduction in the observed TIP by an extractive treatment of films containing

NiDAP and NiRX, prior to thermal ageing [see curves 2 and 3 in Fig. 4A.8, and curves 2 and 4 in Fig. 4A.5] is a clear indication of the unextractable nature of the species involved in the stabilisation of the matrix, which must, therefore, have been formed from the parent nickel complexes [nickel complexes themselves are fully extracted under the experimental conditions used, see Sec. 2A.2.3] during processing. Direct evidence for the bound antioxidant formed from nickel dithiophosphate will be discussed later [Sec. 5.2.1].

For thermally feasible oxidations, higher concentration of oxygen should result in greater formation of disulfide-based oxidation products [oxyacids of sulfur]. Figure 4A.6 displays the improvement in the behaviour of stabilised PE by NiBX in the presence of oxygen. A consequence of this is an improvement in the thermo-oxidative stabilisation efficiency since the oxyacids of sulfur are the real catalysts for decomposing the hydroperoxides^[47,29] which otherwise have a detrimental effect on the polymer stability.

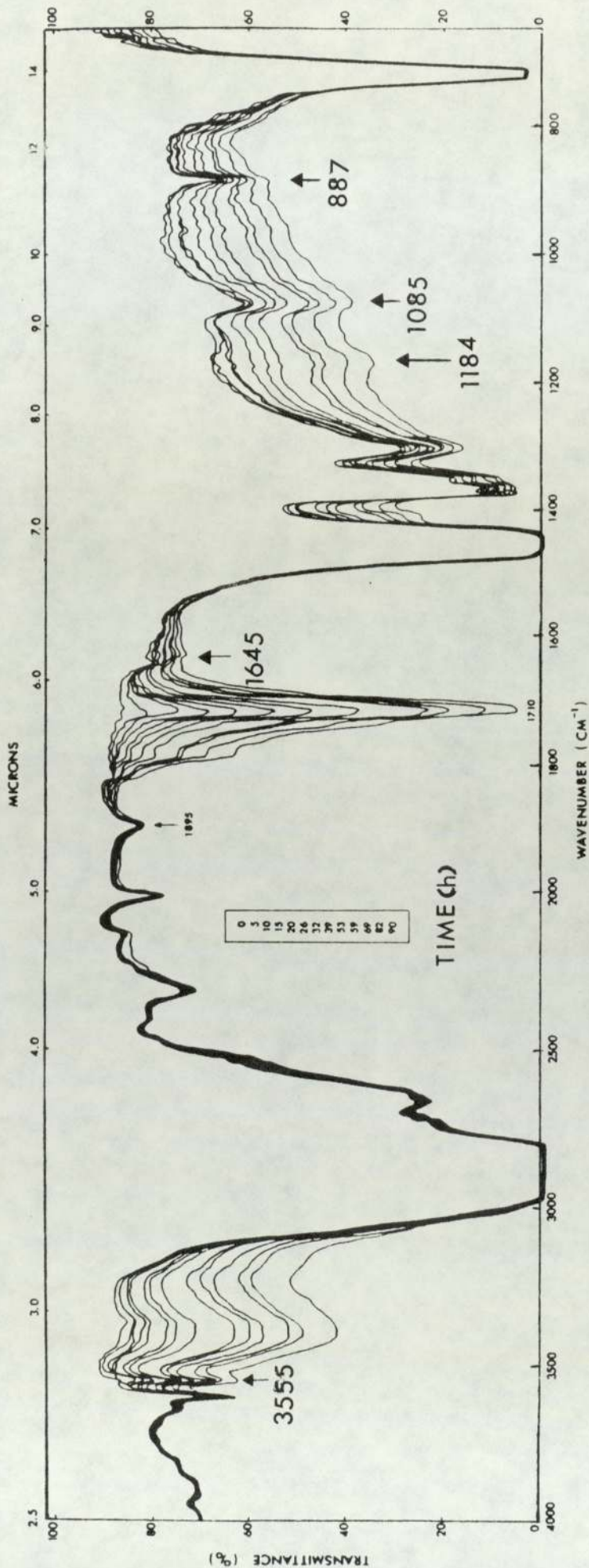


Fig. 4A.1 Changes in the infrared spectra of unstabilised LDPE (10,CM) during photo-oxidation (exposure times shown in hours).

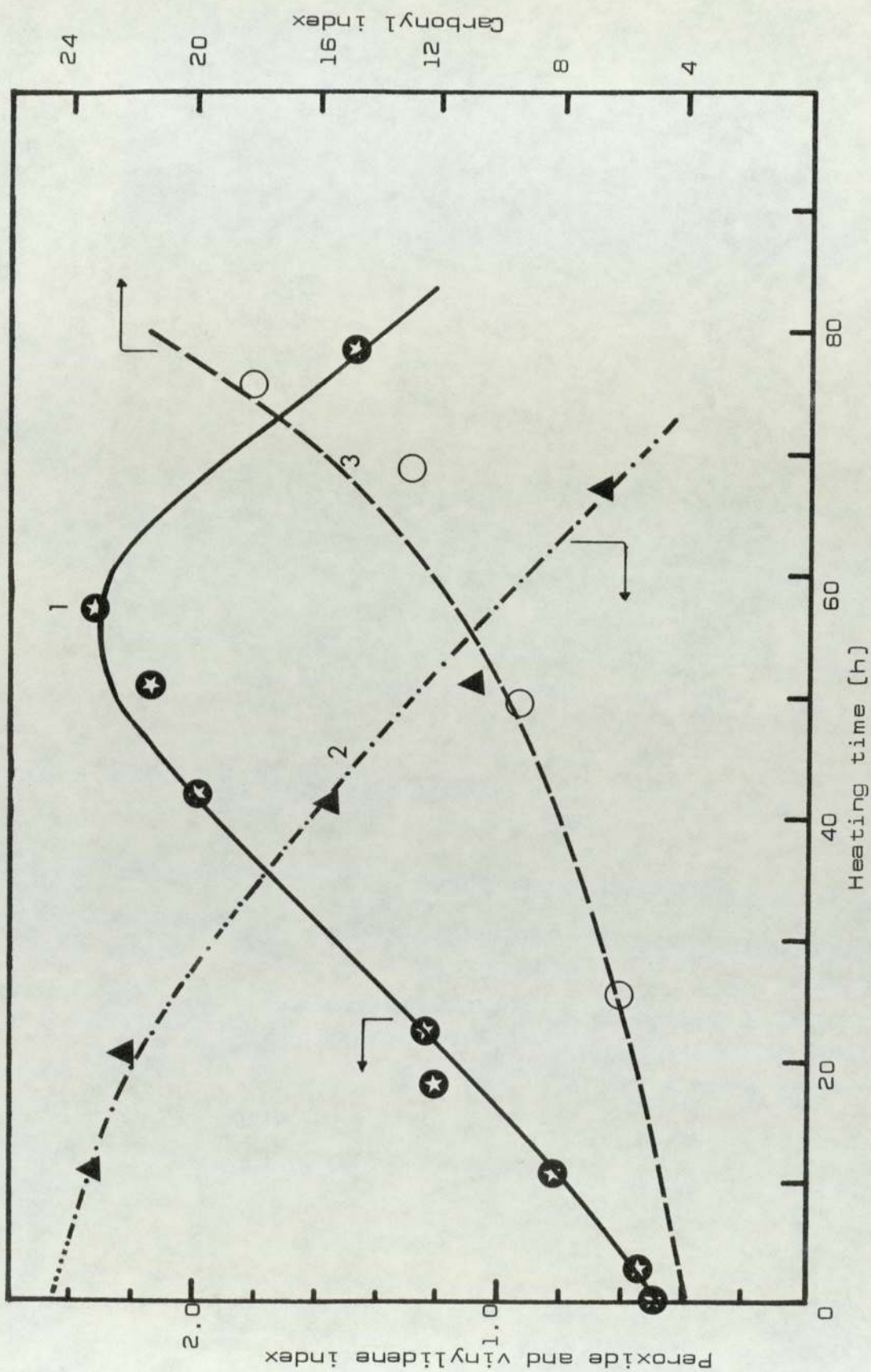


Fig. 4A.1a Changes in functional groups during thermal oxidation (at 110^o) of unstabilised LDPE processed (30,0M) at 150^o. [1] hydroperoxide at 3555cm⁻¹; [2] vinylidene at 887cm⁻¹; and [3] carbonyl at 1710cm⁻¹.

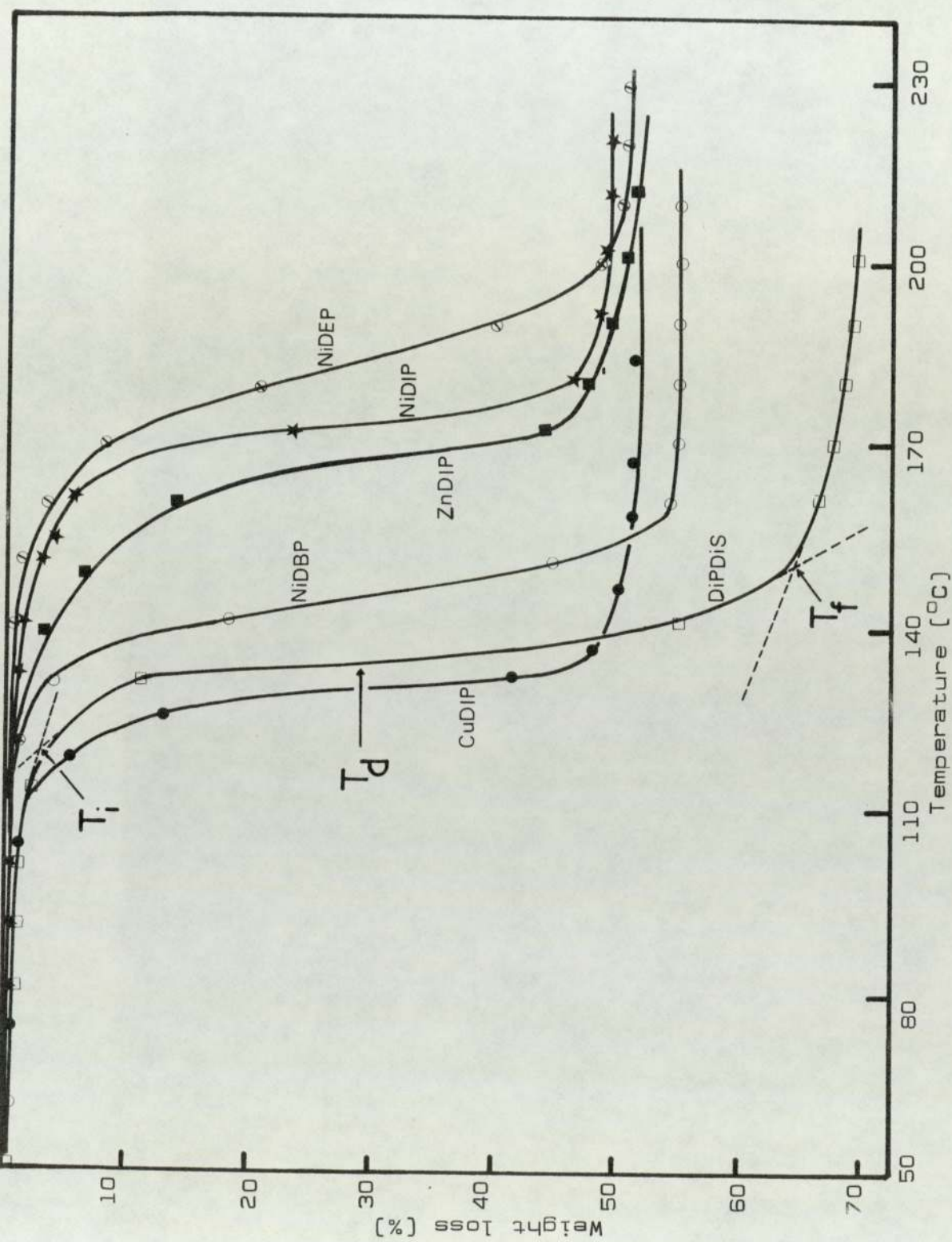


Fig. 4A.2 Non-isothermal weight loss of metal dithiophosphate and di-isopropyl thiophosphoryl disulfide showing T_i , T_D and T_f . [see text for explanation].

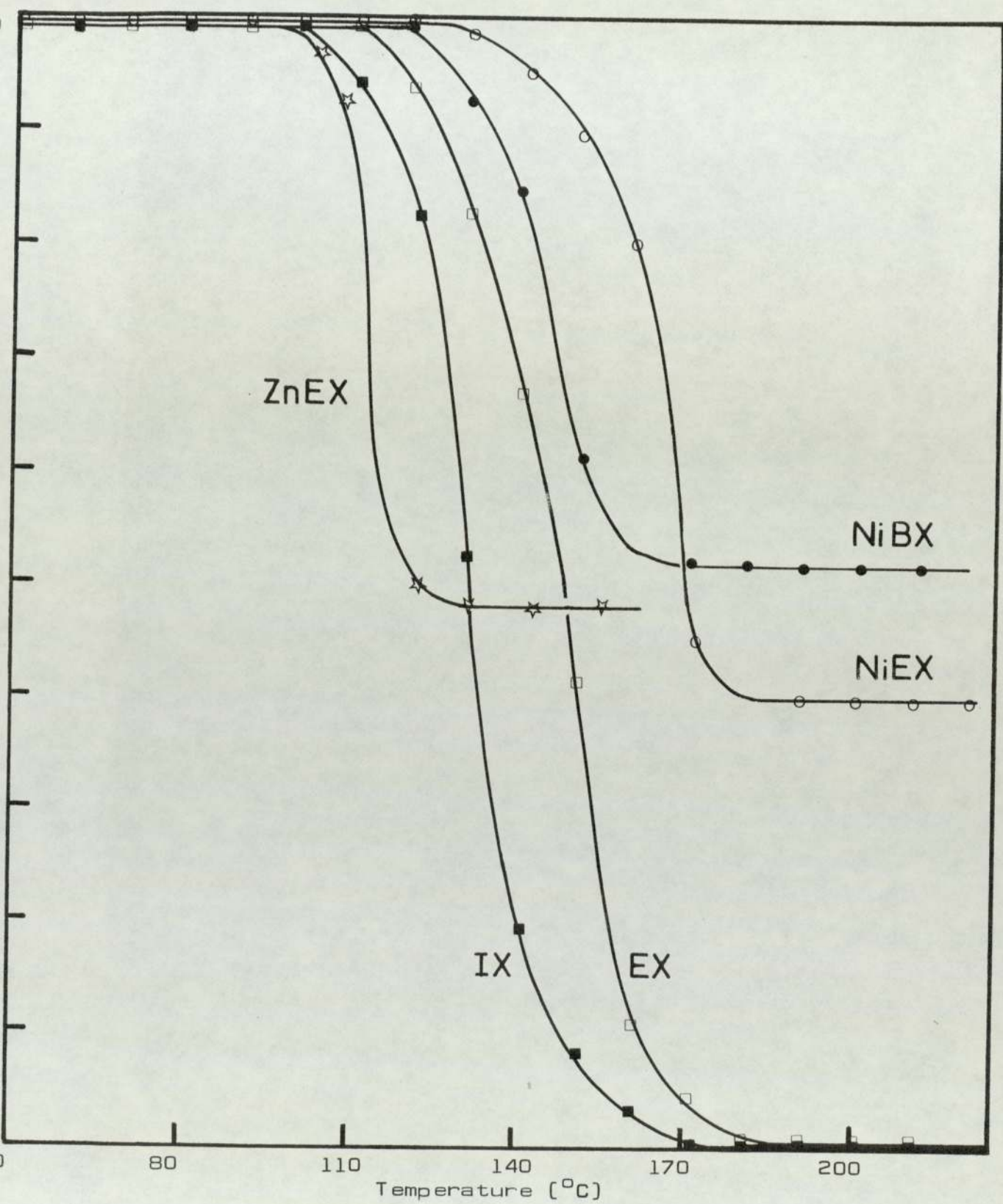


Fig.4A.3 Non-isothermal weight loss of metal alkyl xanthates and dixanthogens

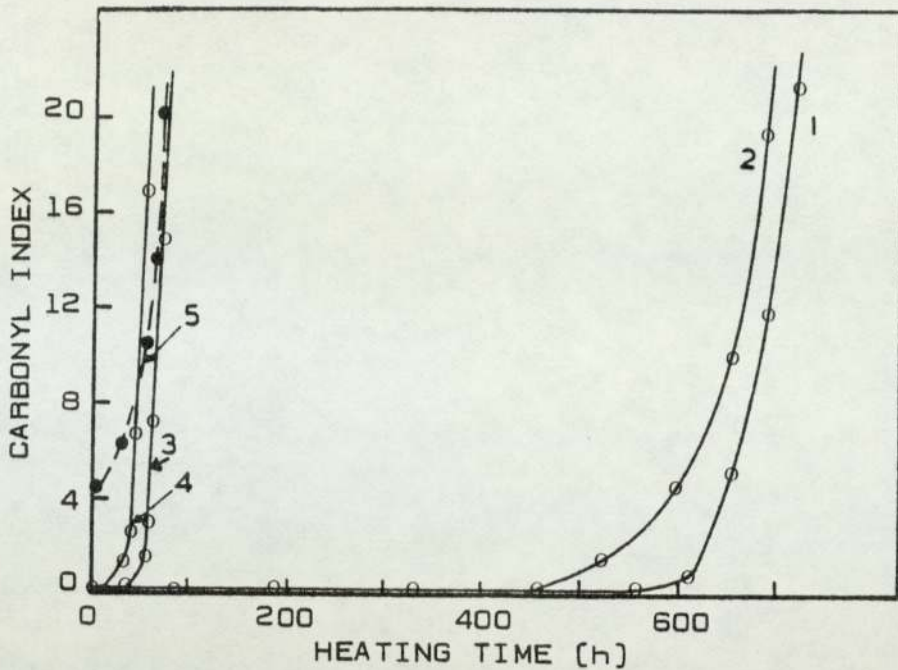


Fig.4A.4 Effect of thermal oxidation [at 110°] in the presence of air on LDPE films containing additives ($2.5 \times 10^{-4} \text{M}/100\text{g}$). [1] NiBX, [2] NiEX, [3] CuBX, [4] ZnEX, [5] control [no additives]. All samples are processed (30,0M) at 150° .

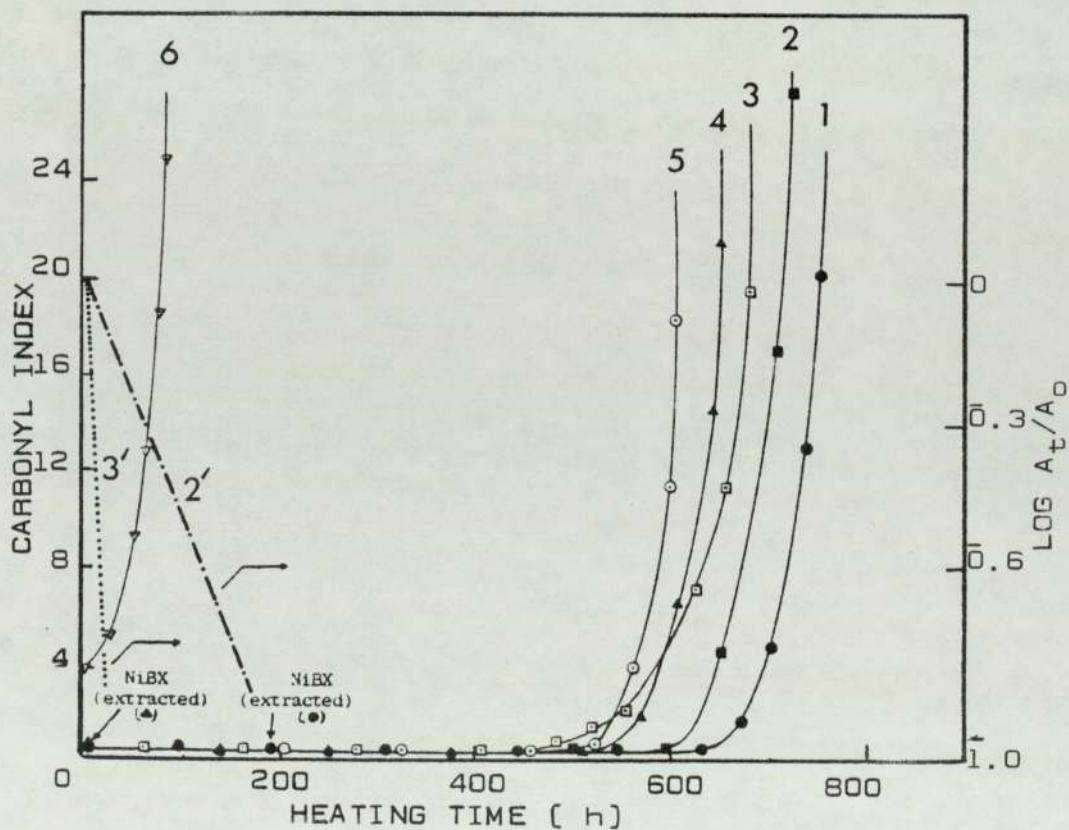


Fig.4A.5 Effect of thermal oxidation [at 110°] in the presence of air on LDPE films containing additives ($2.5 \times 10^{-4} \text{M}/100\text{g}$). [1] NiBX extracted after the destruction of the complex [200h at 110°], [2] NiBX untreated, [3] NiEX untreated, [4] NiBX extracted prior to oven ageing, [5] IX, [6] control [no additives]. All samples are processed (30,0M) at 150° . Kinetics of disappearance of the 316 nm band of untreated NiBX [2'] and NiEX [3'] is also shown.

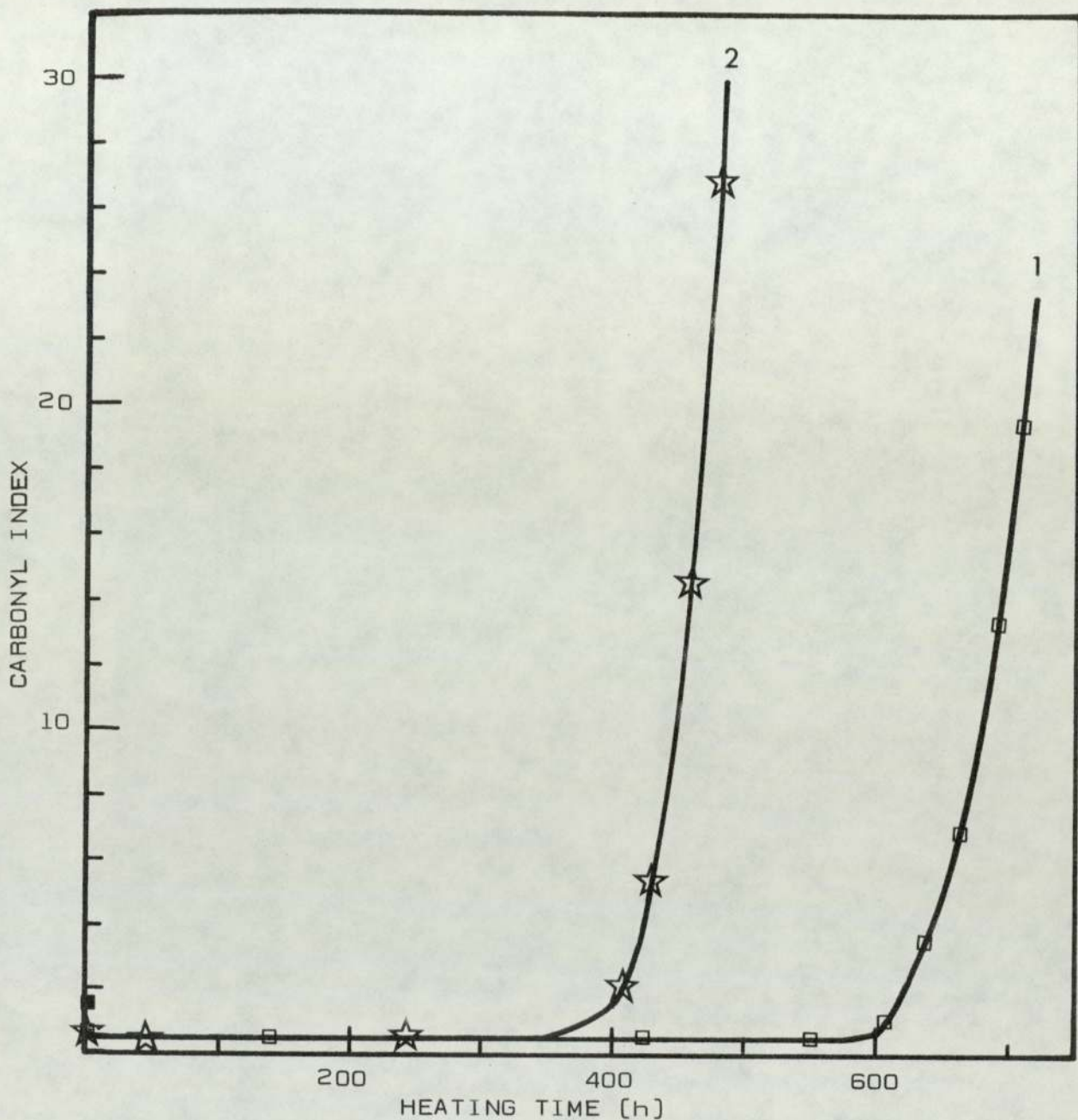


Fig.4A.6 Effect of processing for 30 min. at 150° in an open [1] and closed [2] mixer on thermal oxidation [at 110°] of LDPE films containing NiBX ($2.5 \times 10^{-4} \text{M}/100\text{g}$).

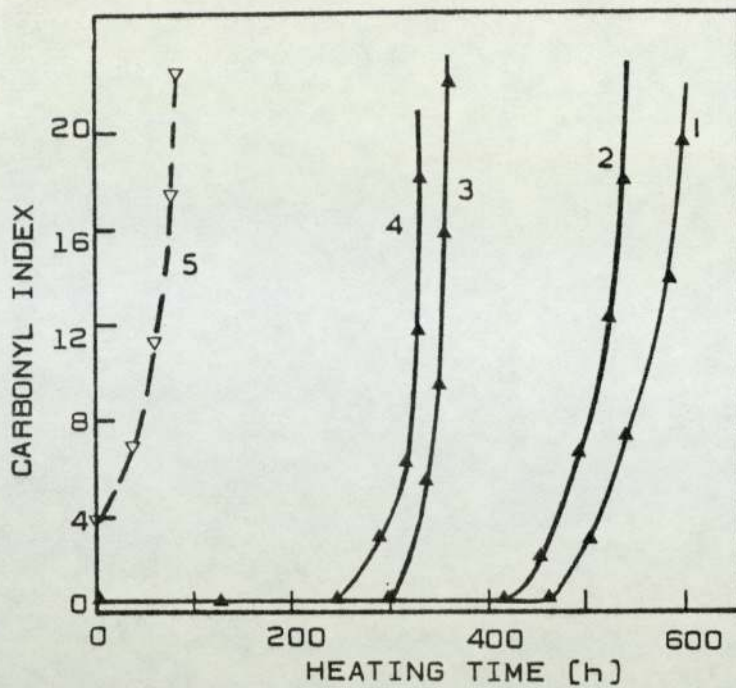


Fig.4A.7 Effect of thermal oxidation [at 110°] in the presence of air on LDPE Films containing additives [$2.5 \times 10^{-4} \text{M}/100\text{g}$] [1] NiDBP, [2] NiDIP, [3] CuDIP, [4] ZnDIP, [5] control [no additive]. All samples are processed [30,0M] at 150° .

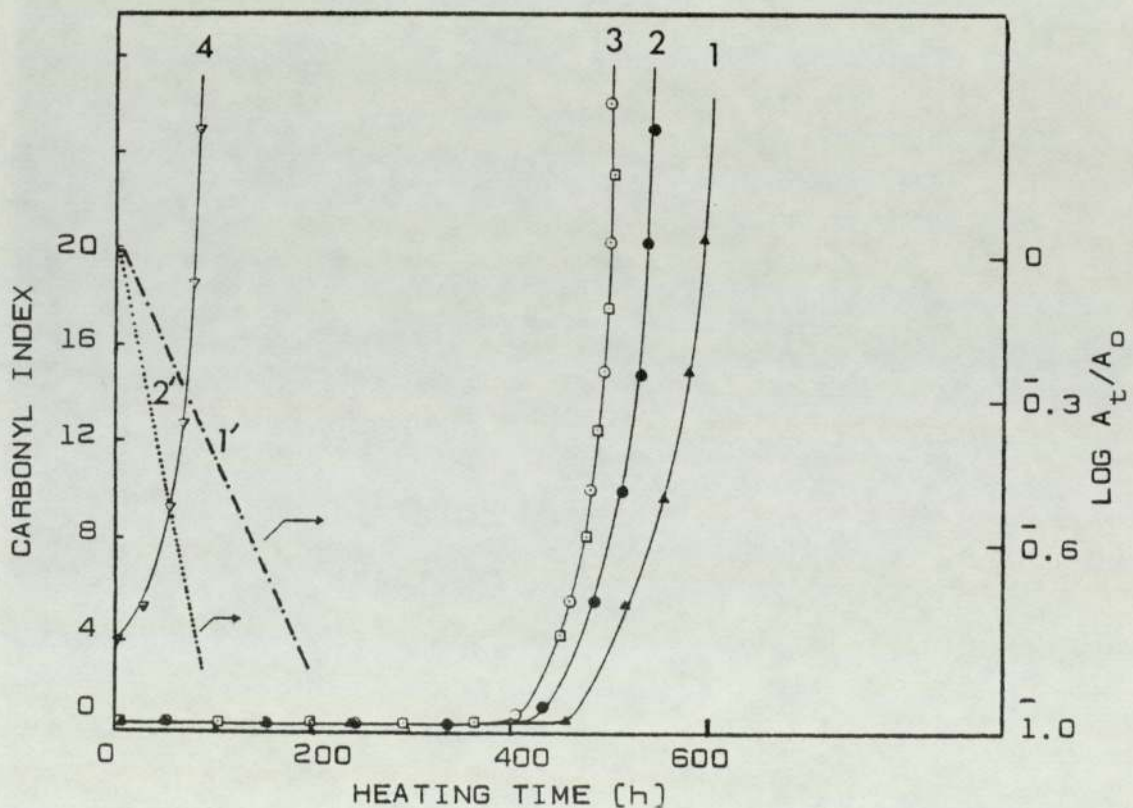


Fig.4A.8 Effect of thermal oxidation [at 110°] in the presence of air in LDPE Films containing additives [$2.5 \times 10^{-4} \text{M}/100\text{g}$], [1] NiDBP untreated, [2] NiDIP untreated, [3] NiDIP extracted and DiPDiS untreated, [4] control [no additives]. Kinetics of disappearance of 316 nm of NiDBP [1'] and NiDIP [2'] is also shown. All samples are processed [30,0M] at 150° .

48. THE INFLUENCE OF METAL DITHIOLATES AND CORRESPONDING
DISULFIDES ON THE PHOTO-OXIDATIVE STABILITY OF LDPE

48.1 OBJECT

In this chapter the photo-oxidative stability of LDPE is examined in the presence and absence of MDRP and MRX, and the derived disulfides. Equimolar synergistic combinations (2.5×10^{-4} M/100g of each component) of these additives and a commercial 'UV-absorber', 2-hydroxy-4-octyloxybenzophenone (HOBP), are also evaluated. Typically the additive (2.5×10^{-4} M/100g) is mixed with unstabilised LDPE and processed for various lengths of time in closed (CM) and open (OM) mixer of the torque-rheometer at 150° . Test films were then prepared from these stabilised PE samples by compression moulding. Sections of comparable thickness (2×10^{-4} cm) are cut from these films and are exposed in the UV-cabinet and subsequently tested. Spectral changes occurring during the course of UV-exposure are followed for these films by IR- and UV-spectrophotometry; additives' lifetimes in the test films are determined, therefore, under these photo-oxidative conditions.

4B.2 RESULTS

4B.2.1 Photo-oxidative Stability of Unstabilised LDPE

The effect of UV-light on films of unstabilised PE [control] was followed by IR spectrophotometry. Figure 4B.1 shows changes in the IR spectra of mildly [10,CM] processed PE, at various intervals during the course of photo-oxidation. Table 4A.1 [see Sec.4A.2.1] lists the various groups which are found in photo-oxidised PE. Of importance here are the functional groups, carbonyl [ca.1710 cm^{-1}], vinyl [909 cm^{-1}] and vinylidene [887 cm^{-1}] which show clear and large changes throughout the useful lifetime of an unstabilised film of LDPE.

4B.2.2 Photo-oxidative Stability of PE in the Presence of MDRP and DiPDiS

Figure 4B.2 compares the effect of processing severity [in open mixer] on the oxidative stability of unstabilised PE [curve 1], and PE which was stabilised by NiDRP [R=I,B] and DiPDiS [curve 3]. The effect of severe [30,OM] and milder [30,CM] processing on the performance of the NiDRP [R=I,B] is shown in figure 4B.3. A long photo-oxidative induction period [PIP] is observed in each case. It is clear that the lifetime of NiDRP [curves 1' and 2'] is directly related to the length of the PIP [see curves 1 and 2].

Examination of figure 4B.3 shows that NiDBP affords greater photo-oxidative stability to LDPE than NiDIP in both closed [cf. curves 6 and 7] and open [cf. curves 1 and 2] mixer. Table 4B.1 gives the induction periods afforded by

each of these complexes under the different processing conditions used. Table 4A.7 [see Sec.4A.3.2] shows the actual amounts of NiDRP which were found to persist in the film specimen under test. Figure 4B.4 shows the changes in the UV-absorption spectra of a mildly [5,CM] processed NiDBP-stabilised PE film during UV exposure. An increase in the window region of NiDBP around 260 nm [which is the region of the disulfide absorption [see Fig.2B.1b, Sec.2B.2.1] accompanies the monotonic decrease of the 316 and 230 nm bands of the nickel complex.

Table 4B.1 Photo-oxidative induction period (PIP) observed for some mildly [30,CM] and severely [30,OM] processed nickel dithiolate-stabilised PE films

Nickel complex	PIP (h)	
	[30,CM]	[30,OM]
NiDBP	900	600
NiDIP	350	200
NiBX	600	340
NiEX	180	undetected

The photo-oxidative stabilisation afforded by DiPDiS [Fig.4B.5] for severely [open mixer] and mildly [closed mixer] processed PE indicates that DiPDiS is a better photo-stabiliser when processed in the presence of an ample supply, i.e. conditions of open mixer, of oxygen [cf. curves 1 and 7]. More severe conditions, therefore, appear to improve the

extent of photostabilisation [cf. curves 7 and 8]. The behaviour of NiDIP [reproduced in Fig.4B.5] displays the opposite effect [cf. curves 2 and 6]. The observation that a photo-oxidative induction period was seen for NiDIP stabilised PE, whereas no real induction period was found for a DiPDiS stabilised film [cf. curve 6 with 7 in Fig.4B.5] suggests, therefore, that a further transformation product is involved in the activity of DiPDiS whereas the metal complex itself is probably the main stabiliser in the case of NiDIP.

Extraction of NiDIP from the stabilised-PE film prior to UV exposure completely removes the induction period which is present in the unextracted stabilised film [cf. curves 2 and 3 in Fig.4B.5]. The photo-oxidative behaviour of the NiDIP-extracted [curve 3] PE film is qualitatively similar to a DiPDiS-stabilised PE film. This similarity becomes self-evident when extracted DiPDiS-stabilised PE film [curve 4] is compared with an extracted film containing NiDIP [curve 3]. Similar findings were obtained with NiDBP [Fig.4B.6].

Figure 4B.7 shows that the photo-oxidative stability of PE is markedly improved by CuDIP [curve 3] compared to the limited stabilisation afforded by ZnDIP [curve 2]. An induction period of ca.450 h was observed for CuDIP-stabilised PE whereas no PIP was observed for ZnDIP-stabilised film.

4B.2.3 Photo-oxidative Stability of PE in the Presence of MRX and RX

The effect of processing severity on the efficiency of NiRX (R=E,B) and disulfides (RX) as antioxidants in PE is

shown in figures 4B.8 and 4B.9. NiBX [curve 1 in Fig.4B.8] affords a clear stabilisation [PIP=340 h] under severe [30,0M] processing conditions and which becomes even greater [PIP=600 h] with milder [30,CM] processing [curve 4'].

In contrast to NiBX, NiEX appears much less effective under these processing conditions: a PIP of 300 h was observed for a mildly processed sample [curve 5 in Fig. 4B.8] and this was drastically curtailed with severe processing [curve 2]. Induction periods afforded by NiRX are shown in table 4B.1. The time of complete disappearance of the NiRX corresponds almost exactly to the end of the PIP [see curves 2 and 2' in Fig. 4B.9]. A similar observation is made for NiDRP [see curves 1 and 1'].

Figure 4B.10 shows changes in the UV absorption spectra of a mildly [5,CM] processed NiEX-stabilised PE film during UV-exposure. As in the case of NiDRP, the disappearance of the parent complex band at 316 nm is accompanied by the appearance of a new absorption feature at 275 nm. This compares well with the results of photolysis of NiRX in solution [Sec.3.2.1.1].

Figure 4B.11 compares the photo-oxidative stability of PE containing NiRX [R=E,B] and RX [R=E,I] at the same molar concentration. Under the severe processing conditions used, NiBX [curve 1] showed a PIP of 340 h whereas NiEX [curve 2] has only a marginal PIP. The effect of extraction on IX-containing PE film [curve 5] is found to effect only a slight reduction in the photo-oxidative stability of PE. Examination of figure 4B.11 indicates that during the first 400 h of

UV-exposure both NiEX [curve 2] and EX [curve 3] appear to impart identical photo-oxidative stability to PE. Since the amount of NiEX remaining in the film under test is only 12% [see table 4A.7, Sec.4A.3.2] of the original complex used, a substantial part of the NiEX unaccounted for must have been transformed to dixanthogen, EX.

The photo-oxidative behaviour of IX- and DiPDiS-stabilised PE, which was processed in open and closed mixer, are compared in figure 4B.12. Of interest here is the reversal in the order of photo-oxidative stability of the polymer in the presence of these disulfides on going from mild to severe processing, i.e. they are more stable under severe conditions; this effect is less pronounced in the case of dixanthogen.

Figure 4B.13 compares the photo-oxidative stability of LDPE in the presence of ZnRX under very mild [5,CM] and severe [30,0M] processing conditions. Compared to the control, ZnEX [curve 5] and ZnIX [curve 6] exhibit pro-oxidant effects for mildly processed ZnRX-containing PE. A somewhat better stabilising effect is seen in the severely processed ZnEX-stabilised PE. CuBX [curve 1] is included for comparison.

4B.2.4 Evaluation of the Photo-oxidative Stability of PE in the Presence of Synergistic Mixtures of HOBP with Metal Dithiolates and Corresponding Disulfides

The effect of HOBP on the oxidative stability of LDPE during processing is compared with that of NiDRP and NiRX at the same molar concentrations in figure 4B.2. Further, the extent of photostabilisation afforded by an equimolar

mixture of HOBP and NiDBP is compared with the behaviour of NiDBP alone under identical conditions (Fig.4B.14). Under mild processing conditions (30,CM) the NiDBP-HOBP combination (curve 2 in Fig.4B.14) imparts greater photo-stabilisation to PE during the induction period (see table 4B.2) than under severe conditions (30,0M); curve 1 in Fig.4B.14.

Table 4B.2 Photo-oxidative induction period (PIP) obtained for some mildly (30,CM) and severely (30,0M) processed stabilised-LDPE films

Stabiliser	Photo-oxidative induction period (PIP) h			
	(30,0M)		(30,CM)	
	Obs.	Calc. ^a	Obs.	Calc. ^a
HOBP	none	-	150	-
NiDBP	600	-	900	-
NiDBP + HOBP	1000	600	1200	1050
DiPDiS	none	-	none	-
DiPDiS + HOBP	600	none	500	150
NiBX	600	-	340	-
NiBX + HOBP	1000	600	-	-
IX	none	-	-	-
IX + HOBP	450	-	-	-

^a Calculated on additive basis of the components.

However, the overall photostabilising effectiveness of NiDBP-HOBP combination, under severe processing conditions, is much greater when compared with the mildly processed combination

Table 4B.3 Comparison of UV-stabilisers in LDPE

[concentration of all additives 2.5×10^{-4}
M/100g]

Stabiliser ^(b)	EMT [h]	Calculation on additive basis [h]	% synergism ^(a)
LDPE [control]	1050	-	-
HOBP	1700	-	-
NiDBP	2800	-	-
NiDBP ^(c)	3300	-	-
NiDBP + HOBP	5500	4500	261
NiDBP + HOBP ^(c)	4000	-	-
DiPDiS	2150	-	-
DiPDiS + HOBP	5500	3850	265
DiPDiS + HOBP ^(c)	2550	-	-
CuDIP	2300	-	-
CuDIP + HOBP	5350	4000	205
NiBX	2500	-	-
NiBX + HOBP	4900	4200	208
IX	1800	-	-
IX + HOBP	4800	3500	255
CuBX	-	-	-
CuBX + HOBP	3300	-	-

$$[a] \% \text{ Synergism}^{[1b]} = \frac{[E_s - E_c] - [(E_1 - E_c) + (E_2 - E_c)]}{E_1 - E_c + E_2 - E_c} \times 100$$

where E_s = embrittlement time of synergist; E_c = embrittlement time of control; E_1 = embrittlement time of antioxidant 1 and E_2 = embrittlement time of antioxidant 2

[b] processed in an open mixer for 30 min.

[c] processed in a closed mixer for 30 min.

[cf. curves 1 with 2 in Fig.4B.14]. This is reflected in longer embrittlement times [table 4B.3] for the severely processed sample. The different extent of conversion of NiDBP into disulfides under mild and severe processing conditions can explain the difference in the antioxidant activity of this same mixture under these conditions.

Examination of curves 3 to 1 in figure 4B.15 reveals the greater photostabilising effectiveness of the DiPDiS-HOBP mixture when processed under severe conditions (see also table 4B.3 for EMT). Compared to a DiPDiS-stabilised PE [control] film, the 1:1 DiPDiS-HOBP combination is ten times more effective [cf. curves 1 with 5, and 3 with 5 in Fig. 4B.15]. Combination of HOBP with NiDBP or DiPDiS, under all processing conditions used here, showed clear synergistic effects [table 4B.3], the effectiveness of which increased with increasing processing severity. Figure 4B.16 compares the considerable stabilisation achieved with DiPDiS [curves 1 and 6], NiDBP [curves 2 and 4] and CuDIP [curves 3 and 5] in the presence and absence of HOBP, respectively. DiPDiS-HOBP [curve 1; see also table 4B.3] offers the best synergistic system.

Synergistic mixtures of HOBP with cuprous and nickel xanthates, or dixanthogen [IX], are also quite good photostabilisers for PE when processed for 30 minutes in open mixer [Fig.4B.17]. These findings are qualitatively similar to those of the synergistic mixtures of dithiophosphates with HOBP.

Figure 4B.18 shows the weight loss curves for pure crystals of DiPDiS (curve 1), HOBP (curve 2) and a mixture of DiPDiS and HOBP (curve 3) (weight of each component and the total weight of the mixture was fixed at 0.035 g). It is clear that HOBP is fairly stable at temperatures well above the processing temperatures for PE (150°). Volatilisation of HOBP begins ca. 150° and a weight loss of 100% is obtained ca. 250° under the experimental conditions used (see Sec.2A.8). The thermal behaviour of DiPDiS has been described earlier (see Sec.4A.2.1). Compared to HOBP, DiPDiS volatilises at much lower temperatures and is almost totally decomposed (with a weight loss of 70%) at around 150° . The TG curves for the mixture of DiPDiS and HOBP indicate an additive weight loss behaviour for both components.

4B.3 DISCUSSION

4B.3.1 Photo-oxidation Stability of Unstabilised LDPE

Photo-oxidised PE films contain the same kind of carbonyl groups as is found in thermally oxidised films^[99]. The importance of hydroperoxides as photo-initiators during the initial stages of photo-oxidation of polyolefins has been well documented^[11,17,20,24,111]; hydroperoxides present initially decay rapidly during photolysis to undetectable level^[45]. This is evident from Fig.4B.1 which shows no hydroperoxide absorption at 3555 cm^{-1} in photo-oxidised films of PE. The contribution of carbonyl groups to the overall degradation is quite extensive as can be seen from IR spectra of a degrading PE film [see Fig.4B.1]. Carboxylic acids [1710 cm^{-1}], the ultimate products of PE photo-oxidation, have been shown^[11,17,20,24,111,112] to result from the photolysis of in-chain ketones. Pronounced changes in the relative contribution of vinylidene [887 cm^{-1}] and vinyl [909 cm^{-1}] groups is a characteristic of photo-oxidised film [Fig.4B.1]: vinylidene decreases and vinyl group increases.

It has been shown^[19] that the effect of prior heat treatment on vinylidene decay during UV irradiation and thermal ageing are similar. Photolysis of carbonyl results in a Norrish II process [see Sec.1.2] since there is a rapid formation of vinyl groups during photolysis of the polymer^[24]. Because of this, changes in vinylidene are more difficult to measure at later stages of photo-oxidation. Impressive correlation has recently been found^[24] between the degree of oxidation of PE and the amounts of carbonyl, vinylidene, and vinyl groups present.

Figure 4B.3 shows the photo-oxidative stability of unstabilised PE [curve 3] processed in the presence of an ample supply of air [30,0M]. It has been shown^[19] that under these conditions maximum amounts of hydroperoxides along with relatively high concentration of vinylidene are present. In addition, the sharp increase in the carbonyl index [see curve 3] which is found [see also reference 19] to occur during the early stages of photo-oxidation is associated with the destruction of hydroperoxides and the concomitant disappearance of vinylidene unsaturation [see decay of absorption at 887 cm^{-1} in Fig.4B.1]. The observed autoretardation in the photo-oxidation of unstabilised PE [curve 3 in Fig.4B.3] has been associated with the reduction in the hydroperoxide concentration by photolysis^[20]. The rapid formation of vinyl groups [see Fig.4B.1] has been correlated^[24] with the photolysis of carbonyl groups via a Norrish II reaction. The formation of aldehydes and carboxylic acids during the later stages of photo-oxidation has been associated^[113,114] with carbonyl photolysis via Norrish I reaction [see Sec.1.2].

4B.3.2 Photo-oxidative Stability of PE in Presence of Nickel Dithiolates and Corresponding Disulfides

It has been shown^[19,24] that processing effects a marked reduction in the UV-stability of unstabilised PE. This has largely been attributed^[19,24] to the formation of hydroperoxides under the thermo-oxidative conditions of processing. The adverse effect of processing on the oxidative stability of unstabilised PE, even before exposure to UV-light, is evident from the initial level of the carbonyl index

obtained under conditions of different processing severity [see curve 1 in Fig.4B.2], i.e. higher carbonyl indices for more severe conditions. Removal of peroxides from unstabilised PE, viz. by heating in the absence of oxygen, was found^[19] to be effective in enhancing the photostability of PE to a level which was comparable to that of unstabilised PE which had not been subjected to processing.

Processing of unstabilised LDPE in the presence of 2.5×10^{-4} M/100g of nickel dithiophosphates and xanthates, and their corresponding disulfides, DiPDiS and RX, did not give rise to increased levels of carbonyl index [Fig.4B.2, curve 3] with increasing processing severity. These compounds must, therefore, be acting to remove hydroperoxides formed during processing. Further, the effectiveness of these additives in decomposing hydroperoxides was shown in the present work [see Sec.7.3] to be chiefly due to the formation of an ionic catalyst which can destroy the hydroperoxides. Similarly, the effectiveness of nickel dialkyl dithiocarbamate [NiDRC] as UV-stabilisers for polyolefins was found^[23,44-46,106,107] to be primarily due to their ability to generate an ionic catalyst for the destruction of hydroperoxides.

In addition to hydroperoxide decomposition, nickel dithiolates function as light stable reservoirs for the catalytic species^[45,46]. Thus both NiDRP and NiRX are very effective UV-stabilisers for LDPE [Fig.4B.3 and 4B.8]; on a molar basis nickel xanthates are less effective. The high molar extinction coefficients [see Sec.2B.2.1 and 2B.3.1] of the metal-ligand bands in these nickel complexes accounts

for much of their UV-stabilisation effectiveness, e.g. by absorption, energy transfer, screening. In the absence of hydroperoxides, the photo-oxidative stability of nickel complexes in inert solvents under similar photolysis conditions was found [see Sec.3.2.1 and 3.2.3] to be quite extensive; this is further support to the above observation on the UV-stabilisation of nickel dithiolates.

Photo-oxidation of NiDRP (R=I,B) stabilised PE film is greatly dependent on the method of sample preparation. PE samples processed in the presence of NiDIP and NiDBP under severe and mild conditions exhibit characteristically different induction periods [cf. curves 6 and 7 with 1 and 2 in Fig.4B.3]. Longer induction periods [see table 4B.1] are obtained with NiDBP under both severe and mild conditions; compare 600 and 900 h for NiDBP with 200 and 350 h for NiDIP. The superior performance of NiDBP is closely linked to its greater compatibility in PE compared to NiDIP [see Sec.2B.4]. The fact that higher concentrations of NiDBP were found to remain in the PE test films when the same molar concentrations of NiDBP and NiDIP were originally mixed with unstabilised PE in the torque-rheometer [see table 4A.7, Sec.4A.3.2] indicates a greater retention of the butyl-derivative by the polymer.

The behaviour of nickel xanthates is similar to nickel dithiophosphates: NiBX is more compatible [see Sec.2B.5] in, and imparts greater UV-stability to, LDPE than NiEX, [Fig. 4B.7 and table 4B.1]. Increased processing severity has a more adverse effect on the performance of NiEX than NiDEP [see table 4A.7, Sec.4A.3.2]. Thus NiEX is more susceptible

to losses during processing. Examination of table 4A.7 and figure 4B.7 reveals that NiEX is considerably less effective as a stabiliser than NiBX under photo-oxidative conditions; under the severe processing [curve 2 in Fig.4B.8] NiEX shows marked reduction in its stabilising effect compared to the case of mild processing [Fig.4B.8, inset, curve 5].

It was shown earlier [see Sec.4A.3.2 and table 4A.7] that a substantial part of NiDRP and NiRX, originally compounded with unstabilised LDPE was converted to the effective thermal antioxidant via the disulfides [see Sec. 7.3]. It is clear, therefore, that there is no direct relationship between the observed thermo-oxidative stabilisation afforded by metal dithiophosphates and the actual amounts of metal dithiolates which had survived the processing stage. This further confirms the all important role of disulfides and their oxidation products which are formed from nickel dithiolates, as oxidation inhibitors during processing and ageing of stabilised LDPE. A linear relationship was found, however, between the observed photo-oxidative induction period and the lifetime of the nickel complexes remaining in the PE films [compare curves 1 and 2 with curves 1' and 2' in Fig.4B.9].

Thus, for example, 36% NiDBP is lost [this includes the conversion to disulfide initially] during severe processing compared to a mere 10% loss under milder conditions.

Earlier studies [23,32,44,47,106,107] and the present work [see Secs.4A.2.3,4A.2.4, and Sec.7.3] clearly argue for the effectiveness of oxidation products formed from the different metal dithiolates as thermal stabilisers for PE rather than the metal complexes themselves. Disulfides are formed initially and these are precursors of a variety of oxyacids of sulfur [Sec.7.3^[32,47]] which are effective catalysts for the ionic decomposition of hydroperoxides. The antioxidant residues formed during the course of thermal oxidative destruction of the metal complexes (NiDRP and NiRX) must become chemically bound to the polymer [see Secs.4A.2, 5.2 and 7.2] giving rise to powerful thermal antioxidant activity and more limited UV-stabilising activity in the tested films. This explains the reason why nickel dithiolate-stabilised PE's [see Sec.4A.2.3 and 4A.2.4] are found to effect greater thermo-oxidative, as against photo-oxidative, stability when processed under severe conditions.

The much weaker photostabilising activity of the bound antioxidant is reflected in the absence of an induction period [curve 7 in Figs.4B.12 and 4B.5, and curve 4 in Fig. 4B.11], compared to the long photo-oxidative induction periods afforded by the corresponding nickel complexes [see curve 6 in Fig.4B.5, and curve 1 in Fig.4B.1]. In fact, these induction periods are not strictly representative of either the nickel complexes or the bound antioxidants, since there is always the simultaneous presence of intact metal complex and metal complex-derived antioxidants. Effectively, therefore, the metal dithiolates behave as inherently

controlled synergistic mixtures. The initial composition of this inherently synergistic mixture is a function of the processing conditions used. Thus, for example, nickel dithiolate-stabilised PE exhibits higher thermo-oxidative stability [see Secs.4A.2.3 and 4A.2.4] when processing is severe [e.g. 30 minutes in open mixer] whereas the highest photo-oxidative stability is attained with the mildest processing time [minimum time in a closed mixer]. Each of these extremes of processing conditions provide inherently synergistic mixtures of widely different compositions and, inadvertently, different thermo- and photo-stabilising effectiveness.

The important role of the metal complex-derived anti-oxidants is elucidated further from examination of the oxidative stability of toluene-extracted PE films containing these metal complexes. Films which were extracted after processing, but before exposure to UV-light, gave no induction period on subsequent UV-exposure [see curve 3 in Fig.4B.5 and curve 2 in Fig.4B.6]. The polymer-bound residues, however, exhibit similar, though reduced, photo-oxidative stability to disulfide-stabilised PE [curve 2 in Fig.4B.5]. Moreover, both disulfide-stabilised and NiDIP-stabilised PE films gave similar photo-oxidative stability after extraction with toluene. This further confirms the bound nature of the antioxidant residues which arise from the nickel complexes and their corresponding disulfides.

It has been suggested previously^[45,46] that stability under photo-oxidative conditions is a basic requirement for the metal complex to act as a UV-stabiliser. Further, these metal complexes^[45,46] were shown to exert an auto-protective effect which permits the controlled release of the effective antioxidant from the complex over a long period. Nickel dithiophosphates and xanthates possess good photolytic stability in solution [see Sec.3.2.1 and 3.2.3]. Furthermore, these complexes were found to photolyse to the disulfide in solution [see Sec.3.2] and in the polymer [Fig.4B.4 and 4B.10]. In PE the disulfides are formed from these complexes during processing and during UV-exposure of the films. Upon UV-exposure, the depletion of NiDRP and NiRX, and the formation of their corresponding disulfides, suggest similar photo-oxidative behaviour of these additives both in the stabilised PE film and in solution [note the increase in the window regions in the UV-spectra shown in Figs.4B.4, 4B.10, and 3.1 in Sec.3.2.1.1].

The importance of oxidation products of simple alkyl disulfides (or monosulfides) as auto-oxidation inhibitors in polymers and model compounds, rather than the disulfides themselves, has been suggested^[115,116]. This is corroborated here from the thermo- and photo-oxidative stability of RX- and DiPDiS-stabilised PE in the presence of an ample supply of air.

The antioxidant behaviour of nickel dithiolates and their corresponding disulfides in affecting thermo- and photo-oxidative stability in LOPE is summarised in table 4B.4. Examination of this table shows that extraction of

NiDRP- and NiRX-stabilised LDPE films does not affect greatly the thermo-oxidative stability of PE. A similar comparison can be made also between extracted and unextracted disulfide-stabilised PE. However, pronounced differences in photo-oxidative stabilities emerge when NiDRP- and NiRX-stabilised PE films were extracted with toluene (extraction causes complete loss of PIP); compare for example curves 1 and 2 in Fig.4B.6, and curves 1 and 3 in Fig.4B.5. Further, the photo-oxidative stability of nickel dithiolates-extracted PE films are quite similar to that of the corresponding extracted disulfide-containing film (cf. curves 3 and 4 in Fig.4B.5).

Table 4B.4 Effects of metal dithiolates on the thermo- and photo-oxidation of LDPE

Antioxidant ^a	UV-exposure		Thermo-oxidation at 110 ^o	
	PIP [h]	Additive disappearance [h] ^b	TIP [h]	Additive disappearance [h]
NiDBP	600	600	450	200
NiDIP	200	200	420	80
NiDiPP(ext) ^c	0	0	400	0
DiPDiS	0	-	400	-
NiBX	340	345	600	200
NiBX(ext) ^c	0	0	500	0
NiBX(ext) ^d	-	-	630	200
NiEX	350	20	450	20
IX	0	-	510	-

a in LDPE at 2.5×10^{-4} mol/100 g processed at 30 mins in open mixer

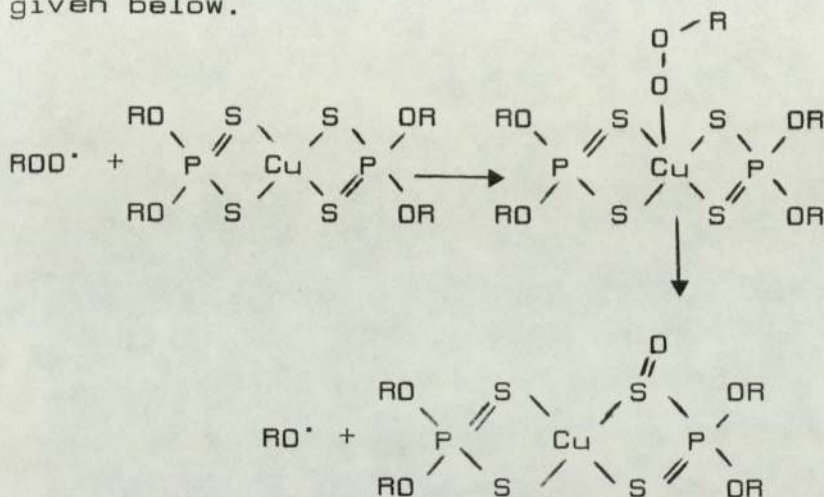
b from disappearance of metal ligand absorption at 316 nm for NiDRP and NiBX

c extracted after processing and before thermal oxidation

d extracted after thermal ageing for 200 h (NiBX destroyed)

4B.3.3 Photo-oxidative Stability of PE in Presence of Zinc and Copper Dithiolates

Studies on model compounds have shown^[117] that copper dithiophosphate is an extremely efficient scavenger of peroxy radicals when compared to nickel and zinc dithiophosphates; long induction periods were obtained^[117] before the substrate oxidation commenced. The proposed^[117] reaction of peroxy radicals with the metal centre of the complex is given below.



If CuDRP can decompose hydroperoxides catalytically then, together with its radical scavenging ability it should exhibit powerful antioxidant activity. This combined mode of action appears to be operating in the polymer. The formation of a DiPDiS-type product from CuDIP was examined earlier (see Sec. 4A.2.4). Results have shown (see Fig.4A.7, Sec.4A.2.4) that CuDIP, like NiDIP, affords good thermo-oxidative stabilisation in PE although with a lower performance than its nickel analogue. Under photo-oxidative conditions, CuDIP-stabilised PE has good stability (PIP=450h) and even better than the nickel analogue (curves 3 and 4 in Fig.4B.7).

The mechanism of action of ZnDIP has been the subject of extensive studies [see Sec.1.4.4]. It has been claimed that ZnDIP is a good hydroperoxide decomposer^[48,50,117-120] and a free-radical scavenger^[39,43]. The ability to scavenge free-radicals and to decompose hydroperoxides catalytically, via the disulfides, in a similar way to that observed for NiDRP [see Sec.7.3.1] is reflected in the good thermo-oxidative stability it imparts to PE [see curve 4 in Fig. 4A.7, Sec.4A.2.4]. ZnDIP, however, has no UV-absorption in the region of interest [$\lambda > 290$ nm]. A basic requirement for a good UV-stabiliser is the ability to absorb UV-light [$\lambda > 290$ nm], and to dissipate it in a non-destructive process. Consistent with this ZnDIP is a poor UV-stabiliser as is evident from the absence of an induction period for ZnDIP-stabilised PE film [see curve 2 in Fig.4B.7].

Under very mild processing conditions, ZnRX (R=E,I) shows a clear pro-oxidant effect [curves 5 and 6 in Fig. 4B.13] in contrast to the photostabilisation (but no induction period) obtained when processed with PE under more severe conditions [curve 2]. This behaviour is, in principle, analogous to that of disulfides where severe processing improves its photostabilising effectiveness [see Fig.4B.12]. This similarity in behaviour, when coupled with similar findings about NiRX, ZnDIP and NiDRP, suggests some formation of dixanthogens under severe processing conditions. A notable difference, however, exists between the behaviour of ZnRX and NiRX. It was suggested from solution photolysis [see Sec.3.2.1.2] that ZnRX yields, under the same conditions, less disulfides than the analogous NiRX. High concentrations of oxygen during the processing of ZnRX with unstabilised PE

allows higher recombination of the radicals formed in competition with the more favourable hydrogen abstraction by the radical from ZnRX. It is important to mention here that, even under the mildest processing used [5,CM], ZnRX-stabilised PE films did not show the characteristic UV-absorption of ZnRX.

4B.3.4 Photo-oxidative Stability of Synergistic Combinations of Dithiolates with HOBP

MDRP and MRX were shown to be good hydroperoxide decomposers [see Sec.7.3] and good UV-absorbers [see Secs. 4B.2.2, 4B.2.3, 3.2.1 and 3.2.3]. Cyasorb UV531 [HOBP] is a well known 'UV-absorber' which combined several admirable characteristics of a photostabiliser. It is relatively inert, does not react with other additives, and is compatible with the polymer^[121]. Its low volatility and excellent UV-stability makes it useful for UV-stabilisation of polymers. This 'UV-absorber' has only a minor stabilising effect on the thermal oxidation of the polymer [curve 2 in Fig.4B.2] compared with nickel dithiolates and their corresponding disulfides.

Compared to the unstabilised film, HOBP-stabilised PE film shows [cf. curves 7 and 8 in Fig.4B.16] a lower rate of carbonyl formation at all stages of photo-oxidation. A much reduced photo-oxidative induction period is observed for severely oxidised PE containing HOBP compared to the mildly oxidised polymer [curves 7 and 5 in Fig.4B.14]. In contrast to the action of HOBP under very severe processing conditions, NiDRP, NiRX and their corresponding disulfides

afford photostabilisation of PE as evidenced by the complete inhibition of carbonyl formation [compare curve 3 with 2 in Fig.4B.2]. Not only was the build-up of carbonyl inhibited during processing, but also the initial rate of carbonyl formation during UV-exposure was much lower than for HOBP; compare for example curves 3-1 with curve 7 in figure 4B.16.

Although pure crystals of HOBP display no weight loss [Fig.4B.18] up to a temperature which is equivalent to the processing temperature of PE, the inability of HOBP to protect the polymer during thermal-oxidation [processing] is a consequence of its inability to inhibit the formation of hydroperoxides^[46]; hence the observed build-up of carbonyl compounds which are formed from the decomposition of hydroperoxide [see curve 2 in Fig.4B.2]. This explains why HOBP is less effective in polymers when processing under severe conditions and hence why it is necessary to protect it. Effective synergism has been reported^[46] for combinations of HOBP with metal dithiocarbamates which destroy hydroperoxides.

The powerful synergisms obtained here from using both nickel dithiolates (NiDRP and NiRX), and their corresponding disulfides in combination with HOBP at different processing conditions is shown in figures 4B.14-4B.17, and table 4B.3. These figures show that in the presence of good hydroperoxide decomposers the deleterious effect of the processing and UV-light on HOBP is minimal.

The excellent photo-oxidative stability afforded by the synergistic mixture of the disulfide, DiPDiS, with HOBP [Fig.4B.15] must, therefore, be at least partly explained in terms of the protection of HOBP by DiPDiS at the processing stage. This protection is so extensive that HOBP appears to suffer minor losses during processing; HOBP protects also the disulfide [or its oxidation products] during UV-exposure and this contributes to the auto-retardation at later stages of photolysis, hence the excellent UV-stabilisation observed for the synergistic mixture.

The prior thermal history of polymers determines, to a major extent, their behaviour during photo-oxidation [17,20,24, 122,123]. The ability of antioxidants or UV-stabilisers to decompose hydroperoxides formed during processing is reflected in their UV-stabilising effectiveness. The antioxidant nature of thiophosphoryl disulfide, DiPDiS, and derived oxidation products, has already been confirmed [see Sec.4.2.4]. Further, the effectiveness of these disulfides was enhanced when the disulfide-stabilised polymer was processed under severe [high concentration of oxygen] conditions [see Fig.4B.12]. Since the photo-stabilising effectiveness of HOBP is considerably impaired under more severe processing [cf. curves 9 with 10 and 4 with 8 in Fig.4B.15], the important role of disulfides and their derived oxidation products in inhibiting the formation of hydroperoxides is clearly evidenced by the behaviour of the synergistic combination shown in curves 3-1 in figure 4B.15. Accordingly, HOBP is allowed to operate, with indifference to the oxidative environment, at the nominal concentration

which was originally incorporated in the polymer. Moreover, the final retardation is a function of the disulfide and its products.

The antioxidant action of nickel dithiophosphate, like many other sulfur-antioxidants^[23,44-46,106,107] lies in its effective hydroperoxide decomposing activity. The present work in model compounds [see Sec.7.3] and in polyethylene [see Sec.4A.3.4] shows that these compounds decompose hydroperoxides in a primarily ionic catalytic process which cannot be attributed to the metal complexes themselves but rather to an acid [or acids] formed from them via their disulfides. This is further confirmed from synergistic combinations of NiDRP with HOBP which show the same order of embrittlement times [table 4B.3] as that which are formed for the combination of disulfides and HOBP at increasing processing severity. A notable feature in both cases of NiDRP and DiPDiS synergistic combinations with HOBP is the apparent auto-acceleration and auto-retardation at the later stages of photo-oxidation, following severe and mild processing, respectively [cf. curves 2 and 1 in Fig.4B.14 with curves 3-1 in Fig.4B.15].

Products formed from the reaction of dithiophosphates with hydroperoxides act to protect HOBP from the deleterious effects of hydroperoxides under both thermal and subsequent photo-oxidative conditions. By analogy with NiDRC, HOBP protects the dithiophosphates, and the disulfides, partly by screening and partly by physical quenching of excited states of carbonyl compounds^[19], in addition to its action as a sacrificial antioxidant in removing chain initiating radicals formed from hydroperoxides and derived carbonyl compounds^[19,45].

HOBP behaves essentially as a screen during the early stages of photo-oxidation^[45] when hydroperoxides are the primary photo-initiators, while it acts by the other two mechanisms at later stages of photolysis.

The initial photolysis of carbonyl in polyolefins, by Norrish II process is known^[38] to be followed by a Norrish I-process upon further oxidation. The former does not give rise to photo-initiating species and will, therefore, play little or no part in the oxidation. However, once the Norrish I process becomes dominant then, HOBP becomes involved in the deactivation of the triplet state of the in-chain carbonyl compounds, giving rise to some auto-retardation at later stages of photo-oxidation.

The photo-oxidation stability afforded by the synergistic combination of DiPDiS, NiDIP and CuDIP with HOBP follows the order, DiPDiS > NiDIP > CuDIP [see curves 3-1 in Fig.4B.16]. Since the amount of disulfides formed from nickel dithiophosphates is directly related to processing severity, and assuming that CuDIP behaves in a similar way to NiDIP, then each of the above synergistic mixtures, exhibit within themselves, greater stabilisation the more severe the processing operation [see for example Figs.4B.14 and 15].

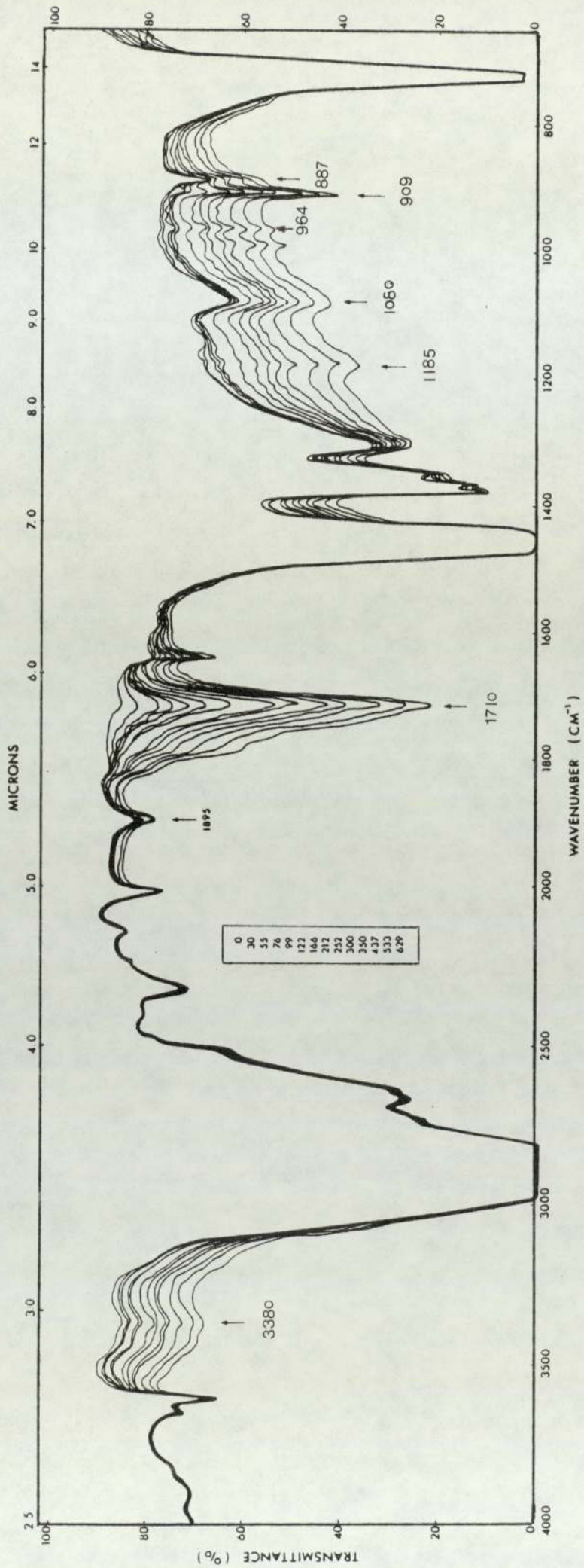


Fig. 4B.1 Infrared absorption spectra recorded during photo-oxidation of unstabilised LDPE film. Irradiation times [h] are shown in the rectangle

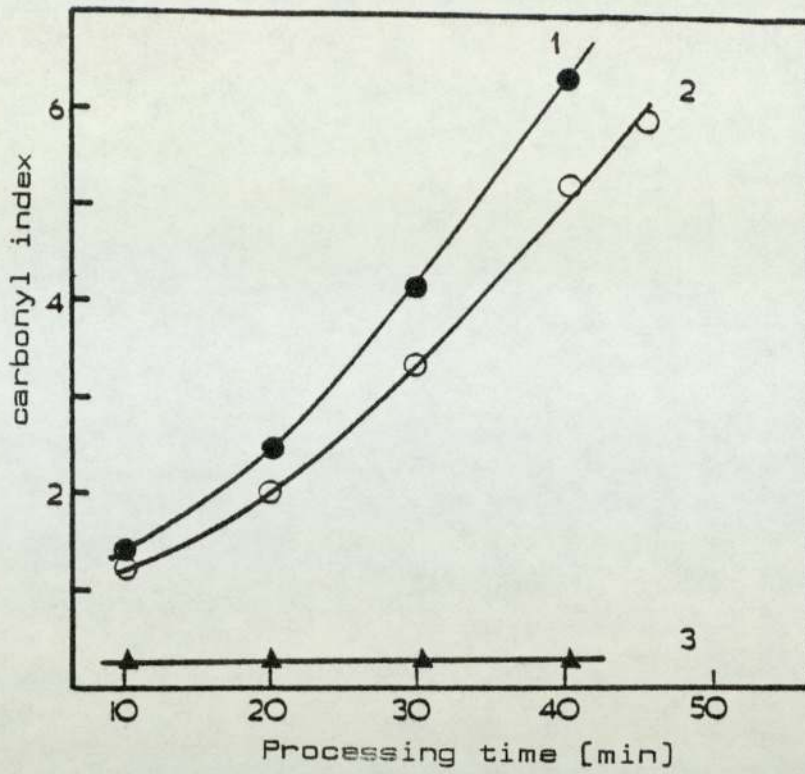


Fig. 4B.2 Effect of processing at 150° on the oxidation of LDPE containing antioxidants [$2.5 \times 10^{-4} \text{M}/100\text{g}$]. [1] no additive [control]; [2] HOBP; [3] NiDRP, DiPDiS, NiRX, IX.

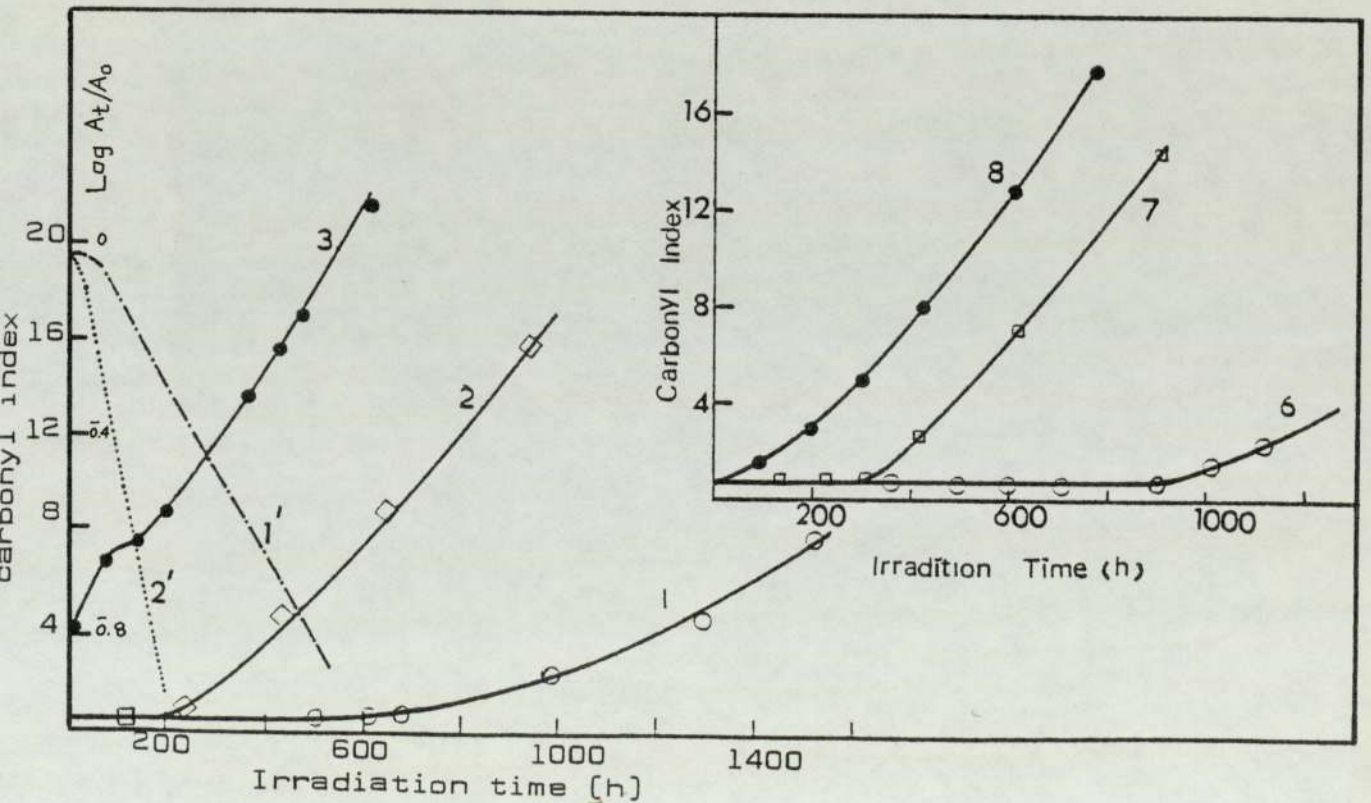


Fig. 4B.3 Effect of processing severity on the photo-oxidation of LDPE containing NiDRP [$2.5 \times 10^{-4} \text{M}/100\text{g}$]. [1] NiDBP; [2] NiDIP; [3] no additive, control; [1-3 processed (30,0M) at 150° . [6] NiDBP; [7] NiDIP; [8] no additive, control [6-8 processed (30,CM) at 150°]. Kinetics of the disappearance of NiDRP [316nm] in the same films is also shown (1' NiDBP).

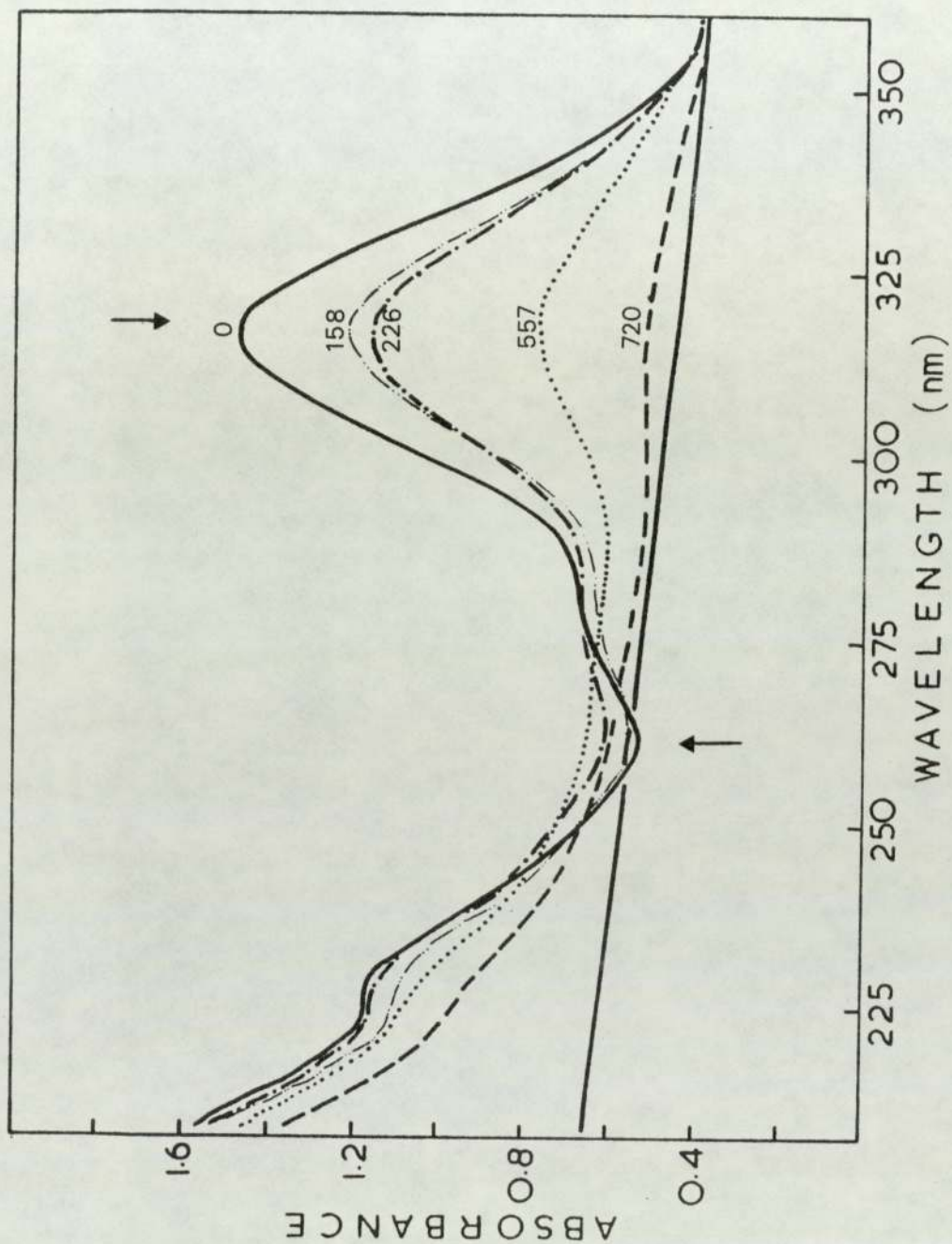


Fig. 4B.4 Changes in UV-absorption spectrum during photo-oxidation of LDPE film containing NiDBP (2.5x10⁻⁴M/100g), processed (5,CM) at 150°C. Numbers on curves are irradiation time in hours.

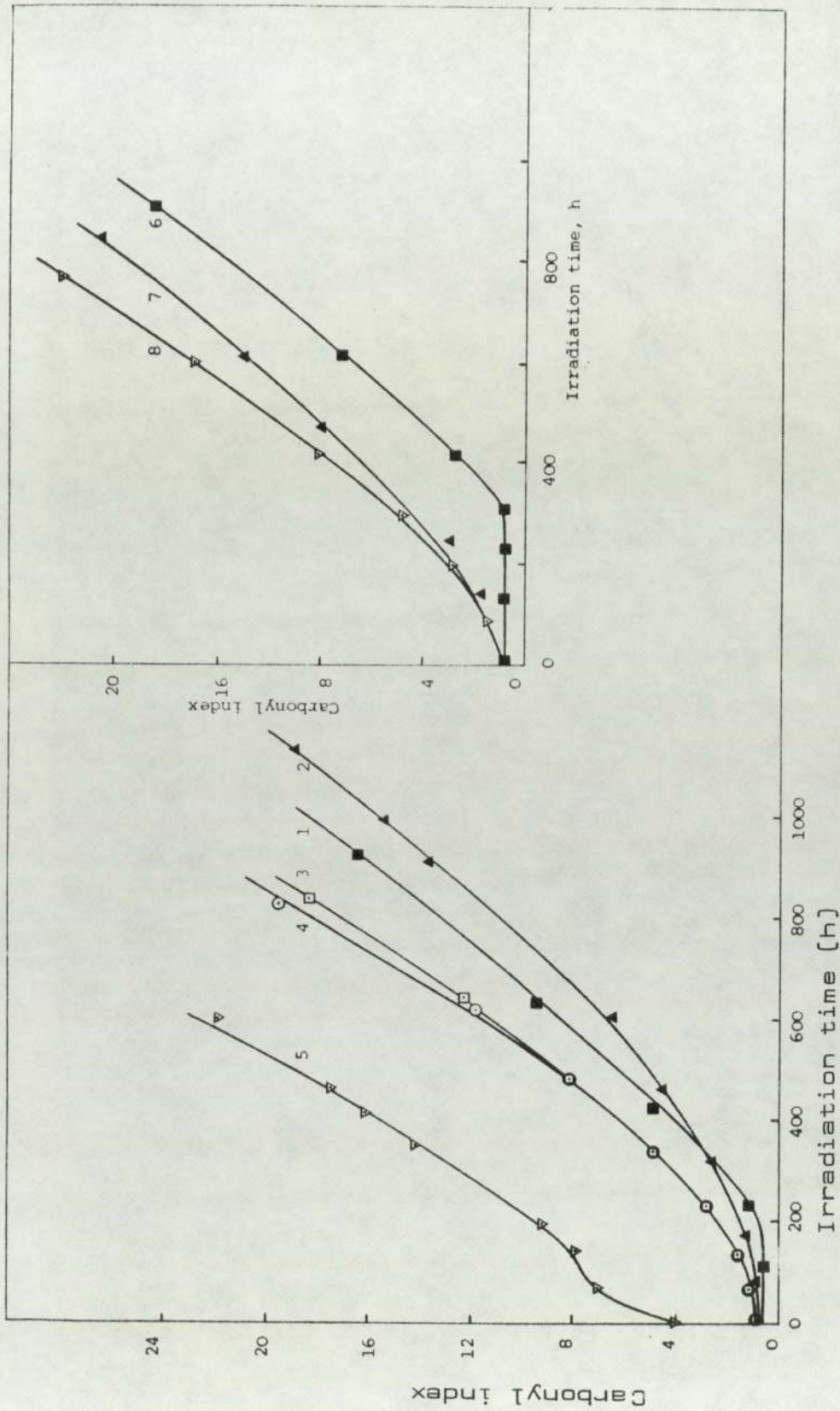


Fig. 4B.5 Effect of additives on photo-oxidation of LDPE [$2.5 \times 10^{-4} M/100g$]. [1] NiDIP; [2] DiPDiS; [3] NiDIP & [4] DiPDiS extracted; [5] control without additives [1-5 all processed at $150^\circ/30, 0M$]; [6] NiDIP; [7] DiPDiS; [8] control without additives [6-8 all processed at $150^\circ/30, CM$].

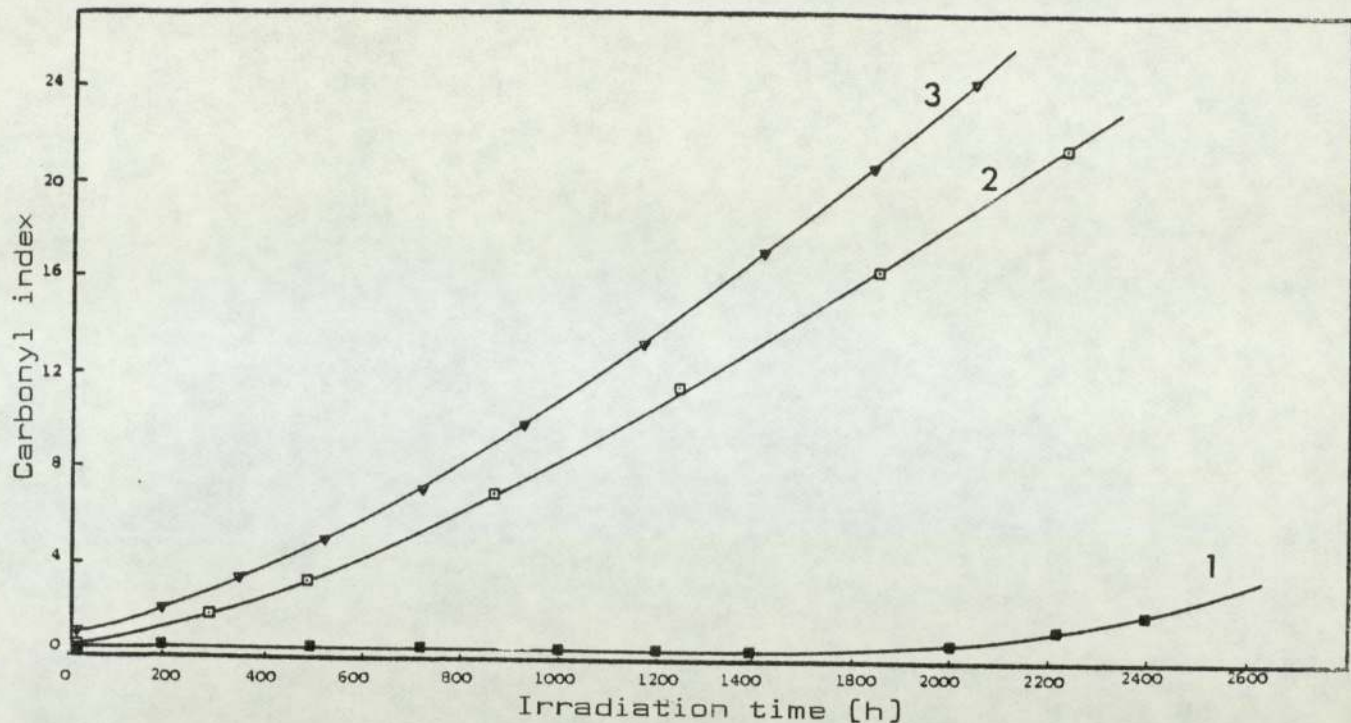


Fig. 4B.6 Effect of NiDBP [extracted and unextracted] on the photo-oxidation of LDPE [processed at 150°/30,CM]; concentration $2.5 \times 10^{-4} \text{M}/100\text{g}$. [1] NiDBP; [2] NiDBP [extracted]; [3] no additive, control.

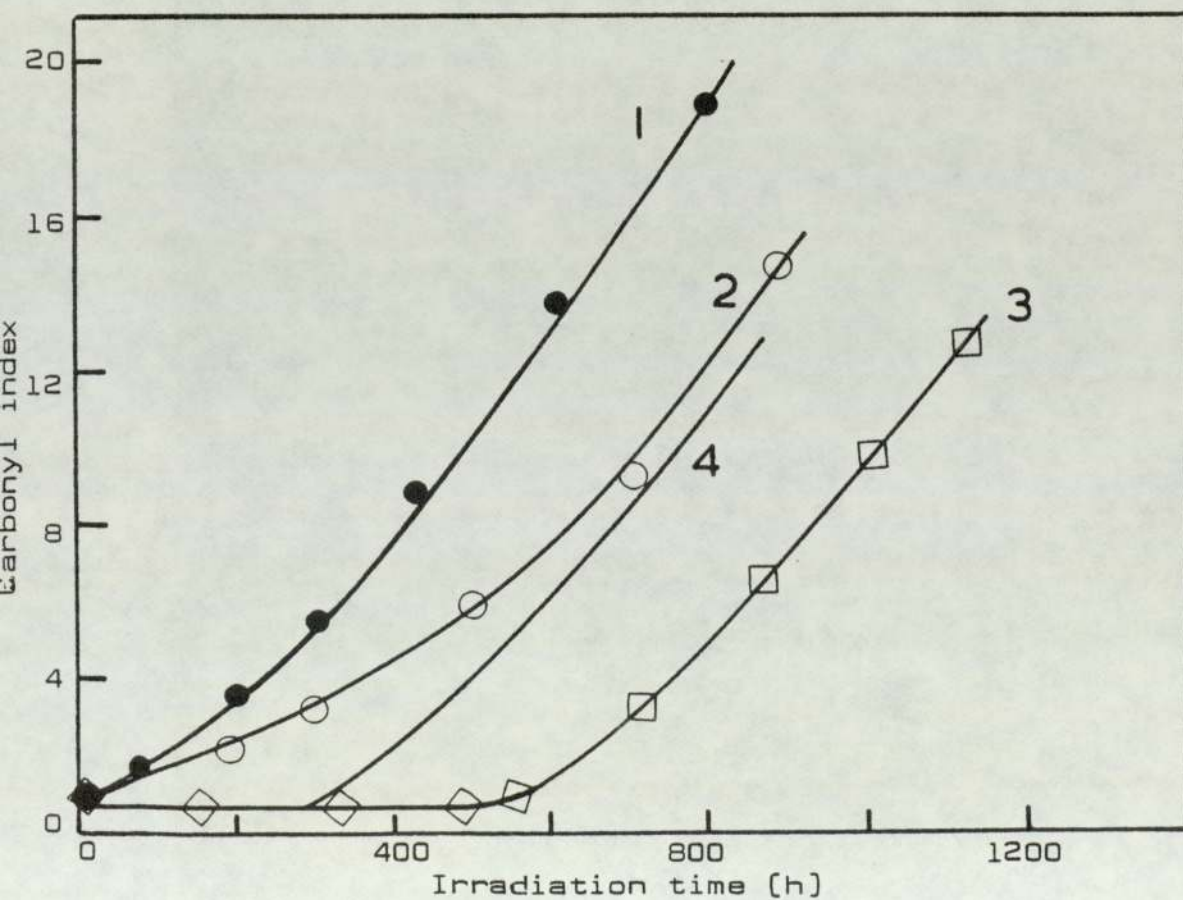


Fig.4B.7 Effect of MDIP on photo-oxidation of LDPE ($2.5 \times 10^{-4} \text{M}/100\text{g}$). 1. control without additive, 2. ZnDIP, 3. CuDIP, 4. NiDIP. All processed at 150°/30 min in closed mixer.

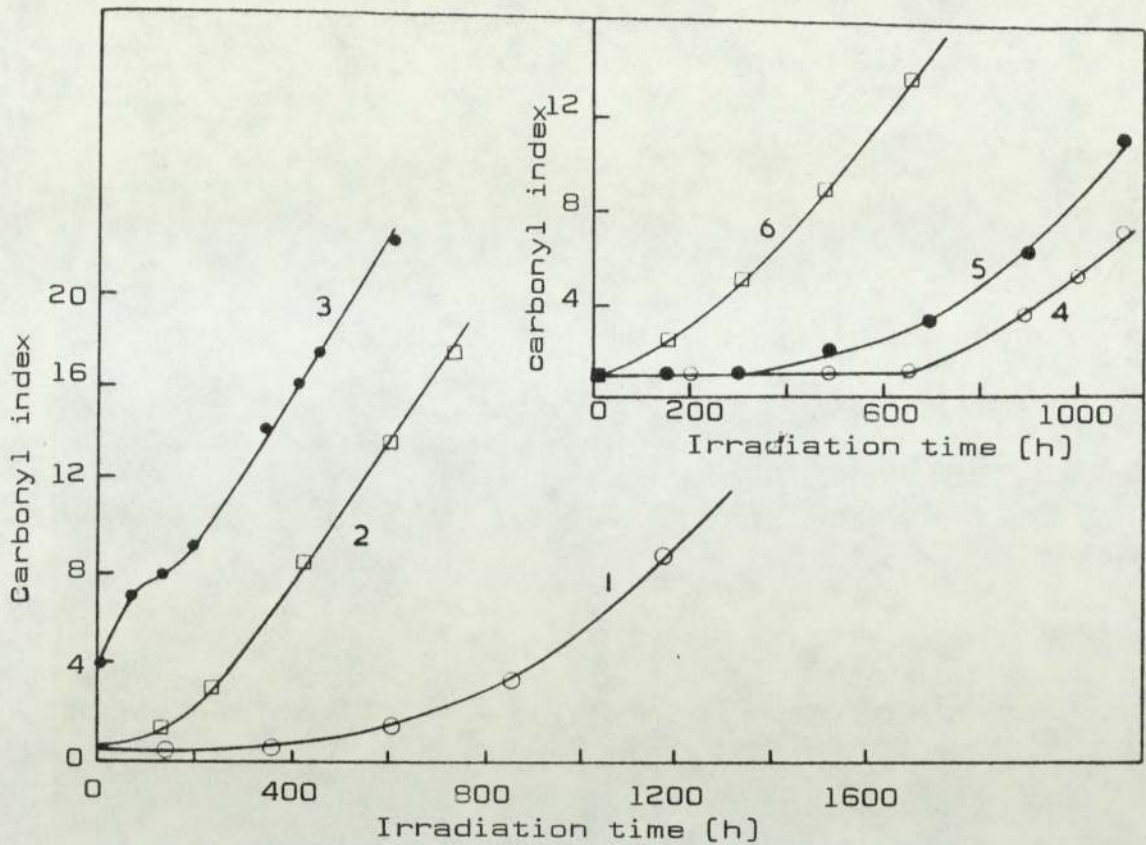


Fig.4B.8 Effect of processing severity [at 150°] on the stabilising effectiveness of NiRX [2.5×10^{-4} M/100g]. [1] NiBX; [2] NiEX; [3] control without additives [1-3 processed for 30 min in open mixer]. [4] NiBX; [5] NiEX; [6] no additive, control [4-6 processed (30,CM) at 150°].

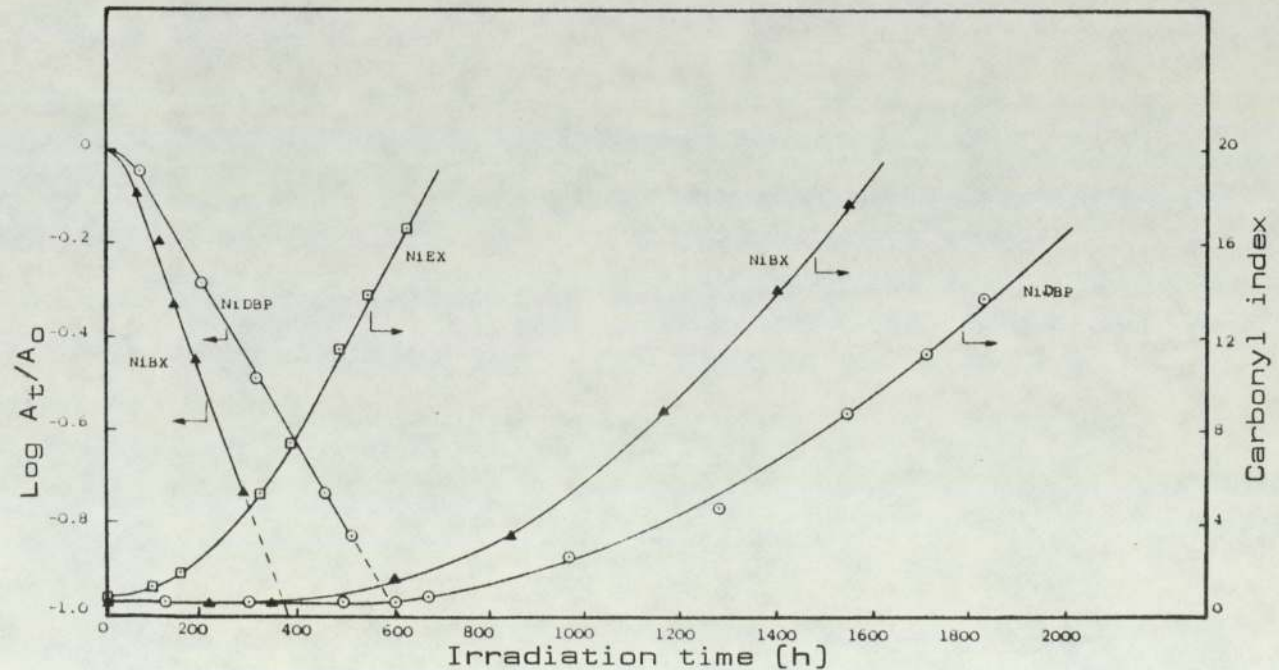


Fig.4B.9 Kinetics of the disappearance of NiEX, NiBX and NiDBP [316 nm] in LDPE during photo-oxidation compared to the changes of carbonyl index under the same conditions [concentration of additives 2.5×10^{-4} M/100g].

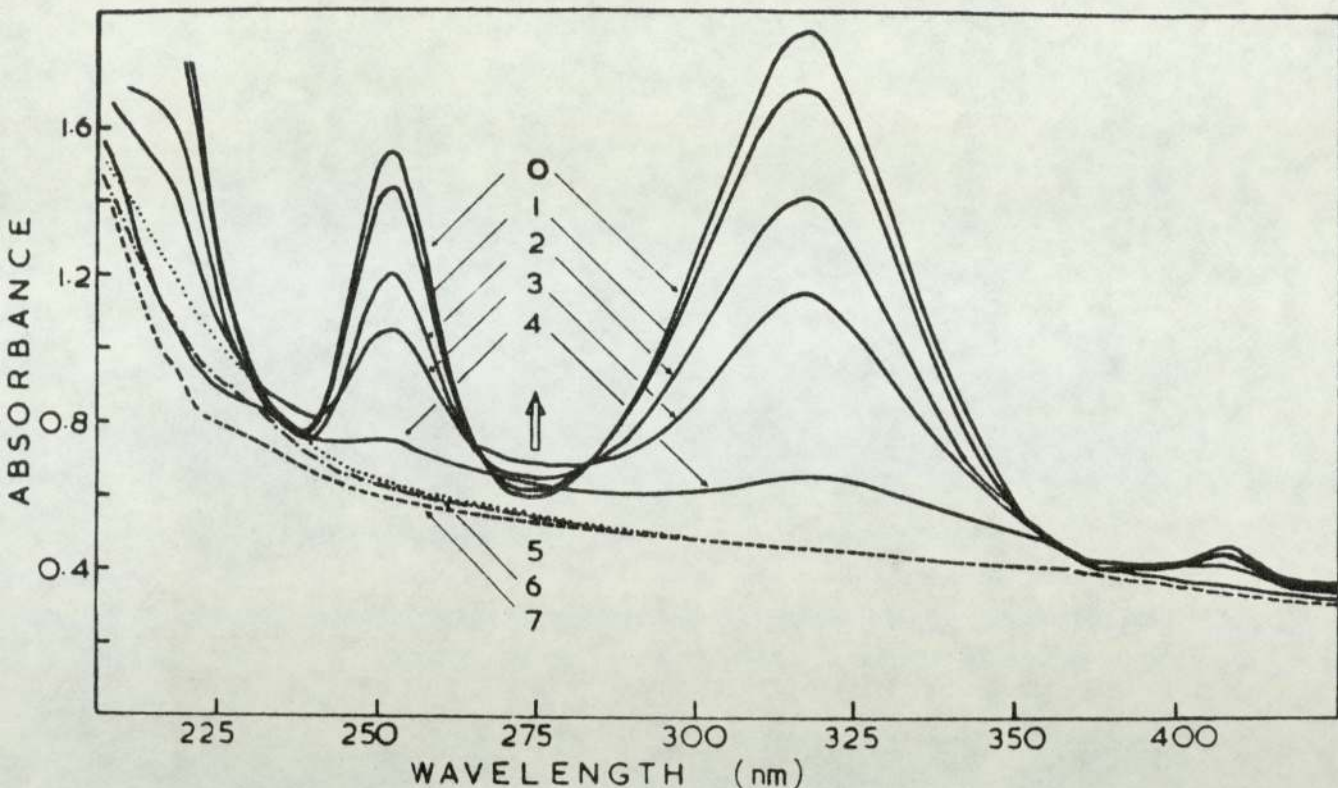


Fig.4B.10 Changes in the UV-spectrum of LDPE film containing NiBX ($2.5 \times 10^{-4}/100g$) during UV-exposure.

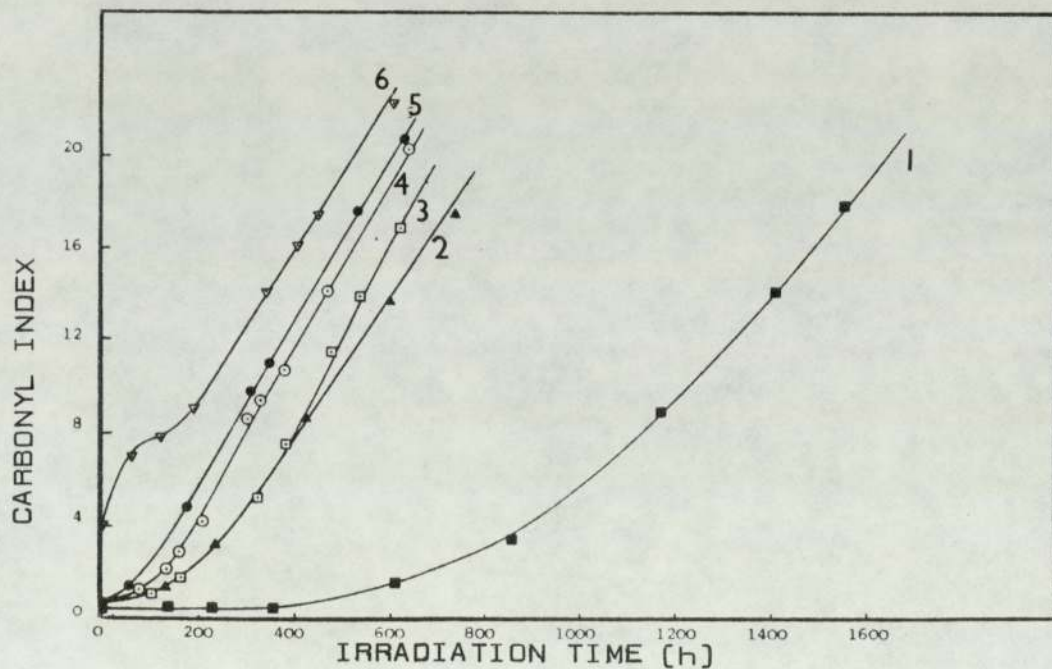


Fig.4B.11 Effect of additives on the photo-oxidation of LDPE processed [30,0M] at 150° , [concentration of additives $2.5 \times 10^{-4}M/100g$]. [1] NiBX; [2] NiEX; [3] EX; [4] IX; [5] IX, extracted; [6] no additive, control.

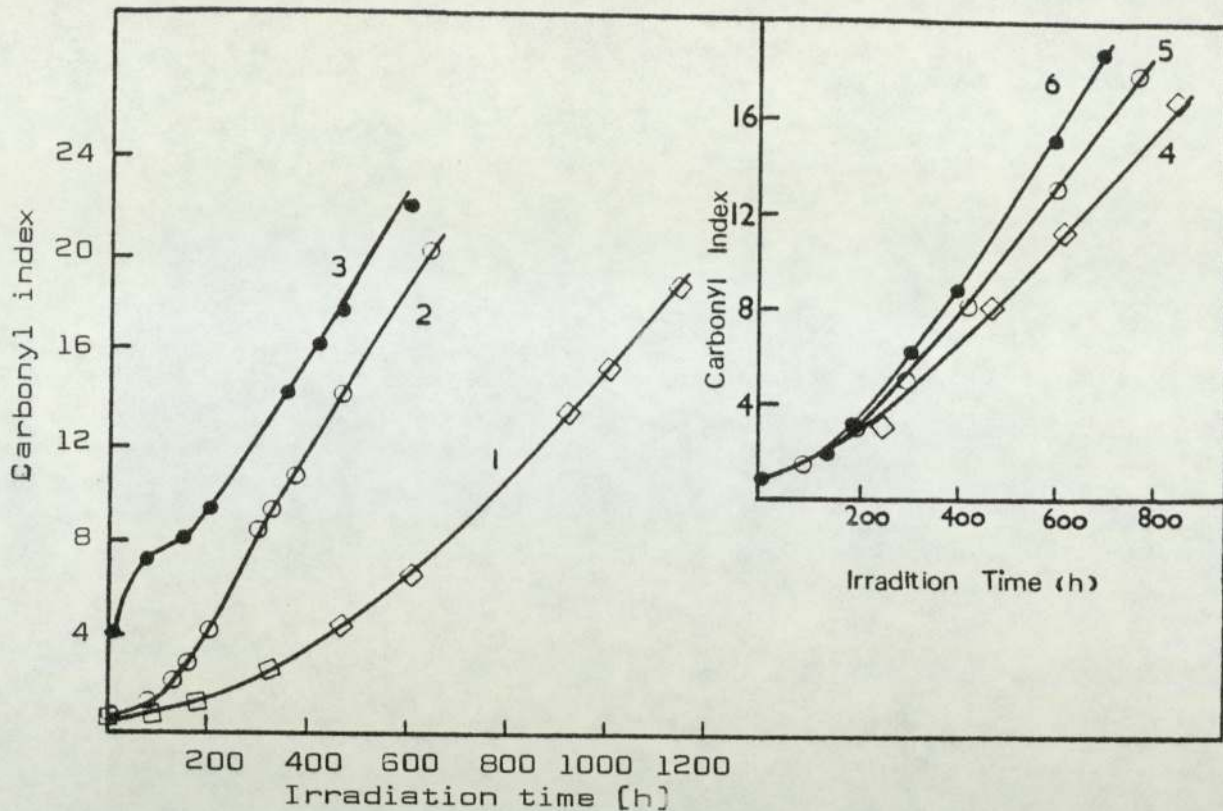


Fig.4B.12 Effect of processing severity on photo-oxidation of LDPE in the presence of disulfides. [1] DiPDiS; [2] IX; [3] no additive, control [1-3 processed [30,0M) at 150°]. [4] DiPDiS; [5] IX; [6] no additive, control [4-6 processed [30,CM) at 150°].

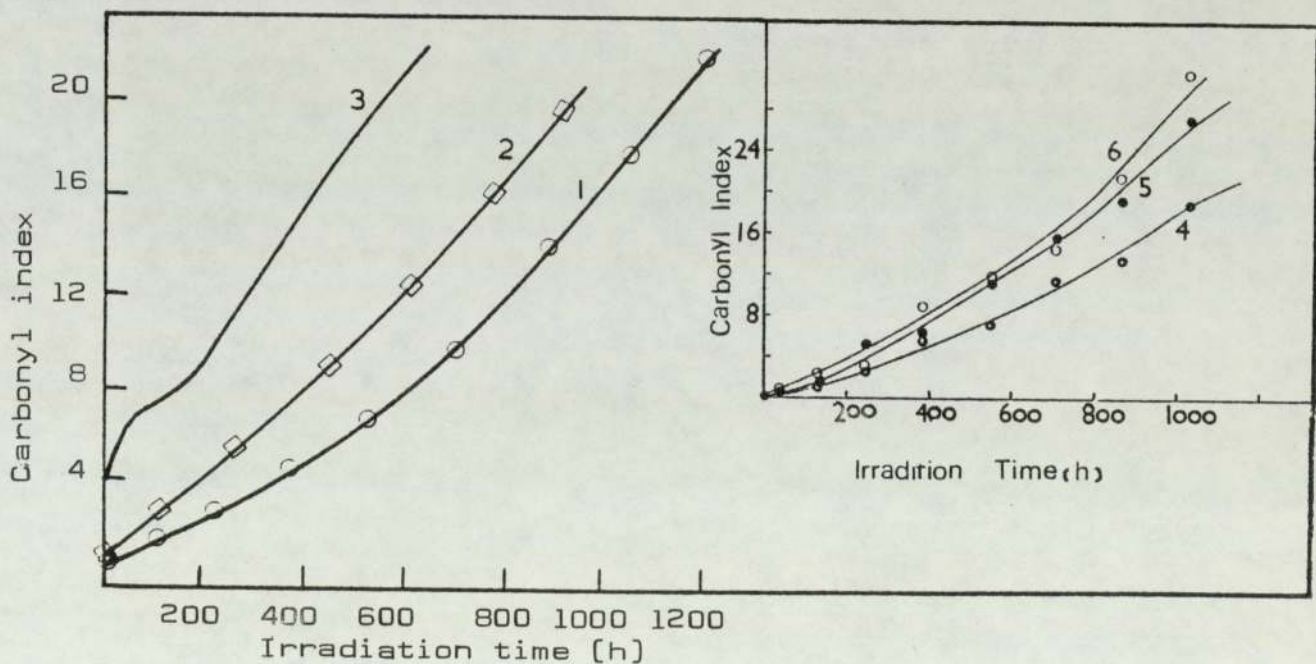


Fig.4B.13 Effect of processing severity on photo-oxidation of LDPE in the presence of metal xanthates. [1] CuBX; [2] ZnEX; [3] no additive, control [1-3 processed [30,0M) at 150°]. [4] no additive, control; [5] ZnEX; [6] ZnIX [4-6 processed [5,CM) at 150°].

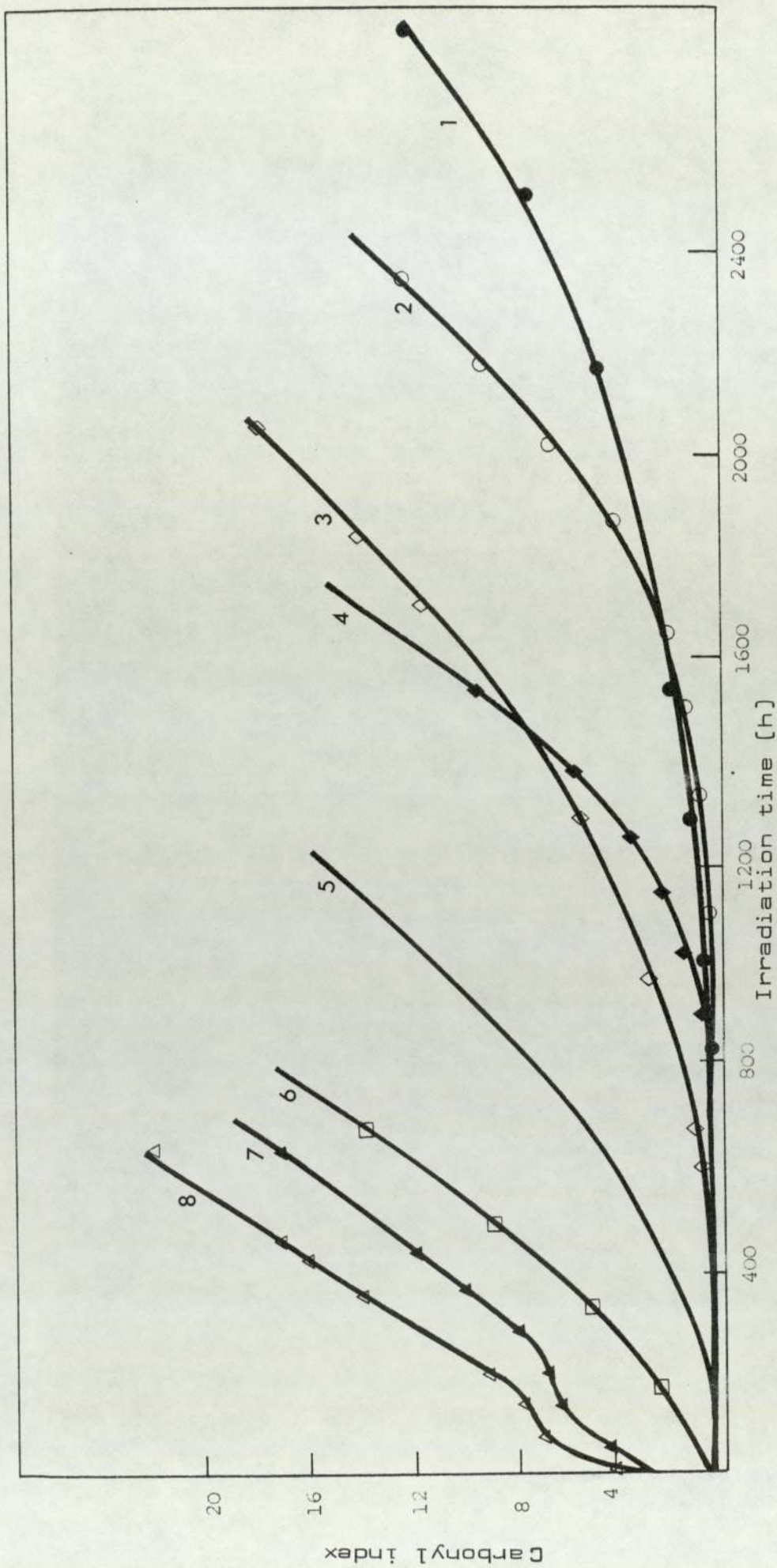


Fig. 4B.14 Effect of processing severity (at 150°) on the stabilising effectiveness of NiDBP and HOBP and their synergistic mixture (all concentrations at $2.5 \times 10^{-4} \text{M}/100\text{g}$).
 1. NiDBP + HOBP (30,0M), 2. NiDBP + HOBP (30,CM), 3. NiDBP (30,CM), 4. NiDBP (30,CM),
 5. HOBP (30,CM), 6. control, no additive (30,0M), 7. HOBP (30,CM), 8. control, no additive (30,0M).

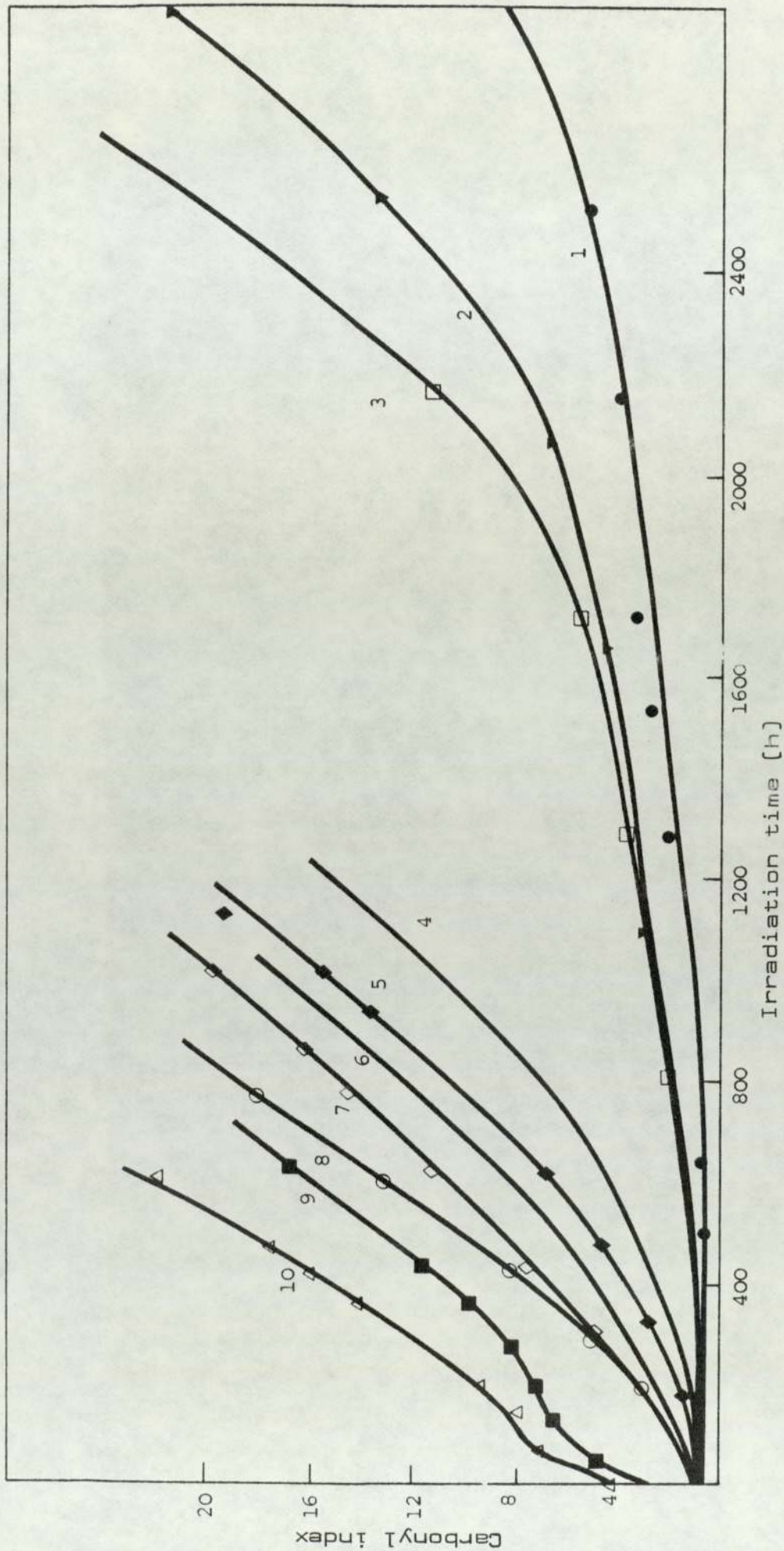


Fig. 4B.15 Effect of processing severity (at 150°) on the stabilising effectiveness of DiPDiS and HOBP and their synergistic mixture [all concentrations at 2.5x10⁻⁴M/100g].
 1. DiPDiS + HOBP (30,0M), 2. DiPDiS + HOBP (10,0M), 3. DiPDiS + HOBP (30,CM),
 4. HOBP (30,CM) 5. DiPDiS (30,0M), 6. HOBP (10,0M), 7. DiPDiS (30,CM), 8. control,
 no additive (30CM), 9. HOBP (30,0M), 10. control, no additive (30,0M).

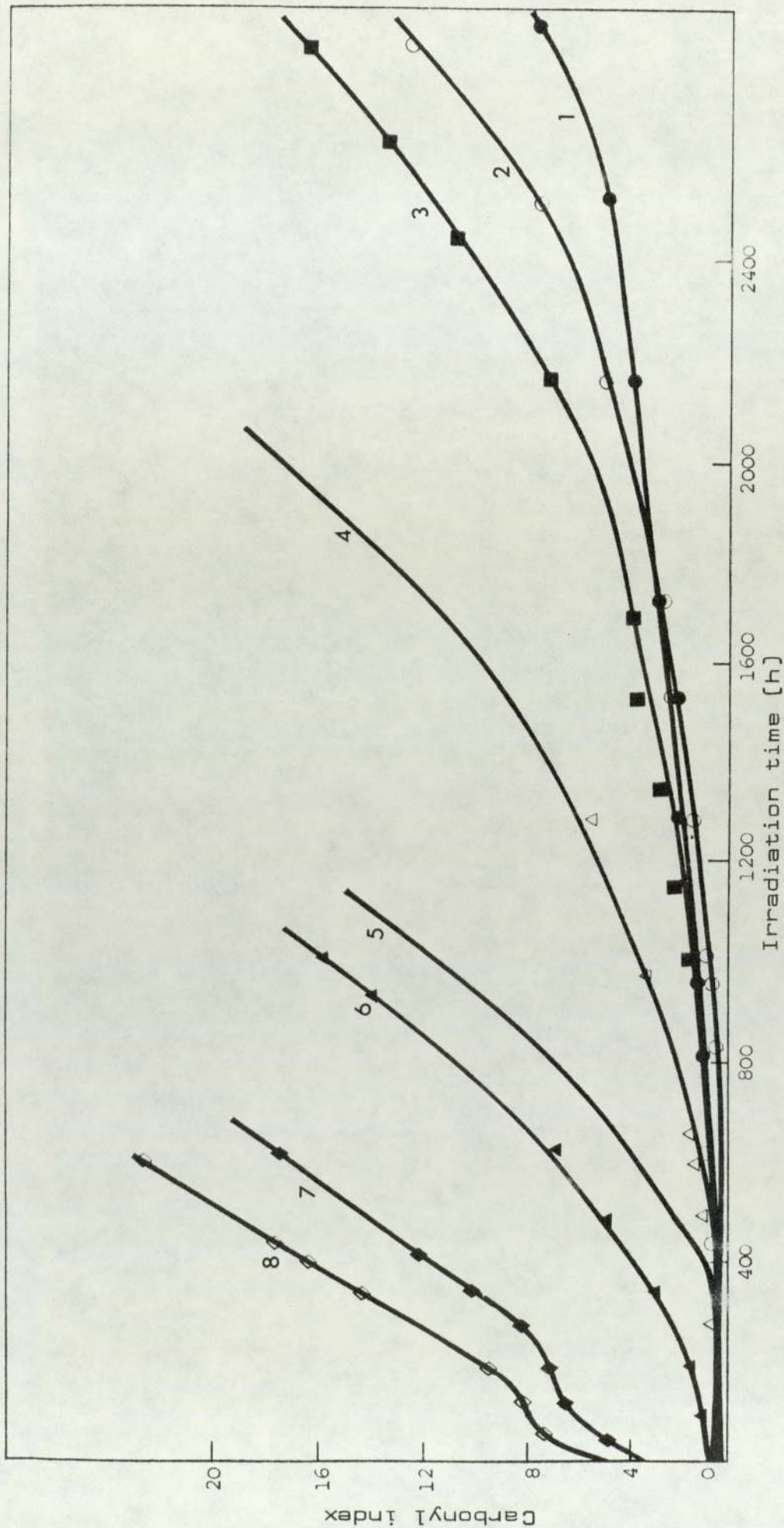


Fig. 4B.16 Effects of MDRP and DiPDiS alone, and in combination with HOBP, on the photo-oxidation of LDPE (30,0M). Concentration of all additives 2.5×10^{-4} M/100g].
 1. DiPDiS + HOBP, 2. NiOBP + HOBP, 3. CuDIP + HOBP, 4. NiOBP, 5. CuDIP, 6. DiPDiS, 7. HOBP, 8. control (without additive).

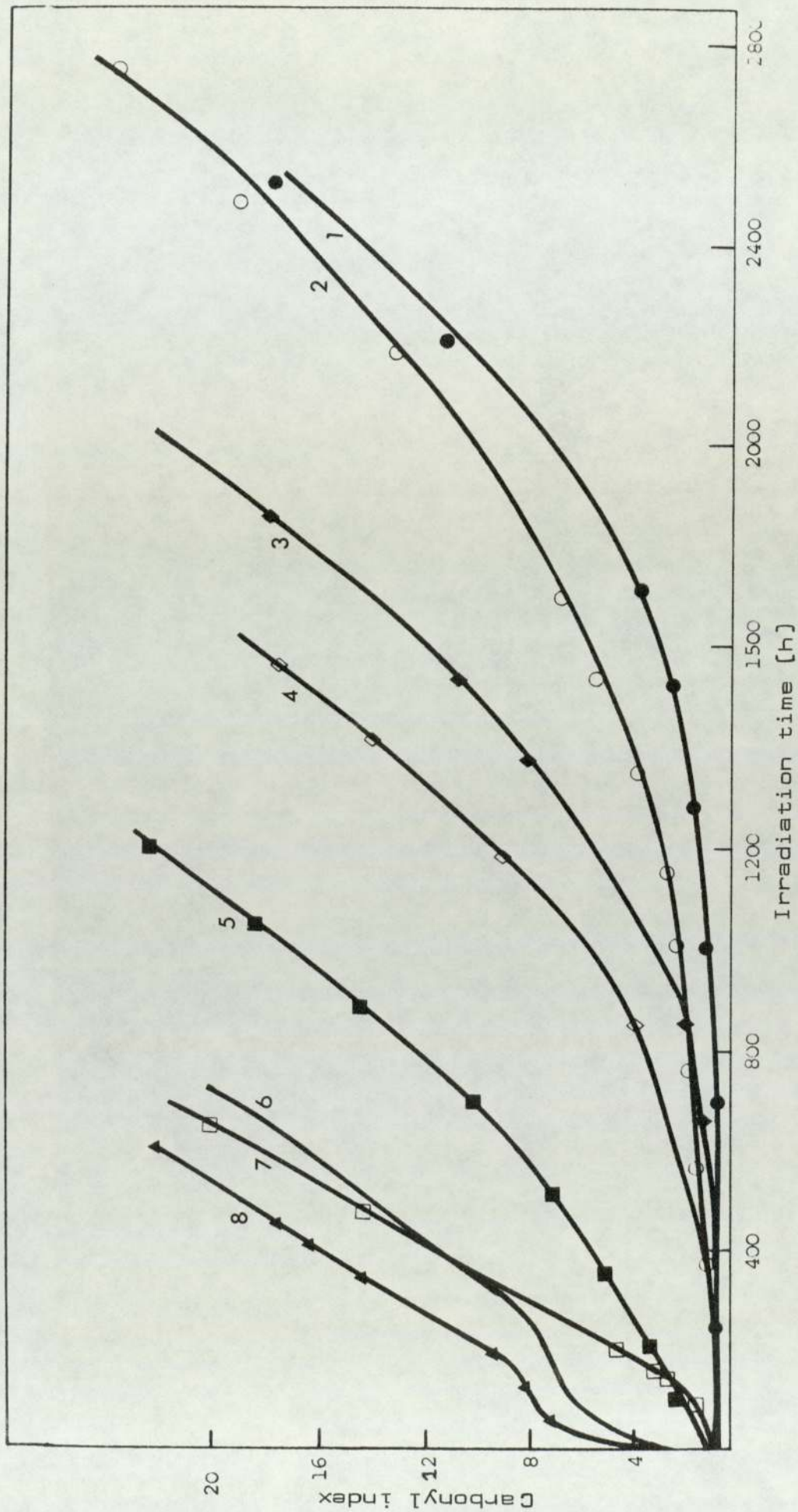


Fig. 4B.17 Effects of MRX and IX alone, and in combination with HOBP, on the photo-oxidation of LDPE (30,0M). Concentration of all additives $2.5 \times 10^{-4} \text{M}/100\text{g}$. 1. NiBX + HOBP, 2. IX + HOBP, 3. CuBX + HOBP, 4. NiBX, 5. CuBX, 6. IX, 7. HOBP, 8. control (no additive).

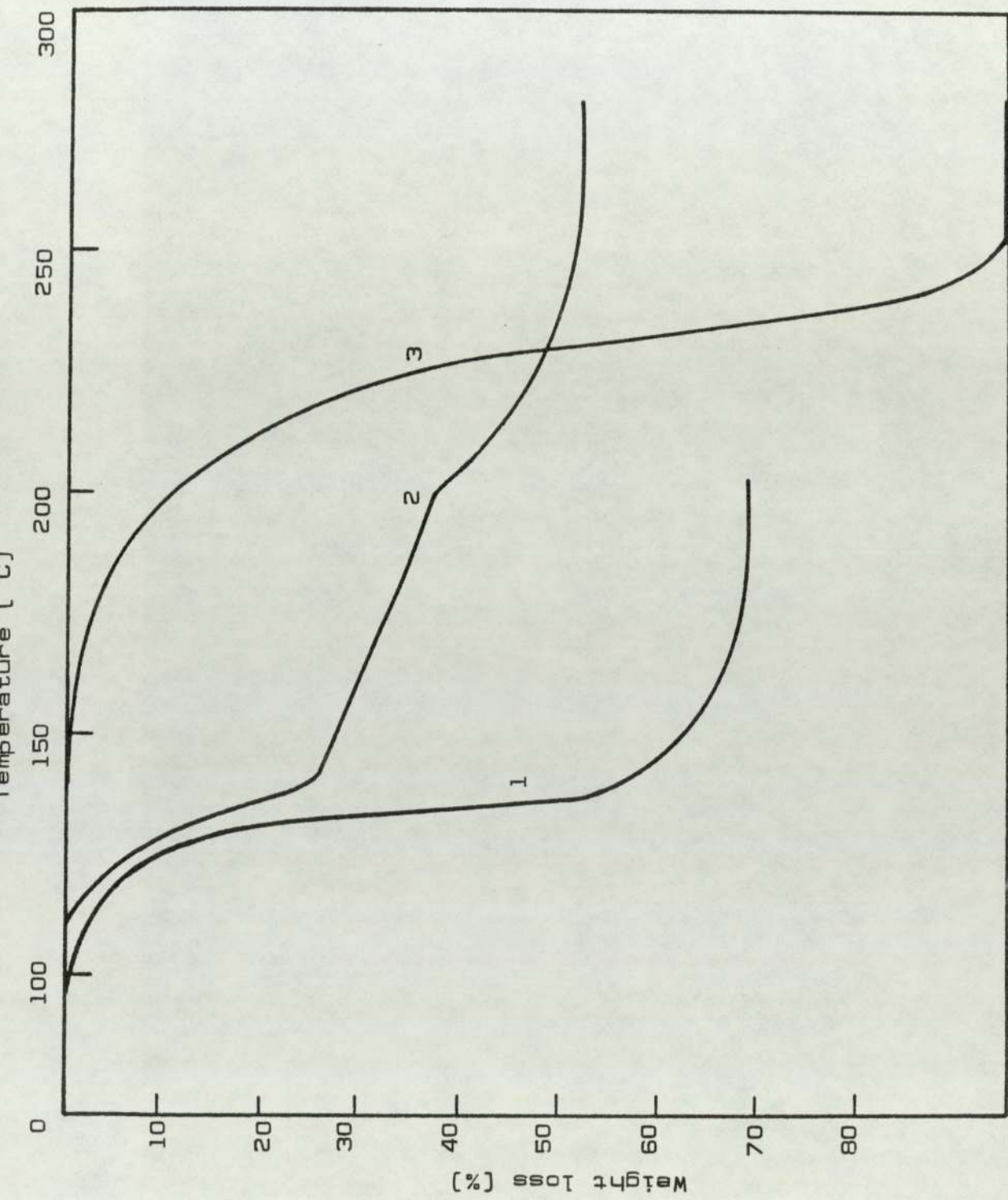


Fig. 4B.18 Non-isothermal weight loss of (1) DiPDiS; (2) DiPDiS + HOBP; (3) HOBP, in air. Weight of each component and the total weight of the mixture is 0.035g.

CHAPTER FIVE

STABILISATION

OF

LOW DENSITY POLYETHYLENE

MASTERBATCHES

5.1 OBJECT

Incorporation of additives into polymers in the form of high concentration masterbatches (MB's) is common industrial practice. The advantages are practical convenience and better dispersion in the polymer. In this chapter a typical stabilised-LDPE MB preparation contains 2.5% additives. For synergistic combinations of dithiophosphates with HOBP a 1:1 molar ratio is used, with 2.5% of each of the additives. In general MB's are processed for 30 minutes in an open mixer (30,0M).

Polyethylene samples containing 0.1% (ca. 2.5×10^{-4} M/100g) hereafter called Diluted Masterbatches (DMB), are subsequently prepared from the masterbatches by dilution with unstabilised polymer. The behaviour of DMB's is then compared with those prepared from normally processed PE samples (NS) containing the same concentration of the additive (2.5×10^{-3} M/100g), ca. 0.1%. DMB samples are subjected to different processing severity to investigate further the conditions under which DMB samples show maximum oxidative stability and how these compare with NS samples.

A UV-cabinet (ca. 30^o) and a Wallace oven (at 110^o and airflow 2.5 cu ft.h⁻¹) are used for light exposure and heat ageing, respectively. UV- and IR-spectrophotometry are utilised, whenever feasible, to follow changes during photo- and thermo-oxidation in MB and DMB films. These films are further extracted with solvents (toluene at 55^o and hexane at room temperature); the extract, and the films before and after extraction are compared, and the effect of extraction on the photo- and thermo-oxidative stabilities of DMB films is examined. Changes in the absorption intensities of different functional groups are measured and reaction schemes are proposed to explain the oxidative behaviour of stabilised PE.

5.2 RESULTS

5.2.1 Spectral Characteristics of MB Films

The presence of additives in LDPE at a concentration of 2.5% MB can be accurately detected and monitored by IR spectrophotometry. Changes in the absorption characteristics of these additives which are affected by processing and accelerated weathering of the stabilised polymer can also be followed. Because of the large amounts of additives used in MB preparation almost all the films appeared coloured whereas DMB and NS films showed almost no colour (see table 5.1).

Table 5.1 Colours of additives in PE, MB, DMB and NS samples

Additive ^a	Solid	MB [2.5%]	DMB [0.1%]	NS [2.5×10^{-4} M/100g] [ca.0.1%]
NiDIP	purple	purple	colourless	colourless
DiPDiS	creamy	creamy	colourless	colourless
HOBP	white	white	colourless	colourless
NiDIP+HOBP	-	purple	colourless	colourless
DiPDiS+HOBP	-	orangish yellow	pale lemon yellow	colourless
DiPDiS+HOBP ^b	-	creamy	colourless	colourless

a processed in an open mixer for 30 min.

b processed in a closed mixer for 10 min.

Figures 5.1-5.3 compare the IR spectral regions of PE films prepared from MB's containing NiDIP, DiPDiS and HOBP, with the IR spectra of the pure additives. Normally, when ca.0.1% additive concentration is present in the polymer, most of the characteristic bands of the additives are too weak to be observed. Thus, for example, only the absorption ca.1000 cm^{-1} can be seen as a weak band in the IR spectrum of a NS of NiDRP-stabilised-LOPE film.

Severe processing of NiDIP-stabilised-PE MB revealed no change in the IR-absorption characteristic of NiDIP when compared with a KBr pellet spectrum of the additive (cf. Fig.5.1a and b), nor was there any increase in the carbonyl absorption region (ca.1710 cm^{-1}). Moreover, NiDIP-stabilised-PE MB film which was extracted with toluene gave a similar IR spectrum (Fig.5.1a) to that of an unstabilised PE [control] film (Fig.4B.1, Sec.4B.2.1). Complete extraction of NiDIP from the stabilised MB film was evident from the complete disappearance of the original purple colour of the stabilised PE-film.

The IR spectrum for a typical MB preparation of PE containing DiPDiS is shown in Fig.5.2a). By comparison with the KBr pellet spectrum (Fig.5.2b) the severe processing (30,0M) has effectively removed the characteristic P=S band (ca.640 cm^{-1}) while neither the P-O-C (ca.970 cm^{-1} and 1020 cm^{-1}) nor the P-S (ca.495 cm^{-1} and 455 cm^{-1}) are greatly effected (e.g. P-O-C (1000 cm^{-1}) and P-S (485 cm^{-1}) in the polymer. Furthermore, toluene extraction of DiPDiS-stabilised-PE MB film did not effect a substantial change in the IR spectral characteristics of the film.

Figure 5.3 displays the IR spectrum of unexposed MB-film containing HOBP. A KBr-pellet spectrum in the region of interest [Fig.5.3] shows absorption characteristic at 1630 cm^{-1} [carbonyl], 1600 cm^{-1} , 1578 cm^{-1} and 1500 cm^{-1} [skeletal ring vibration]. A significant amount of carbonyl absorption ca. 1710 cm^{-1} [from the polymer matrix] in the IR spectrum of HOBP-stabilised-PE MB [Fig.5.3] film is evident. Thus under severe processing conditions [30,0M] HOBP is unable to protect the polymer since it is adversely effected by hydroperoxides [38,46]. The 1620 cm^{-1} band observed in the IR spectrum of the MB films [Fig.5.3] could have resulted from a mixing of two bands at 1600 and 1630 cm^{-1} as a result of the polymer-HOBP system.

Figure 5.4 compares IR spectral regions of MB film containing the synergistic combination NiDIP-HOBP. No difference was found between the IR spectrum of this synergised MB film [Fig.5.4] and the superimposed spectra of MB films containing NiDIP [Fig.5.1a] and HOBP [Fig.5.3] separately. The characteristic bands of HOBP [1578 cm^{-1} and 1620 cm^{-1}] and NiDIP [1020 cm^{-1} and 970 cm^{-1}] appear quite strongly in the spectrum of the MB film [see Fig.5.4]. Of great importance here is the observation that the 1710 cm^{-1} carbonyl band is absent in the MB film containing NiDIP-HOBP combination [Fig.5.4] when compared to the NiDIP-free analogue [Fig.5.3].

Similarly, a comparison of the IR spectrum of MB-film containing DiPDiS-HOBP [30,0M] [Fig.5.5a and the superimposed spectra of MB films containing DiPDiS [Fig.5.20] and HOBP [Fig.5.3] separately, indicates the absence of

carbonyl absorption (ca. 1710 cm^{-1}) for the DiPDiS-HOBP combination, and that the characteristic bands of DiPDiS (1000 cm^{-1} and 485 cm^{-1}) and HOBP (1620 cm^{-1} and 1578 cm^{-1}) remain unaffected under the processing conditions used for MB preparation containing the synergistic combination [see Fig.5.5a]. Under milder (10,CM) conditions, however, a DiPDiS-HOBP-stabilised-PE MB film reveals significant departure from the results obtained under severe (30,OM) processing conditions and at the same 2.5% additive concentration. Thus, absorption bands which are ascribed to DiPDiS (1000 cm^{-1} and 485 cm^{-1}) are absent and the IR bands of HOBP showing enormous reduction in their intensities [compare the 1620 cm^{-1} band in Fig.5.5b (10,CM) with that in Fig.5.5a (30,OM)]. This observation was further confirmed from a comparison of UV-spectra of MB films containing HOBP-DiPDiS and processed under severe (30,OM) and mild (10,CM) conditions: the amount of HOBP left in the film was greater for the severely processed sample [cf. curves 1 and 3 in Fig.5.6]. Furthermore, extraction of DiPDiS-HOBP-stabilised MB film by toluene [Fig.5.5a] led to the disappearance of all the characteristic IR absorptions of HOBP, whereas characteristic absorptions due to DiPDiS were unchanged [see 1000 cm^{-1} and 485 cm^{-1} bands in Fig.5.5a].

Films prepared from severely processed (30,OM) stabilised-PE MB were found to be opaque to UV-light below 370 nm [see for example curve 1 in Fig.5.6]. The UV-spectrum of a DMB film containing DiPDiS-HOBP combination (0.25%) is, therefore, shown instead [Fig.5.7a, curve 1]. Unexpectedly, four new bands were found to occur with band maxima around 395 nm, 330 nm, 312 nm and 286 nm. HOBP itself exhibits two broad

absorption bands at 325 nm and 285 nm. Under photo-oxidative conditions the 395 cm^{-1} band decreases in intensity with a simultaneous increase in the intensity of the 285 nm band. Changes in the UV-spectrum of the DMB film following periods of photolysis in the UV-cabinet is shown in Fig.5.7a.

NS film of PE [10,0M] containing 1:1 synergistic combination of DiPDiS and HOBP does not show these new absorptions. Since DiPDiS, in an NS film, does not absorb light above 300 nm, the UV-spectrum of the DiPDiS-HOBP DMB film [Fig.5.7a] must be associated with HOBP and products of its reaction with DiPDiS. Moreover, both toluene [at 55°C] and hexane [at room temperature] were able to extract [from the DiPDiS-HOBP stabilised PE-MB and DMB films] the species responsible for these spectral features [Fig.5.7b]. The UV-spectrum of di-2-hydroxybenzophenone dithiophosphoric acid [HBPA [I], Sec.2A.5.1.7] is shown in figure 5.7c.

NiDIP-HOBP-stabilised-PE MB film processed under identical conditions [30,0M] to the DiPDiS-HOBP MB film, on the other hand, did not show any new UV-spectral features. Further, extraction of the NiDIP-HOBP-stabilised PE MB film with hexane revealed that, apart from the UV-absorption of NiDIP and HOBP, no additional spectral features were observed in the extract [see Fig.5.7d]. HOBP is completely extracted from the MB-PE films. Fig.5.7e shows the UV-spectrum of a hexane extract of HOBP-MB film which is identical to the spectrum of a neat HOBP solution. The extracted film, on the other hand, showed similar UV-spectrum to the unstabilised control film.

5.2.2 Photo-oxidation of Stabilised LDPE in Masterbatch Preparation

Identically processed [10,CM] PE films of DMB and NS, containing ca.0.1% stabiliser [e.g. NiDIP] show similar photo-oxidative behaviour [Fig.5.8 inset]; compare curves 7 and 8 which show a PIP of ca.350 h and 400 h for DMB and NS samples, respectively. Figure 5.8 compares the photo-oxidative behaviour of MB films containing NiDIP [curve 2], DiPDiS [curve 4], the synergistic combinations DiPDiS-HOBP [curve 3], and NiDIP-HOBP [curve 1]. A very low carbonyl index prior to UV-exposure is clearly evident in all these films. Moreover, the initial stage of photo-oxidation of these stabilised films was marked by the slow formation of carbonyl groups. Furthermore, DiPDiS-HOBP MB appears to exert an auto-retarded oxidation [curve 3 in Fig.5.8] during the early stages of photo-oxidation, whereas NiDIP-HOBP MB affords an extensive PIP [curve 1 in Fig.5.8]. In contrast to this, an MB of NiDIP-stabilised PE [curve 2 in Fig.5.8] shows an initial auto-retarded oxidation similar to that observed for DiPDiS [curve 4 in Fig.5.8] though to a much **less**-er extent. Based on the initial auto-retarded step, the effectiveness of the above photostabilisers in the MB films follow the order: NiDIP > DiPDiS-HOBP > DiPDiS. Figure 5.8 further shows that the increase in the carbonyl index is only slight ($\leq 0.5-9$ units) was obtained [curves 2-4] even after 1300 hours exposure in the UV-cabinet. This initial increase in carbonyl index [autoretarded step] is followed by a complete inhibition for a very long time.

Figure 5.9 shows the changes in functional groups observed during photo-oxidation of synergistically (HOBP-DiPDiS combination) stabilised-LDPE MB film. Clearly a correlation does exist among the indices shown: carbonyl [ca. 1710 cm^{-1}], curve 2, carbonyl vibration of HOBP [ca. 1620 cm^{-1}], curve 3, and bound P-S [ca. 485 cm^{-1}] curve 1.

Figure 5.10 compares the effect of different processing conditions on the photo-oxidative stability of dilutions prepared from DiPDiS-HOBP-stabilised-PE MB samples. It is clear that both components in this combination exert their effects synergistically and that under the same processing conditions similar results are obtained for DMB and NS films (cf. curves 2 and 1 in Fig.5.10). Further, figure 5.10 confirms earlier results regarding the greater importance of retardation during the later stages of oxidation with more severe processing in the presence of DiPDiS (cf. curves 2 and 3 with 4). Photo-oxidation of DMB film prepared from DiPDiS-HOBP-stabilised PE reveals the short-lived nature of the new spectral features (see Sec. 5.2.1 and inset of Fig.5.7a).

5.2.3 Thermal Oxidation of Stabilised PE in Masterbatch Preparation

Figure 5.11a shows the thermo-oxidative behaviour of normally processed NiDIP-stabilised LDPE films before (curve 4) and after (curve 2) extraction with toluene at 55° . This is compared with a DMB (curve 3) film (final concentration of NiDIP is 0.125%) and an extracted (curve 1) analogue. No significant difference was found between the oxidative

stabilities of NS and DMB films whether extracted or not [compare TIP=350 h for extracted and 400 h for unextracted film]. Figure 5.11b compares the thermo-oxidative behaviour of normally stabilised NiDIP-LDPE films, before [curve 1] and after [curve 3] extraction, with MB [undiluted] films which were similarly [30,0M] processed [curve 2] and extracted [curve 4]. It is clear that MB film [e.g. curve 2 in Fig. 5.11b] exhibited a similar thermo-oxidative stability to both the diluted MB film [curve 3 in Fig.5.11a] and the normally processed PE film [curve 4 in Fig.5.11a] for the same additive used. In contrast to this, NiDIP-MB film which was extracted with toluene showed lower oxidative stability [TIP=175 h] when compared to NS NiDIP-stabilised LDPE [TIP=350 h] which was similarly extracted.

DiPDiS-HOBP stabilised MB-film was extracted with toluene, before placing in the Wallace oven at 110° , under conditions which were shown to extract HOBP completely [as judged from the disappearance of the 1620 cm^{-1} band]. There was a good correlation between changes in the indices for the carbonyl [1710 cm^{-1} , curve 1] and P-S [485 cm^{-1} , curve 2] absorptions [Fig.5.12], under these ageing conditions. This correlation is comparable with an earlier one observed during photo-oxidation of DiPDiS-HOBP-MB film though the changes involved here are much less. The slow initial increase in the carbonyl index [curve 1 in Fig.5.12] is clearly associated with the simultaneous decrease in the P-S index [curve 2 in Fig.5.12].

The non-extractability of the thiophosphoryl group in the DiPDiS-stabilised-PE MB film as judged from the IR absorption spectra before and after extraction [no change in the P-O-C (1000 cm^{-1}) and P-S (485 cm^{-1}) bands] indicates that changes observed in the 485 cm^{-1} band during ageing in the case of DiPDiS-HOBP MB must be directly related to the changes in the grafted P-S groups. This confirms the bound nature of the thiophosphoryl residue, or its oxidation products. Furthermore, the increase in the carbonyl absorption was extremely slow and only after very long periods in the oven did the film gradually lose its clarity. The colour changed from clear yellow to dark yellow, brown and opaque dark brown (after 1500 h) and at a point where the carbonyl index was still fairly low [carbonyl index ca.3], see curve 1 in Fig.5.12]. Concurrently, during this period, the P-S index [curve 2 in Fig.5.12] which showed an initial drop appeared to autoretard at an index value of ca.0.6 (after 1200 h).

5.3 DISCUSSION

5.3.1 Photo-oxidative Stabilisation of Masterbatch Preparation

The protection of HOBP by DiPDiS during processing of an equimolar combination of HOBP-DiPDiS with LDPE has already been demonstrated in the previous chapter. It was further shown [see Sec.4B.2.4] that the extent of this protection was proportional to the processing time in an open mixer. DMB and NS films of HOBP-DiPDiS-stabilised PE are shown in the present chapter to exhibit similar photo-oxidative stability when processed under identical conditions [curves 1 and 2 in Fig. 5.10]. The observation that a greater degree of stabilisation was afforded by DMB samples when processed under more severe conditions [curves 4 and 2 in Fig. 5.10] corroborates earlier findings on the important role of oxygen in the stabilisation process [see Secs.4B.3.2 and 4B.3.4]. Stabilisation of severely processed DiPDiS-HOBP masterbatch, and its dilutions, is the result of contributions from the newly formed species [see Sec.5.2.1] with one of its absorptions occurring at 395 nm [Fig. 5.7a, curves 1 and 3], their transformation products during photolysis [as indicated for example by the increase in the 286 nm band [Fig.5.7a, curves 2 and 4] and any HOBP which has been protected by DiPDiS during processing but whose UV-absorption is masked by the new spectral features [see Fig. 5.7a]. However, a mildly processed DiPDiS-HOBP masterbatch does not show the new spectral features mentioned above [cf. curves 3 and 2 in Fig.5.6]. Examination of figures 5.6 and 5.7a shows that a smaller amount of HOBP has survived the milder processing conditions used for a DiPDiS-HOBP masterbatch.

It is known that HOBP is adversely effected by hydroperoxides [38,46] when processed alone in LDPE. Increasing processing severity increases the removal of HOBP. The marked improvement observed in the photo-oxidative stability of PE when an equimolar combination of HOBP and DiPDiS is used must be associated initially with the ability of DiPDiS to protect HOBP against hydroperoxides. Greater amounts of oxygen have apparently been harnessed by DiPDiS to give a higher yield of oxidation products which are responsible for the protection of HOBP at the processing stage [see Sec.5.3.3.3]. It is clear, therefore, that the O_2 :DiPDiS ratio must determine the ratio of oxidised:unoxidised DiPDiS. This, in turn, determines the thermo-oxidative stability of the polymer during processing and ageing or subsequent photo-oxidation [see Sec.5.3.3]. Under the same processing conditions, therefore, a higher proportion of the original DiPDiS will remain unoxidised in the MB sample when compared to the NS sample since a 25-fold excess DiPDiS is used in the former. This conclusion is strengthened further by the observation that DMB films, prepared from the same MB sample [30,0M], when subjected to more severe processing conditions (e.g. 30,0M), exhibited greater photo-oxidative stability compared to a mildly processed [10,CM] DMB film [cf. curves 4 and 2 in Fig.5.10].

There seems little doubt, therefore, that oxygen is a prerequisite for effective oxidative stability in formulations containing DiPDiS alone, or in combination with HOBP [as external synergist] or NiDIP [as auto synergist]. The fact that DMB and NS samples of stabilised LDPE exhibit similar photo-oxidative stabilities for the same additive and for identical processing conditions is also evident in the case of the nickel complex: compare DMB and NS Films containing NiDIP [curves 7 and 8 in Fig.5.8].

IR spectrophotometry can be used to follow accurately changes in the characteristic absorptions of the additives in MB (2.5%) films (see for example Fig.5.1a), whereas NS (ca.0.1%) films show extremely weak IR absorptions for the same additive. Because of the observed similarity between DMB and NS films insight into the mechanism of antioxidant action of these additives may, therefore, be gained indirectly from the study of MB films.

IR spectral features of NiDIP-stabilised PE MB indicate that NiDIP is not grossly effected during severe processing when compared with the KBr spectrum of the stabiliser [cf. Figs. 1a and 1b]. It is clear, therefore, that MB films containing NiDIP, DiPDiS and HOBP display almost only the IR spectra of the individual additives when present separately. The photo-oxidative stabilisation afforded by each of these additives in MB films, however, reveal considerable differences in the initial effectiveness of these antioxidants (when compared to the control). An initial fast auto-retarding step was found to occur in the case of DiPDiS [Fig.5.8, curve 4] to a much greater extent than for a NiDIP [Fig.5.8, curve 2] stabilised MB film.

The bound nature of the antioxidant is confirmed for the case of DiPDiS-stabilised-PE MB from the observation [Fig.5.2a] that stabilised films gave almost identical intensities of IR absorptions at 1000 cm^{-1} [due to P-O-C group] and 485 cm^{-1} [due to P-S absorption] before and after extraction of the films with toluene. In the same manner, the bound nature of the DiPDiS-based antioxidant in equimolar synergistic combinations of HOBP with DiPDiS in a PE-MB was

confirmed from the observation that HOBP was completely removed following extraction with toluene [Fig.5.5a] whereas no change in the intensity of P-O-C and P-S absorption bands was evident. The observation that DMB and NS-films containing DiPDiS in the presence and absence of HOBP display similar photo-oxidative behaviour [e.g. curves 1 and 2 in Fig.5.10], and the non-extractability of the thiophosphoryl residue with toluene leads to the conclusion that bound antioxidants are also present, though undetectable, in NS films.

5.3.2 Thermo-oxidative Stabilisation of PE-MB Preparations

The similarity in thermo-oxidative stabilities of NiDIP stabilised-PE DMB and NS films [e.g. curves 1 and 2 in Fig. 5.11a] supports the earlier conclusion [see Sec.5.2.2] that their oxidative behaviour will be similar provided they contain the same additive concentration and have been identically prepared and tested. The presence of bound antioxidant was established earlier [see Secs.5.3.1 and 4A.3.2] and examination of the effect of hot toluene extraction on the thermo-oxidative behaviour of the stabilised PE films supports this further. Thus, for example, complete removal of NiDIP [from DMB and NS films] by toluene, at 55^o, [as confirmed by the complete disappearance of the UV-absorption of NiDIP] did not effect a significant reduction in the thermo-oxidative induction period [cf. curves 2 with 4 and 1 with 3 in Fig.5.11a]. This observation is similar to that discussed previously for NS film containing

similar disulfide [IX] which was similarly aged in a Wallace oven [see curve 5 in Fig.4A.5, Sec.4A.2.4]. It is clear, therefore, that during processing the nickel complex gives rise to DiPDiS initially which undergoes further oxidation, the extent of which is dependent on the amount of oxygen present [see Fig.4A.6 in Sec.4A.5, and Sec.5.3.3]. These oxidised products might also act as bound-antioxidants in the mechanism of stabilisation of PE.

The shorter thermo-oxidative induction period observed for a NiDIP-MB film extracted with toluene [curve 4 in Fig.5.11b] when compared to a similarly stabilised extracted DMB film [curve 4 in Fig.5.11a] is additional evidence for the lower extent of conversion of the metal complex to the corresponding disulfide [and hence less bound antioxidant] at low oxygen ratios [in the presence of high additive concentration in the MB].

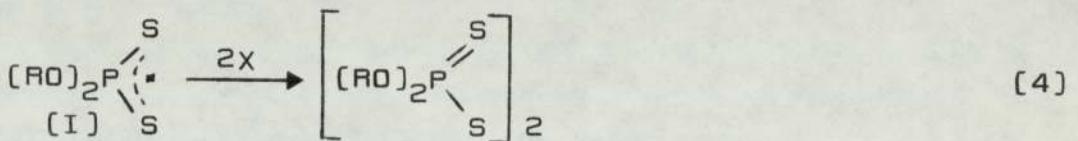
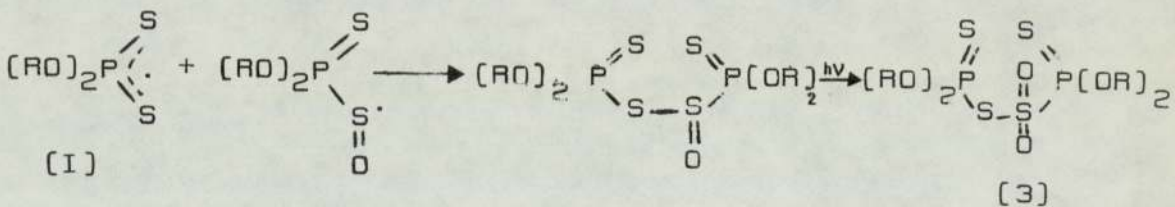
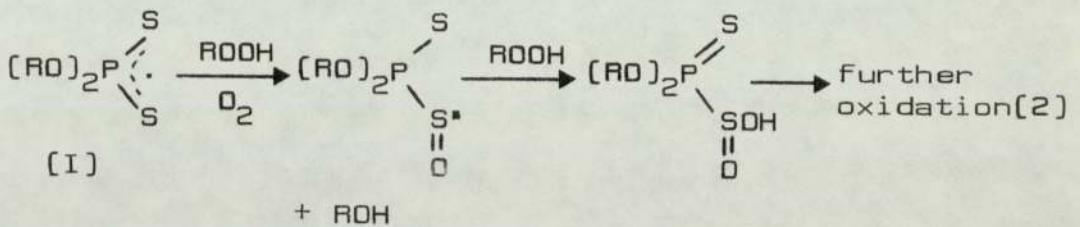
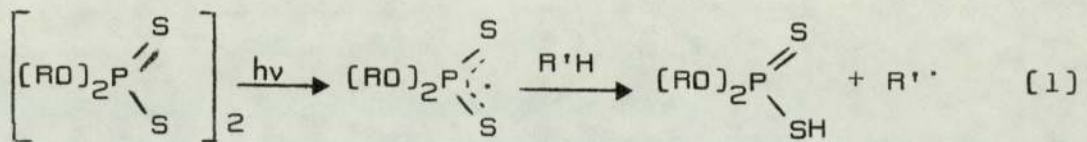
The initial rapid oxidation step which is observed in extracted MB containing DiPDiS-HOBP [curve 1 in Fig.5.12] is similarly explained on the basis of the presence of low oxygen [and hence hydroperoxide availability] relative to the high concentration of the additives under the MB conditions. It seems likely that some un-oxidised free thiyl radicals results. The latter are known^[29] to be more reactive than the corresponding sulphinyl radical. Alternatively, less sulfur acids are formed under milder processing conditions.

5.3.3 Mechanisms of Stabilisation of PE in MB
Preparations using Different Antioxidants

5.3.3.1 DiPDiS

The initial fast auto-retarding step observed during photo-oxidation of stabilised PE-MB containing DiPDiS (Fig. 5.8, curve 4) can be explained in terms of the following competitive reactions [scheme 5.1].

Scheme 5.1 Photo-oxidation Pathways for DiPDiS



Process (4) is a termination step which leads to the regeneration of the parent disulfide, DiPDiS. Process (1) is responsible for the initial rapid oxidation, whereas processes (2) and (3) are responsible for retardation which leads to inhibition in the case of the MB film [curve 4 in Fig. 5.8].

It was shown earlier [see Sec.3.3.3] that DiPDiS does not decompose TBH at room temperature unless photo-initiated by light. The formation of an unknown intermediate was found to occur at $\lambda_{\text{max}} = 250 \text{ nm}$ and which disappeared on further photolysis [see Fig.3.16, Sec.3.3.3]. It is feasible, therefore, that a radical of the type $[(\text{RO})_2\text{PSSO}]$ [process 2] and the thiosulfinate product [process 3] are associated with the 'inhibition' which is observed after the initial retarded step [curve 4 in Fig.5.8] rather than DiPDiS itself.

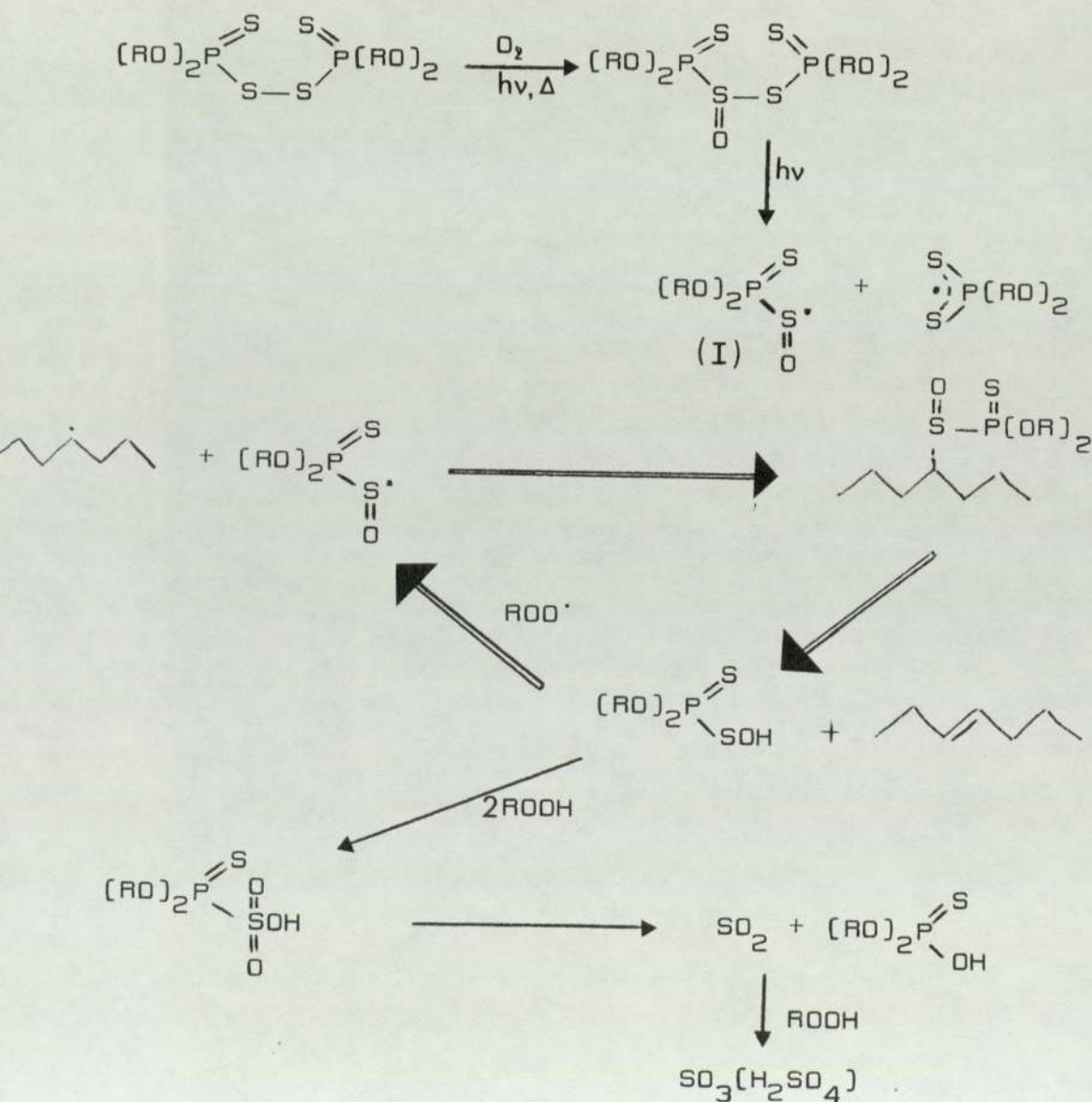
Other workers [29,47,115,116,124,125] have demonstrated the inhibitory role of disulfides [and monosulfides] during the oxidation of polymers and in the thermal auto-oxidation of model compounds. It was further shown [115,116,124], however, that the inhibitory effect could not be attributed to these disulfides [or monosulfides] themselves but rather to certain of their oxidation products. Moreover, it was shown [124] that the only active oxygenated products formed from the reaction of hydroperoxides with disulfides and monosulfides, to which effective inhibition could be attributed, were the thiosulfinate, RSSR , and sulfoxides, RSR , respectively. It is clear, therefore, that disulfides [or monosulfides] function as reservoirs from which the active inhibitor can be generated as required when hydroperoxides are formed during auto-oxidation of the substrate.

Oxidation of the disulfide during processing results in a reaction similar to process [2] in Scheme 5.1. Increasing processing severity therefore, leads to greater amounts of sulfur acids which are catalysts for hydroperoxide decomposition. Thus process [1], Scheme 5.1, becomes secondary under severe processing conditions in view of the depletion of the disulfide via oxidative reactions. Under the same conditions of

processing, therefore, a twenty five-fold increase in the concentration of the additive, e.g. in MB preparation, and in the presence of the same 'fixed amount' of oxygen which is normally available during the preparation of NS-PE film should result in a preponderance of radicals via process (1), i.e. less sulfur acid formation. Indeed, the importance of oxygen and oxidation products is best illustrated by the photo-oxidative behaviour of DMB films which were processed in the presence of excess [30,0M] and limited [5, CM] amounts of oxygen (as discussed earlier [see Sec.5.3.3.1 and curves 4 and 2 in Fig.5.10]).

The extent of the radical-generating process (1) can only be inferred from the initial auto-oxidation process for the case of DiPDiS when compared with NiDIP [see Fig.5.8, curves 2 and 4 and Sec.5.3.3.2]. It is well known^[8,11] that the thermal processing history of the polymer exerts its effect in the subsequent UV-lifetime of fabricated plastics. In effect, therefore, the ratio of oxygen:radical $[(RO)_2PSS']$ during processing, predetermines the mode of photo-oxidative behaviour of stabilised PE. The appearance of the initial auto-retarded step is the resultant effect of the two radicals $[(RO)_2PSS']$ and $[(RO)_2PSS'O]$ which exert opposite effects, i.e. oxidation engendered by process (1), and an antioxidant effect imparted by processes (2) and (3). Moreover, grafting of the radical $(RO)_2PSS'$ [or its oxidised form] during processing of PE-MB containing DiPDiS is supported from the observation that the IR-absorption of P-O-C

and P-S with MB films showed no change before and after extraction with toluene [see Fig.5.2a]. Thus grafting as well as the proposed formation of a Lewis acid [see Scheme 5.2] are responsible for the antioxidant activity of DiPDiS as evidenced from the low initial carbonyl index [curve 3 in Fig.5.8], and its good performance as a melt stabiliser [see Sec.6.2.2]. Photo-initiated grafting of radicals is also feasible and could occur simultaneously with a regenerative process [Scheme 5.2] which accounts for the long inhibition observed in DiPDiS-stabilised-PE MB film.



Scheme 5.2 Regenerative mechanism giving rise to the antioxidant species

5.3.3.2 NiDIP

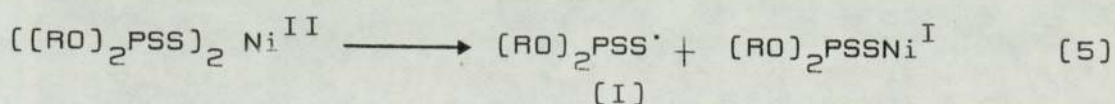
NiDIP-stabilised-PE MB film shows an initial rapid oxidation, albeit to a lesser degree [carbonyl index levels off at ca.3-4] when compared with DiPDiS-MB analogue [cf. curves 2 and 4 in Fig.5.8]. This slower rate of the initial rapid oxidation is explained in terms of the low rate of conversion of NiDIP into DiPDiS [See Sec.3.2.3], i.e. lower thiophosphoryl $[(RO)_2PSS^{\cdot}]$ radical formation, compared to the DiPDiS-stabilised-PE MB case [process 1 in Scheme 5.1].

Photo-induced decomposition of NiDIP is catalysed by oxygen [see Scheme 3.1 in Sec.3.3.2]. The amount of oxygen which is available during the processing of stabilised-PE MB samples dictates, therefore, the fate of the metal complex. Four processes are important during the decomposition of the metal complex via a radical-generating process [see Scheme 5.3 and Scheme 3.1 in Sec.3.3.2].

1. Radical-nickel complex fragment which can lead to the regeneration of the parent complex through 'in-cage' recombination.
2. Radical-radical coupling which accounts for the formation of disulfides.
3. Radical-substrate interaction which can result in grafting [sulfur radicals adding to macroradicals] or in a fast oxidation [radicals abstracting hydrogens from the substrate]. This process may account for stabilisation or degradation depending on the reactivity of the sulfur-centred radicals toward addition and hydrogen-abstraction, and in competition with process 4.

4. Radical-oxygen reaction giving rise to varying degrees of oxidation of sulfur-centred radicals. These radicals can bind to the matrix [see process 3].

It was shown earlier [see Sec.3.3.2] that the presence of oxygen promotes processes 2 and 3 at the expense of 1. Thus high oxygen concentration interferes with radical reactions, possibly through a 'poisoning' of the metal centre and/or via process 4, thereby effectively competing with the otherwise most favoured reaction pathway, i.e. radical-fragment recombination. The regeneration process 1 was shown^[95] to be quite extensive at very low oxygen concentration for the metal complex NiDBC. Consequently, formation of disulfides via process 2, metal complex-induced decomposition of hydroperoxides^[42], and reaction of hydroperoxides with the thiol group of dithiophosphoric acid [process 3] are unimportant. In the complete absence of oxygen, therefore, process 1 is expected to predominate and an equilibrium [reaction 5] will be established. The stability of the dithiophosphoryl



radical [I] to some extent determines the nature of this equilibrium together with the hydrogen-donating ability of the substrate.

Process 3 could be directly related to the fate of the radicals [I] which are neither scavenged by oxygen [process 4]

nor 'trapped' by the parent metal-fragment (process 1). Radicals which escape reaction pathways 1 and 2 may undergo addition reactions and become grafted to the polymer network. This is supported by the observation that P-O-C and P-S IR-absorptions for DiPDiS-stabilised-PE MB's were unaffected upon hot toluene extraction (see Fig.5.2a, and Scheme 5.2).

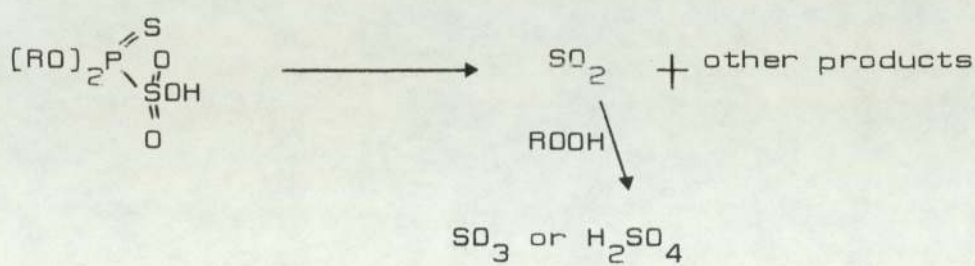
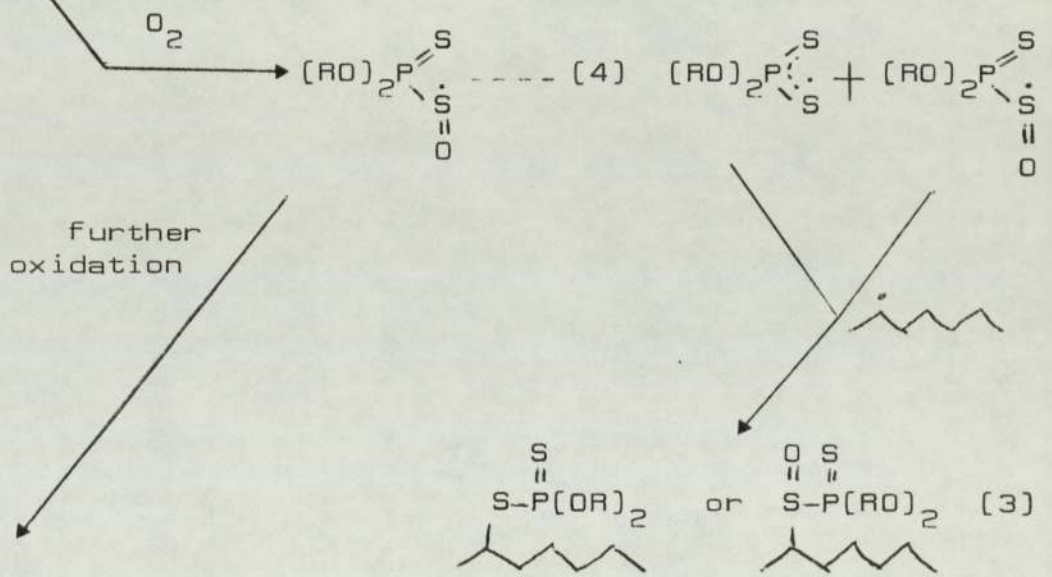
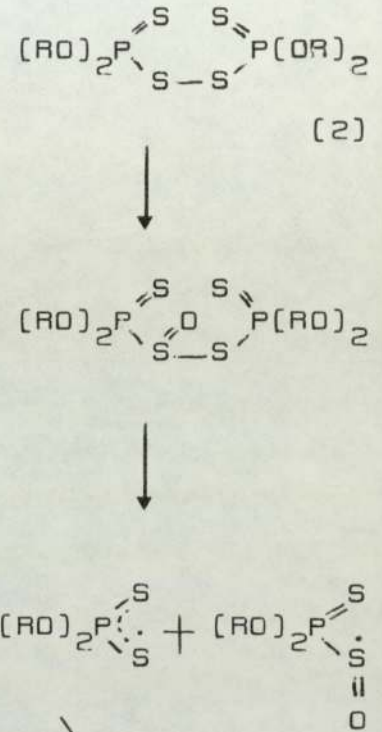
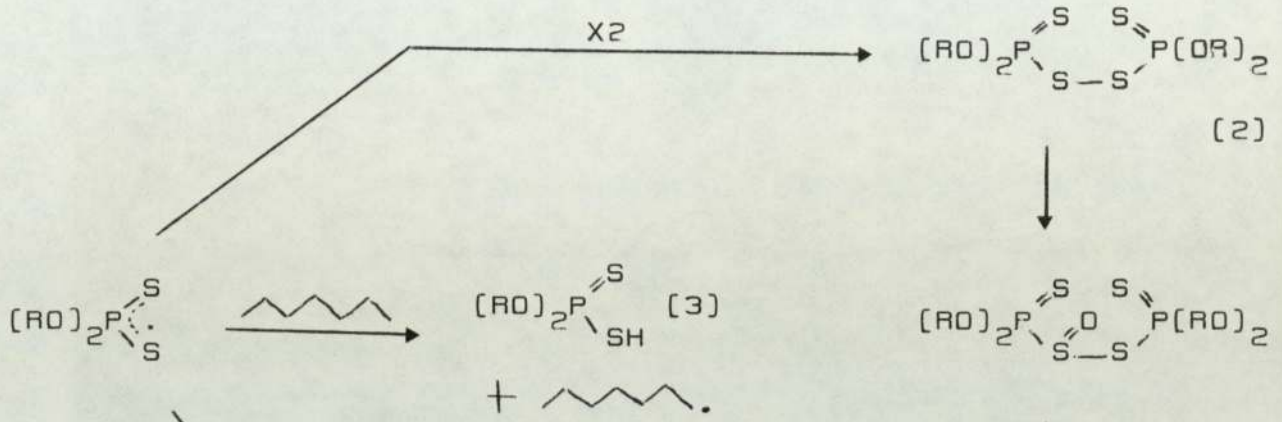
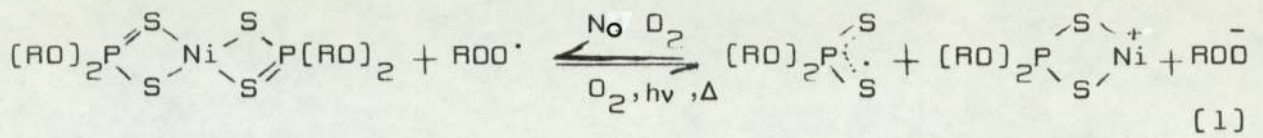
In the case of NiDIP-stabilised-PE MB, however, a slow rate of conversion of the metal complex into disulfide (as a result of process 1) would account for the limited significance of process 3 (i.e. grafting) because of higher competition by oxygen for these radicals (process 4). The absence of residual P-S and P-O-C IR-absorption after toluene extraction (see Fig.5.1a; compare with Fig.5.2a for DiPDiS) indicates the decisive role of process 1 in the case of NiDIP.

Other radicals which will abstract hydrogens from the polymer backbone will create macroradicals which can in turn, either propagate in a chain-type process and act as sites for oxygen uptake or, cross links to other macroradical^[23]. The former will result in fast oxidation which is clearly in accord with the present work at higher radical:oxygen ratios (curve 2 in Fig.5.8) in view of the high concentration of the additive being used in master-batch preparations. In this sense, the dithiophosphoryl radical is 'initiating degradative photo-oxidation'.

The observation that fast oxidations were not found to occur in NS of stabilised-PE samples containing NiDIP [see Fig.4B.3, Sec.4B.2.2] must be rationalised on the same basis. A high oxygen to radical ratio drives the reaction favourably toward disulfide formation [process 2] and other oxidised forms of these radicals [process 4], interfering effectively with process 1. The functional dependence of the photo-oxidative induction period on the concentration of NiDIP in NS films of stabilised PE [see Sec.4B.2.2 and Fig.4B.3] is indicative of the importance of process 1. Photo-oxidation of NiDIP in hexane systems [see Sec.3.2.3 and Fig.3.12] showed a similar result where the more concentrated photolysates gave proportionately longer periods of photo-stability. Although process 2 is favoured by the presence of oxygen, the actual conversion of radicals into disulfides [see Sec.3.2.3] is attenuated because of processes 3 and 4.

The following scheme outlines the conditions under which the different processes [1-4] become important though the pathways shown are not mutually exclusive.

Scheme 5.3 Outline of the important processes during decomposition of nickel dithiophosphate



5.3.3.3 Synergistic Combinations of NiDIP and DiPDiS with HOBP

Photo-oxidation of DiPDiS and DiPDiS-HOBP stabilised-PE MB films show an initial fast step which is slower in the case of the synergistic combination (curves 3 and 4 in Fig.5.8). Under MB conditions, radicals produced from DiPDiS (upon UV-exposure) are formed in high concentration and are expected to attack the matrix and, at least initially, photosensitise oxidation via production of a high concentration of thiyl and macro alkyl radicals (see reaction 3, Scheme 5.3). The slower step observed in the presence of HOBP is explained on the basis of the greater percentage of light being preferentially absorbed by HOBP. Thus photolysis of DiPDiS proceeds much more slowly (than in the absence of HOBP) whether by direct absorption of light by HOBP^[46] or, indirectly, via a deactivating secondary process^[38,46] involving energy transfer from the excited state of DiPDiS to HOBP. Benzophenones in general^[127], and HOBP in particular^[128], have a limited compatibility in PE and PP. Accordingly, exudation or blooming of HOBP may take place during the various stages of MB-preparation before, and during, UV-exposure. It was also suggested^[127] that exuded benzophenones (during UV-exposure) can act as screens, providing enhanced protection of the substrate. Although blooming was evident in HOBP-stabilised PE-MB, and to a much lesser extent in the case of NiDIP-HOBP PE-MB, no such effect was observed with DiPDiS-HOBP-stabilised-PE MB processed under exactly the same conditions. Evidently, DiPDiS has radically affected HOBP under the conditions of MB preparation, resulting in a more compatible benzophenone reaction product (see Fig.5.7a).

The apparent absence of an initial fast process during photolysis of NiDIP-HOBP stabilised PE-MB [curve 1 in Fig. 5.8], in contrast to the initial fast oxidation which was observed for NiDIP-stabilised-PE MB [see curve 2 in Fig.5.8], is postulated here to result from the combined effect of NiDIP and HOBP during photo-oxidation of the stabilised film and the lower yield of dithiophosphoryl radicals which could be generated in the presence of HOBP on account of its screening/quenching^[38] action [as mentioned above], since blooming was also observed in films stabilised by the NiDIP-HOBP combination. A lower radical concentration, in turn, implies a higher contribution from other competing reactions [see Schemes 5.1-3] including the oxidation of radicals, disulfide formation and radical addition to unsaturated sites on the matrix [grafting].

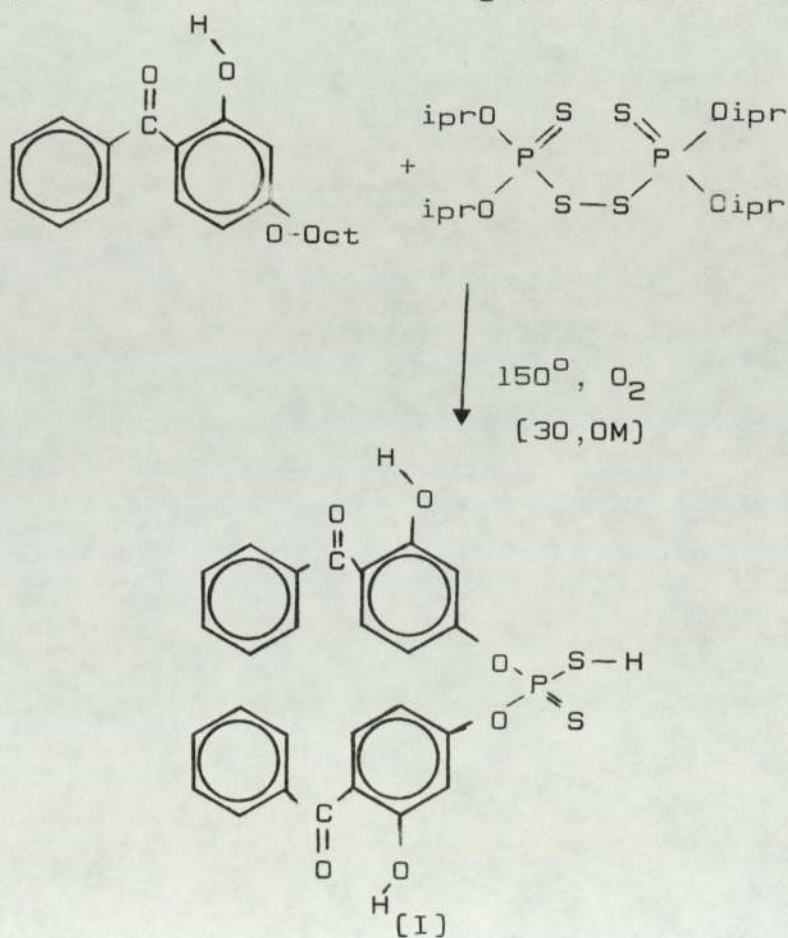
In contrast to the new UV-spectral features [at 395 nm, 330 nm, 312 nm and 285 nm] which are observed in severely processed [30,0M] DiPDiS-HOBP-stabilised-PE MB films [as seen in a hexane extract of this MB-film in Fig.5.7b], no new 395 nm band was observed in NiDIP-HOBP stabilised PE-MB film, prepared under identical processing conditions [30,0M]. This is to be expected due to the low formation of DiPDiS from NiDIP under the MB conditions [see Sec.5.3.3.2].

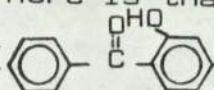
The photo-oxidative instability of the species responsible for the new spectral features observed in the severely processed [30,0M] DiPDiS-HOBP-PE MB and DMB films [see inset in Fig.5.7a] contrasts with its stability under thermo-oxidative conditions [inset in Fig.5.12]. Furthermore,

the gradual colour changes which were observed for HOBP-DiPDiS-stabilised-PE MB film [from bright yellow to brown] with prolonged UV-exposure must be associated with absorption characteristics of the new species which were found to be extractable by toluene and by hexane.

Similarly, under thermo-oxidative conditions, the colour of the MB film changed to a very dark brown [almost opaque] colour after prolonged ageing [ca.1000 h]. It is suggested here that a 'cross-product' acid of the type DiPDiS-HOBP may explain the photo- and thermo-oxidative behaviour observed. Although the nature and identity of the 'cross-product' acid has not yet been thoroughly investigated a possible assignment is, 0,0-di-2-hydroxybenzophenone dithiophosphoric acid [I].

A suggested route to this is given below:



it assumes an exchange reaction between the (RO) groups of the interacting species. Thermodynamic considerations must obviously be a deciding factor on the feasibility of such a reaction. The contention here is that the (iPrO-P) bond is somewhat weaker than the [] bonds, i.e. aryloxy group interacts more strongly with phosphorus than an alkoxy group. Although thermodynamic data are not available to ascertain this, it is worth mentioning here that the reaction between isopropanol and P₂S₅ proceeds at a much lower temperature than an analogous reaction between 2,4-dihydroxy benzophenone and P₂S₅ [see Sec.2A]. Dithiophosphoric acids are known^[78] to undergo reactions with high molecular weight alcohols in which their alkoxy groups can be exchanged [see Sec.2B.1].

This tentative scheme is based on the observation that O,O-di-2-hydroxybenzophenone dithiophosphoric acid (I) displays a UV-absorption spectrum [Fig.5.7c] which appears to be similar to the new spectral features described earlier [cf.Fig.5.7a or b]. A 'cross-product' of this kind would be expected to be rather unstable towards UV-light on account of the instability of the acid moiety. Thermo-oxidative treatment should readily oxidise the S-H to disulfide^[77,92] initially, followed by subsequent oxidation by hydroperoxides formed during heat ageing of PE^[19]. The formation of this disulfide during thermo- and photo-oxidation is supported by the simultaneous build-up and disappearance of the 285 nm (disulfide) and 395 nm (acid) bands respectively [curves 3 and 4, Fig.5.7a]. The apparent insensitivity of the 285 nm band to prolonged UV-exposure after the complete disappearance of the 395 nm band supports the disulfide nature of this newly formed species of which the 2-hydroxybenzophenone moiety forms an integral part.

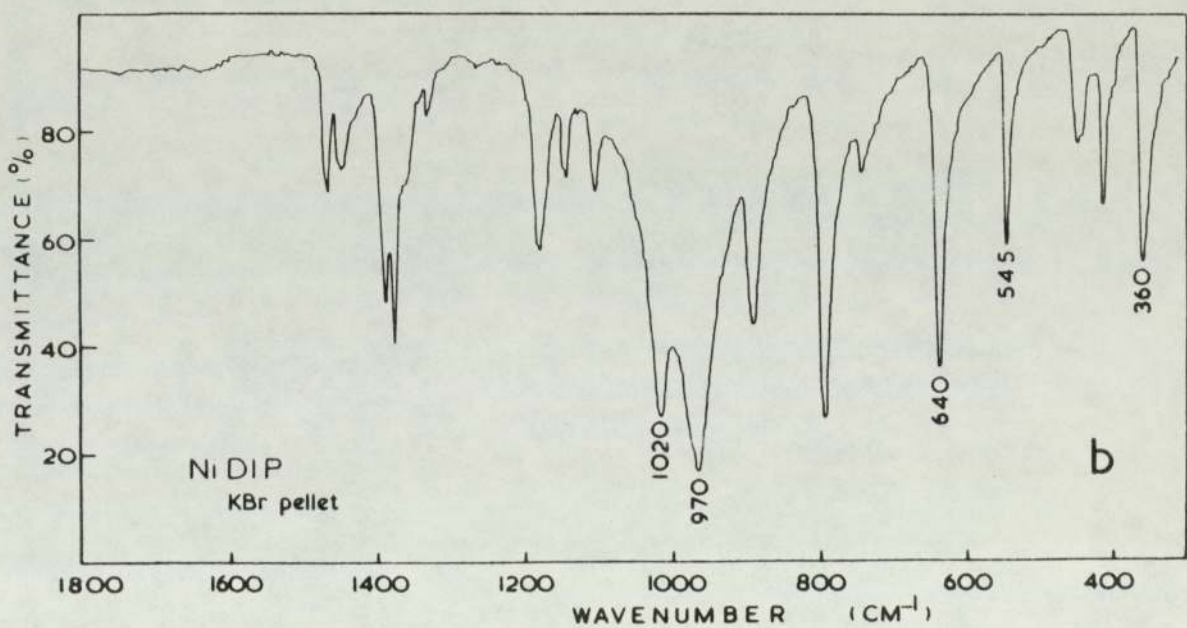
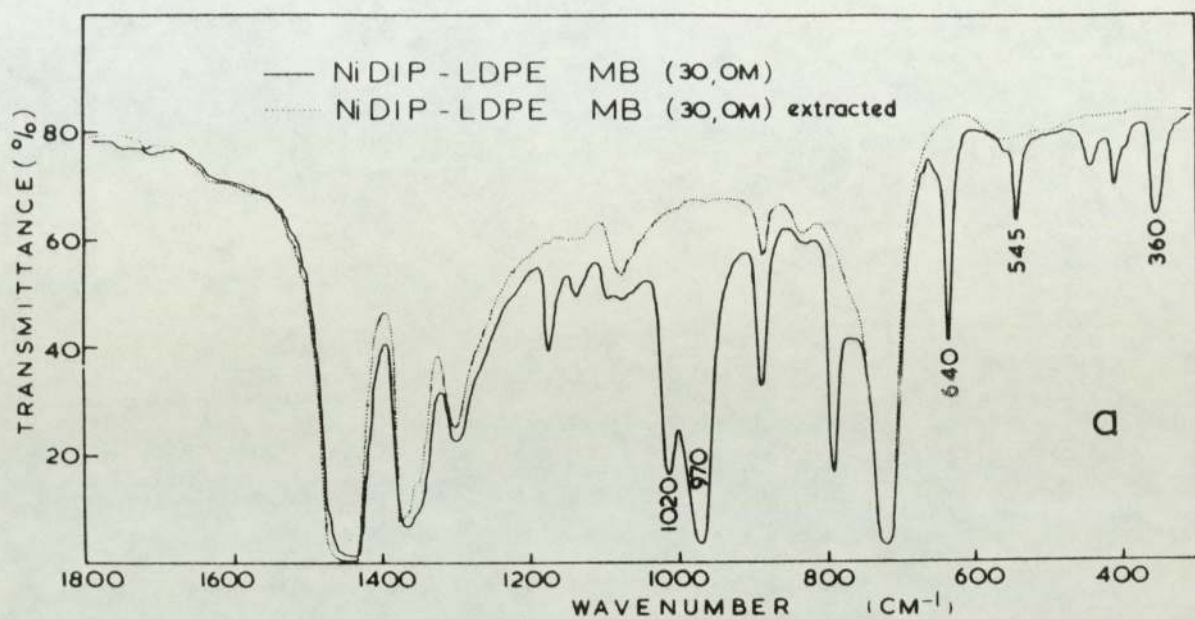


Fig.5.1 Infrared spectra of [a] extracted and unextracted LDPE MB containing NiDIP [2.5%], and [b] KBr-pellet containing NiDIP [ca.1%]

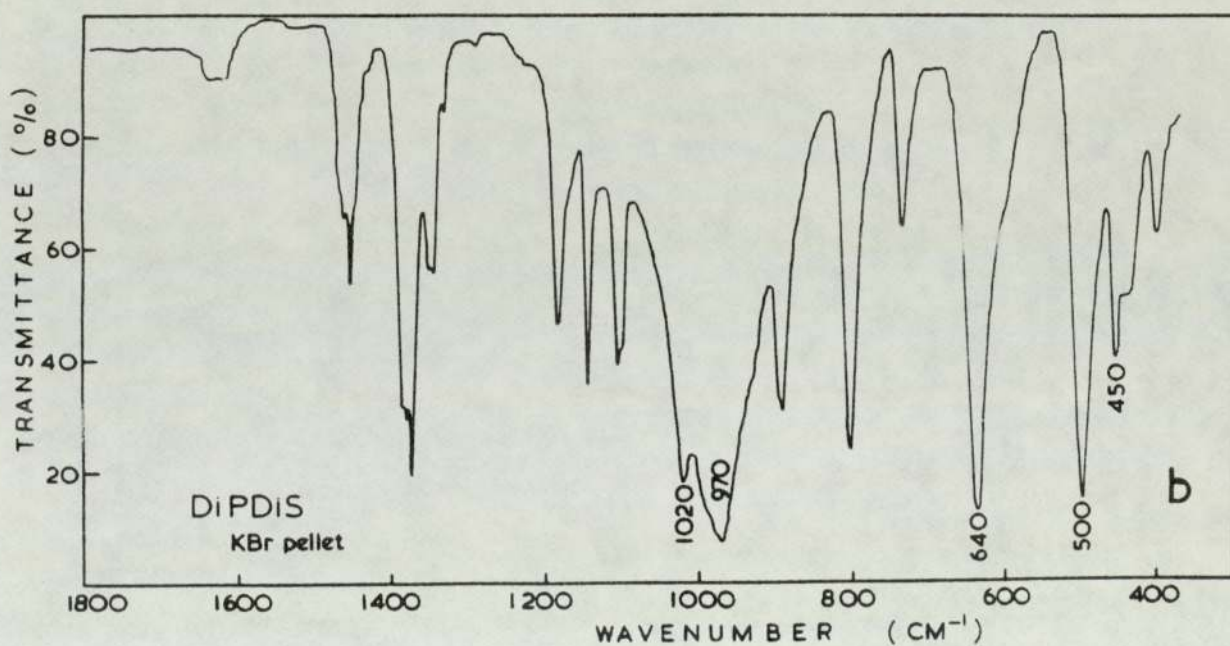
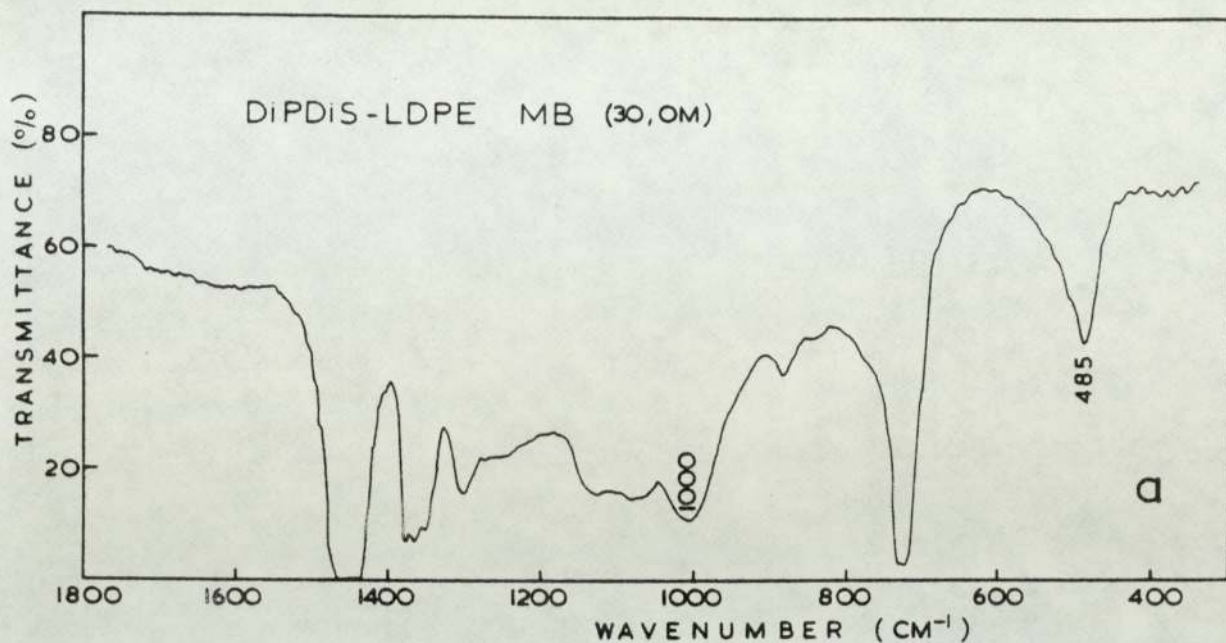


Fig.5.2 Infrared spectra of [a] DiPDiS [2.5%] stabilised -LDPE MB film before and after extraction and [b] DiPDiS [ca.1%] in KBr pellet.

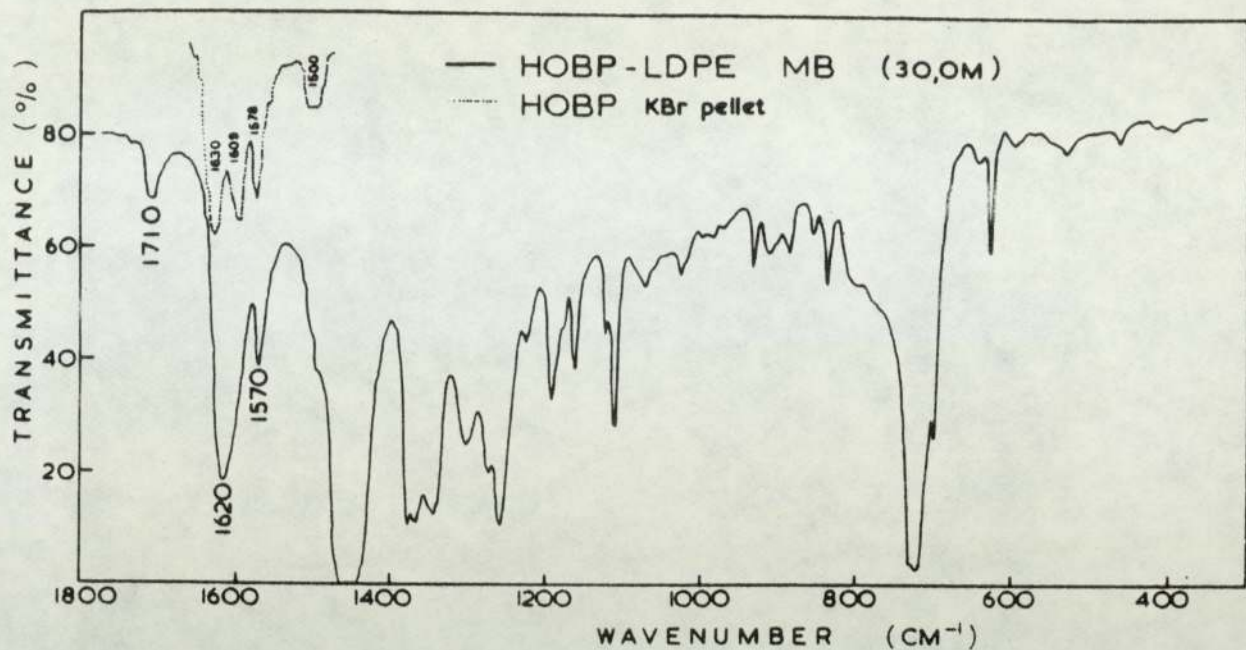


Fig.5.3 Infrared spectra of HOBP [2.5%] stabilised-LDPE MB film and that of HOBP [ca.1%] in a KBr pellet

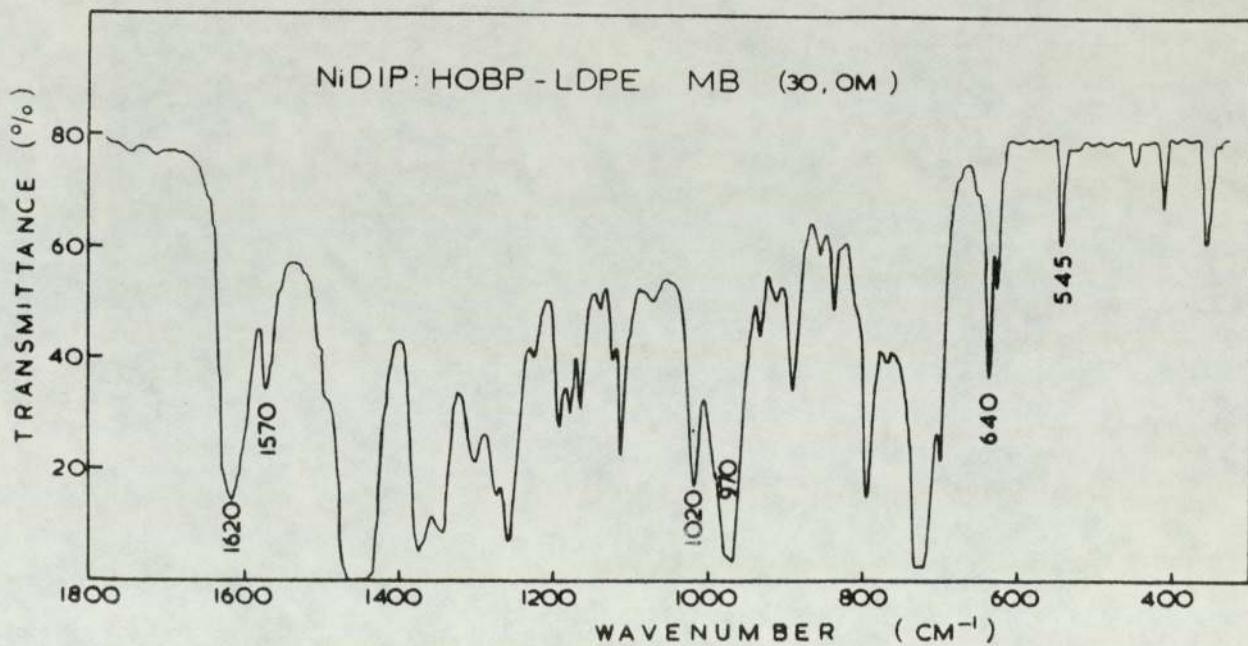


Fig.5.4 Infrared spectrum of NiDIP-HOBP [2.5% each] -stabilised-LDPE MB film

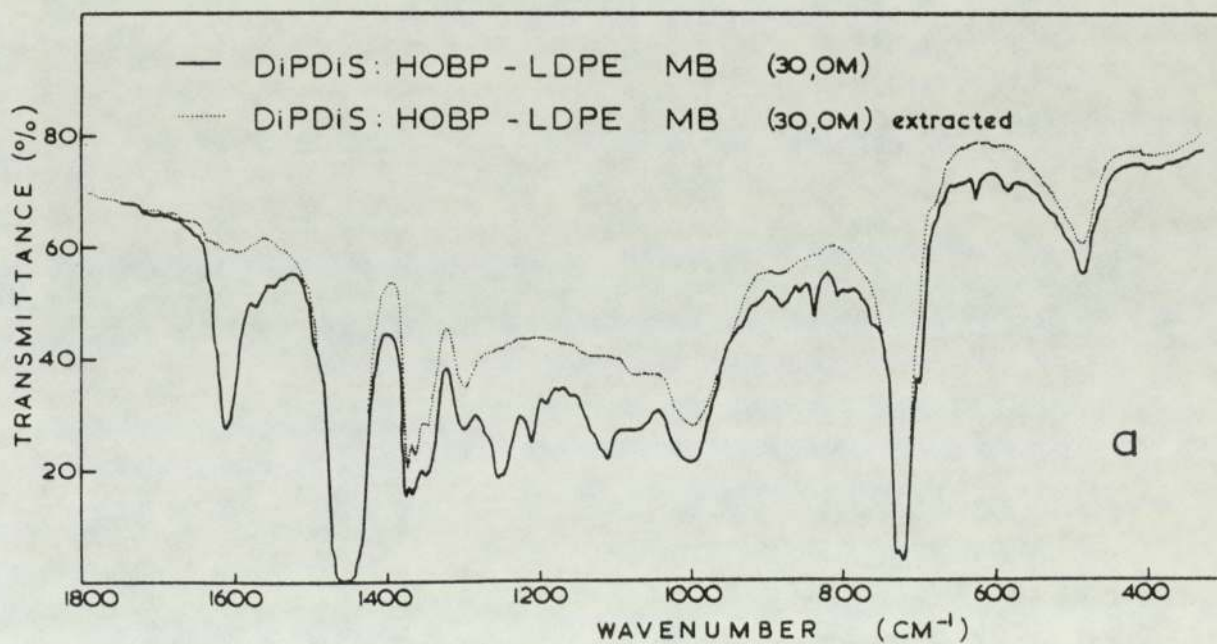
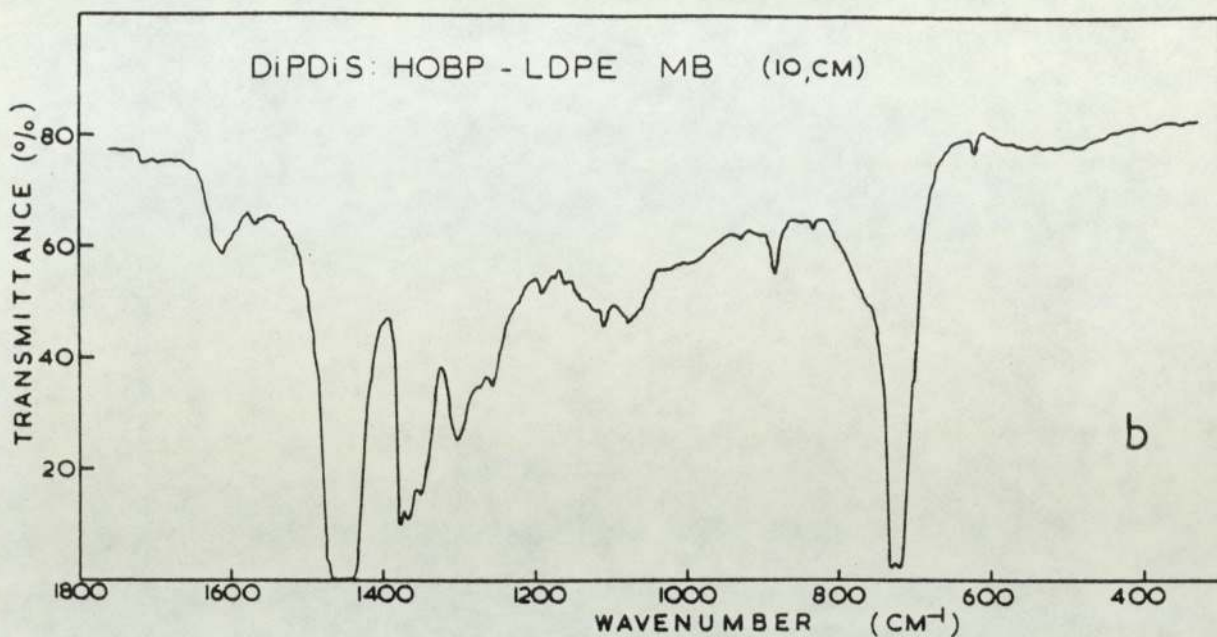


Fig.5.5 Infrared spectra of [a] extracted and unextracted films of severely processed DiPDiS-HOBP [2.5% each] stabilised LDPE MB, and [b] unextracted mildly processed analogue

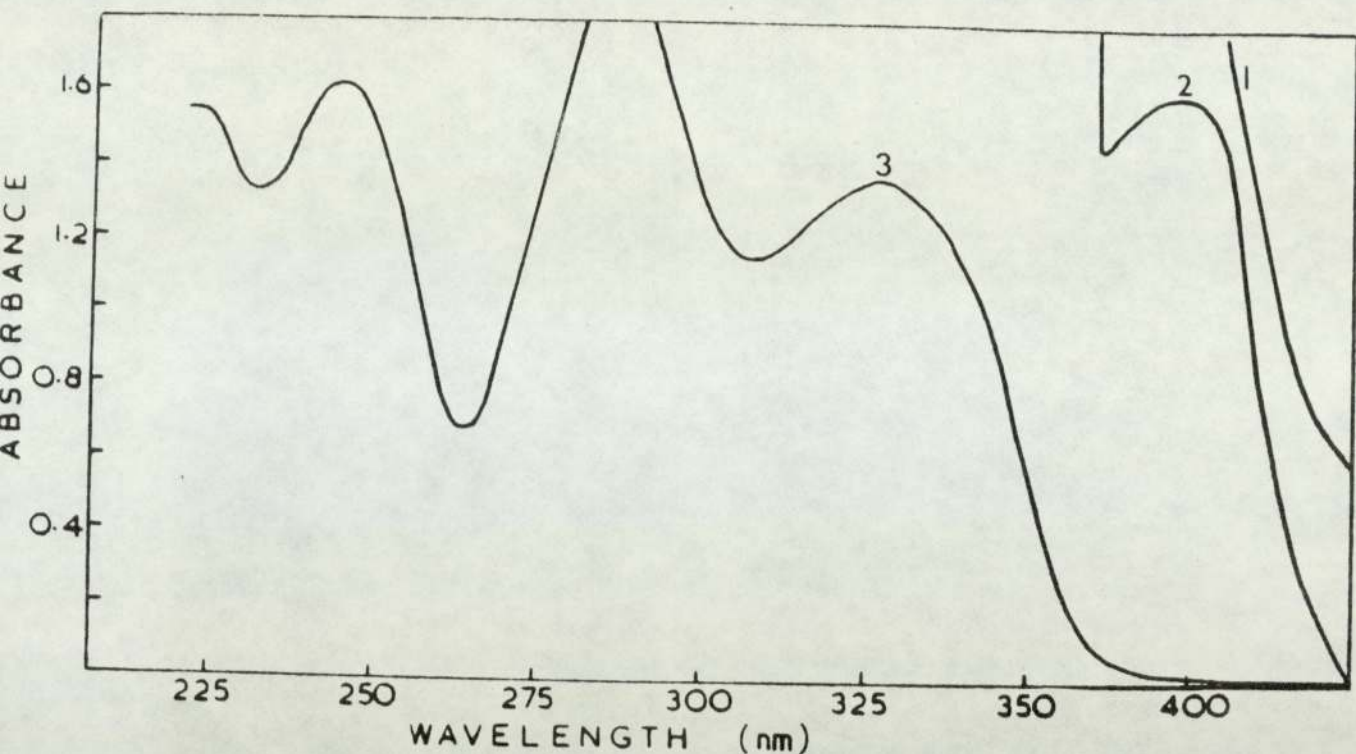


Fig.5.6 UV-absorption spectra of MB films of DiPDiS-HOBP stabilised-LDPE processed for 1. [30,0M], 3. [10,CM]. Spectrum 2 is same as 1 except for a baseline shift in order to show the maximum of the new absorption at 395 nm which is found in severely processed MB film.

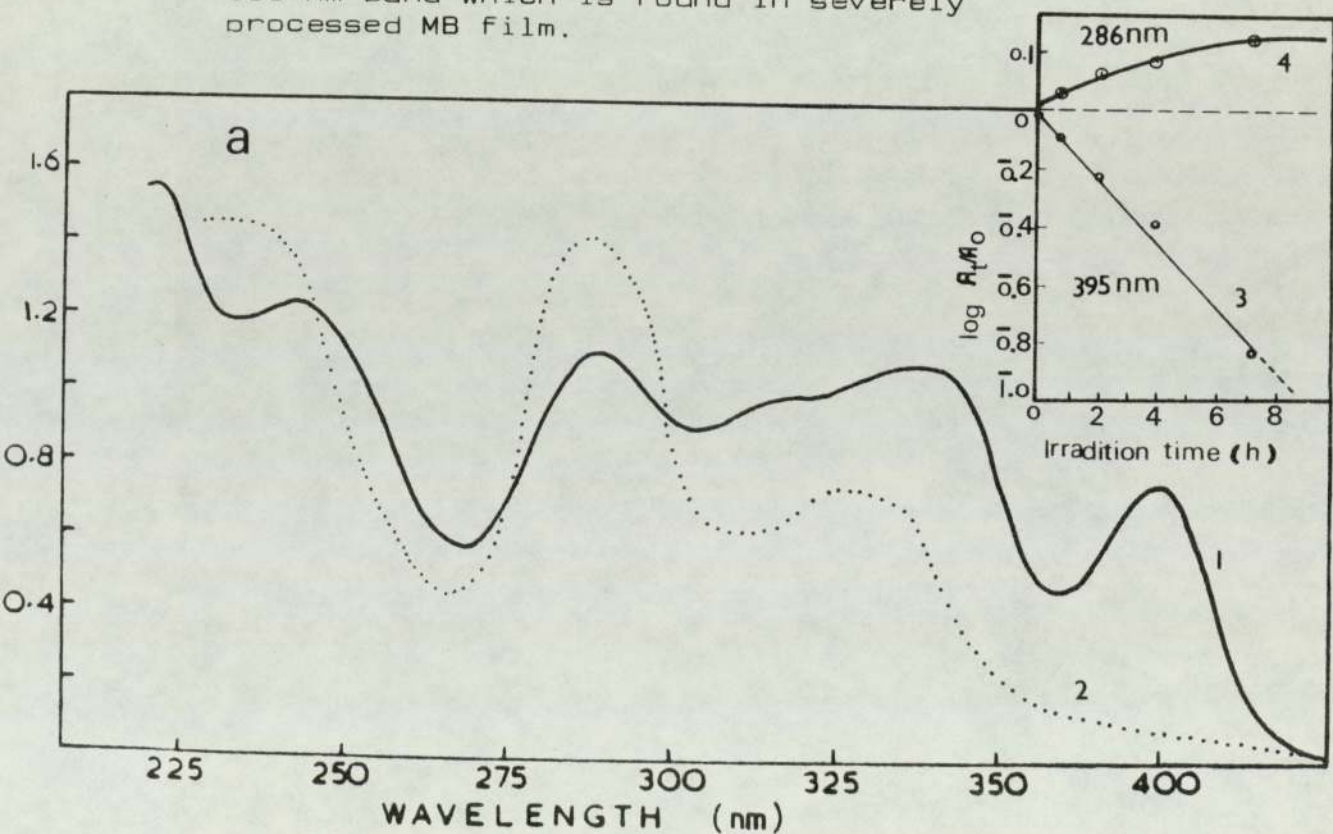


Fig.5.7a UV-absorption spectrum of DMB Film of DiPDiS-HOBP stabilised (0.25%)-LDPE processed for [10,0M] before [1] and after 8hr UV-exposure [2]. The original MB was processed under severe conditions [30,0M]. The kinetics of disappearance of the 395 nm band [3] and the build up of products absorbing in the region 286 nm [4] is shown in the inset.

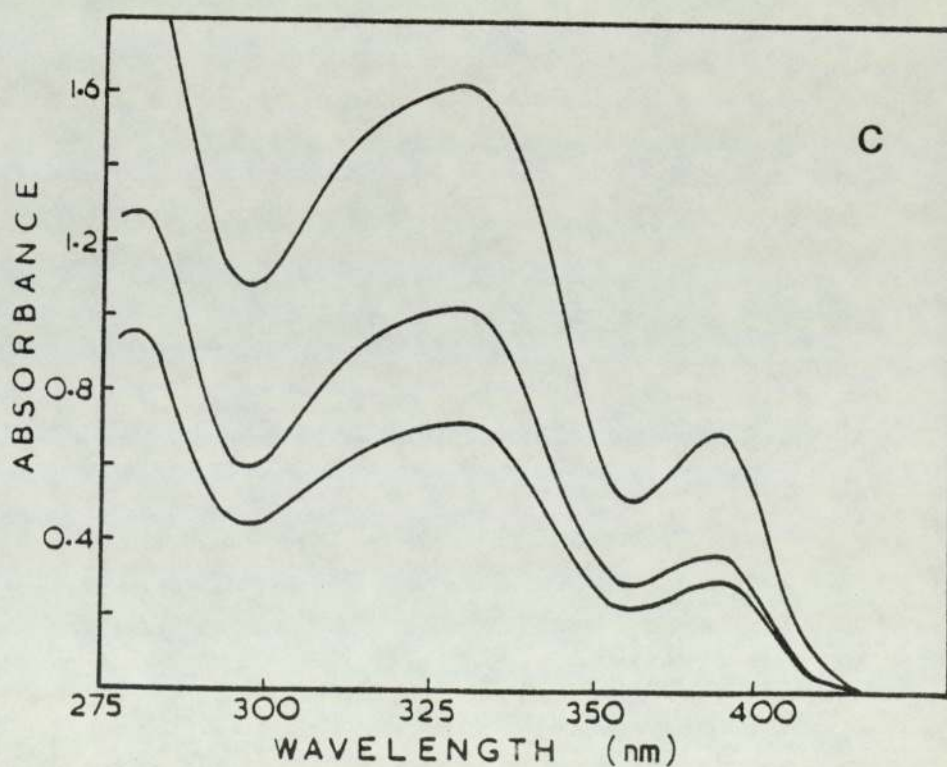
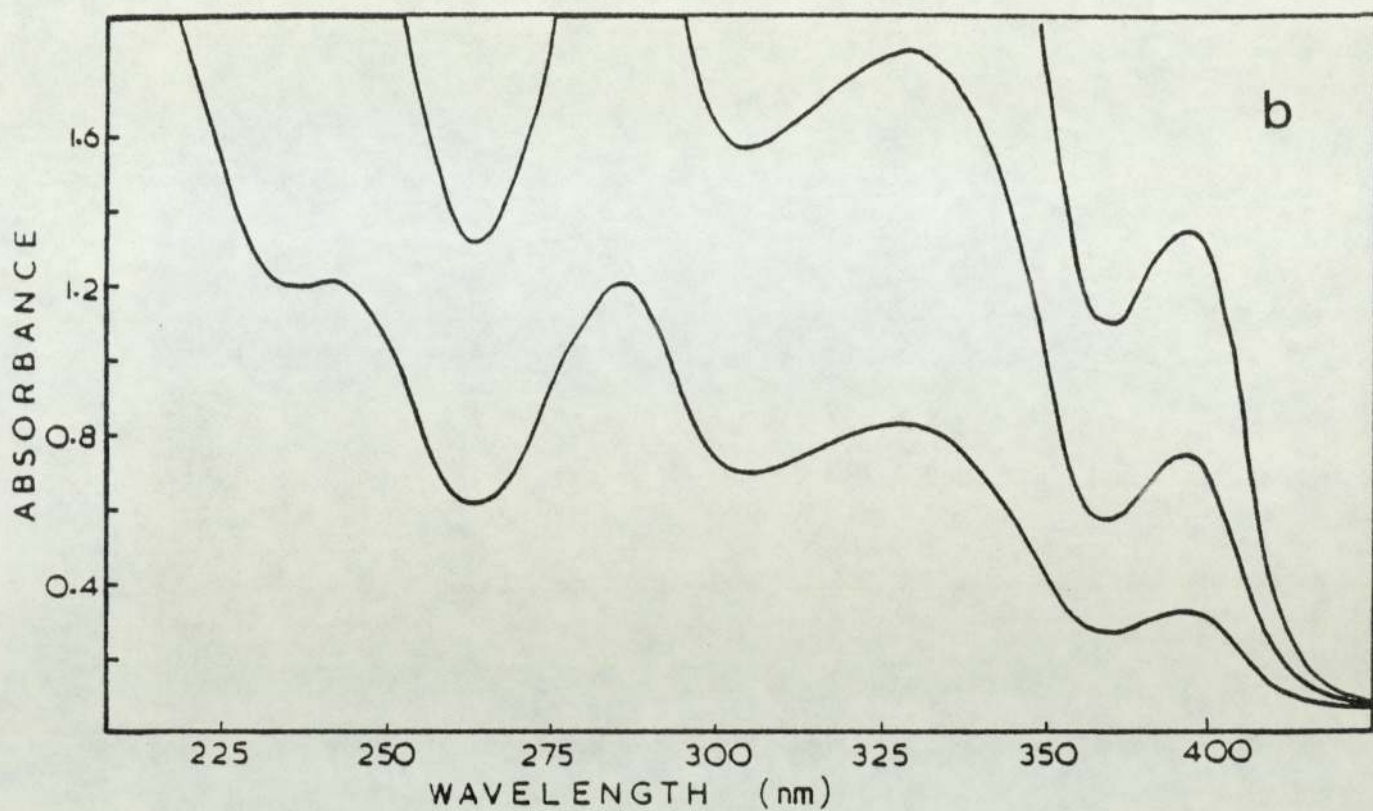


Fig.5.7 UV-absorption spectra of [b] hexane extract of MB Film of DiPDiS-HOBP (30,0M), and [c] O,O-di-2-hydroxybenzophenone dithiophosphoric acid in toluene. Absorption at higher concentrations are also shown.

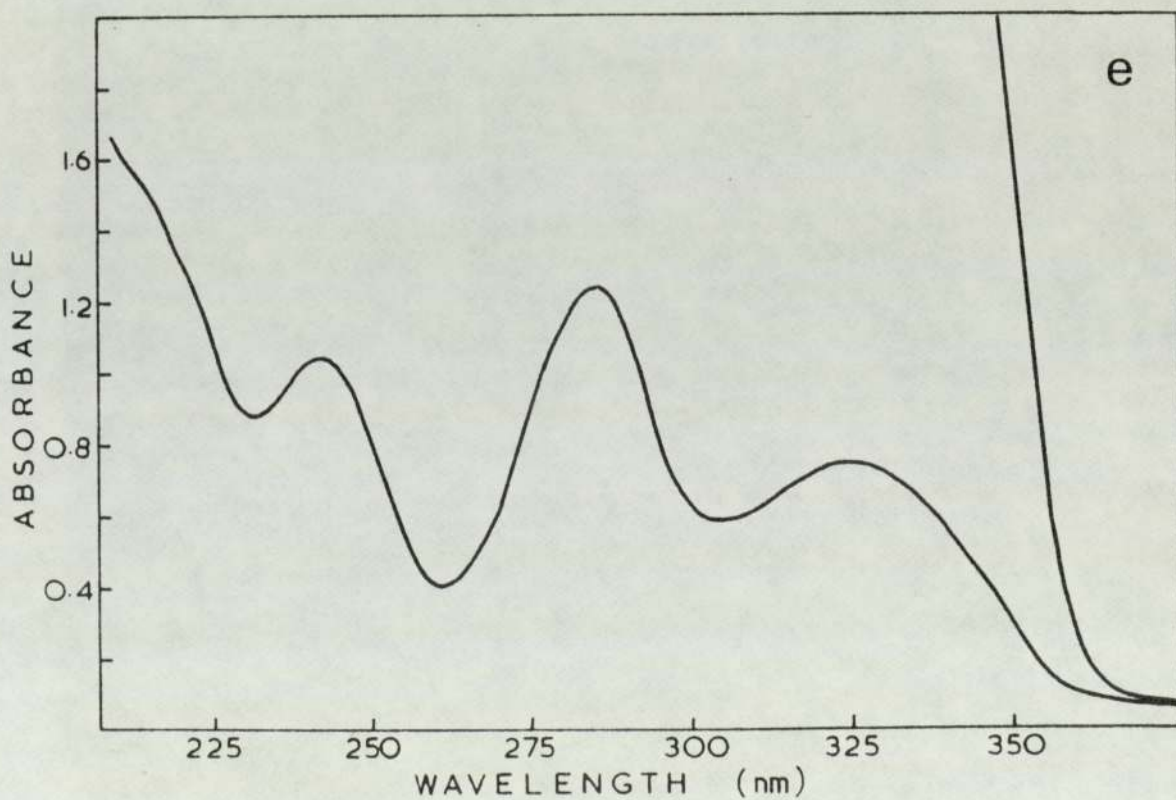
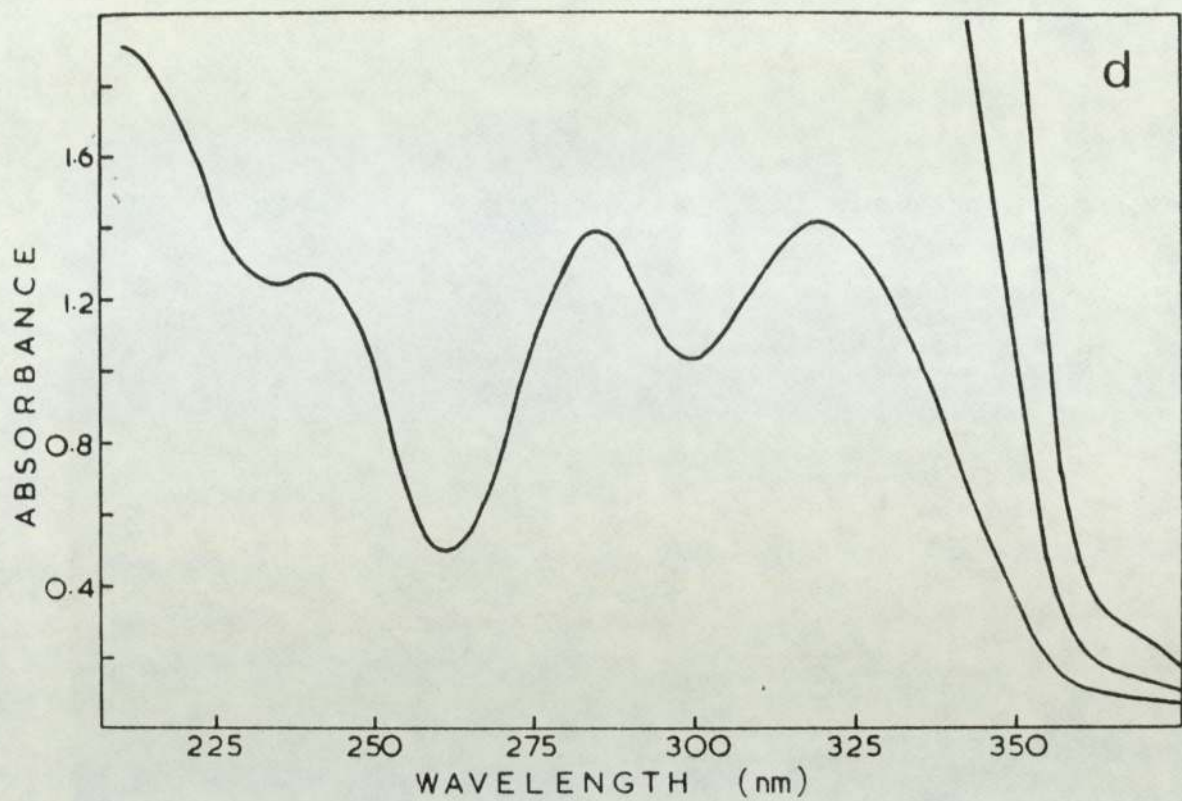


Fig. 5.7 UV-absorption spectra of hexane extract of MB films of NiDIP-HOBP [d] and HOBP [e] stabilised-LDPE [30,0M]. Absorptions at higher concentrations are also shown.

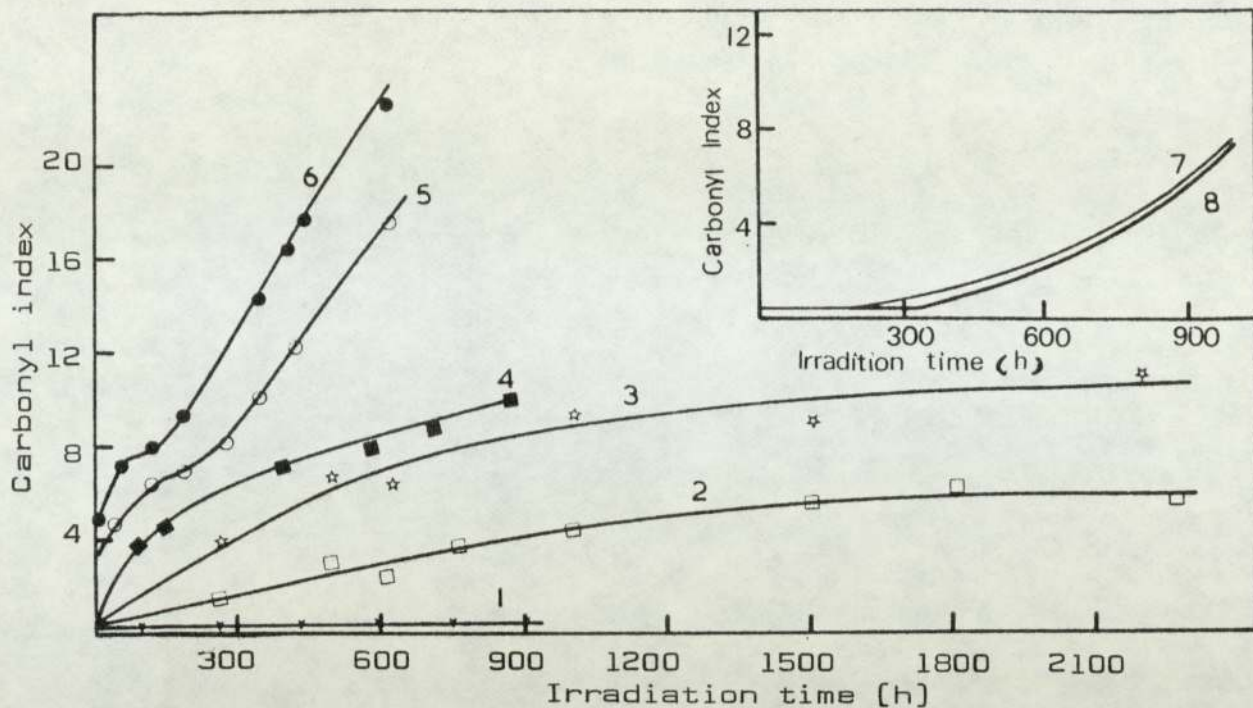


Fig.5.8 Effect of additive [2.5%] on photo-oxidative stability of LDPE-MB films. [1] NiDIP + HOBP, [2] NiDIP, [3] DiPDiS + HOBP, [4] DiPDiS, [5] HOBP at ca.0.1%, [6] control without additive. 1-6 all processed [30,0M] at 150°. Inset compares the photo-oxidative stability of a 0.1% DMB of NiDIP [7] and 0.1% NS of NiDIP [8] processed [10,CM] at 150°.

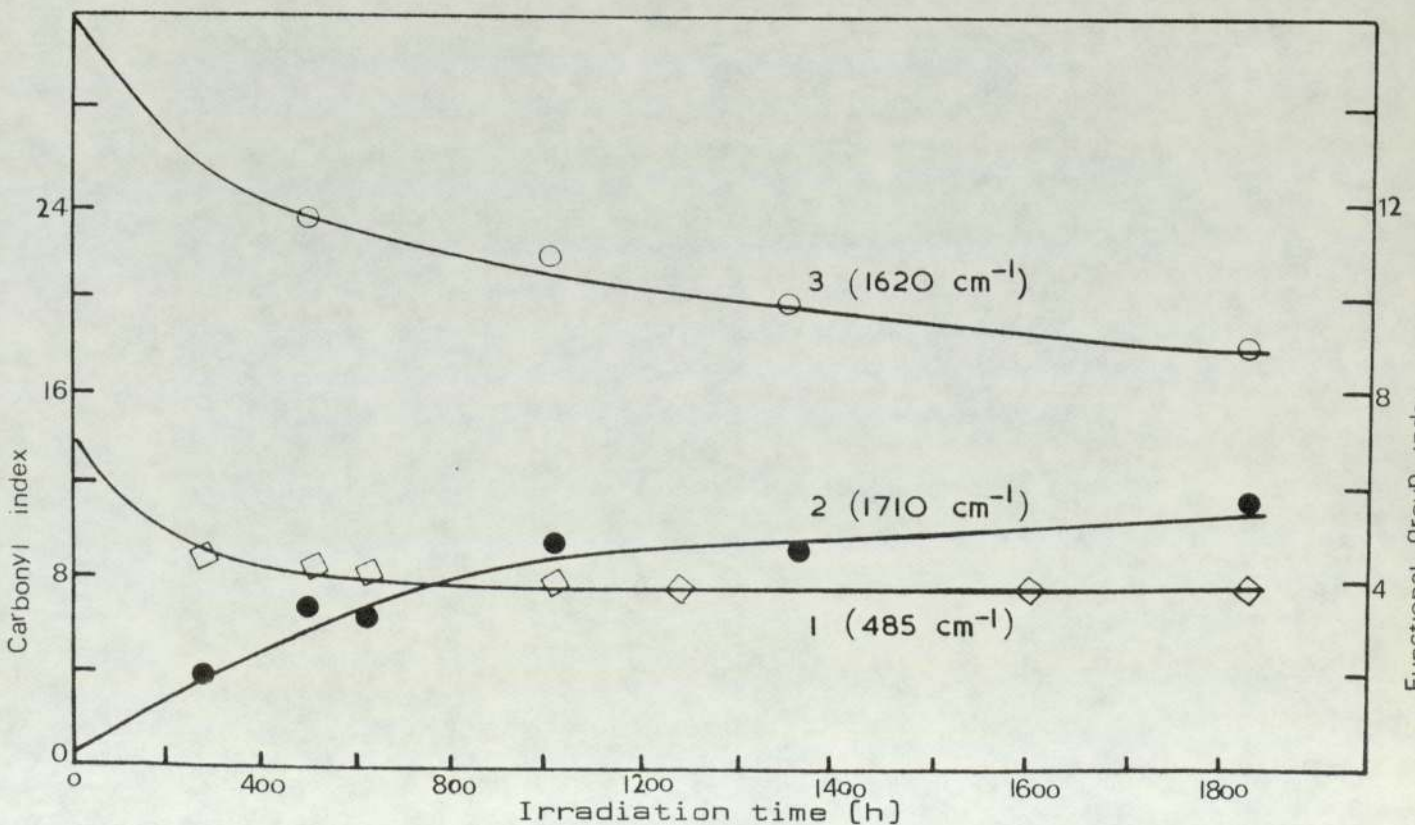


Fig.5.9 Changes of Functional groups during photo-oxidation of LDPE-MB [2.5%] of DiPDiS + HOBP processed [30,0M] at 150°. [1] P-S, [2] formed C=O, [3] C=O in HOBP.

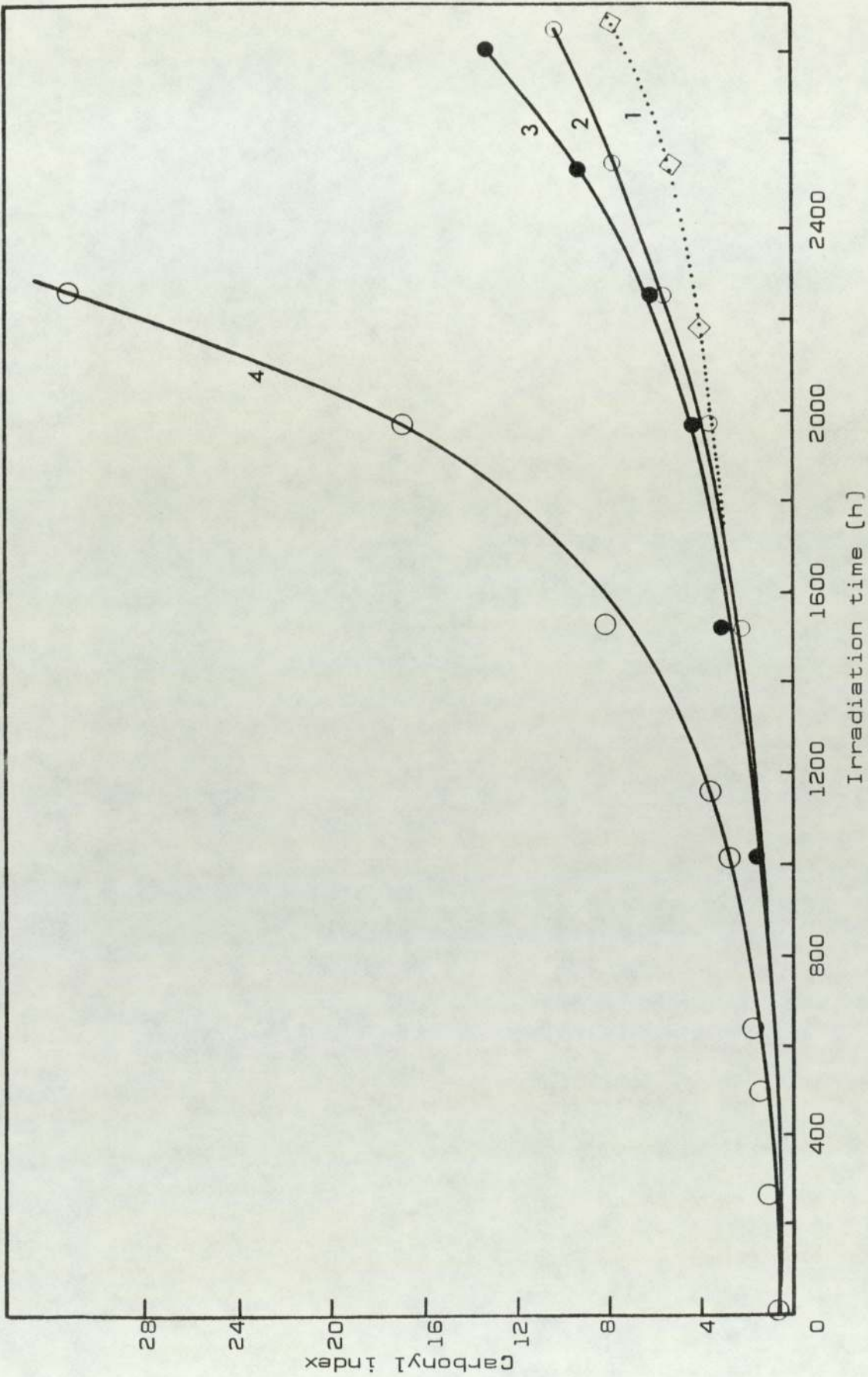


Fig.5.10 Effect of processing severity on the photo-oxidative stability of LDPE-DMB (0.125%) containing DiPDiS + HOBP (original MB processed [30,0M] at 150°). [2] 30,0M; [3] 10,0M; [4] 5,CM. The effect of a LDPE-NS containing DiPDiS + HOBP [1], [0.1% each] processed [30,0M] at 150° on photo-oxidative stability of LDPE is compared also.

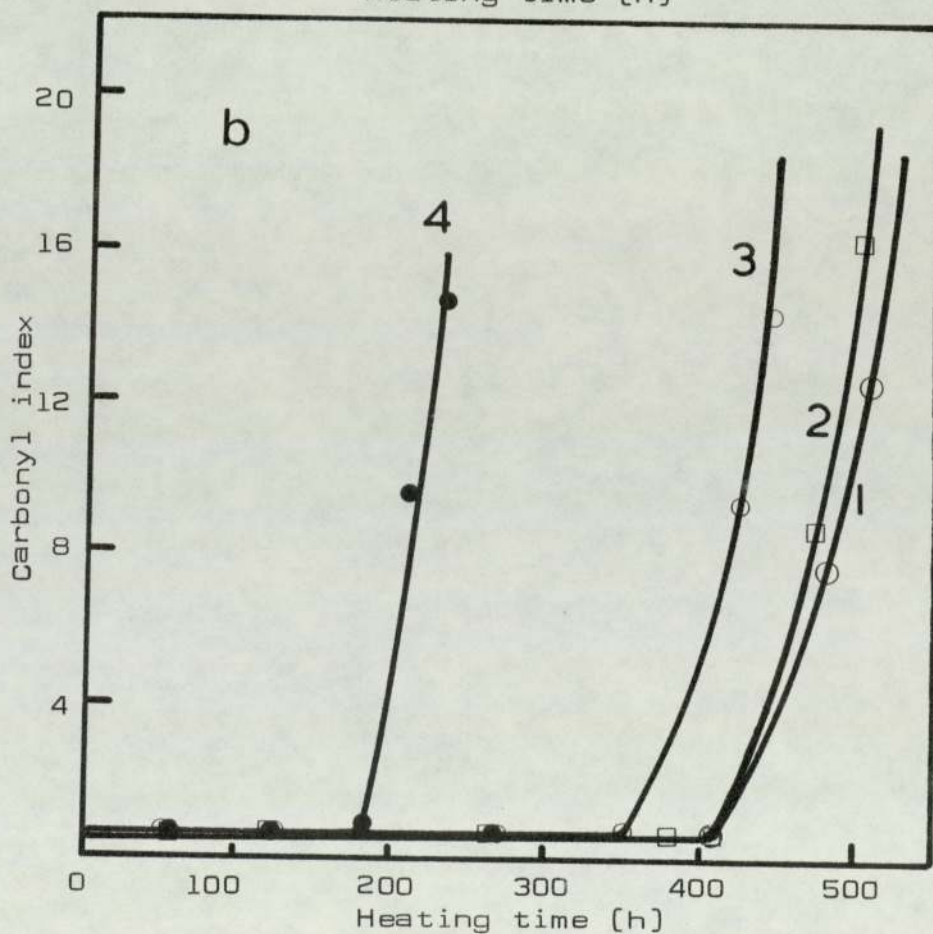
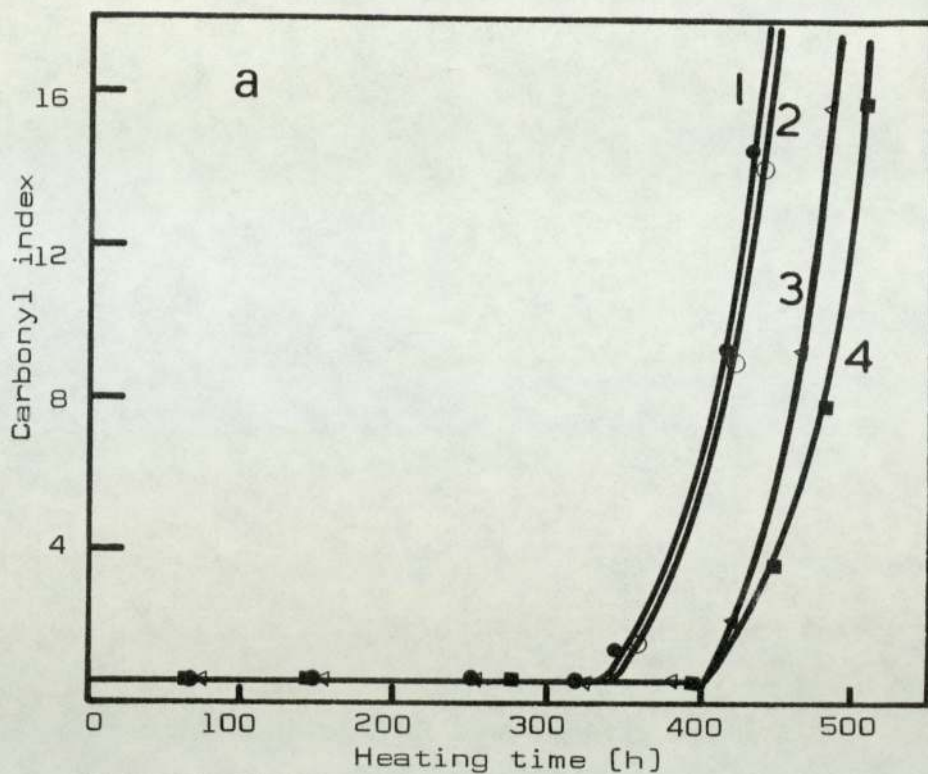


Fig.5.11 Effect of additives on thermo-oxidation (at 110^o) of LDPE films. All samples processed (30,0M) at 150^o.
 (a) [1] NiDIP, DMB extracted; [2] NiDIP, NS extracted; [3] NiDIP, DMB; [4] NiDIP, NS.
 (b) [1] NiDIP, NS; [2] NiDIP, MB; [3] NiDIP, NS extracted; [4] NiDIP, MB extracted.

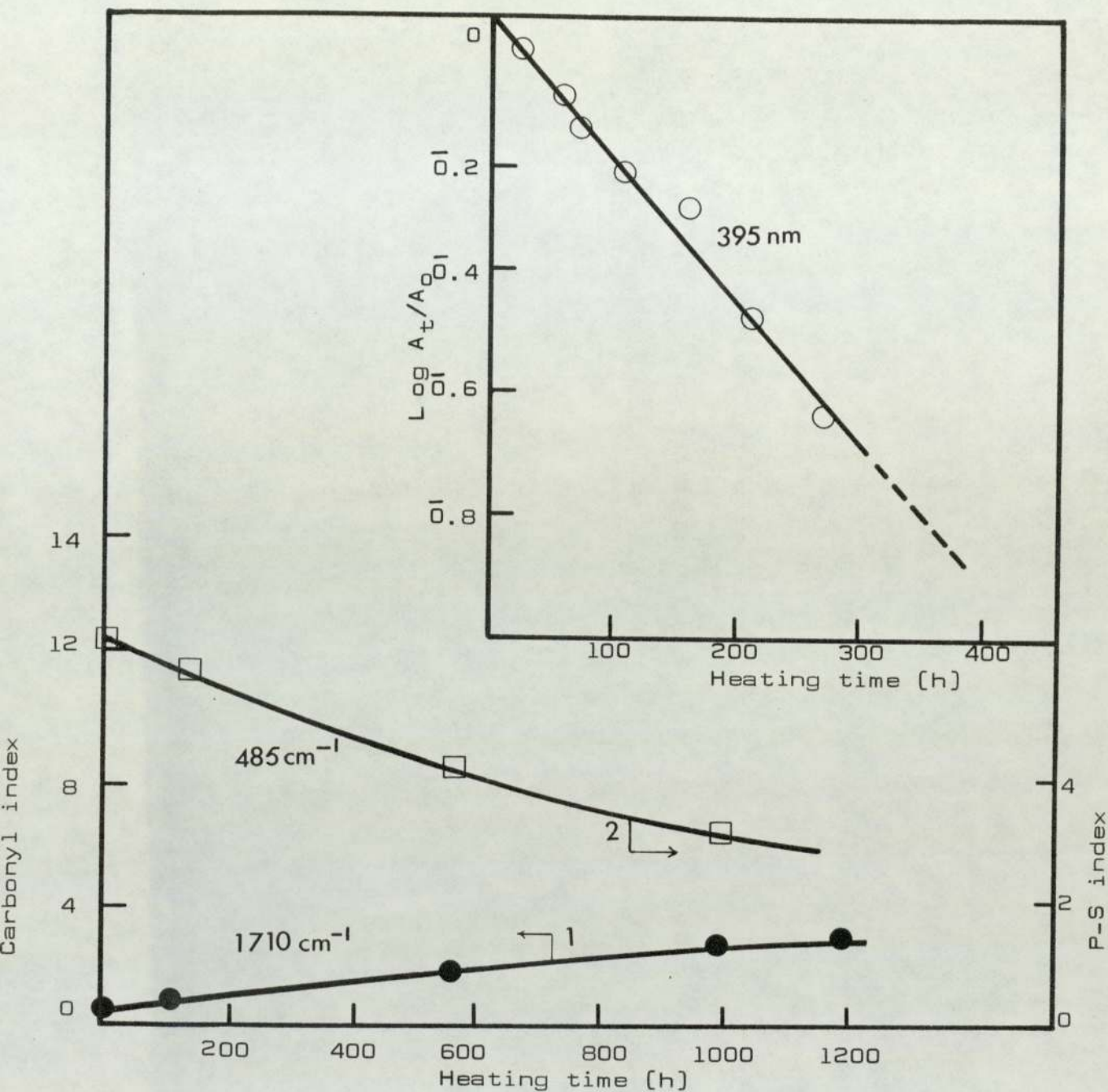


Fig.5.12 Changes of carbonyl [1] and P-S [2] indices with heating time [Wallace Oven, 110°] of an extracted LDPE MB-containing the combination DiPDiS-HOBP processed [30,0M] at 150°. Concentration of MB 2.5%. Inset shows kinetics of disappearance of 395 nm band of an unextracted PE film containing DiPDiS-HOBP [DMB, concentration 0,25%, 30,0M].

CHAPTER SIX

S T A B I L I S A T I O N

O F

P O L Y P R O P Y L E N E

In this chapter photo- and thermo-oxidative stability of PP is examined in the presence and absence of 2.5×10^{-4} M/100g of NiDBP, NiBX and DiPDiS. PP films are exposed to light in the UV-cabinet [sec.2A.3.1] at about 30° and aged at 140° in a Wallace oven [air flow $2.5 \text{ cu ft. h}^{-1}$]; see Sec.2A.3.2.

Combinations of each of the above additives with HOBP on a 1:2 molar basis, and with Irganox 1076 on a 1:1 molar basis [with 2.5×10^{-4} M/100g additive and 5×10^{-4} M/100g HOBP] are also examined as described above. Changes in the UV- and IR-spectra of these films are followed at intervals during UV-exposure and oven ageing. Unless stated otherwise, stabilised and unstabilised PP samples were processed in a closed mixer (10,CM) of the torque-rheometer at 180° . DiPDiS-based oxidation products formed by reaction of the polymer hydroperoxides with the disulfide are hereafter called DiPDiSO.

6.2 RESULTS

6.2.1 Photo- and Thermo-oxidation of PP

Examination of the IR spectra of photo-oxidised PP film [Fig.6.1] revealed two broad absorption bands with peaks at 3400 cm^{-1} and 3340 cm^{-1} . The band at 3340 cm^{-1} [$\epsilon = 70\text{ L.M}^{-1}\text{ cm}^{-1}$] has been ascribed^[15c] to hydrogen-bonded hydroperoxides which are produced by the oxidation of the tertiary C-H bonds. In thermally oxidised PP film no band was found to occur at 3555 cm^{-1} which is normally associated with non-hydrogen-bonded hydroperoxide groups in thermally oxidised LDPE.

The IR-absorption band at 1685 cm^{-1} , which is ascribed^[15c] to conjugated carbonyls initially present in the polymer, disappeared on UV-exposure. Photo-oxidation of PP film led to the formation of carboxylic acid [$\text{ca.}1710\text{ cm}^{-1}$] as a major product. In addition, broad and ill-defined absorptions [$\text{ca.}1715\text{-}1750\text{ cm}^{-1}$] due to aldehydes, esters and ketones [$\epsilon_{1715} = 220\text{ L.M}^{-1}\text{ cm}^{-1}$]^[15c] were observed. It has been shown^[15c] that the aldehyde and ketone content of degraded PP is 16% and 42% following photo- and thermal oxidation, respectively.

Vinyl [909 cm^{-1}] and vinylidene [887 cm^{-1}] absorptions, which are clearly observed during photo-oxidation of LDPE [see Sec.4B.2.1], are not observed in oxidised or unoxidised PP because of the large number of wagging and bending vibrations exhibited by PP in this region. The broad IR band at 1645 cm^{-1} [see Fig.6.1] is due to olefinic unsaturation.

6.2.2 Photostabilisation of PP by NiDBP, NiBX and DiPDiS and their Combination with HOBP and Irganox 1076

The effect of processing severity on the photo-oxidative stability of NiDBP-, DiPDiS- and HOBP-stabilised PP is shown in figure 6.2. It is clear that severe processing [10,0M] adversely effects the photo-oxidative stability of NiDBP and HOBP stabilised PP [curves 6 and 2] when compared with mildly processed [10,CM] analogues [curves 7 and 4]; see also table 6.1. In contrast to this severely processed [10,]M) PP in the presence of DiPDiS exhibits greater photo-oxidative stability when compared to a mildly processed [10,CM] analogue [cf. curves 5 and 3, in Fig.6.2, table 6.1]. DiPDiS was found to be good melt stabiliser (MFI = 0.194) for PP even under severe processing [10,0M] conditions.

A comparison between figures 6.2 and 4B.12 [Sec.4B.2.2] reveals the greater photo-stabilising effectiveness of DiPDiS when used with PP compared with its performance in LDPE. Compared to the control, mildly processed DiPDiS-stabilised PP [curve 3 in Fig.6.2b] exhibits appreciable photo-oxidative stability whereas the stabilised PE-analogue, at the same molar concentration [curve 4 in Fig.4B.12], shows only an insignificant improvement compared to its control.

All the stabilised PP films, in the presence of NiDBP [2.5×10^{-4} M/100g], DiPDiS and HOBP are colourless. The UV-spectrum of NiDBP-stabilised-PP film processed in a closed mixer for 10 min. is shown in Fig.6.3, and compared with that of a similarly processed film in PE. It is clear from this figure that a greater part of NiDBP was consumed during

Table 6.1 Comparison of UV-stabilisers in PP. Concentration of additives 2.5×10^{-4} M/100g except that concentration of (b) and of HOBP in the combination with other antioxidants is 5×10^{-4} M/100g. Unless stated otherwise all processings are for 10 min. in a closed mixer at 180°

Antioxidant	EMT (h)	
	Obs.	Calc. [a]
control [no additive]	90	-
HOBP ^[b]	835	-
HOBP	295	-
1076	420	-
DiPDiS ^[c]	400	-
DiPDiS	285	-
NiDBP	1370	-
NiBX	360	-
NiDBP ^[c]	780	-
DiPDiS + HOBP	1470	1120
NiDBP + HOBP	3000	2205
CuDIP + HOBP	1800	-
NiBX + HOBP	2450	1195
DiPDiS + 1076	400	700
NiDBP + 1076	1400	1790

[a] The effect of synergist or antagonist calculated on additive bases

[c] Processing in an open mixer for 10 min. at 180°

processing in PP [curve 1] as compared to that in PE [curve 2] under similar conditions. The greater loss of nickel complex in PP samples [curve 1 in Fig.6.3] is attributed to the higher processing temperatures (180°) and the more oxidisable substrate. Under these conditions more conversion of the nickel complex to the corresponding disulfide and its oxidation products are expected (see also Sec.5.3.3.2). These products must, therefore, be largely responsible for the marked increase in the absorption (see curve 1 in Fig.6.3) below ca.270 nm, see Sec.2B.2.1, Fig.2B.2, and which, in turn, effects the shape of the UV-absorption spectrum of NiDBP in the PP film. The outstanding observation in the case of NiDBP stabilised PP film [inset in Fig.6.3] is that the low concentration of NiDBP which survived the processing stage, has a long lifetime [ca.1000 h] in the UV-exposed film.

The processing severity received by a PP sample containing NiRX (R=E,B) precludes the survival of the nickel complex even under the mildest conditions [5,CM]. Thus instead of the characteristic UV-absorption of NiRX [Fig.6.4], a new absorption ca.278 nm emerged. Similarly, processing of PP containing CU(I)EX under identical conditions [5,CM], revealed the same new absorption features [curve 3 in Fig.6.4]. A PIP of 150 h [and EMT of 360 h], however, was found [Fig. 6.5 and table 6.1] for PP film containint NiBX.

Figure 6.6 compares the effect of the commercial UV-absorber, HOBP, on the photo-oxidative stability of mildly processed [10,CM] PP containing NiDBP, CuDIP and DiPDiS [HOBP:additive is 2:1, additive 2.5×10^{-4} M/100g]. An

autoaccelerating photo-oxidation characterises the behaviour of HOBP-stabilised-PP [curve 2 in Fig.6.6] whereas NiDBP-HOBP and CuDIP-HOBP combinations [curves 4 and 5] confer extensive photostabilisation with an induction period [PIP 2000 h and 1200 h respectively, see table 6.1]. DiPDiS-HOBP-stabilised PP [curve 3 in Fig.6.6] showed a relatively small but definite induction period [380 h] which was followed by a prolonged period of retarded oxidation. Both the metal complexes [M=Ni,Cu] and their corresponding disulfide, DiPDiS, synergise effectively with HOBP [see table 6.1].

The effect of a synergistic combination of NiBX-HOBP on the photo-oxidative stability of PP [see curve 4 in Fig.6.5, and table 6.1], under identical processing conditions, is less than NiDBP-HOBP combination.

Preliminary experiments were done on extrusion of PP films containing the combinations of NiDBP and DiPDiS with HOBP at 230^o [1:2, additive molar concentration 6×10^{-4} M/100g] using the Brabender plastograph. The UV-absorption spectra of both extruded films of NiDBP-HOBP and DiPDiS-HOBP-stabilised PP under the above conditions, reveal the presence of a new spectral feature at 395 nm [Fig.6.7] which is very similar to that observed for severely processed [30,0M] PE, MB and DMB of DiPDiS-HOBP [but not for NiDIP-HOBP-PE MB combination using the torque-rheometer at 150^o [see Fig.5.7a, Sec.5.2.2]. This indicates an interaction between HOBP and the other components of the synergistic mixtures which is favoured by an oxidisable substrate and severe processing.

This is further supported by the fact that in PE, while this band is formed when DiPDiS-HOBP synergistic mixture was severely processed [30,OM], no such feature was found when the same synergistic combination was processed in PE under mild [10,CM] conditions [see curves 2 and 3 in Fig.5.6, Sec. 5.2.2]. No further examination of the extruded films was undertaken in view of shortage of time.

The photo-oxidative stability of a typical commercial hindered phenolic antioxidant (Irganox 1076, see table 2A.1) in the presence and absence of NiDBP and DiPDiS [at equimolar concentration] is shown in Fig.6.8. Whereas Irganox 1076, in the presence and absence of DiPDiS [curves 3 and 4] auto-accelerate from the beginning of UV-irradiation, the NiDBP-Irganox 1076 combination [curve 5] affords a long PIP. Table 6.1, however, shows that the combination of both, NiDBP and DiPDiS with Irganox 1076 under photo-oxidative conditions have an antagonistic effect.

6.2.3 Effect of Nickel Dithiolates and their Corresponding Disulfides on Thermo-oxidative Stability of PP in the Presence and Absence of Irganox 1076

Thermo-oxidative stability and EMT of PP films stabilised with NiDBP, DiPDiS and NiBX processed under identical conditions [10,CM] are shown in Fig.6.9 and table 6.2. It is clear that the disulfide, DiPDiS, offers a better thermo-oxidative stability than its own nickel complex [curves 4 and 3 in Fig.6.9]. Furthermore, NiBX offers better thermo-oxidative stabilisation to PP than NiDBP. This behaviour is similar to that observed earlier [see Figs.

4A.5 and 4A.8 in Sec.4A.2.3 and 4A.2.4) in the case of PE. Fig.6.10 compares the thermo-oxidative stability of equimolar ratio of similarly processed (10,CM) combination of NiDBP and DiPDiS with Irganox 1076. Clearly both the nickel complex and its corresponding disulfide have synergised with Irganox 1076 [table 6.2].

Table 6.2 Effect of thermal oxidation (at 140° on the lifetime of PP Films containing 2.5×10^{-4} M/100g of the appropriate antioxidant

Antioxidant	EMT (h)	
	Obs.	Calc. [a]
control (no additive)	1	-
1076	230	-
DiPDiS	24	-
NiDBP	18	-
NiBX	20	-
DiPDiS + 1076	300	254
NiDBP + 1076	540	248

[a] The effect of synergist calculated on additive bases.

6.3 DISCUSSION

6.3.1 Thermo- and Photo-oxidative Stability of PP

PP is more prone to oxidation than LDPE. One of the reasons for this is its labile hydrogen, which is lost readily in the rate determining step^[7] during auto-oxidative chain reaction. The methyl group inductively enhances electron density on the carbon atom being oxidised and delocalises the electron by hyperconjugation^[7]. Experimentally, this is manifested by much shorter embrittlement times.

It has been shown^[17] that PP is markedly sensitised to UV-light by the thermal-oxidative conditions of the processing operation. As in the case of LDPE (see Sec.4B.2.1), hydroperoxides rather than carbonyl has been shown^[17] to be the main photo-initiators during the early stages of photo-oxidation of PP.

The ready formation of peroxidic groups in PP is clear since these are detectable^[17] even in the most mildly processed PP. In contrast to LDPE where the hydroperoxides present initially decay rapidly to an undetectably low value^[45], the hydroperoxide level in PP increases rapidly to a maximum, during the first 30 h of UV-exposure, prior to its decay. Hydrogen bonded hydroperoxides (IR band at 3340 cm^{-1} , see Fig.6.1), rather than the free hydroperoxides, normally observed in LDPE (ca. 3555 cm^{-1}) occur in PP. The absence of a free hydroperoxide absorption in photo- or thermally-oxidised PP has been explained^[15c] in terms of intra-molecular hydrogen bonding formation between neighbouring hydroperoxide groups.

6.3.2 Effect of NiDBP, NiBX and DiPDiS on Oxidative Stability of Polypropylene

NiDRP is rather unstable at the high processing temperature of PP [see Sec.2B.3 and 4A.2.2]. Clearly, therefore, severe processing is detrimental to the nickel complex [see Fig.6.2], the photo-stabilisation afforded by the complex is almost halved (cf. curves 3 and 5 in Fig.6.2) with increased processing severity. In contrast to this poor performance by NiDRP, the corresponding disulfide, e.g. DiPDiS, however, has almost double its photostabilisation effect under the same severe processing conditions [table 6.1].

By analogy with simple disulfides, e.g. alkyl and aryl disulfides [as against their oxidation products] which themselves have been found^[130] to be poor hydroperoxide decomposers, the actual process of decomposition of hydroperoxides in the case of the thiophosphoryl disulfide [DiPDiS] is, therefore, a function of its oxidation products.

The importance of oxygen in enhancing the oxidative stability of DiPDiS-stabilised-PP was clearly demonstrated [see table 6.1]. The antioxidant mode of action in this case must, therefore, be directly proportional to the amount and nature of oxidation products since PP processed at 180^o [and similarly for LDPE at 150^o, see Sec.4B.2.4] in an open mixer gave consistently better photo-oxidative stability than from a closed mixer [see table 6.1].

The antioxidant properties of DiPDiS and its oxidation products [DiPDiSO] are gradually destroyed by light [see Fig.3.16, Sec.3.2.3]. The absence of a period of complete inhibition i.e. no PIP during UV-exposure of DiPDiS-stabilised PP film [curves 3 and 5 in Fig.6.2] supports this conclusion. The overall photostabilisation observed must be associated with retarded oxidation on prolonged exposure. This behaviour is characteristically dependent on the thermal oxidative history of the stabilised polymer. Severely processed samples were found, therefore, to display, at later stages of photo-oxidation, a greater degree of retardation which leads in effect to better overall photostabilisation [cf. curves 3 and 5 in Fig.6.2].

It has been shown^[46] previously that HOBP is an indifferent antioxidant during processing and behaves essentially as a screen during the early stages of photo-oxidation when hydroperoxides are the primary photo-initiators. The effect of processing on HOBP is to reduce its effectiveness as a UV-absorber [cf. curves 2 with 4 in Fig.6.2]. The inability of HOBP to inhibit the formation of hydroperoxides during processing, and to destroy them during subsequent UV-exposure^[45], contrasts strongly with the hydroperoxide decomposer [PD] role of DiPDiS [see Sec.7].

A combination of HOBP [UV-stabiliser] and DiPDiS [PD] should, therefore, lead to extensive stabilisation. Indeed, the components of this combination behaved as effective synergists [curve 3 in Fig.6.6]. This was verified from a comparison of EMT [see table 6.1] of this combination [at a 2:1 molar ratio] with the additive effects of the two

components of the DiPDiS-HOBP system. The deleterious effects of processing on HOBP was, therefore, minimised via the powerful hydroperoxide decomposing activity of DiPDiS [see for example curve 3 in Fig.6.6], and this is expected to assume greater importance under more severe processing conditions [by analogy with LDPE, cf. curves 3 and 1 in Fig. 4B.15, Sec.4B.2.4]. The UV-protective action of HOBP subsequently exerts its effect and prolongs, therefore, the persistence, and hence the activity, of DiPDiS and/or DiPDiSO during UV-exposure. The synergistic system of DiPDiS-HOBP combines, therefore, the desirable features of both components: a long PIP afforded by the protected UV-stabiliser coupled with the stabilisation afforded initially and subsequent auto-retardation by the peroxide decomposer.

The synergistic effect observed for the combination NiDBP-HOBP [curve 5 in Fig.6.6] can be similarly rationalised. During processing a certain amount of the nickel complex is converted into the corresponding disulfide. The extent of this conversion is directly proportional to the amount of oxygen present. Subsequent oxidation of DiPDiS is similarly effected by the level of oxygen present. NiDRP is itself a good UV-stabiliser [see Sec.4B.2.4]. During photo-oxidation, therefore, a period of complete inhibition [i.e. PIP] is expected. The length of the PIP observed in the case of NiDBP-stabilised PP films [e.g. curve 7 in Fig.6.2] correlates well with the lifetime of NiDBP actually present in the film [and which has survived thermal oxidation during the processing stage], see also inset in Fig.6.3. More severe processing produces higher levels of DiPDiSO formation coupled with a

greater loss of the nickel complex. The photo-oxidative behaviour of a severely processed NiDBP-stabilised film is characterised by a shorter PIP when compared to a mildly processed analogue [cf. curves 6 and 7 in Fig.6.2].

Unlike HOBP, NiDRP is a good PD [see Sec.7.2.1]. In addition, its UV-absorption in the 300 nm region is much higher than HOBP [e.g. for ca.316 nm $\epsilon_{\text{complex}} \approx 3\epsilon_{\text{HOBP}}$]. NiDIP also has been found^[22] to affect photostabilisation by a screening mechanism. In a synergistic mixture [see also PE], therefore, the combined effects of photostabilisation afforded by NiDRP and the amounts of HOBP left intact should impart a markedly extended PIP. This was indeed the case for UV-exposed PP films containing the synergistic combination of NiDBP-HOBP [curve 5 in Fig.6.6 and table 6.1]. In the presence of a limited amount of oxygen, processing [10,CM] of PP sample containing NiDRP may produce a sufficient amount of DiPDiSO to ensure that the survival of the nickel complex is maximal.

A notable difference emerges on comparing the synergistic combination NiDBP-HOBP with DiPDiS-HOBP. Since DiPDiS-stabilised PP film does not show PIP, the period of inhibited photo-oxidation afforded by DiPDiS-HOBP system [curve 3 in Fig.6.6] must be partly due to the DiPDiS or its oxidation products which have been protected [by HOBP] from photolysis, thereby becoming a more effective peroxide decomposer [UV-stabiliser]. In the case of NiDBP-HOBP-stabilised PP film [curve 5 in Fig.6.6] the exact role of each component is less clear.

Dixanthogens were shown [Sec.4A.2.3] to be formed during processing of PE containing NiRX. The relative instability of NiRX [see Sec.2B.4] toward the higher processing temperature [180^o], together with the oxidisability of PP, is expected to lead to higher yields of dixanthogens. Dixanthogens are known^[56c] to yield alkyl carbonate, ROC(S)OR, and alkyl xanthate ester, ROC(S)SR. Ethyl xanthate ester shows^[90] continuous UV-absorption with a band at λ_{\max} 278 nm ($\epsilon \approx 11,200$). The bands observed when NiRX (R=E,B) and CuEX were processed with PP at 180^o appear quite similar, and is suggestive of the formation of alkyl xanthate ester. The occurrence of this ester may account for the lower photostability of NiBX inPP when compared to its stability in PE.

The outstanding photo-stabilisation afforded by NiDBP when present alone in PP film [curve 7 in Fig.6.2] cannot be explained only on the basis of the 'residual' amounts of the complex which appeared to have survived the processing operation [see Fig.6.3]. A regenerative mechanism is proposed [Scheme 6.1] to explain this [compare with a similar scheme for LDPE, Scheme 5.2, Sec.5.3.3.1].

The commercial hindered phenolic antioxidant, Irganox 1076, was found^[40] to exert synergistic and antagonistic effects when used in combination with metal dithiocarbamates (M=Ni, Zn) under thermo- and photo-oxidative conditions, respectively. Similarly, Irganox 1076 was found here to be synergistic [Fig.6.10] with the hydroperoxide decomposers, DiPDiS [curve 2 in Fig.6.10 and curve 3 in Fig.6.8] and NiDBP [curve 3 in

Scheme 6.1 Regenerative mechanism for stabilisation of PP

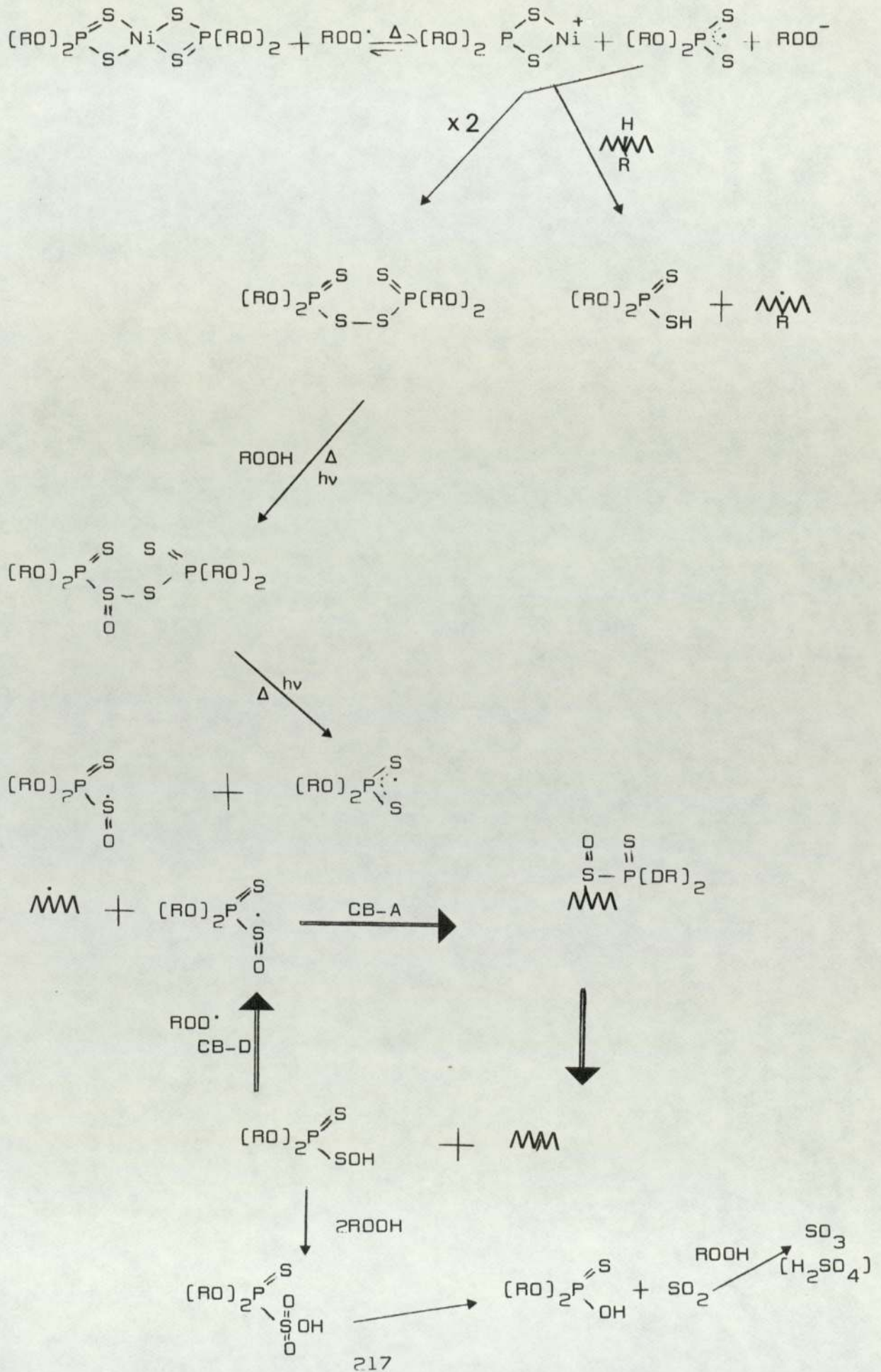


Fig.6.10 and curve 5 in Fig.6.8] under thermal-oxidative conditions and antagonistic [Fig.6.8] under photo-oxidative conditions. As a hindered phenolic antioxidant, Irganox 1076 [AH] undergoes^[1d] a chain transfer reaction with a propagating PP peroxy radical [PPDO[•]] by donating its hydrogen, forming hydroperoxide and a stable phenoxy radical [A[•]].



Self association of this radical [X2] or further reaction with [PPDO[•]] leads to termination^[1d].

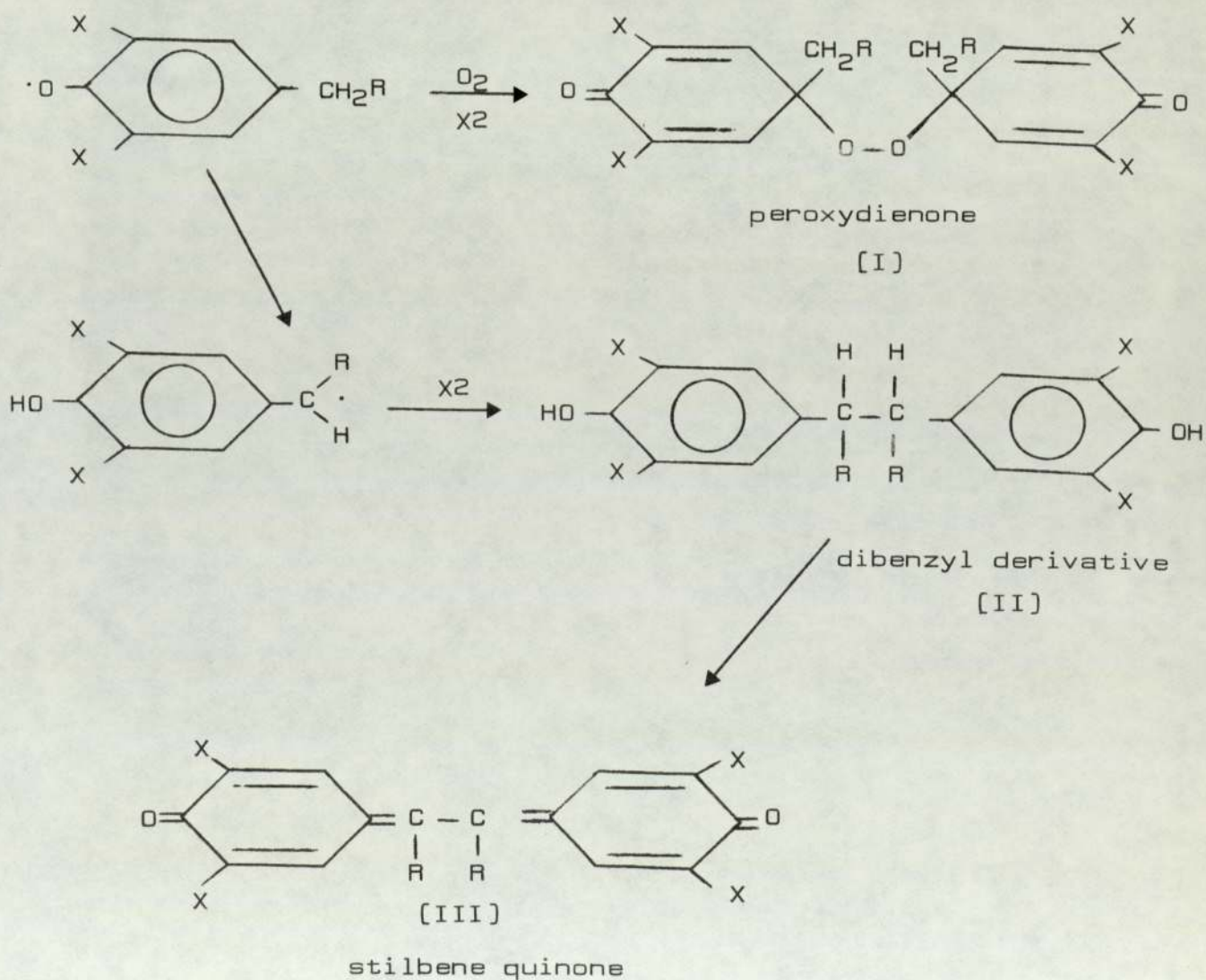


Table 6.1 shows clearly that the combination of the PD (DiPDiS and NiDBP) with the C-B antioxidant Irganox 1076, exerts an antagonistic effect. In these two component systems, the phenol photosensitises the decomposition of the dithiophosphates leading to a decrease in their effectiveness [Fig.6.8 and table 6.1]. This is due to^[46] the presence of quinonoid products [stilbene quinones (III) and peroxydienone (I)] which are the major products of the normal function of phenols as antioxidants^[46]. The antagonistic behaviour of Irganox 1076 contrasts with the excellent synergism afforded by the combination of the UV-absorber, HDBP, with the above PD's NiDBP and DiPDiS [see Fig.6.6 and table 6.1]. This confirms the different roles of HDBP and Irganox 1076 as UV-stabiliser and melt stabiliser, respectively.

NiDBP and DiPDiS are compared as thermal-oxidative stabilisers in PP [see Fig.6.9 and table 6.2]. The disulfide confers better thermo-oxidative stability through its oxidation products, DiPDiSO, the active PD's. The thermo-oxidative stabilising effectiveness of the nickel complex, on the other hand, is mainly due to the amount converted into the corresponding disulfides. Nickel xanthate [curve 3 in Fig.6.9] confers better thermo-oxidative stability than the nickel dithiophosphate [curve 2 in Fig.6.9] in a way similar to that discussed for LDPE [see Sec.4A.3.2].

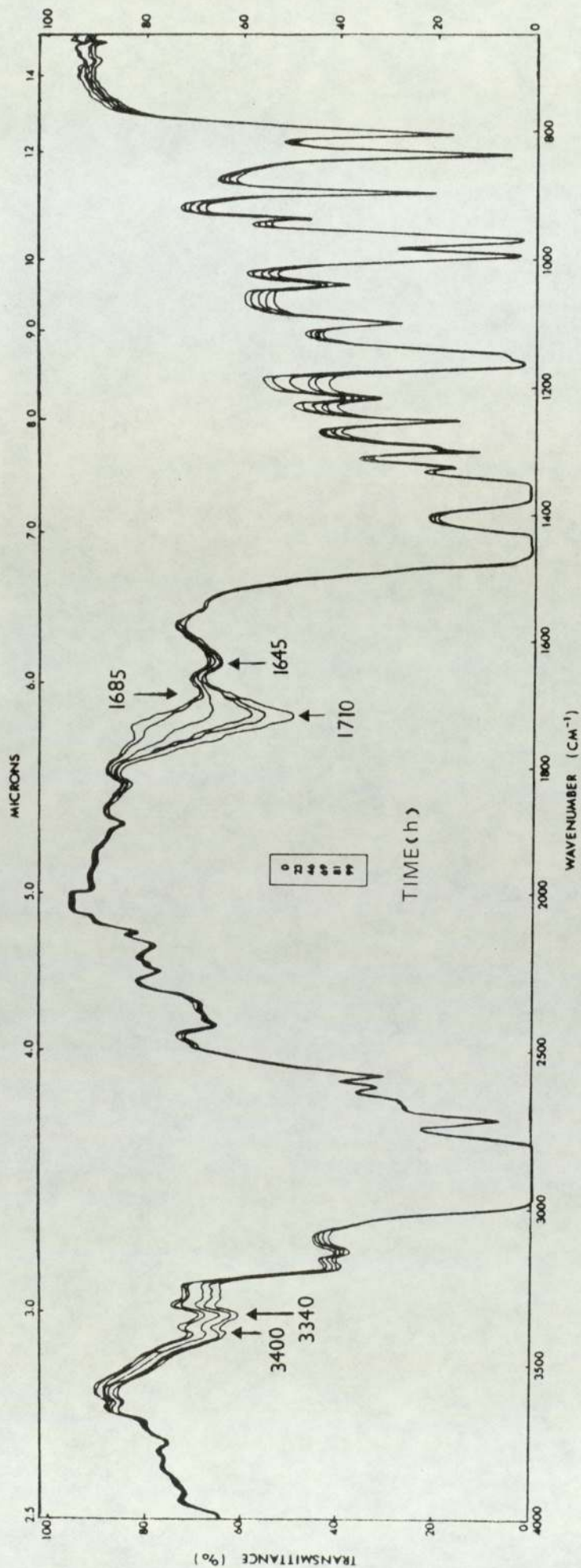


Fig. 6.1 Infrared absorption spectra of unstabilised PP during photo-oxidation. [Exposure times are shown in hours].

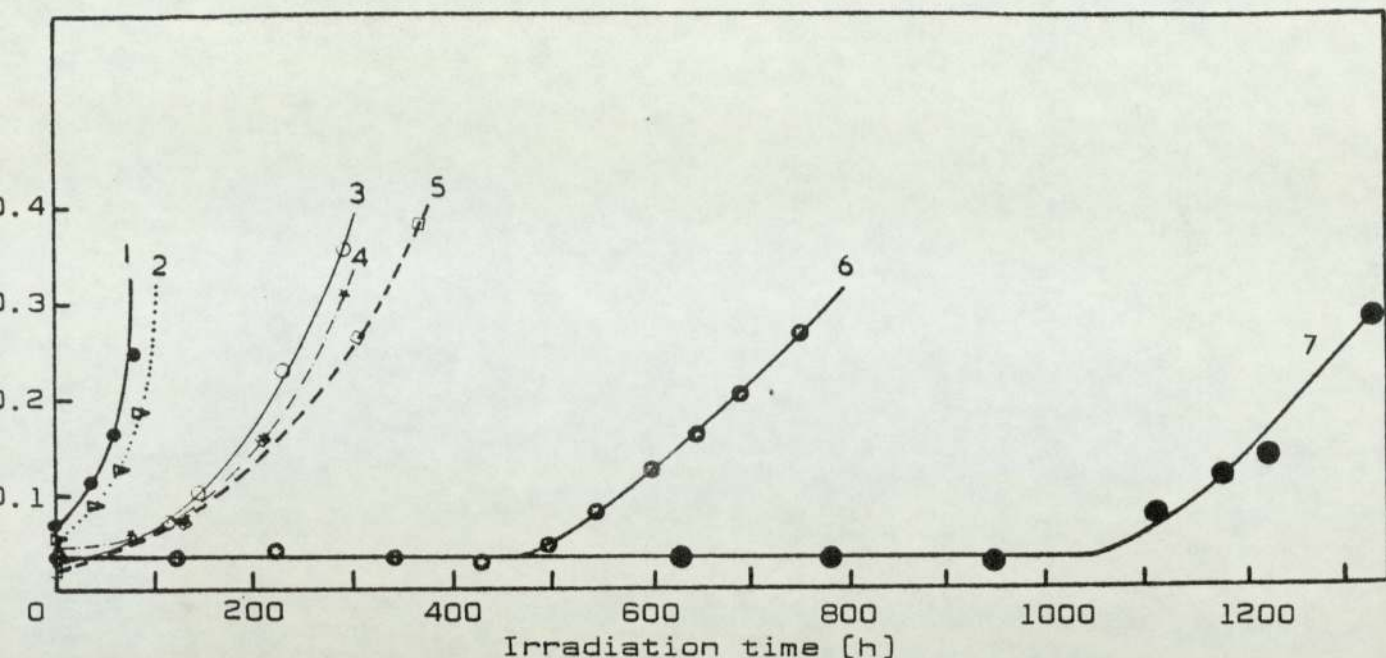


Fig. 6.2 Effect of different processing conditions [at 180^o] on the stabilising effectiveness of additives ($2.5 \times 10^{-4} \text{M}/100\text{g}$) in PP Films. [1] no additive [control]; [2] HOBP [10,0M]; [3] DiPDiS, [10,CM]; [4] HOBP [10,CM]; [5] DiPDiS [10,0M]; [6] NiDBP [10,0M]; [7] NiDBP [10,CM].

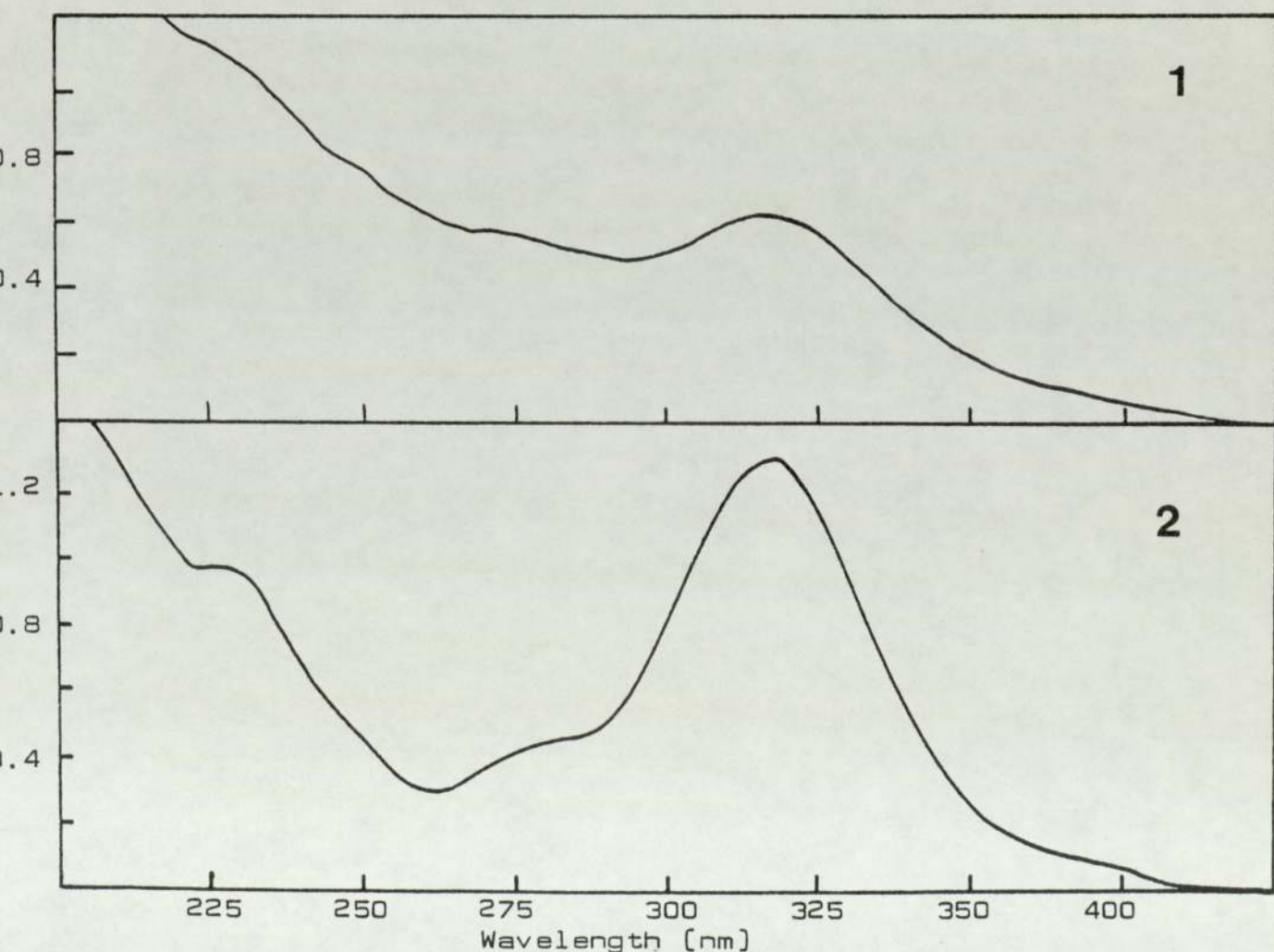


Fig. 6.3 UV-absorption spectra of NiDBP in PP [1] and in LDPE [2] films.

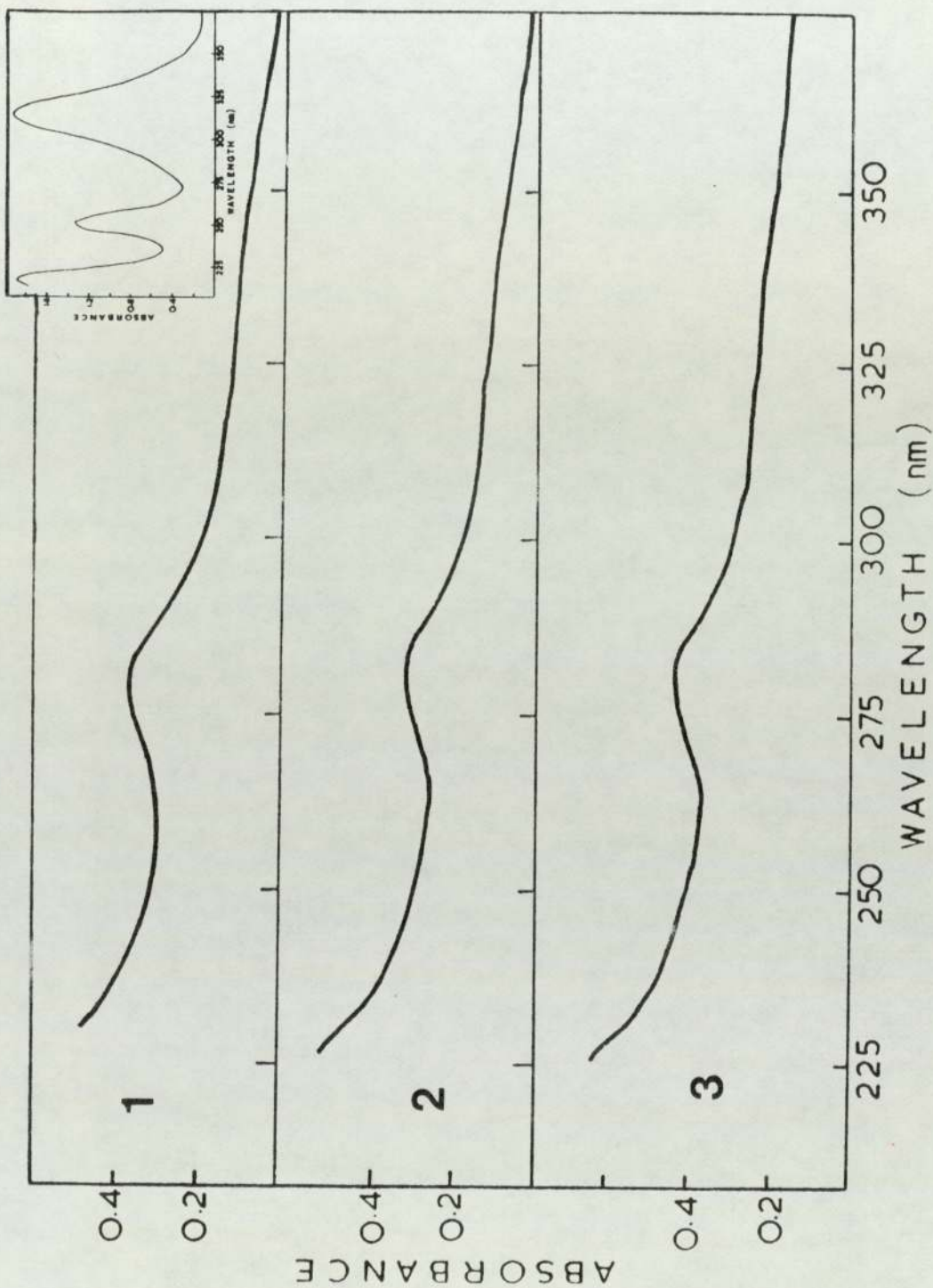


Fig. 6.4 UV-absorption spectra of stabilised PP films. The different processing conditions at 180° and the additives are shown (1) NiEX (5,CM); (2) NiBX (10,CM); (3) CuEX (5,CM). Inset shows UV-absorption spectra of NiBX in LDPE (10,CM).

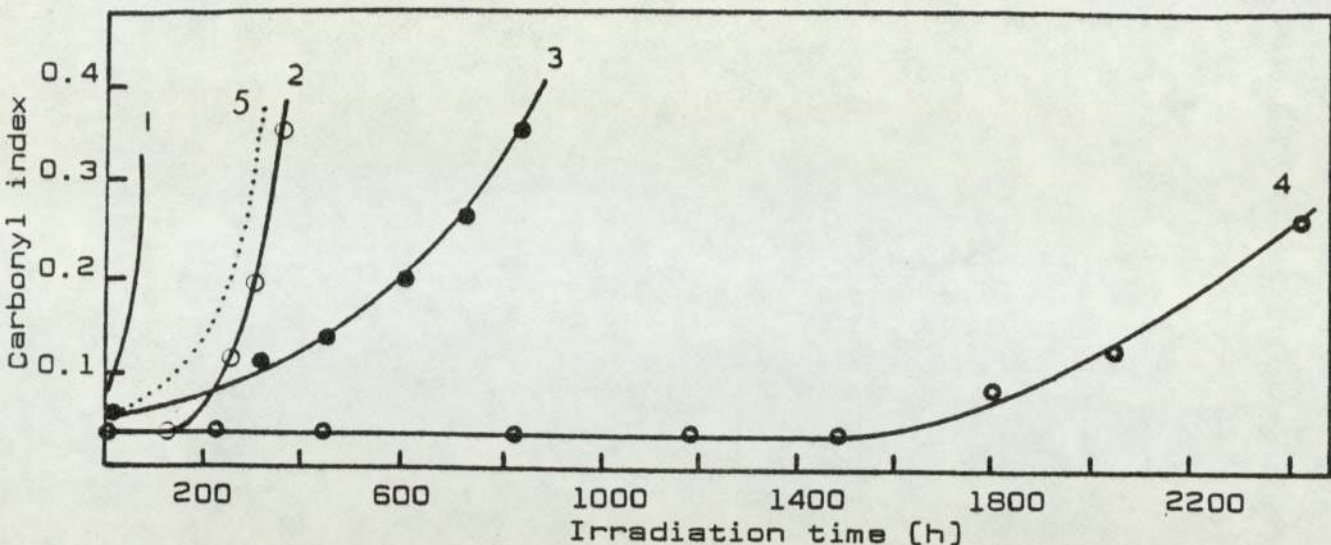


Fig. 6.5 Effect of NiBX ($2.5 \times 10^{-4} \text{M}/100\text{g}$), alone, and in combination with HOBP ($5 \times 10^{-4} \text{M}/100\text{g}$) on the photo-oxidation of PP films. All films were processed (10,CM) at 180° . [1] no additive, control; [2] NiBX; [3] HOBP; [4] NiBX + HOBP; [5] HOBP at $2.5 \times 10^{-4} \text{M}/100\text{g}$.

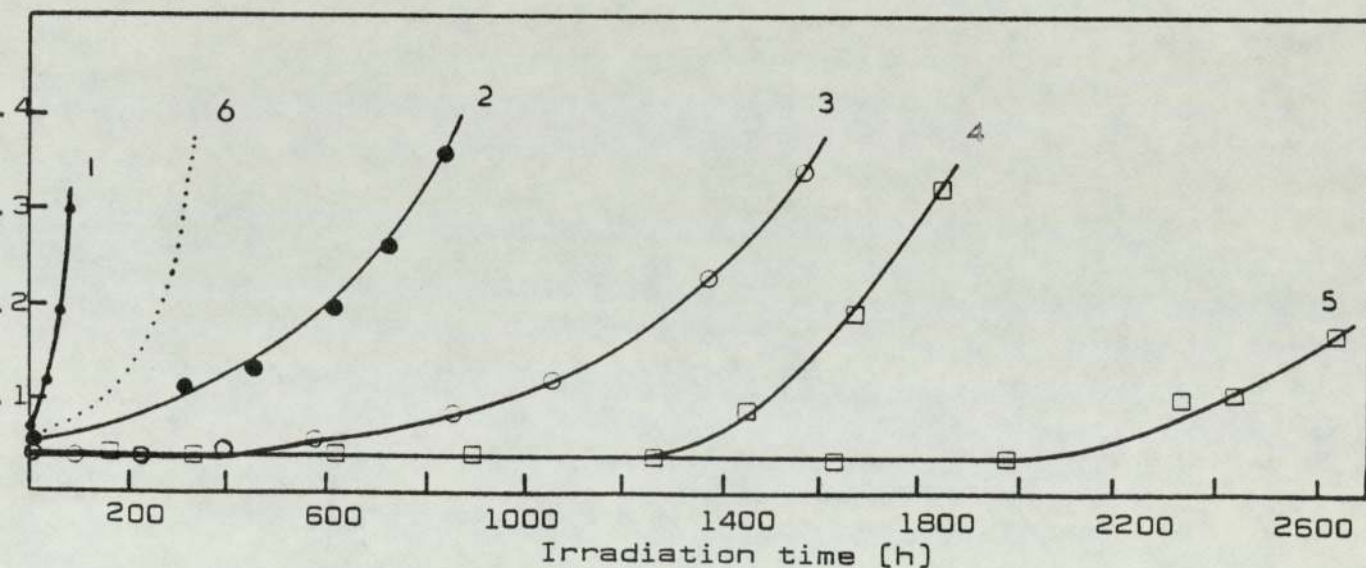


Fig. 6.6 Effect of dithiophosphates ($2.5 \times 10^{-4} \text{M}/100\text{g}$), alone, and in combination with HOBP ($5 \times 10^{-4} \text{M}/100\text{g}$) on the photo-oxidation of PP films. All films were processed (10,CM) at 180° . [1] no additive, control; [2] HOBP; [3] DiPDiS + HOBP; [4] CuDIP + HOBP; [5] NiDBP + HOBP; [6] HOBP at $2.5 \times 10^{-4} \text{M}/100\text{g}$.

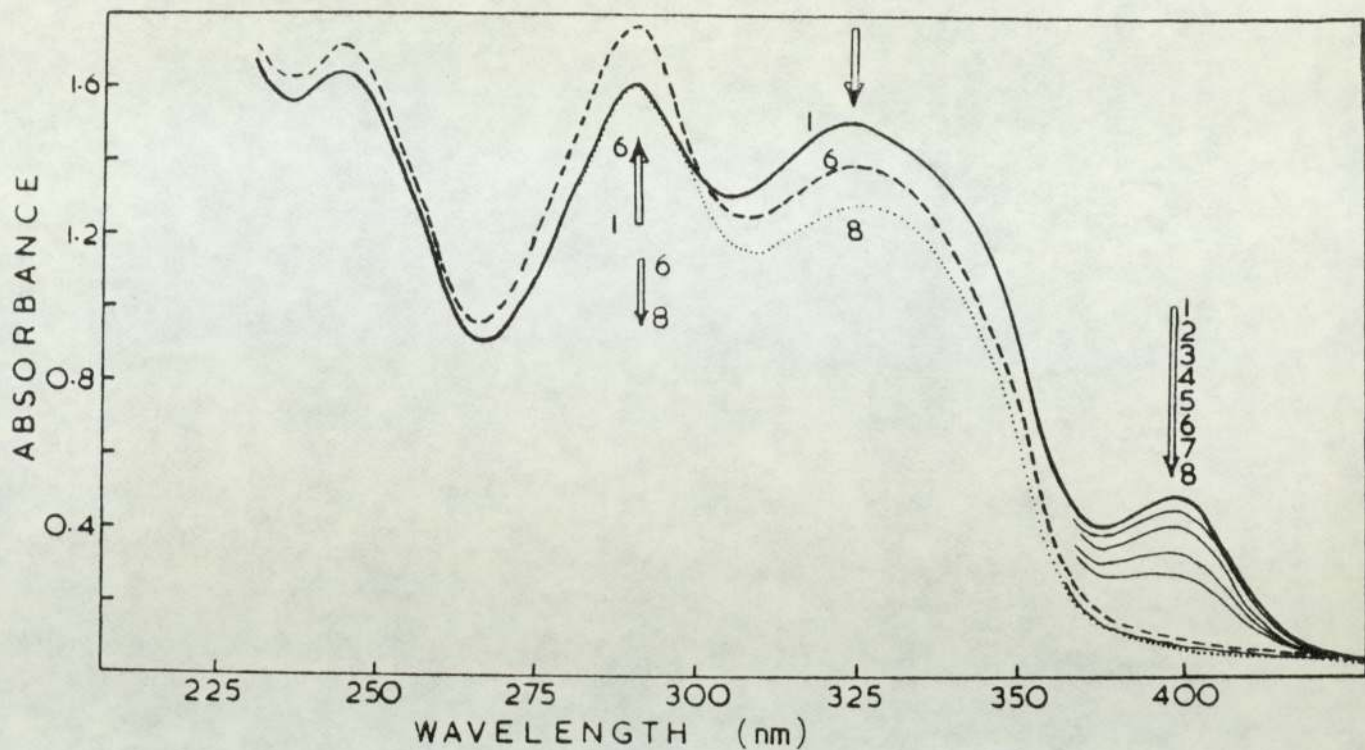


Fig. 6.7 Changes in the UV-spectra during photo-oxidation of PP film containing NiDBP + HOBP; processed in a Brabender plastograph at 220°.

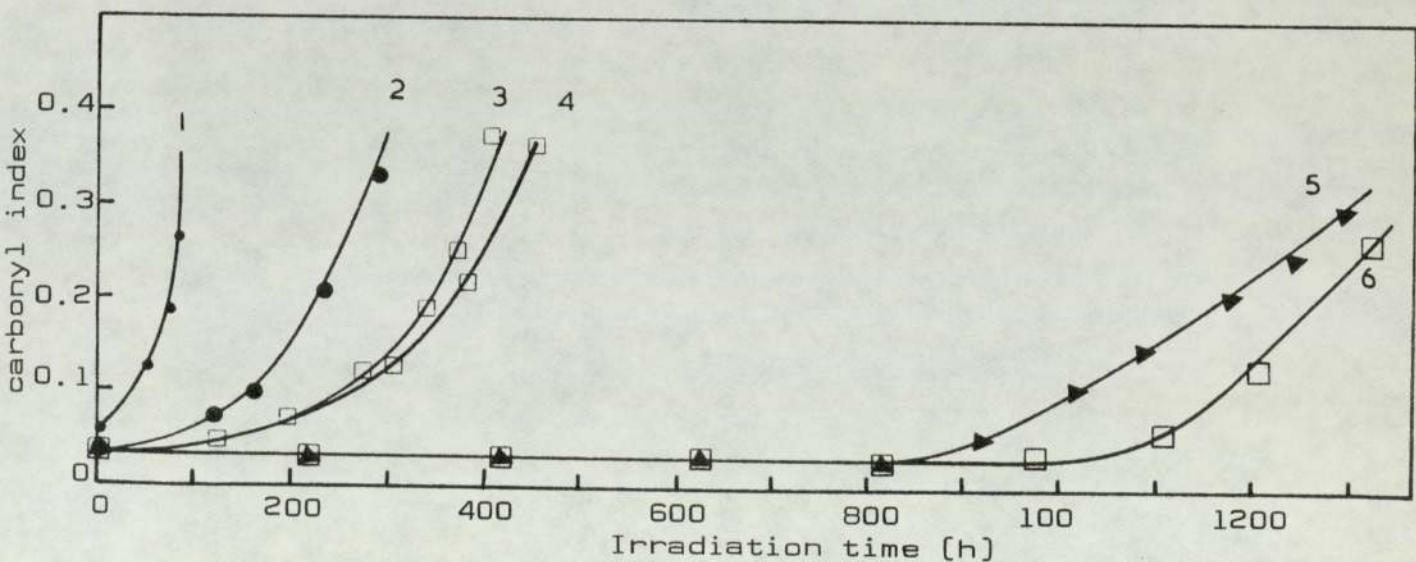


Fig. 6.8 Effect of dithiophosphates, alone, and in combination with Irganox 1076 on the photo-oxidation of PP. Additive concentration $2.5 \times 10^{-4} \text{M}/100\text{g}$. [1] control without additives; [2] DiPDiS; [3] DiPDiS + Irg.1076; [4] Irg.1076; [5] NiDBP + Irg.1076; [6] NiDBP. PP was processed (10,CM) at 180°.

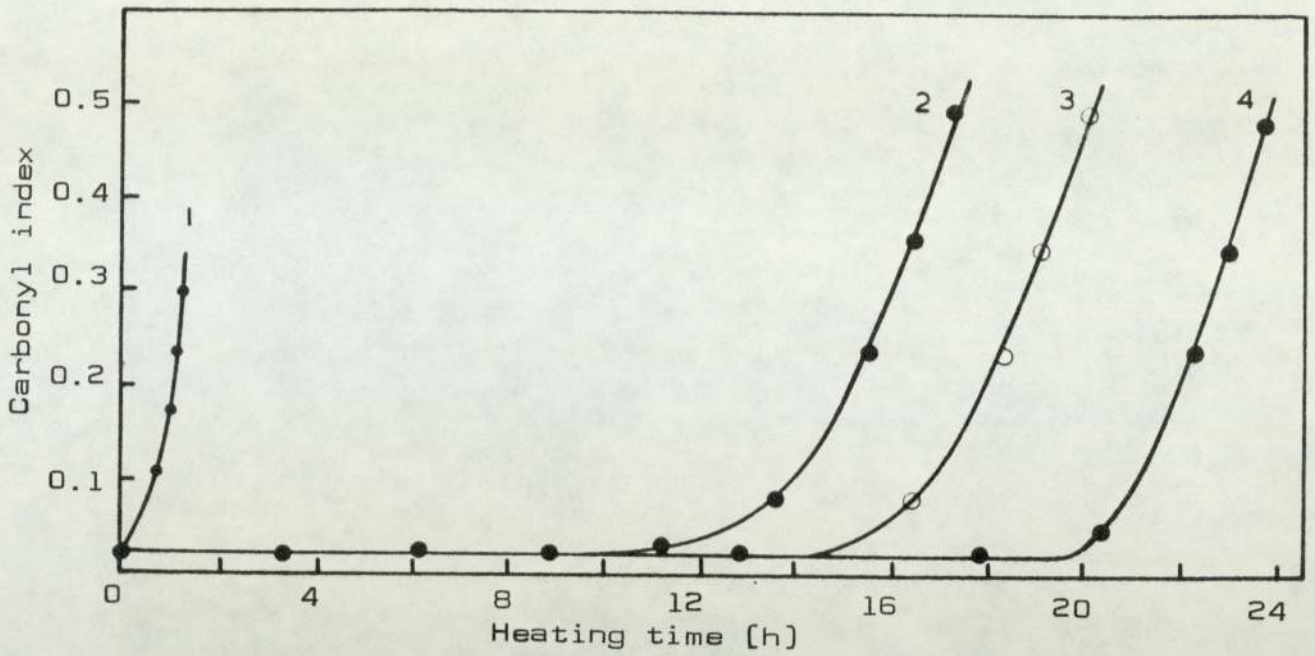


Fig. 6.9 Effect of NiDBP [2], NiBX [3] and DiPDiS [4] on the thermo-oxidation of PP at 140°. Concentration of all additives is $2.5 \times 10^{-4} \text{M}/100\text{g}$ [10,CM].

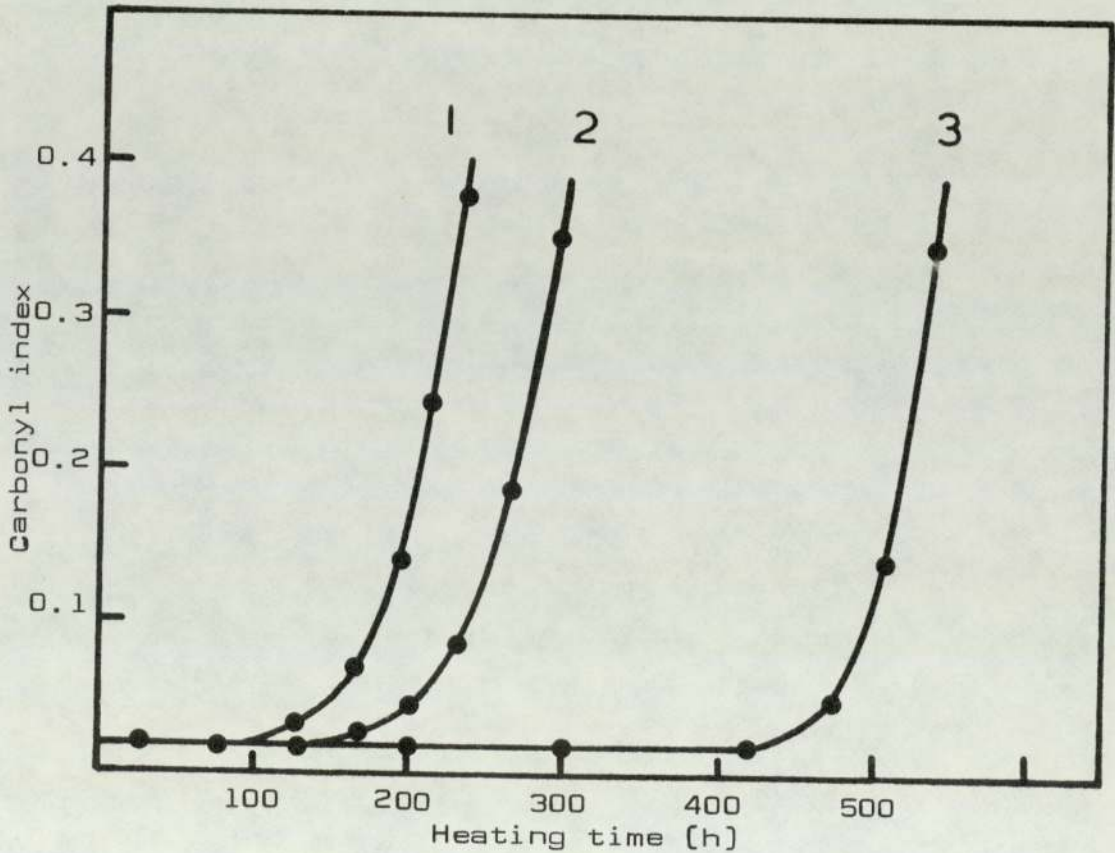


Fig. 6.10 Effect of additives [$2.5 \times 10^{-4} \text{M}/100\text{g}$], in combination with Irganox 1076, on thermo-oxidation of PP at 140°. [1] Irg.1076; [2] DiPDiS + Irg.1076; [3] NiDBP + Irg.1076. PP samples were processed at 180°.

CHAPTER SEVEN

DECOMPOSITION OF HYDROPEROXIDES

IN

MODEL COMPOUNDS

In this chapter thermal decomposition of cumene hydroperoxide (CHP) in chlorobenzene (at 110^o) and dodecane (at 150^o) is investigated in the presence and absence of NiDBP, NiBX, NiDBC, and DiPDiS. Kinetics of disappearance of CHP and the additives are examined at different molar ratios and concentrations.

Several methods are used to follow and monitor changes in the decomposition reactions of CHP. Iodometry is used to determine CHP, IR-spectrophotometry, thin layer chromatography (TLC) and gas/liquid chromatography (GLC) are used to follow intermediates and products, and UV-spectrophotometry to monitor, qualitatively, the build up of products and to determine, quantitatively, the rates of disappearance of the additives at room temperature, 30^o, and at 70^o. Results show the importance of ionic catalytic decomposition pathways when compared to the homolytic catalytic decomposition of CHP.

7.2.1 Thermal Decomposition of CHP in the Presence and Absence of Nickel Dithiolates in Chlorobenzene at 110^o

The effect of the metal dithiolates NiDBP, NiDBC and NiBX [at 2×10^{-4} M] on the mode of decomposition of CHP [at 1×10^{-2} M] in chlorobenzene at 110^o is shown in figure 7.1a. In the absence of these complexes, CHP was found to be quite stable [see control curve in Fig.7.1a]. Chlorobenzene itself is an inert solvent and is thermally stable at 110^o.

The decomposition curves of CHP; in the presence of nickel dithiolates at a ratio of CHP:additive = 50 or 100 [Fig.7.1] reveal three characteristic features:

- 1) rapid initial catalytic stage
- 2) a secondary induction period [IP] leading into,
- 3) a slower first order catalytic reaction.

First order rate constants obtained for the second catalytic stage are $7.1 \times 10^{-2} \text{ s}^{-1}$ [NiDBP], $6.0 \times 10^{-3} \text{ s}^{-1}$ [NiDBC], and $6.1 \times 10^{-3} \text{ s}^{-1}$ [NiBX].

The effect of varying the concentration of NiDBP [2.5×10^{-5} – 1×10^{-4} M] on the kinetics of decomposition of CHP [1×10^{-2} M] in chlorobenzene at 110^o is displayed in figure 7.2. These results show that on going from the catalytic to stoichiometric ratios, i.e. 500:1 to 1:1, the secondary induction period appears to be by-passed, with notable increase in the contribution of the first catalytic stage. Figure 7.2 further shows that the first catalytic stage is much faster at higher concentrations of the metal

complex, i.e. at low CHP:NiDBP molar ratio, but assumes an all-important role near the stoichiometric ratios. Thus at the higher ratios of hydroperoxide to additive, decomposition of CHP proceeds at a slower rate.

Further examination of Figure 7.2 reveals an inverse relationship between the amount of CHP initially decomposed, and the length of the induction period which precedes the final decomposition stage. This second catalytic (and final) stage in the decomposition of CHP (at $1 \times 10^{-2} \text{M}$) displays first order kinetics (inset in Fig.7.2). Figure 7.3 reveals the linear relationship between the number of moles of CHP which are decomposed during the first stage per mole of NiDBP at different additive concentrations (see also Fig.7.2). At $[\text{CHP}] 1 \times 10^{-1} \text{M}$ and $1 \times 10^{-2} \text{M}$, the decomposition of CHP by NiDBP ($1 \times 10^{-2} \text{M} - 1 \times 10^{-5} \text{M}$) proceeds in essentially the same manner except for the kinetics of the second catalytic stage which was found to be second order at the higher CHP concentration (cf. insets in Figures 7.4 and 7.2).

Decomposition of CHP ($1 \times 10^{-1} \text{M}$) by NiDBP and NiDBC ($8 \times 10^{-4} \text{M}$) at 110° (Fig.7.5a) and 70° (Fig.7.5b) shows NiDBC to be a more effective PD; compare this with Fig.7.1 where at the lower concentration of CHP ($1 \times 10^{-2} \text{M}$) and nickel dithiolates ($2 \times 10^{-4} \text{M}$), NiDBP was found to be better. Furthermore, the kinetics of disappearance of CHP (1×10^{-2}) and NiDBP ($8 \times 10^{-4} \text{M}$) during their reaction in chlorobenzene at 70° are compared (inset in Fig.7.5b). It is clear that the metal complex was almost entirely consumed prior to the onset of the second catalytic stage. The kinetics of disappearance of the three nickel dithiolates ($8 \times 10^{-4} \text{M}$ and $4 \times 10^{-4} \text{M}$),

NiDRC, NiRX, and NiDRP during the induced decomposition of CHP [$1 \times 10^{-1} \text{M}$] at 70° are compared in Fig.7.5c.

At even higher CHP concentration [$5 \times 10^{-1} \text{M}$], and at 125 fold excess, CHP was found [see Fig.7.6] to be virtually destroyed by the three nickel dithiolates [$2 \times 10^{-3} \text{M}$] in a much shorter time than that which is permitted by the analytical method employed here [see Sec.2A.5.2]. The results shown in figure 7.6 should not be confused with the fast initial catalytic stage which were observed earlier in figures 7.1-7.5. Analysis of the products from this reaction [table 7.1] showed them to be those expected from the second ionic catalytic stage.

Table 7.1 Products formed from the decomposition of CHP
[$5 \times 10^{-1} \text{M}$] by nickel dithiolates [$2.3 \times 10^{-3} \text{M}$]
in chlorobenzene at 110°

Additive	% theoretical yield		
	phenol	α -me-styrene	acetophenone
NiDBP	90.8	2.4	6.8
NiDBC	89.0	5.3	5.7
NiBX	76.6	18.0	5.4

7.2.2 Auto-oxidation of Dodecane in the Presence and Absence of NiDBP and DiPDiS at 150^o

CHP-induced oxidation of dodecane was studied at 150^o both in the absence and presence of NiDBP. Figure 7.7 shows the behaviour of CHP in additive-free dodecane [curves 1 and 2]. A notable increase in peroxide content of the reaction mixture [curve 1] is found [see Sec.2A.5.1 for experimental details]. For the purpose of analysis, the reaction vessel was opened to the atmosphere only briefly, and for the purpose of sampling, while still under continuous flow of nitrogen. Results of several experiments of CHP-induced oxidation of dodecane in the complete absence of oxygen [closed system] are shown [curve 2] [see Sec.2A.5.1 for experimental details]. Each of these experiments furnished a single point on this curve. A comparison between figures 7.1a and 7.7 shows that thermal decomposition of CHP in dodecane [in a closed system] and in chlorobenzene are similar.

The generally lower peroxide content [curve 2 in Fig. 7.7] when compared to the control curve in Figure 7.1a, is attributed to the higher temperature used in the decomposition studies of CHP in dodecane. The results of a set of experiments in which the oxidation of dodecane [in a closed system] was followed at 150^o and in the absence of CHP [blank run] is also shown [curve 6 in Fig.7.7]. The small increase in peroxides, which sets-in only after ca.3 hours is a consequence of the residual amounts of oxygen present in the nitrogen used during these experiments.

Figure 7.7 shows [curves 3-5] the effect of increasing the concentration of NiDBP on the general behaviour of CHP decomposition in dodecane at 150° . The three stages of hydroperoxide decomposition, clearly observed here, are similar to those found earlier [see Sec.7.2.1 and Fig.7.1].

In order to identify the second stage, catalytic decomposition of CHP with the presence of disulfide, DiPDiS was investigated under the same conditions as in NiDBP. Results shown in figure 7.8 indicate the absence of a secondary induction period which must, therefore, be associated with the metal complexes [see for example Figs. 7.7 and 7.1]. After a transitory faster step, the reaction of CHP (1×10^{-2} M) with DiPDiS (10^{-3} , 10^{-4} M) follows first order kinetics [curves 1-3 in inset of Fig.7.8], which, in turn, is faster than the second catalytic stage from a corresponding reaction of CHP with NiDBP at the same molar concentration [curves 4 and 5 in Fig.7.8].

7.2.3 Photodecomposition of CHP in the Presence of NiDBP and DiPDiS

In the absence of additives, CHP was found to undergo slow but gradual decomposition when a chlorobenzene solution containing the hydroperoxide (1×10^{-2} M) was exposed to UV-light [see control in Fig.7.9]. Photodecomposition of CHP was greatly facilitated when NiDBP (1×10^{-4} M) is present [curve 2 in Fig.7.9]. It is clear that the features displayed by the decomposition curve of CHP in the presence of the nickel complex, in light, are identical to those obtained during thermal reaction at 110° [cf. curve 2 in

Fig.7.9 with Fig.7.1). Furthermore, figure 7.9 displays the rapid destruction of the nickel complex under these photo-oxidative conditions [curve 2']. The effect of DiPDiS [curve 3] on the photodecomposition of CHP in chlorobenzene under the same conditions, was similarly found to correlate well with results of thermal decomposition of CHP [cf. with Fig.7.8).

Photodecomposition of CHP in dodecane, in the presence of NiDBP, is also shown [inset in Fig.7.9]. Albeit the similarity in the overall features of the decomposition curves, a slower rate of decomposition of CHP is noted here when compared with analogous curves in chlorobenzene [curve 2]. The reactive nature of chlorobenzene^[131] and the long wavelength absorption arising from the contact charge-transfer interaction between chlorobenzene and oxygen^[132] was, therefore, avoided by the use of dodecane. The faster rate observed in the case of chlorobenzene must be a consequence of the solvent.

In the presence of a large excess of NiDBP, i.e. at a molar ratio of NiDBP:CHP = 100, photodecomposition of CHP was found to be very rapid [Fig.7.10]. Only a slight decrease in the concentration of the nickel complex was noted. The decrease was found to be simultaneous with the fast hydroperoxide decomposition. The final dark purple colour of the solution was, therefore, hardly effected.

7.2.4 Kinetics of Disappearance of Additives

The disappearance of nickel dithiolates during induced-decomposition reaction with CHP (1×10^{-1}) at 30° and 70° in dodecane was followed by UV-spectrophotometry at the fixed wavelength shown: 316 nm [for NiDRP and NiRX] and 325 nm [for NiDRC]. All the nickel complexes decayed according to first order kinetics [Fig.7.11]: the decay rates are fastest for NiDRC and slowest for NiDRP [see Fig.7.12]. Thermal decomposition of CHP (1×10^{-1} M) at 70° and the disappearance of the additives (8×10^{-4}) are shown in figure 7.5b for comparison. Furthermore, rates of disappearance of these additives were effected by variations in the ratio [CHP]:[additive], with additive concentrations in the range 4×10^{-4} to 8×10^{-4} M, in the presence of CHP at 1×10^{-1} M; higher ratios led to faster decay of the additives.

7.2.5 Product Analysis

1. By Gas Liquid Chromatography

Products obtained following thermal decomposition of CHP in chlorobenzene [at 110°], both in the presence and absence of additives, were analysed by GLC. Kinetics of formation and disappearance of products were also followed during the course of the reaction. Triphenyl phosphine was used to affect reduction of unreacted CHP to α -cumyl alcohol [α, α -dimethyl benzyl alcohol]. The product yield of the alcohol was corrected with the aid of a calibration graph [see Sec.2A.7.1]. Product distribution for the reaction of CHP (1×10^{-2} M) with NiDBP at different molar ratios [10-120] is shown in figure 7.13. It is clear that α -cumyl alcohol and

acetophenone are exclusively formed at, and below, molar ratio of 10. This situation is drastically altered at higher ratios, when products (phenol and α -methyl styrene) of the ionic reaction [see Sec.7.3] predominates, i.e. CHP:NiDBP > 10. Under the experimental conditions used for the thermal decomposition studies (i.e. at 110° and continuous purging with N_2) volatile products of the reaction, e.g. acetone, are not retained in the reaction medium. The formation of acetone was shown, however, to occur simultaneously with phenol by IR spectrophotometry [see Sec.7.2.5.2].

Figure 7.14 displays the product distribution of the reaction of CHP ($1 \times 10^{-2} M$) with DiPDiS, under the same experimental conditions described above, at different molar ratios. Phenol and α -methyl styrene are the major decomposition products of CHP in this case (e.g. at CHP:NiDBP = 10). Both products were found to occur in appreciable amounts even at stoichiometric ratios (ca.36% phenol). Products of the free-radical catalytic decomposition pathway i.e. acetophenone and α -cumyl alcohol, occur at a constant (ca.20% of the total) value at molar ratios > 50. The relative yield of products obtained from the induced decomposition of CHP ($5 \times 10^{-1} M$) by nickel dithiolates (NiDBP, NiDBC, NiBX) at $2 \times 10^{-3} M$, in chlorobenzene at 110° , is shown in Table 7.1.

Kinetics of formation of products during the decomposition reaction of CHP ($1 \times 10^{-2} M$) with NiDBP ($1 \times 10^{-4} M$) at 110° , in chlorobenzene, is shown in figure 7.15 at a fixed molar ratio, i.e. 100, the build-up of ionic products during the progress of the reaction, at the expense of free-radical reaction products, is clearly evident.

Figure 7.16 displays the kinetics of formation of CHP ($5 \times 10^{-1} \text{M}$) decomposition products in the presence of NiDBP ($1 \times 10^{-2} \text{M}$) at 110° in chlorobenzene. The distribution of the products changes dramatically during the first few minutes and is completely reversed after 7 minutes in favour of phenol and α -methyl styrene. α -cumyl alcohol and acetophenone are the major products of the reaction at the earlier stages of CHP decomposition by NiDBP.

2. By Infrared (IR) Spectrophotometry

Products from thermal decomposition of CHP ($1 \times 10^{-2} \text{M}$) in chlorobenzene at 110° , in the presence of NiDBP (1×10^{-4}) were also determined by following the IR-characteristic absorptions of the products [Fig.7.17].

The formation of intermediates from both peroxide and nickel complex is clearly demonstrated during the course of CHP decomposition by NiDBP. IR-absorptions, which are attributed to sulfonic acid (1260 cm^{-1} , 1320 cm^{-1}), sulfoxides (1060 cm^{-1}) and thionophosphoric acid (580 cm^{-1} , 825 cm^{-1}), appear to increase during the IP and, undergo decomposition beyond their maximum value. The onset of their decomposition coincides with the onset of the second catalytic stage in CHP decomposition [curve CHP in Fig.7.17]. Figure 7.17 further shows that following the decomposition of these moieties, i.e. sulfonic, sulfoxides, and thionophosphoric acid, the yield of the ionic products, e.g. phenol [$\text{ca. } 3570 \text{ cm}^{-1}$], increase sharply [curve phenol in Fig.7.17].

The simultaneous formation of phenol (3570 cm^{-1}) and acetone (1705 cm^{-1}) is clearly demonstrated (Fig.7.18a) during the decomposition of CHP ($5 \times 10^{-1}\text{M}$) in chlorobenzene at room temperature in the presence of NiDBP ($2 \times 10^{-3}\text{M}$). Coupled with the formation of acetophenone ($1670\text{-}1685\text{ cm}^{-1}$), the IR-results confirm the earlier GLC analyses (Sec.7.2.5.1), and the predominance of phenol at longer reaction times. Similar findings were also realised from decomposition reactions of CHP by NiDBC under exactly identical experimental conditions (see Fig.7.18c).

3. By Thin-layer Chromatography

The formation of reaction intermediates and products from the decomposition of CHP in chlorobenzene (at 110°) in the presence of NiDBP and DiPDiS was followed by TLC (see Sec.2A.7.2). Authentic compounds, prepared in chlorobenzene, were used for comparison (Fig.7.19).

Figure 7.19 shows that NiDBP, α -cumyl alcohol and phenol are to varying extents immobilised by silica gel, i.e. they remain near the starting point, compared to DiPDiS and α -methyl styrene, which lag only slightly behind the solvent front. The position of acetophenone is intermediate (see Fig.7.19) between these extremes.

Figure 7.20 reproduces results of TLC analysis for CHP ($5 \times 10^{-1}\text{M}$) reaction with NiDBP ($1 \times 10^{-2}\text{M}$) at 110° . This same reaction was also analysed by GLC (see Fig.7.16). The rapid destruction (within 7 minutes) of the nickel complex by CHP is clearly demonstrated here from the decreasing size of the shaded area (which is proportional to the concentration of

the complex). Both acetophenone and α -methyl styrene, along with DiPDiS, are formed initially (Fig.7.20). The irregular shape of the spots (for the latter compounds) is suggestive of unresolved components; at longer reaction the shape of these spots reverts to a more circular shape (normally obtained for plates developed in one dimension) indicating a 'pure' component, attributed here to α -methyl styrene. The formation of α -cumyl alcohol toward the end of the reaction is discounted on the basis of GLC analysis (see Sec.7.2.5, Fig.7.16).

The stoichiometric reaction between DiPDiS ($1 \times 10^{-2} \text{M}$) and CHP, and the reaction between NiDBP ($2 \times 10^{-3} \text{M}$) and CHP (5×10^{-1}) in chlorobenzene, at 110° , were also followed by TLC (Fig.7.21). At the stoichiometric ratio of DiPDiS:CHP, phenol and α -methyl styrene were found to 'co-exist' in addition to small amounts of acetophenone; this confirms the GLC results described earlier (see Fig.7.14 and Sec.7.2.5.1).

TLC analysis of products for a stoichiometric reaction between CHP ($1 \times 10^{-2} \text{M}$) and NiDBP, in chlorobenzene at 110° and under an inert atmosphere, is shown in Figure 7.22. The persistence of the metal complex was indicated from TLC spots (during the reaction) and from the persistence of colour of additive (at the end of the reaction). Similar to the case of DiPDiS:CHP reaction, acetophenone was found to occur initially also (cf.Figs.7.21 and 7.22).

The formation and persistence of DBDiS during the first three minutes of the reaction between CHP and NiDBP is clearly evidenced in figure 7.22. The fact that the spots

appearing at $R_f = 0.8$ disappear within 4 minutes of the CHP-induced decomposition reaction of NiDBP would suggest them to be due to DiPDiS. The general appearance of these spots (when compared with the authentic samples) encourage this assignment further [cf. Figures 7.19 and 7.22].

4. By UV-Analysis

Careful analysis of decomposition products of CHP, in the presence of NiDBP, NiBX and DiDBC, in hexane at room temperature and at 70° , has indicated the formation of phenol, alongside α -methyl styrene. The presence of the other products i.e. acetophenone and α -cumyl alcohol prohibits a proper assessment of the contribution of each of these products. It was possible, however, to establish, on a qualitative basis, the dominant presence of phenol and that its formation coincides with the disappearance of the metal complexes [Fig.7.23]. Coupled with earlier quantitative results on product analysis, this finding adds further strength to the fact that the ionic catalytic nature of CHP decomposition is a consequence of oxidation products of the nickel complex rather than the complex itself.

7.3 DISCUSSION

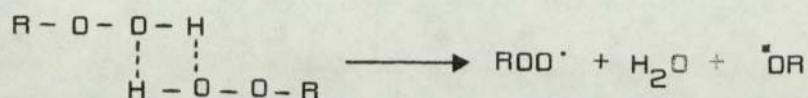
7.3.1 Thermal Decomposition of CHP in the Presence and Absence of Nickel Dithiolates in Chlorobenzene at 110^o

Nickel dithiolates were found to decompose CHP via two distinct catalytic processes: an initial stage, favoured at low molar ratio of CHP-to-complex, and a second stage that assumes greater significance at higher ratios [see Fig.7.1a].

The rapid initial catalytic stage [Fig.7.1a] accounts for the homolytic decomposition products [i.e. α -cumyl alcohol, α -methyl styrene, and acetophenone] of CHP [Fig.7.13] during its reaction with nickel dithiolates in chlorobenzene at 110^o under an inert atmosphere [see Sec.2A.5.1]. This process has been the subject of considerable study^[40,133] by fast kinetic techniques which were used to support the homolytic cleavage of the peroxide bond in CHP.

The formation of ionic products, e.g. phenol and acetone [see Fig.7.13], is a consequence of the second catalytic stage during the decomposition of CHP by each of the nickel complexes. The relative contribution of homo- and hetero-lytic decomposition pathways is critically dependent on the molar ratio [see Fig.7.2] of CHP to additive [NiDBP, NiRX, NiDBC] and on the total concentration of CHP and nickel complexes [cf. Figs.7.2 and 7.4 for NiDBP; cf. Figures 7.1 [NiDBP] with 7.5 [NiDBC]]. ZnDRP has been reported^[50] to show similar concentration-dependent rate processes.

The second catalytic stage is relatively slower than the first and shows first-order kinetics at low CHP (e.g. 1×10^{-2} M) concentration [see inset in Fig.7.2], but was shown to behave according to second order kinetics (Fig.7.4) at higher concentration of CHP (1×10^{-1} M). The second-order behaviour may be ascribed to CHP association at high concentrations. Second-order rates of disappearance of CHP have been shown^[74] for oxygen-free environment and were supposed to proceed via the dimer:



The relative contribution of the initial catalytic process to the overall peroxide decomposing activity of NiDBP decreases with additive concentration and is minimal above the stoichiometric ratio (~ 12) of CHP:additive, which is the stoichiometry required for the oxidation of every sulfur atom to SO_3 in NiDBP [see Fig.7.13]. This is clearly shown (Fig.7.3) from the linear relation between the amount of hydroperoxide initially decomposed and the concentration of the nickel complex at $[\text{CHP}] = 1 \times 10^{-2}$ M.

The formation, accumulation, and destruction of the products which are precursors of the secondary stage catalysts (Figs.7.17 and 7.22) in the kinetics of CHP decomposition is evidenced by the presence of the induction period (Fig.7.1). This is a period of slow steady-state build-up of some sulfur-oxygenated reactive intermediate [see later discussion]. Its length is dictated by the dynamics of the equilibrium [and underlies the apparent period of

inactivity of the metal complex] which verges on instability in the case of NiDBP [curve NiDBP in Fig.7.1a]. Doubling the molar ratio of CHP to additive, i.e. at 100:1, results [see Fig.7.1b] in slower decomposition of CHP [at all stages]. The same order of peroxide decomposing activity, however, is retained by the additives: NiDBP > NiBX > NiDBC.

In contrast to the linear relation found for the initial catalytic stage [Fig.7.3] an inverse relationship is found between the length of the induction period and the concentration of the nickel complex. Therefore, longer times are needed for the accumulation of sufficient active intermediate products which are necessary for the triggering of the second catalytic stage. A converse relationship has been reported^[118] for ZnDIP, where the length of induction period was found to be linearly proportional to concentration.

The fact that nickel complexes are not themselves responsible for the catalytic decomposition of CHP is clear from the observation that these complexes were essentially destroyed before the onset of the second catalytic stage [see Fig.7.5b]. **Trans** Reaction products observed during the secondary induction period were found to include disulfide, phenol, acetophenone, α -methyl styrene, and cumyl alcohol [see Figs. 7.15 and 7.22]. Both IR and TLC analyses [Secs. 7.2.5.2 and 7.2.5.3] provide unequivocal evidence [Figs. 7.17 and 7.22] in support of the formation and accumulation of reactive intermediates during the apparent period of inactivity of the additive 'system'. This justifies the statement that oxidation products of nickel dithiolates which are formed during the induction period are responsible

for the second ionic catalytic decomposition during thermal [at 110^o in chlorobenzene] reactions of CHP with nickel dithiolates, and that all the metal complex is decomposed before the onset of the second catalytic stage.

Decomposition of CHP [1×10^{-5} M] by nickel dithiolates [2×10^{-3} M] suggests a greater contribution from the ionic pathway in the case of NiDBP when compared to NiBX. This conclusion is supported by the greater amounts of ionic products obtained in the presence of NiDBP (see table 7.1). Furthermore, the absence of an observable induction period [to CHP] coupled with the appearance of high percentage of phenol [table 7.1 and Fig.7.6], which is a product of an ionic catalytic process, is taken as evidence for the 'rapid switching' of the dynamics of decomposition from the initial rapid to the final catalytic stage on a time scale which is much too short to be followed by the experimental set-up used in the present study. This choice of hydroperoxide concentration [i.e. 5×10^{-1} M] was made to achieve similar levels of hydroperoxide as those found^[19] to occur for polymer hydroperoxides, which gave maximum hydroperoxide concentration for unstabilised PE when processed in an open mixer for 30 min. at 150^o. Additives were normally incorporated in the polymer at a loading of ca.0.1% [2.5×10^{-4} M/100g], see Sec. 4B.1. An important conclusion to be drawn from fig.7.6 is the extraordinary effectiveness of nickel dithiolates in affecting hydroperoxide decomposition at these high hydroperoxide concentrations.

It is well known^[1e,28] that the nature and extent of decomposition products formed from CHP are diagnostic of the processes occurring during catalytic decomposition of the hydroperoxide. The formation of phenol and acetone in a heterolytic process, compared to acetophenone, which results from a homolytic cleavage, was discussed earlier[Sec.7.3.1]. The formation of α -cumyl alcohol, however, may be explained in terms of both a homolytic cleavage and stoichiometric reduction of hydroperoxides. On the other hand, the presence of α -methyl styrene among the products indicates the presence of an acid catalyst and is, therefore, generally associated with the ionic pathway in the catalytic decomposition of CHP^[134,1e].

The nature of the ionic catalyst formed from nickel dithiolates and its effect on product distribution were concluded from the study of several decomposition reactions of CHP in the presence of NiDBP at different molar ratios of CHP-to-additive [Fig.7.2].

The observation that α -methyl styrene, rather than α -cumyl alcohol [Fig.7.13] occurs as a product at all CHP:NiDBP ratios greater than 10, argues strongly in favour of the formation of a strong Lewis acid [species], during CHP decomposition which is capable of catalysing the dehydration of the alcohol to α -methyl styrene. A striking similarity is apparent from a comparison between product distribution from CHP decomposition in the presence of NiDBP [Fig.7.13] with that observed in the presence of SO_2 ^[28].

The general appearance of the different decomposition curves [Fig.7.1] and the similarity in the ionic decomposition products [table 7.1 and Figs.7.18b and c] of CHP in the presence of each of the three nickel dithiolates, under similar experimental conditions, is suggestive of a similar mechanism of action which must be associated with similar active intermediates. This conclusion is supported also by the behaviour of DiPDiS [see Sec.7.2.2 and later discussion].

There appears to be some conflict in the earlier literature on the formation of disulfide, and its intermediacy, during the peroxide decomposing action of ZnDIP^[50,118,135]. Although the mechanism of action of all nickel dithiolates is expected to be similar, the discussion that follows deals with NiDBP only.

The formation of the disulfide during the stoichiometric reaction of CHP ($1 \times 10^{-2} \text{ M}$) with NiDBP ($1 \times 10^{-2} \text{ M}$) was illustrated by TLC [Sec.7.2.5.3] to occur initially during the first three minutes of the reaction, after which it disappears completely [Fig.7.22].

Although the conditions used for TLC analysis [see Sec.7.2.5.3] does not provide an unequivocal identification of α -methyl styrene and DBDiS, the formation of the former is excluded on the following grounds.

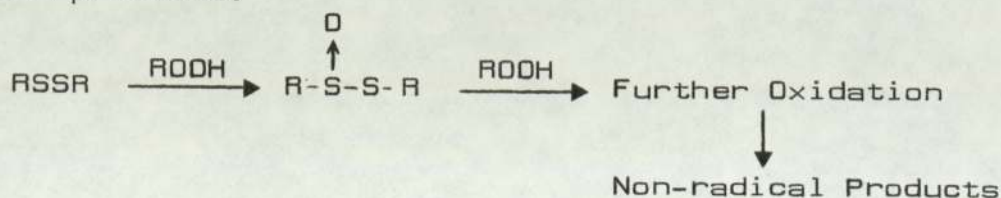
1. Since α -methyl styrene is a stable product, it should persist throughout the course of the reaction, as indeed was found to be the case in other reactions [see Figs.7.15 and 7.16]. TLC results [Fig.7.22], however, show only a transitory existence of the product in question.

2. At this molar ratio, i.e. CHP/NiDBP=1, product analysis by GLC did not reveal the formation of α -methyl styrene.

The formation of disulfide from the corresponding nickel complex in the presence of hydroperoxide at 110° is, therefore, established. The presence of disulfide under conditions of stoichiometric reactions could suggest similar product formation during the initial transformation reactions of the nickel complex in the presence of different molar ratios of CHP.

The above process is entirely analogous to the formation of ionic catalyst for hydroperoxide decomposers from MBT and its metal complexes through the intermediacy of disulfides [47] and is also consistent with the mechanism proposed [28,32] for the antioxidant function of MDRC in hydroperoxide-initiated systems.

Disulfides (and sulfides) have been shown [39,119] to be unable themselves to inhibit oxidation of substrates but rather the inhibition was attributed to products formed from them as peroxides accumulate in the substrate [29,47,125]. It has been proposed [130,136] that peroxides formed in the substrate, at high temperatures, oxidise the disulfides to thiosulfinates and that effective inhibition then results from peroxide decomposition by the thiosulfinate or subsequent reaction products.



Similarly, thiophosphoryl disulfide has been found in the present work to be unable to affect thermal decomposition of t-butyl hydroperoxide (TBH) at room temperature, nor is it destroyed, unless photo-initiated, by UV-light (see Sec.3.2.3).

7.3.2 Auto-oxidation of Dodecane in the Presence and Absence of NiDBP and DiPDiS at 150^o

Dodecane is used here as a simplified model for PE without the additional unsaturation and oxygen-containing functional groups which are normally present in commercial PE. In addition to the basic reaction of CHP with nickel dithiolates (see Sec.7.2.1) at 150^o, auto-oxidation of dodecane may be induced also by CHP. The ability of the nickel complex to destroy CHP and hydroperoxide-derived from the auto-oxidised substrate (i.e. dodecane) can, therefore, also be evaluated.

The notable increase in peroxide content of the reaction mixture (curve 1 in Fig.7.7) indicates the ease with which dodecane is auto-oxidised under the experimental conditions used (see Sec.7.2.2 and Sec.2A.5.1). The behaviour of the CHP-induced oxidation of dodecane (curve 1 in Fig.7.7) under these conditions, is very similar to the oxidation of unstabilised LDPE when processed in an open mixer at 150^o^[19]. The large increase in the peroxide content (curve 1 in Fig.7.7) is comparable with the generally accepted pattern of oxidation of unstabilised PE^[13]. In the complete absence of oxygen, however, dodecane is inert.

During processing of NiDBP-stabilised PE, the ratio of the nickel complex to polymer hydroperoxide, at any moment in time, is quite high. This situation arises as a result of

the concentration of the complex initially used (i.e. compounded) and because of its excellent hydroperoxide decomposing activity. The high ratio of NiDBP:CHP (100:1) is, therefore, of practical significance [see Fig.7.10].

The low rate of consumption of NiDBP, when present at high NiDBP:CHP ratio, has already been substantiated from experiments on stabilised LDPE [see Sec.4B.2.4] for samples which were prepared under mild and severe processing conditions. As in the case of solution studies [Sec.3.2.3], the nickel complex in the test film was found to persist for a considerable length of time on UV-exposure [see for example Fig.4B.9, Sec.4B.2.4]. This is further proof for the excellent auto-inhibiting role of the nickel complex when present in the polymer at these molar ratios.

At the same molar ratio, reactions of CHP ($1 \times 10^{-2} \text{ M}$) with NiDBP and DiPDiS in dodecane at 150° reveal two major points of departure for the disulfide-CHP reaction [cf.Figs.7.7 with 7.8):

1. absence of induction-period
2. small contribution of the initial catalytic stage to the overall decomposition process.

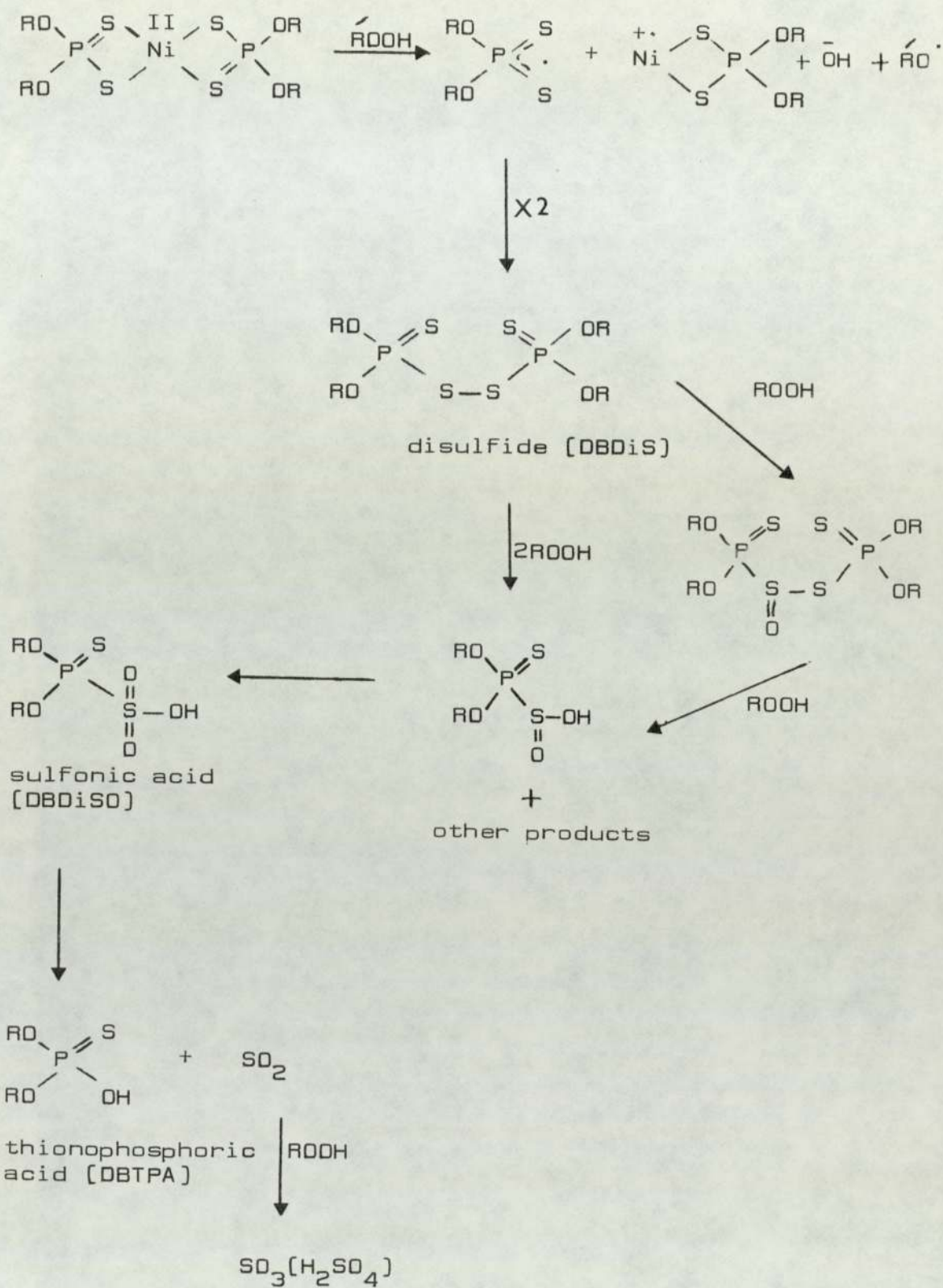
Product analysis for CHP-disulfide reaction [Fig.7.14] further confirms that, at all ratios of CHP:disulfide, ionic decomposition products are favoured. Thus, for example, 36% phenol is obtained from a 1:1 reaction [Fig.7.14] while for ratios higher than 50:1 the contribution of the free radical step to the overall decomposition remains constant at under 20%.

Evidently, the heterolytic decomposition of CHP prevails in the presence of DiPDiS and is even quite significant for stoichiometric reactions. Disulfides have been found^[43] to be unreactive toward $ROO\cdot$ & in this respect, the behaviour of the disulfide contrasts with its metal complex precursor. Moreover, the latter shows total homolytic decomposition of CHP near the stoichiometric ratio [see Fig.7.13].

An initial catalytic stage [homolytic decomposition of hydroperoxide] and an induction period [during which time reactive intermediates and ionic catalysts for hydroperoxide decomposition are formed] must, therefore, be characteristic of the metal complex peroxidolytic action.

Scheme 7.1 shows an outline of processes involved during the conversion of NiDBP [in the presence of CHP at 100 fold excess] to the powerful antioxidant [sulfonic acid, DBDiSO] which catalyses the decomposition of CHP [forming phenol and acetone, see Figs.7.17,18,15] and inhibits hydroperoxide-initiated oxidation.

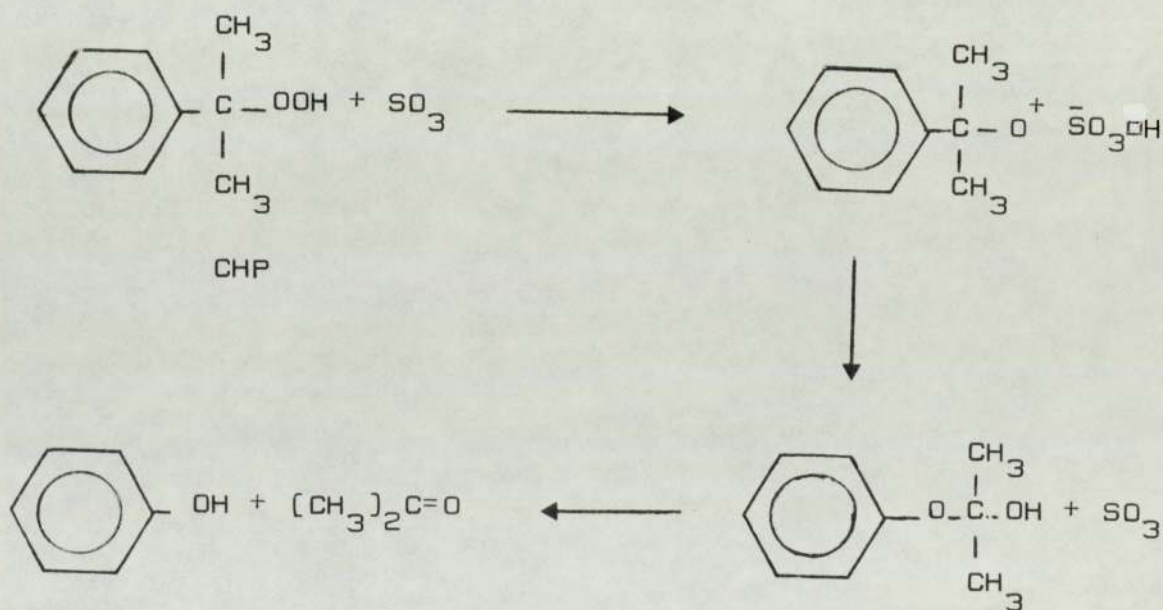
In the reaction of NiDBP [$1 \times 10^{-4} M$] with CHP [$1 \times 10^{-2} M$], sulfonic acid and, at a slower rate, thionophosphoric acid [DBTPA] are formed slowly during the induction period [see Fig.7.17], whereas no phenol is found initially, i.e. during the build-up of DBDiSO and DBTPA. However, phenol is observed after about 10 minutes [from the start of the reaction] and toward the end of the induction period, which, coincides with the decomposition of these oxidation intermediates. The further decomposition of these intermediates is seen to be directly involved in the formation of the ionic catalysed product, phenol. Thus DBTPA, formed via the decomposition of



Scheme 7.1 Antioxidant mechanism of NiDRP

DBDiSO, appears to level-off following an initial decomposition. The resulting SO_3 or H_2SO_4 may, therefore, account for the formation of phenol and acetone during CHP decomposition [Scheme 7.2].

The precursor to all these oxidation intermediates, e.g. DBDiSO and DBTPA, must be the initial transformation product [the disulfide, DBDiS] formed [within the first few minutes] from the nickel complex during its reaction with CHP as was confirmed by TLC [Fig.7.22]. The importance of heterolytic decomposition during the initial stages of CHP metal complex reaction, and the predominance of the heterolytic mechanism of decomposition, and at higher ratios of CHP:NiDBP, is, therefore, fully established and confirmed.



Scheme 7.2

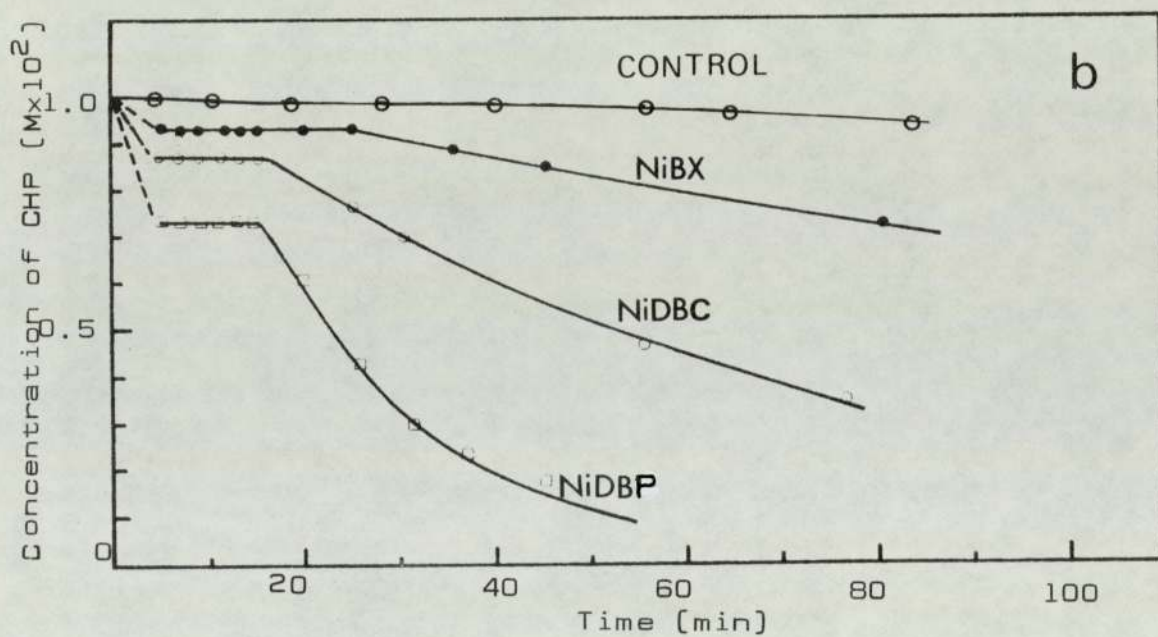
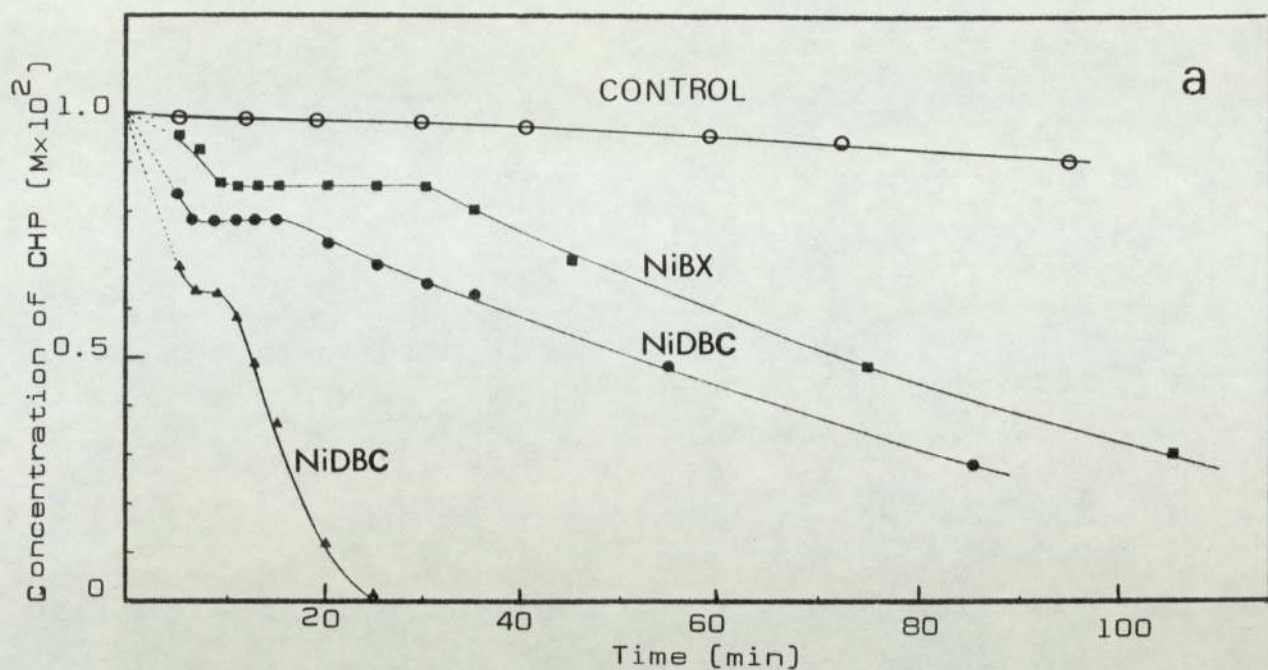


Fig. 7.1 Decomposition of CHP (a. $1 \times 10^{-2} \text{ M}$; b. $1 \times 10^{-2} \text{ M}$) in chlorobenzene at 110° in the presence of nickel dithiolates (a. $2 \times 10^{-4} \text{ M}$; b. $1 \times 10^{-4} \text{ M}$). Decomposition of CHP in the absence of additives is shown [control].

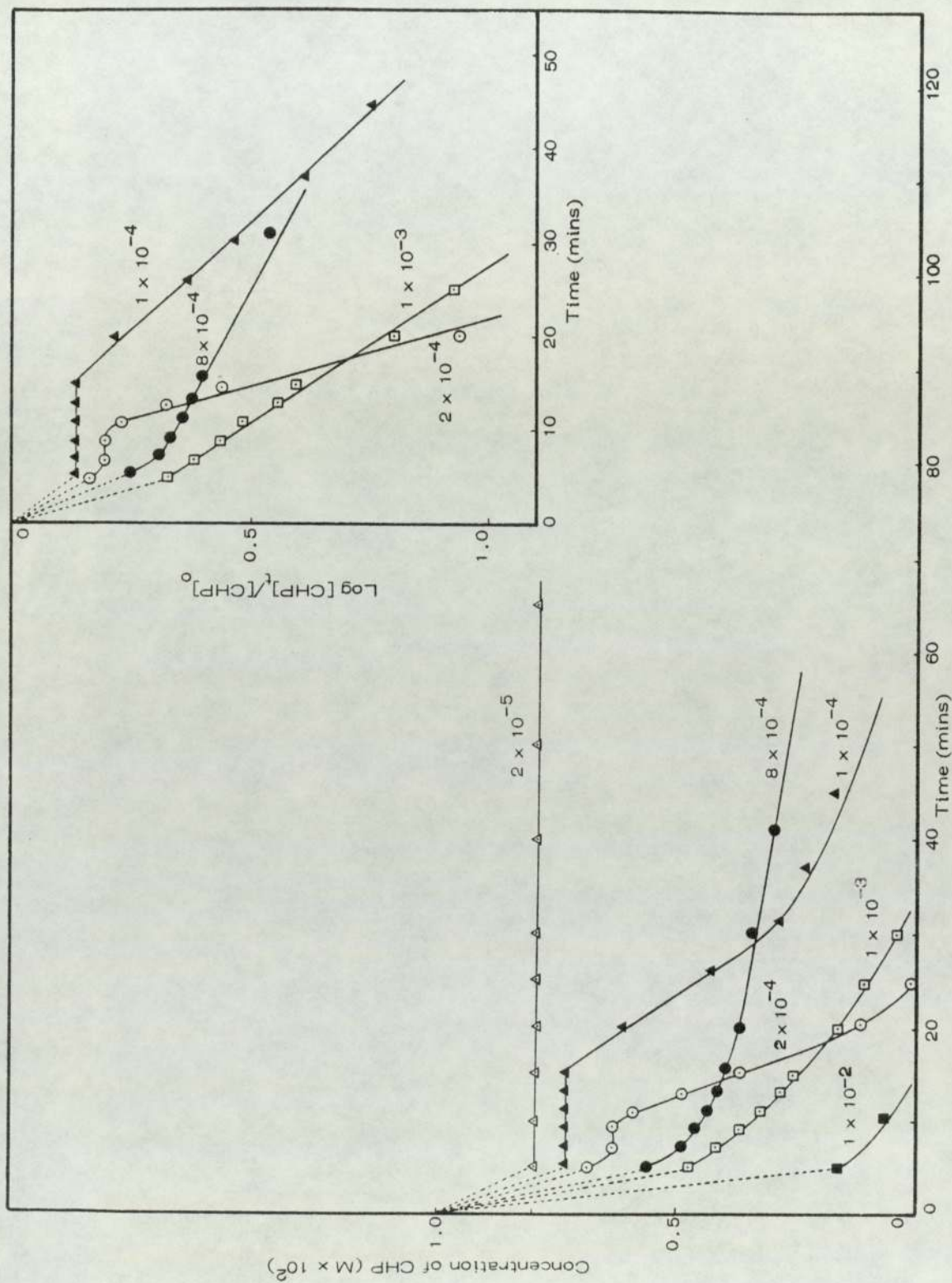


Fig. 7.2 Decomposition of CHP ($1 \times 10^{-2} M$) in chlorobenzene at 110° in the presence of NiDBP at the molar concentrations shown. [The inset shows first order kinetic plots for the third stage of some of these reactions].

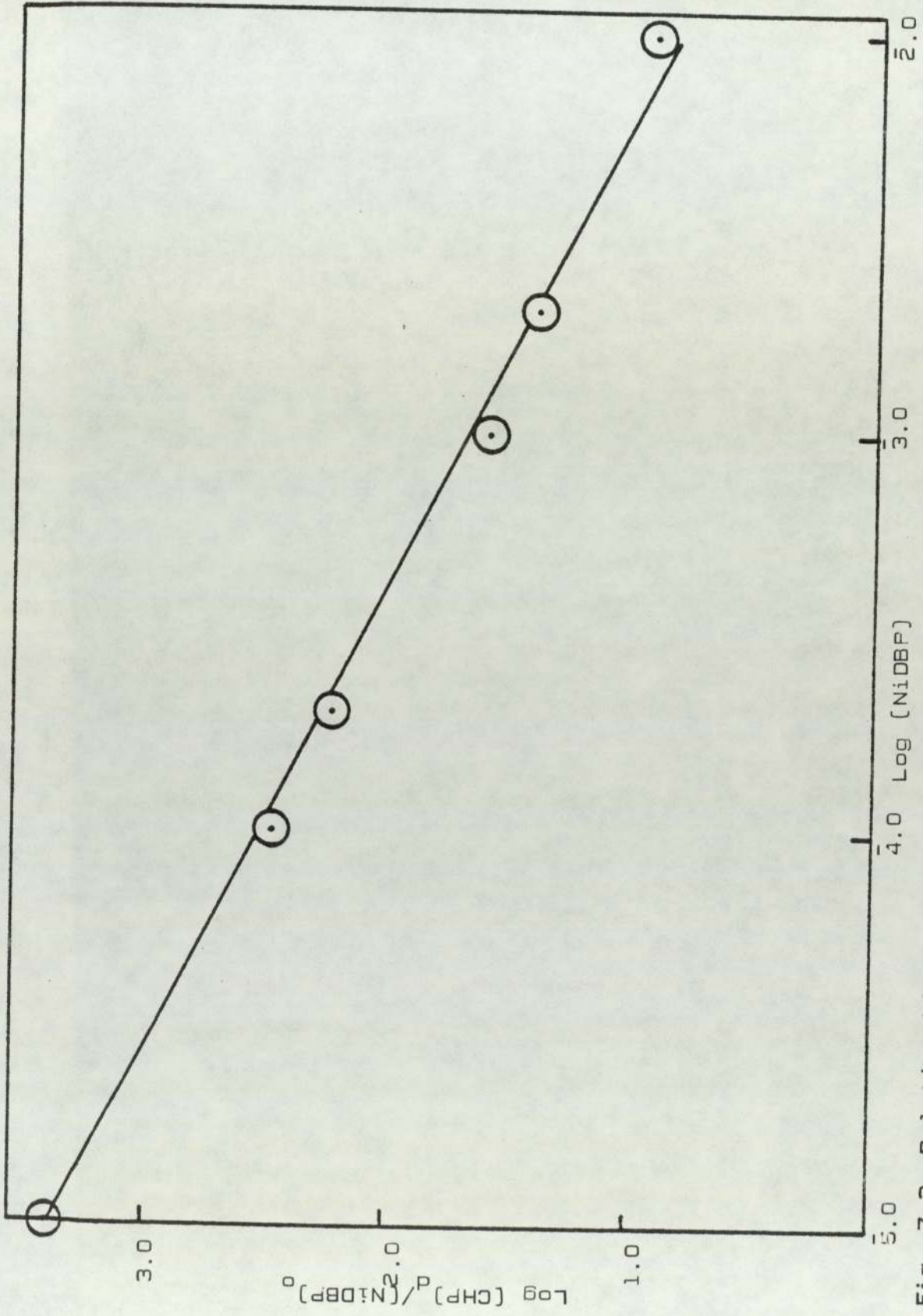


Fig. 7.3 Relationship between number of moles of CHP decomposed during the first stage per mole of NiDBP at different additive concentration. CHP concentration is $1 \times 10^{-2} \text{M}$.

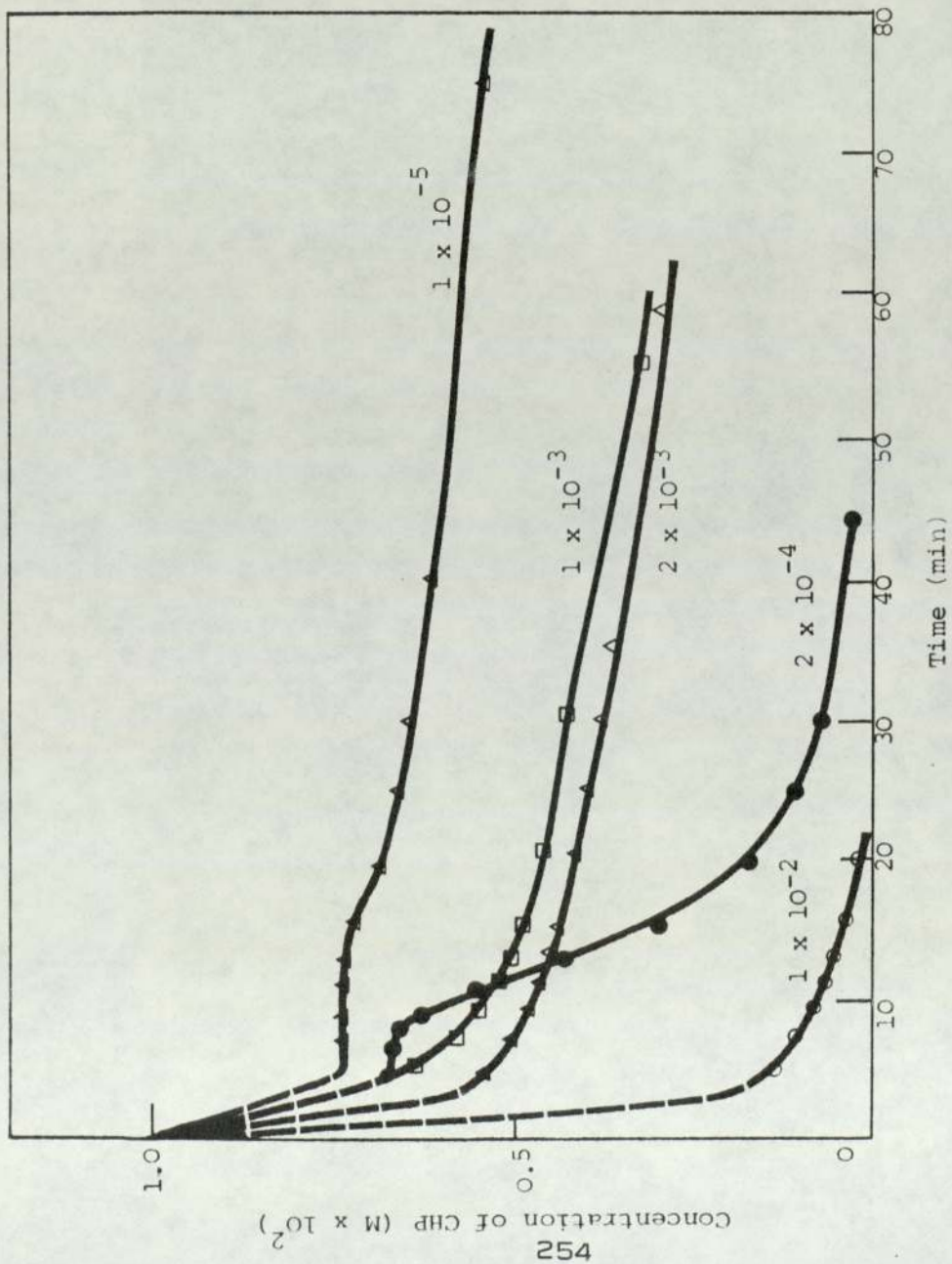
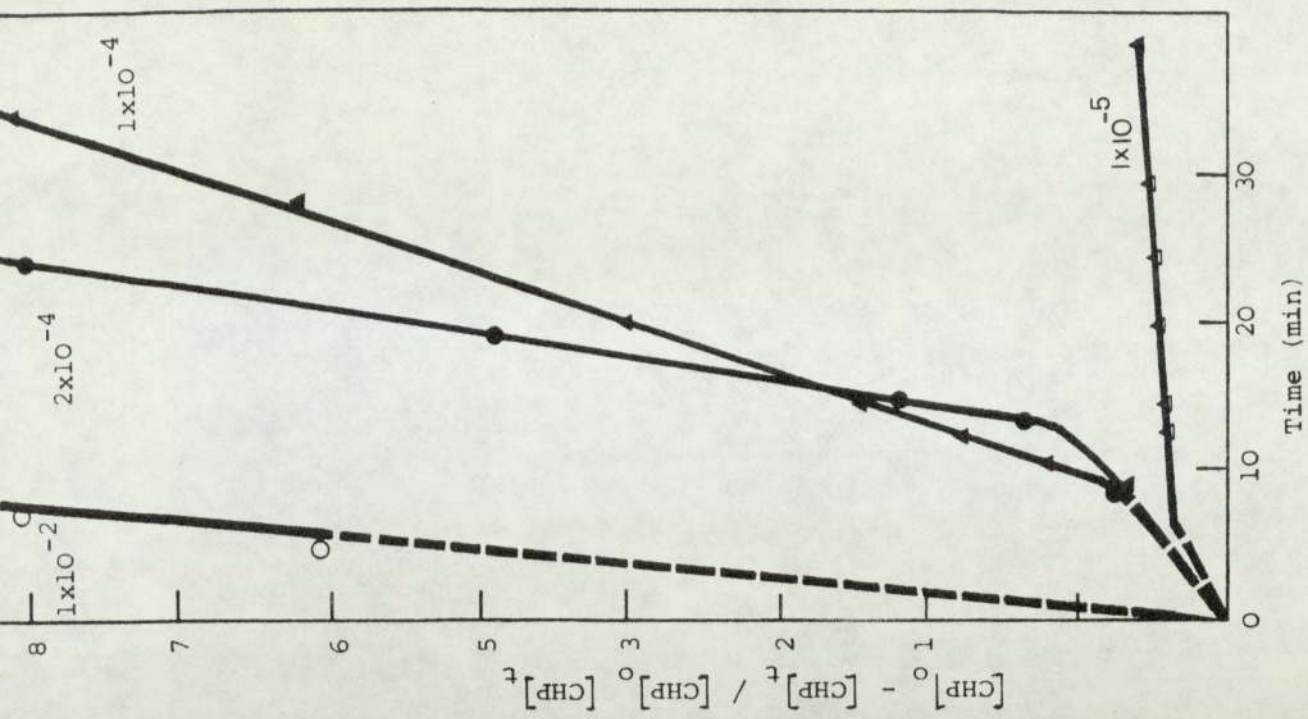


Fig. 7.4 (above) Decomposition of CHP ($1 \times 10^{-1} M$) in chlorobenzene at 110° in the presence of NiDBP at the molar concentration shown. (right) Second order kinetic plots for the third stage of some of these reactions.



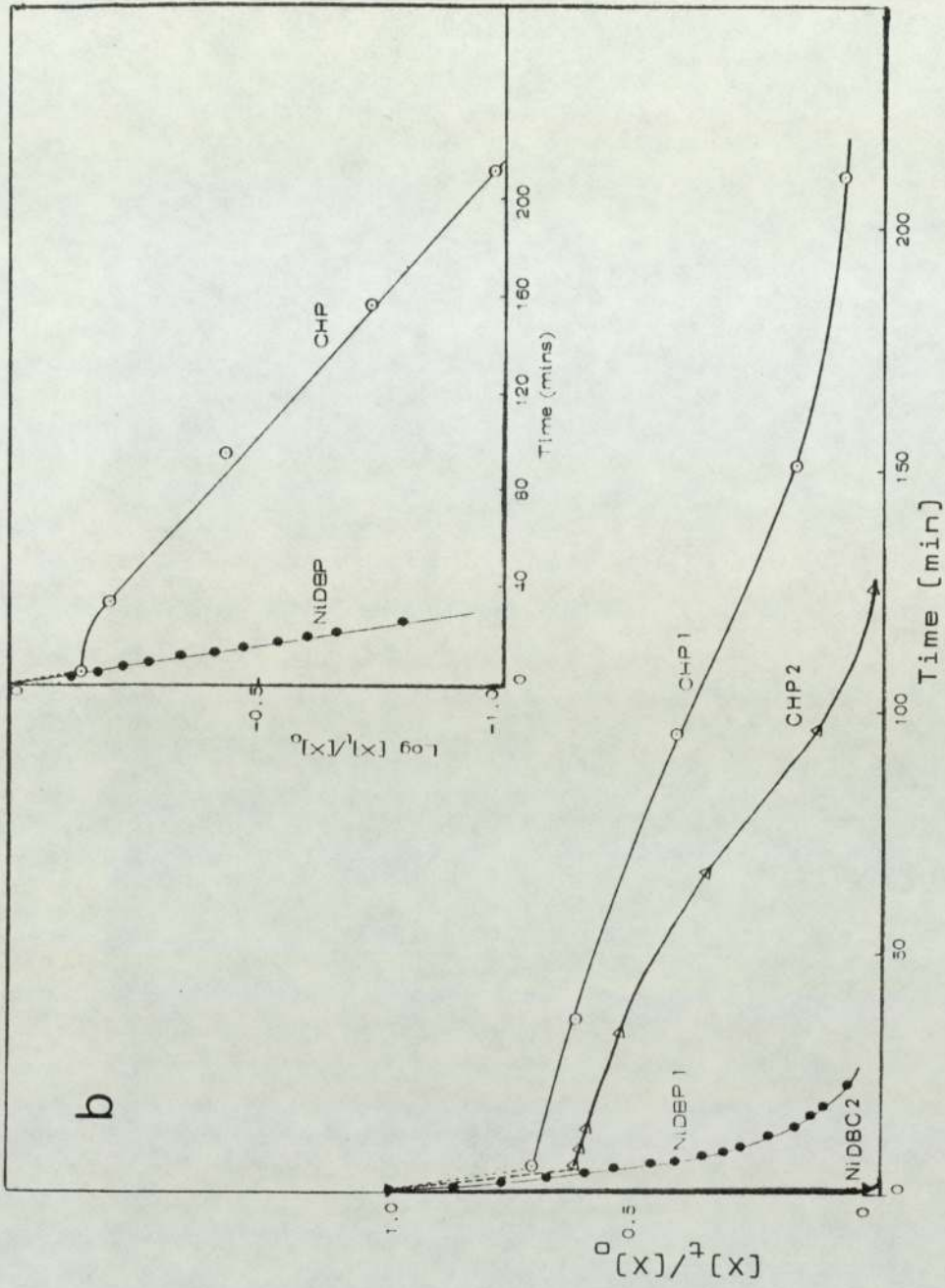
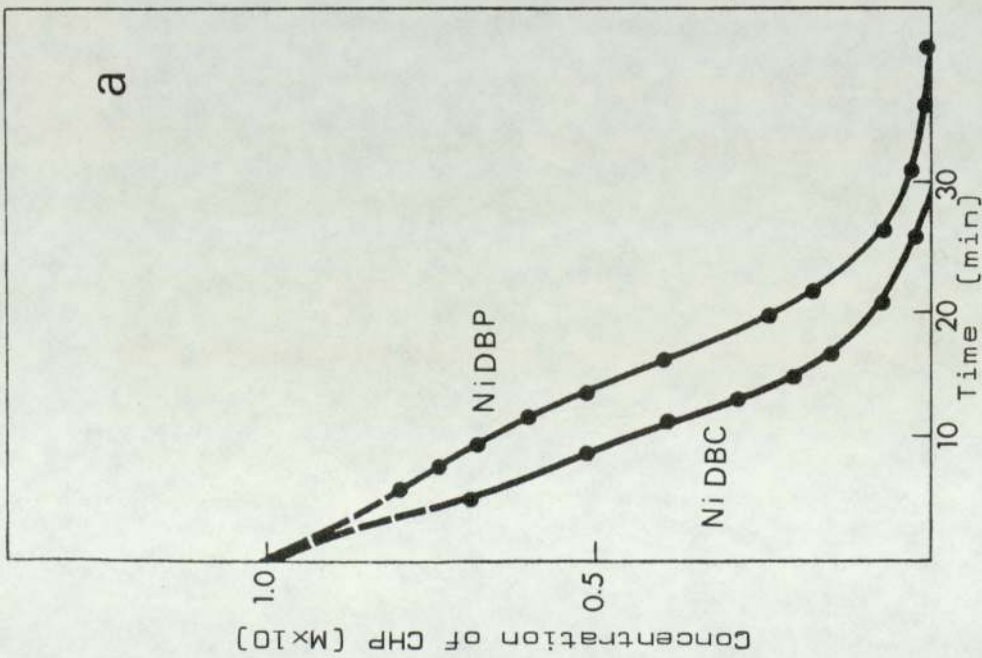


Fig. 7.5 Decomposition of CHP in chlorobenzene (a) $1 \times 10^{-1} \text{M}$ at 110° ; (b) at $1 \times 10^{-2} \text{M}$ at 70° in the presence of nickel dithiolates ($8 \times 10^{-4} \text{M}$) and the associated decay of the nickel dithiolate UV-absorbance (in b). (The inset in (b) shows first order kinetic plots for the same reaction of NiDBP.)

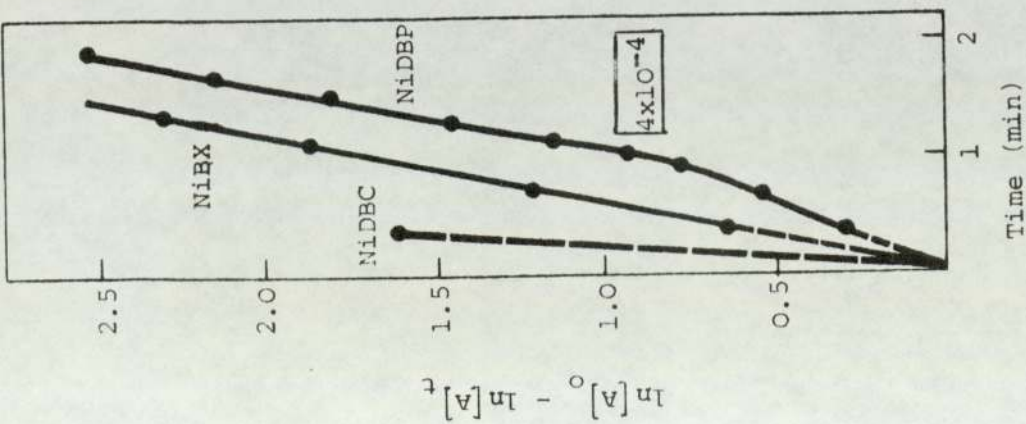


Fig. 7.5c First order decay of nickel dithiolates in the presence of CHP (1×10^{-1}) in heptane at 700 at different additive concentrations (shown in rectangles).

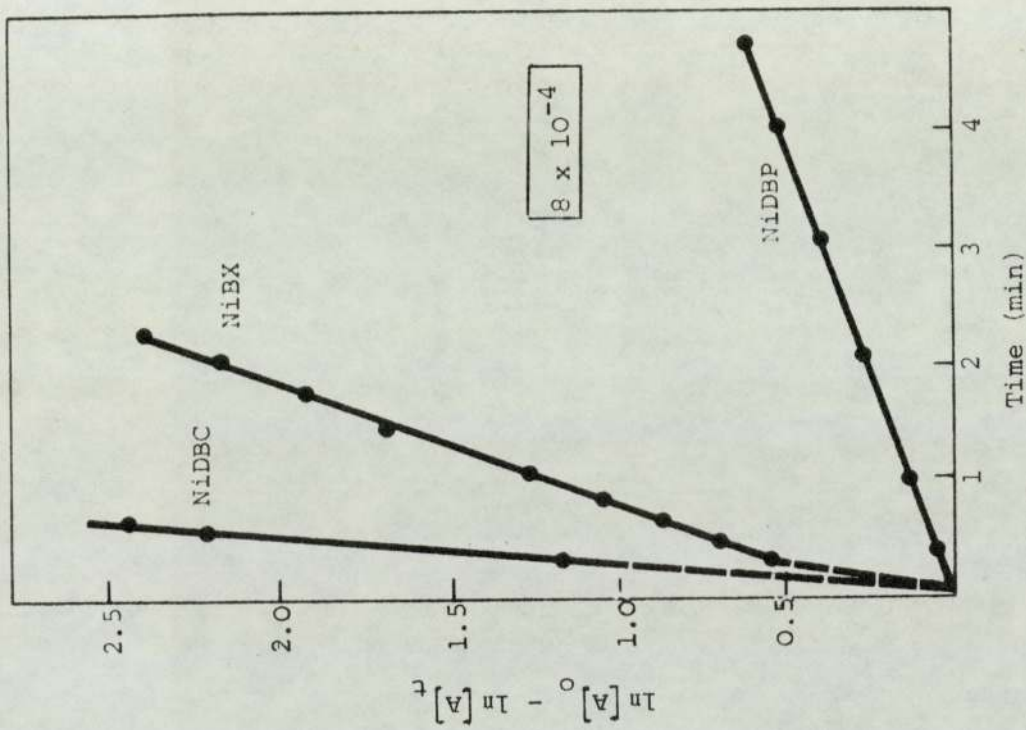
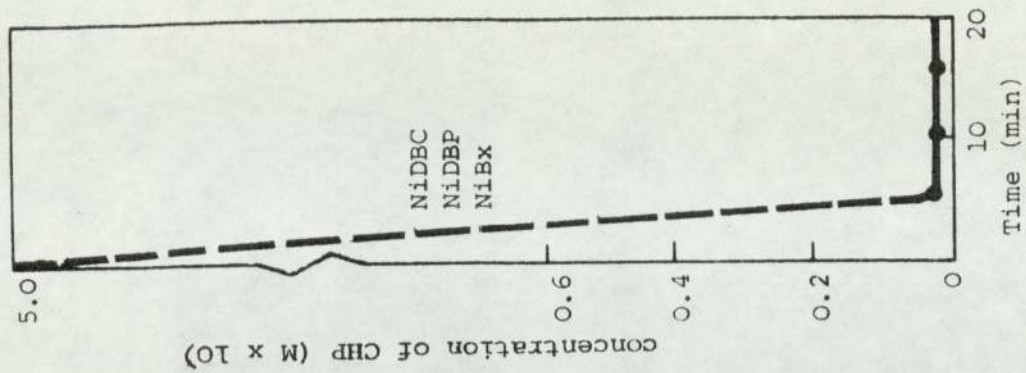


Fig. 7.6 Decomposition of CHP ($5 \times 10^{-1} M$) in the presence of NiDBC, NiDBP, NiBX (2×10^{-3}) in chlorobenzene at 110



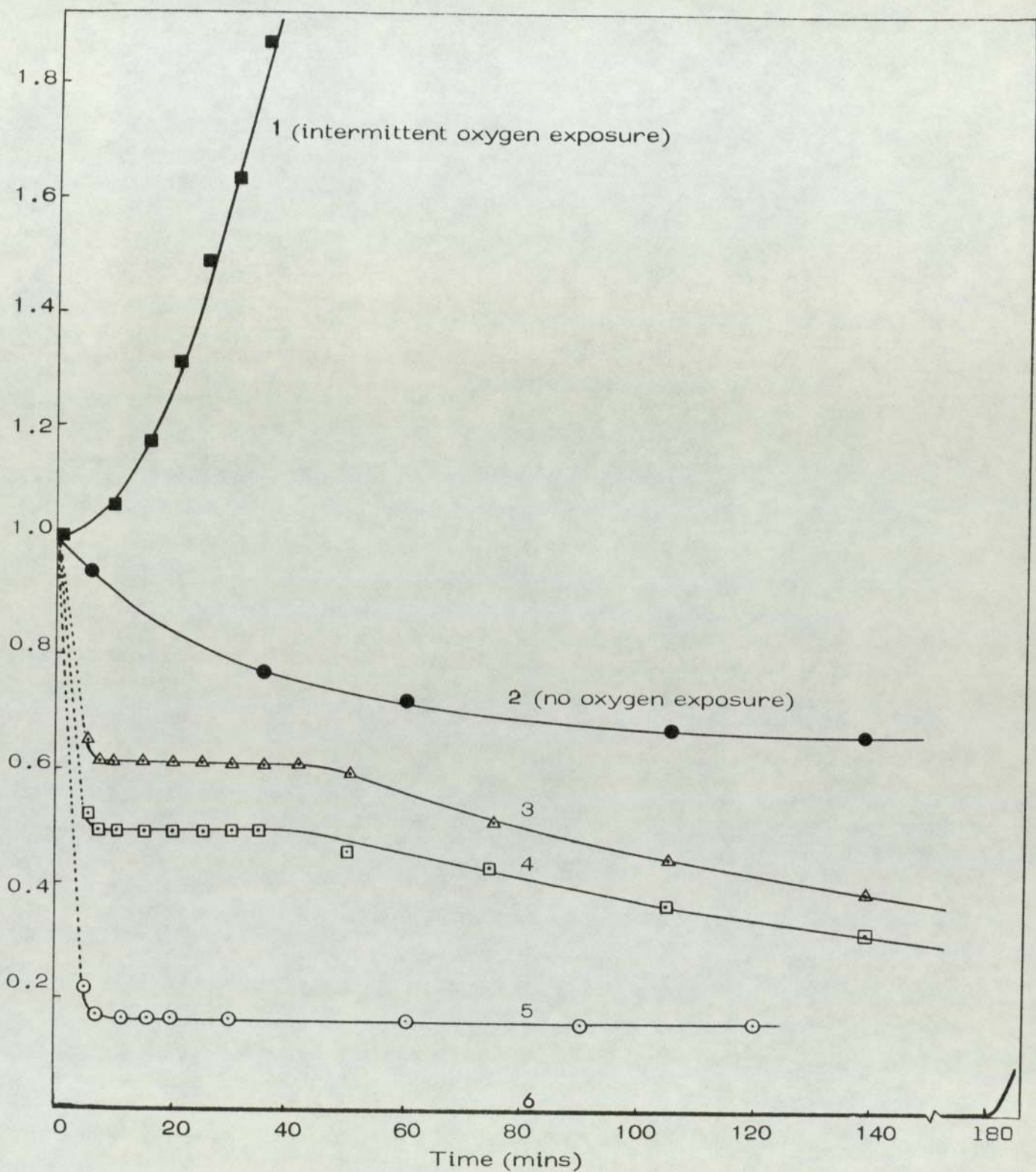


Fig. 7.7 Change in CHP concentration ($1 \times 10^{-2} \text{M}$) in dodecane at 150° , 1. intermittent O_2 exposure, no additive; 2. no O_2 exposure, no additive; 3. NiDBP (1×10^{-4}); 4. NiDBP ($2 \times 10^{-4} \text{M}$); 5. NiDBP ($10 \times 10^{-4} \text{M}$); 6. Blank run [no added CHP].

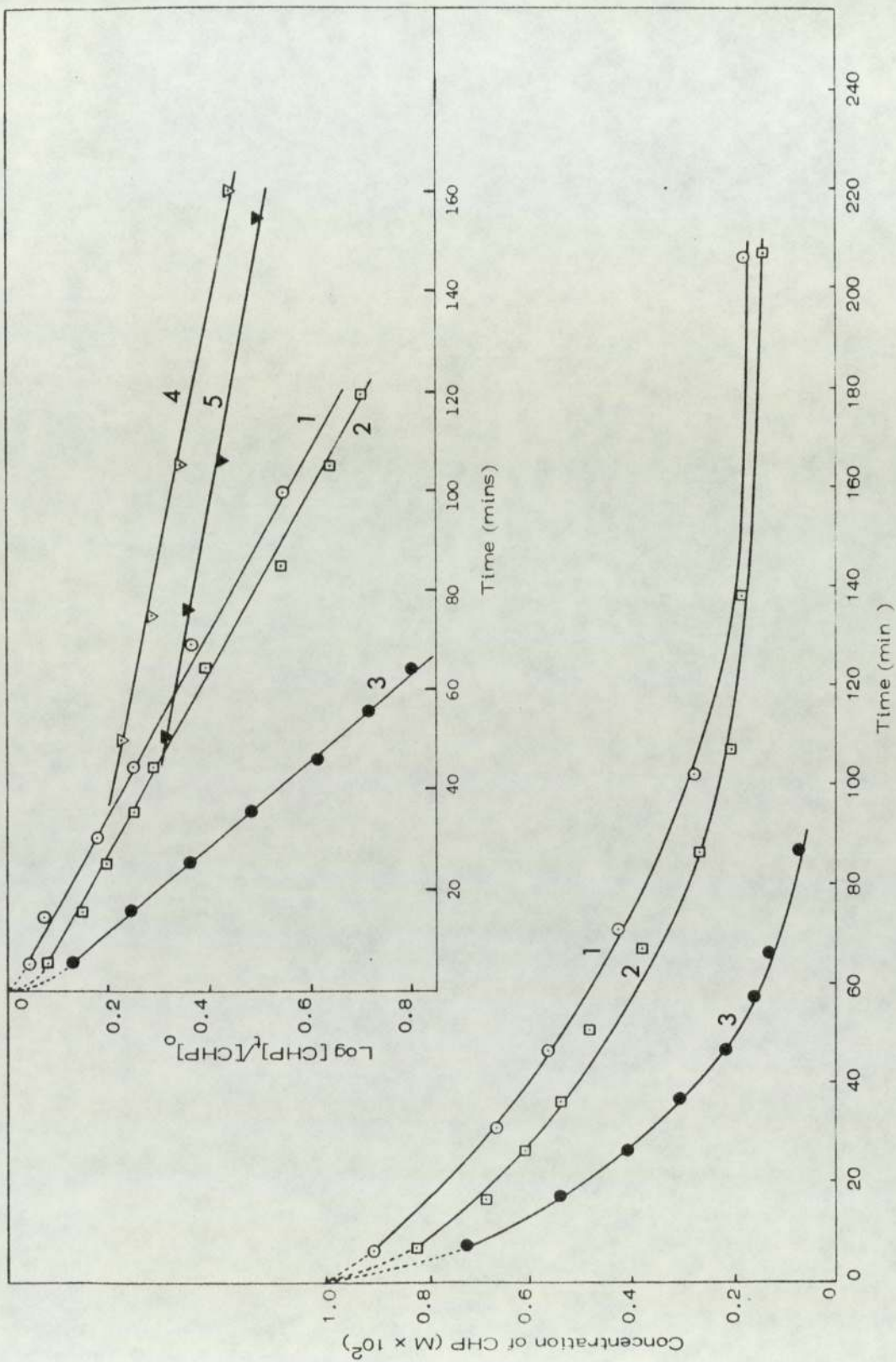


Fig. 7.8 Decomposition of CHP ($1 \times 10^{-2} M$) in dodecane at 150° in the presence of DiPDiS at the molar concentrations indicated below. [Inset compares first order kinetics for the reactions of DiPDiS and NiDBP with CHP under identical conditions. The plots for NiDBP are those obtained from the third stage of the reaction]. 1. DiPDiS ($1 \times 10^{-4} M$); 2. DiPDiS ($2 \times 10^{-4} M$); 3. DiPDiS ($10 \times 10^{-4} M$); 4. NiDBP ($1 \times 10^{-4} M$); 5. NiDBP ($2 \times 10^{-4} M$).

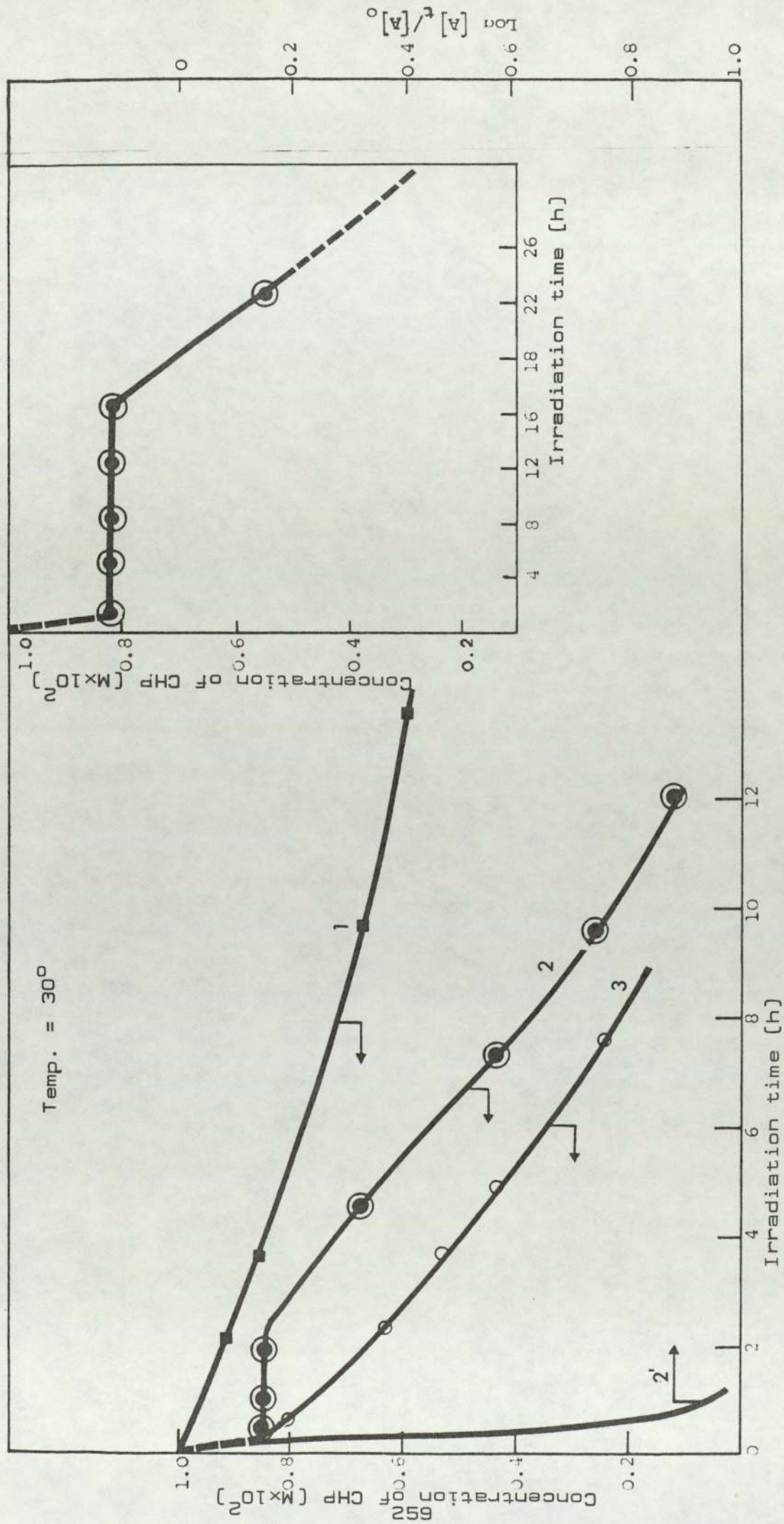


Fig. 7.9 Decomposition of CHP ($1 \times 10^{-2} \text{M}$) in chlorobenzene in the absence of additives (1) and by NiDBP (2) and DiPDiS (3) in the presence of light, and the associated decay of the NiDBP UV-absorbance (2'). The inset shows the decomposition of CHP ($1 \times 10^{-2} \text{M}$) in 4 -dodecane by NiDBP in the presence of light. Concentration of the additives $1 \times 10^{-4} \text{M}$.

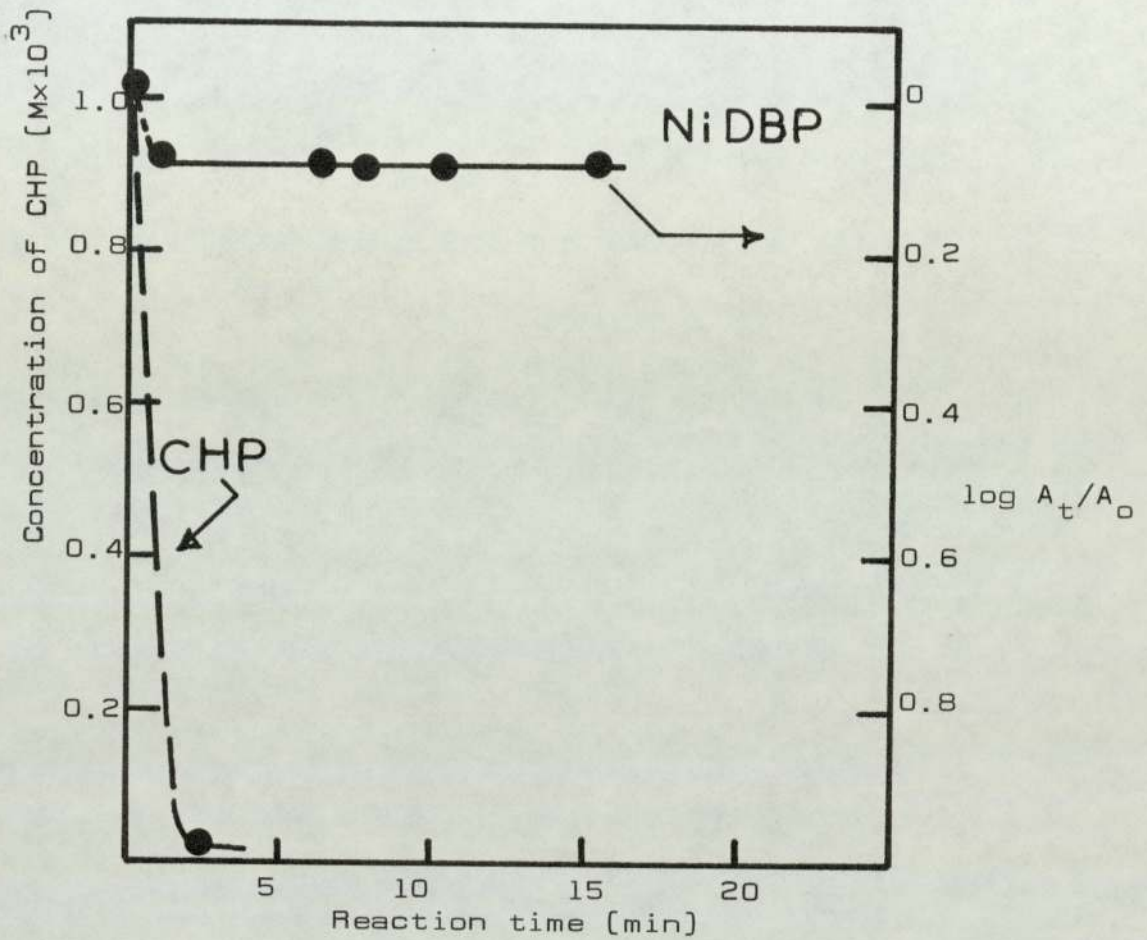


Fig. 7.10 Decomposition of CHP (1×10^{-3} M) in the presence of NiDBP (1×10^{-1} M) in chlorobenzene when irradiated with UV-light. Kinetic of disappearance of 316 nm of NiDBP under the same conditions is also shown.

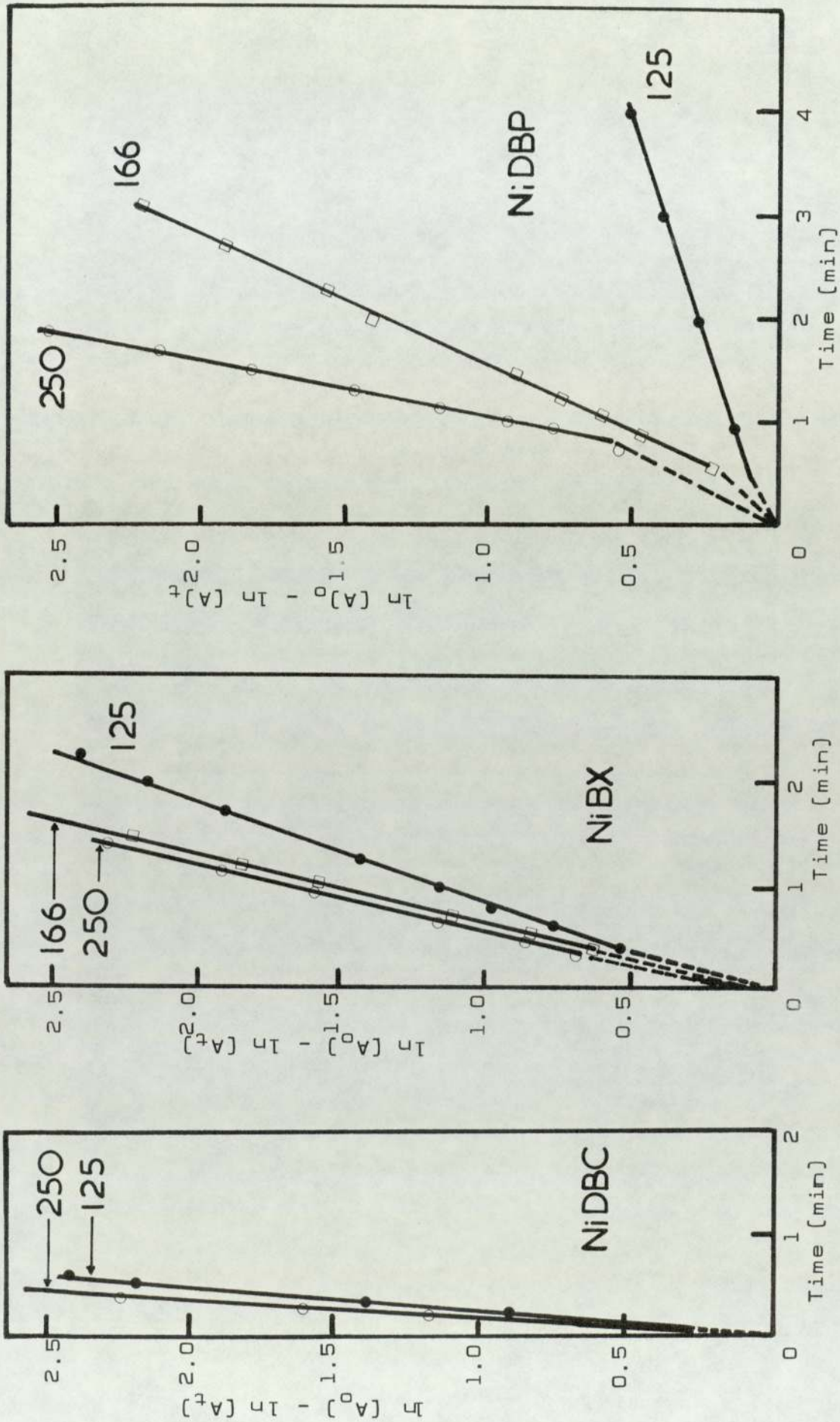


Fig. 7.11 First order plots for the decay of Ni dithiolates (at different molar concentration) in heptane at 70° in the presence of CHP (1×10^{-2}). Numbers on curves are ratios of CHP/additive.

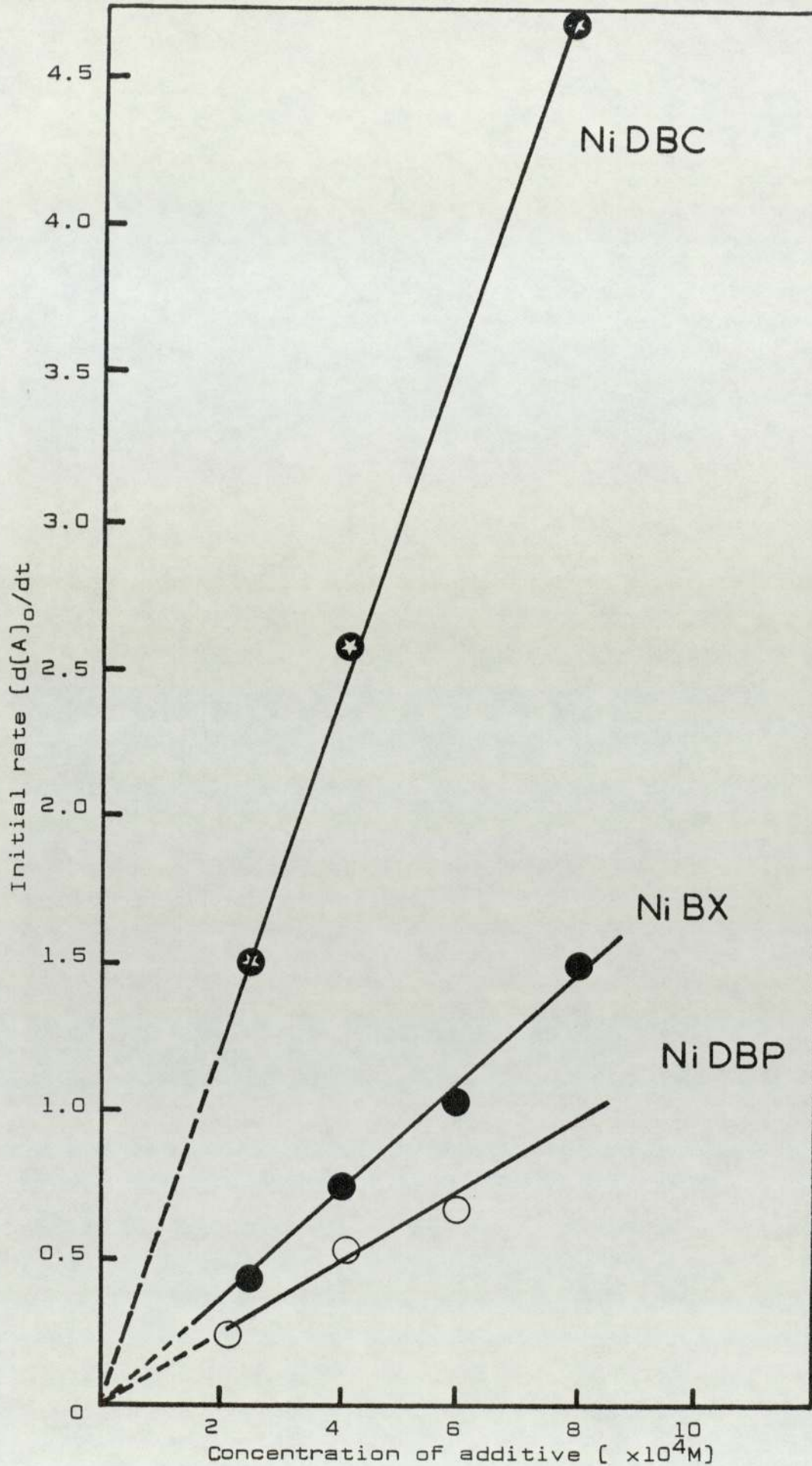


Fig. 7.12 Initial rate of disappearance of 316 nm [NiDBP, NiBX] and 325 nm [NiDBC] over a wide range of concentrations during the reaction of nickel dithiolates with CHP ($1 \times 10^{-1} M$) at 70° in dodecane.

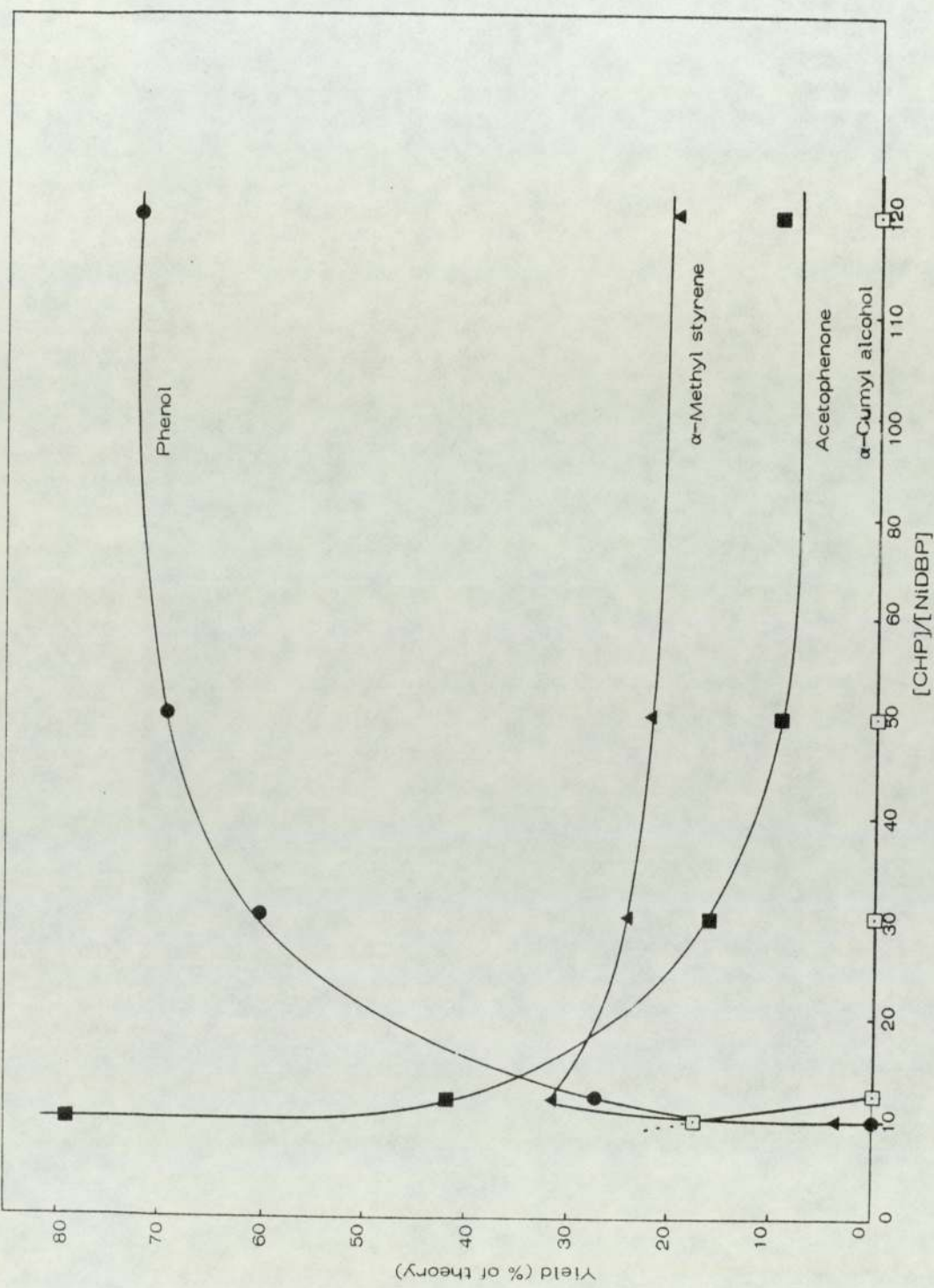


Fig. 7.13 Product yields after reaction of NiDBP with CHP at 110° in chlorobenzene at various molar ratios [CHP]/[NiDBP].

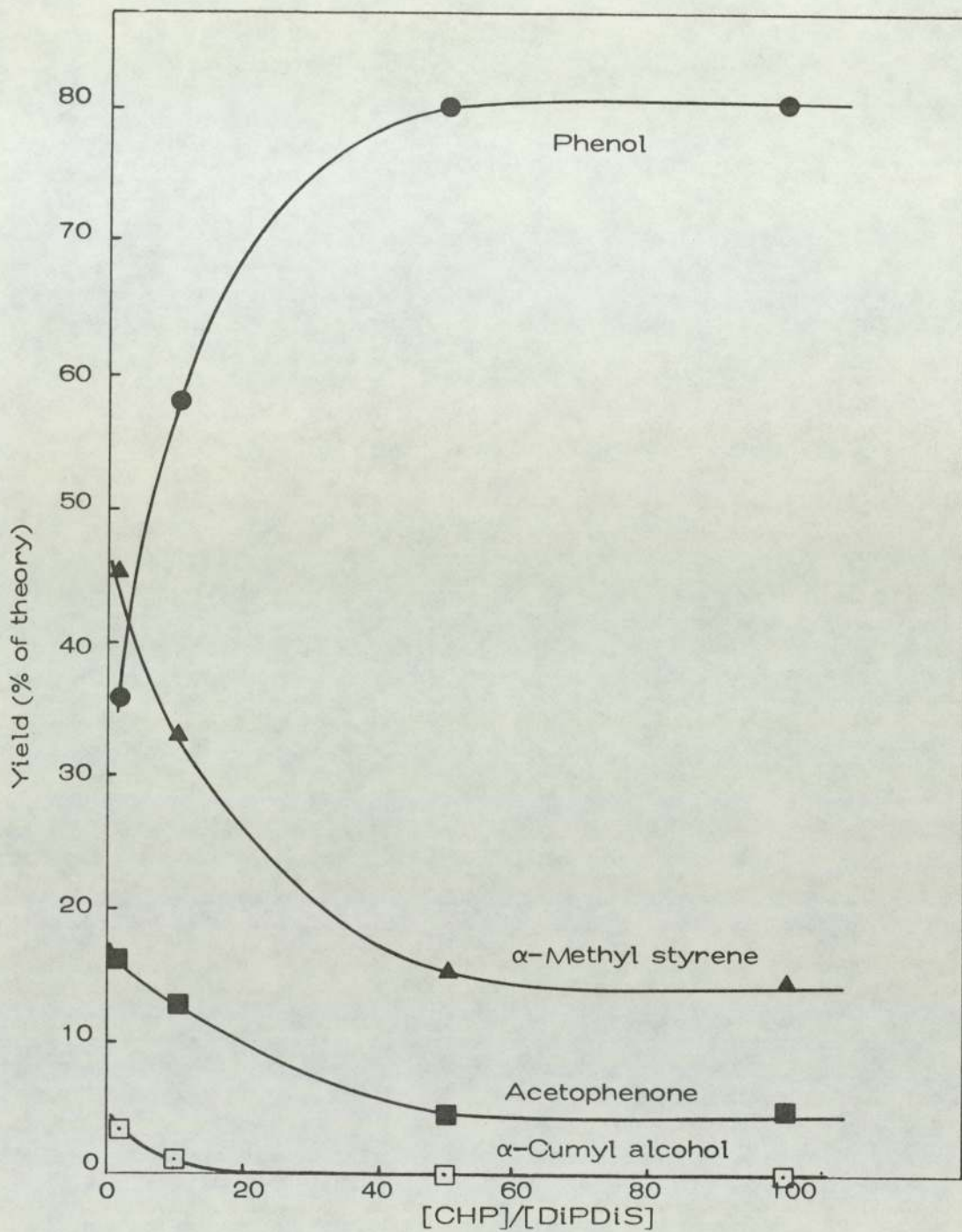


Fig. 7.14 Product yields after complete reactions of DiPDiS with CHP at 110° in chlorobenzene at various molar ratios [CHP]/[DiPDiS].

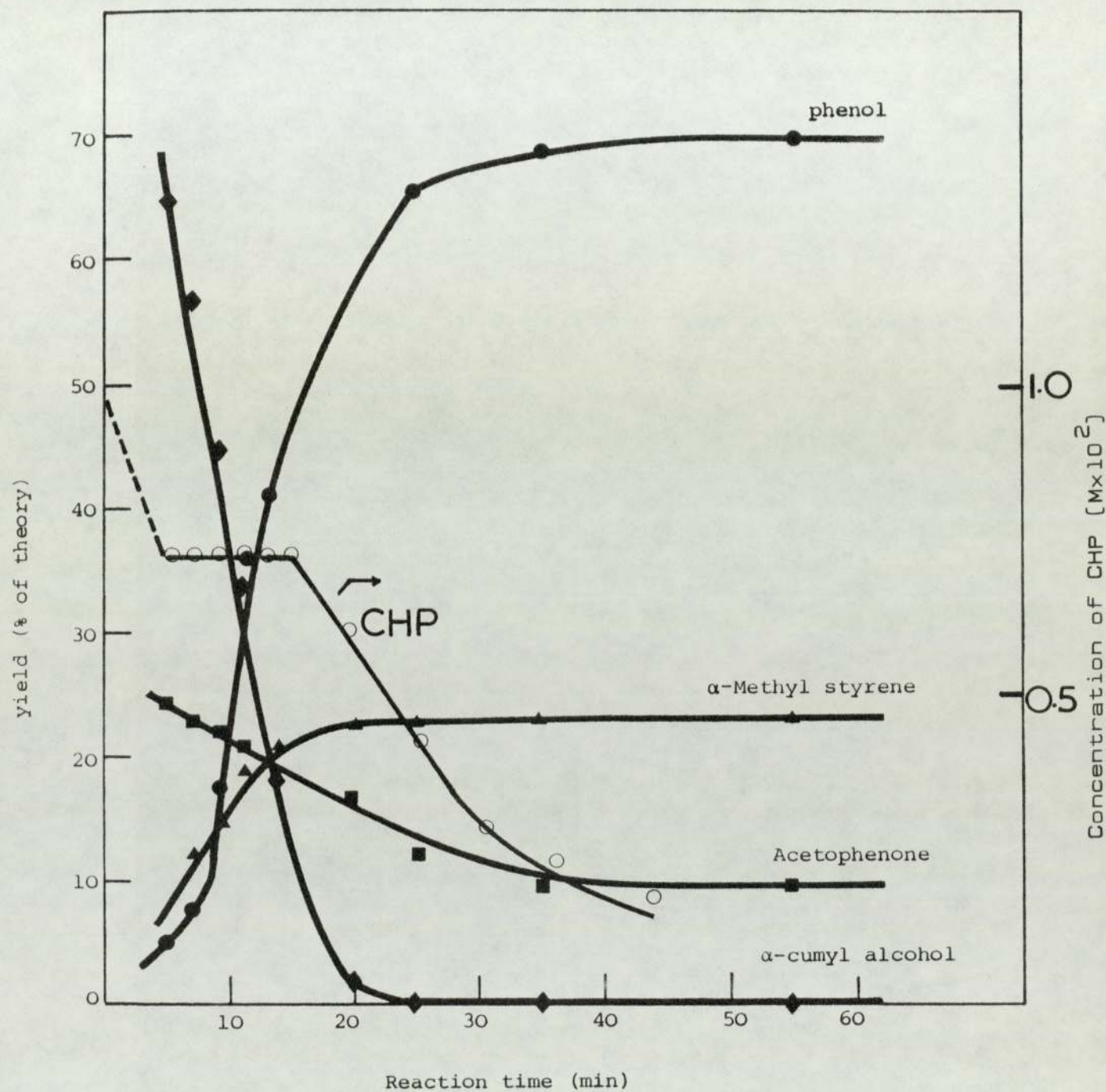


Fig. 7.15 Kinetics of alternative ionic and radical product from the reaction of CHP ($1 \times 10^{-2} \text{M}$) and NiDBP ($1 \times 10^{-4} \text{M}$) in chlorobenzene at 110° . CHP decomposition curve for the same reaction is also shown.

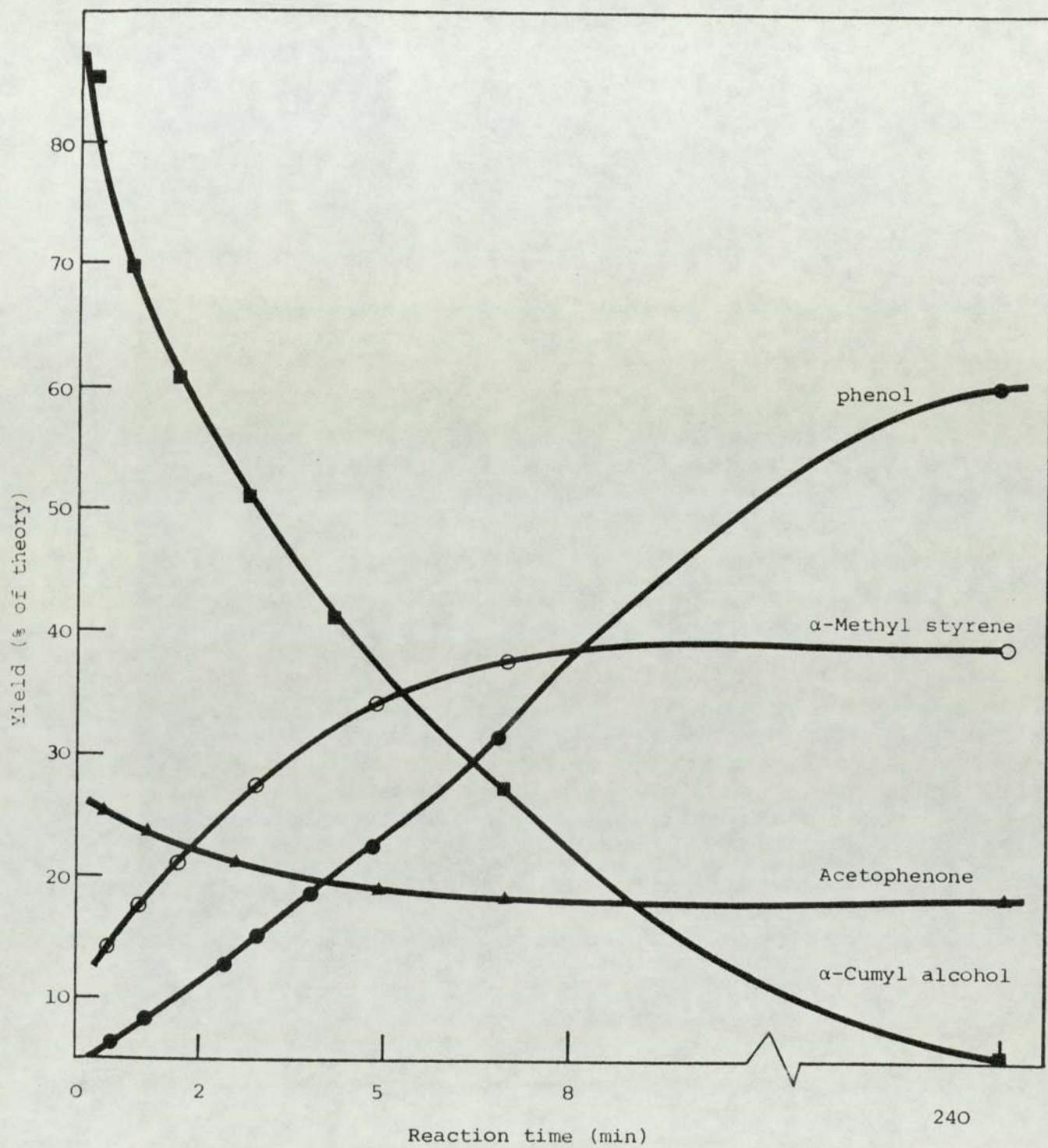


Fig. 7.16 Kinetics of alternative ionic and radical product formation from the reaction of CHP ($5 \times 10^{-1} \text{M}$) and NiDBP ($1 \times 10^{-2} \text{M}$) in chlorobenzene at 110° .

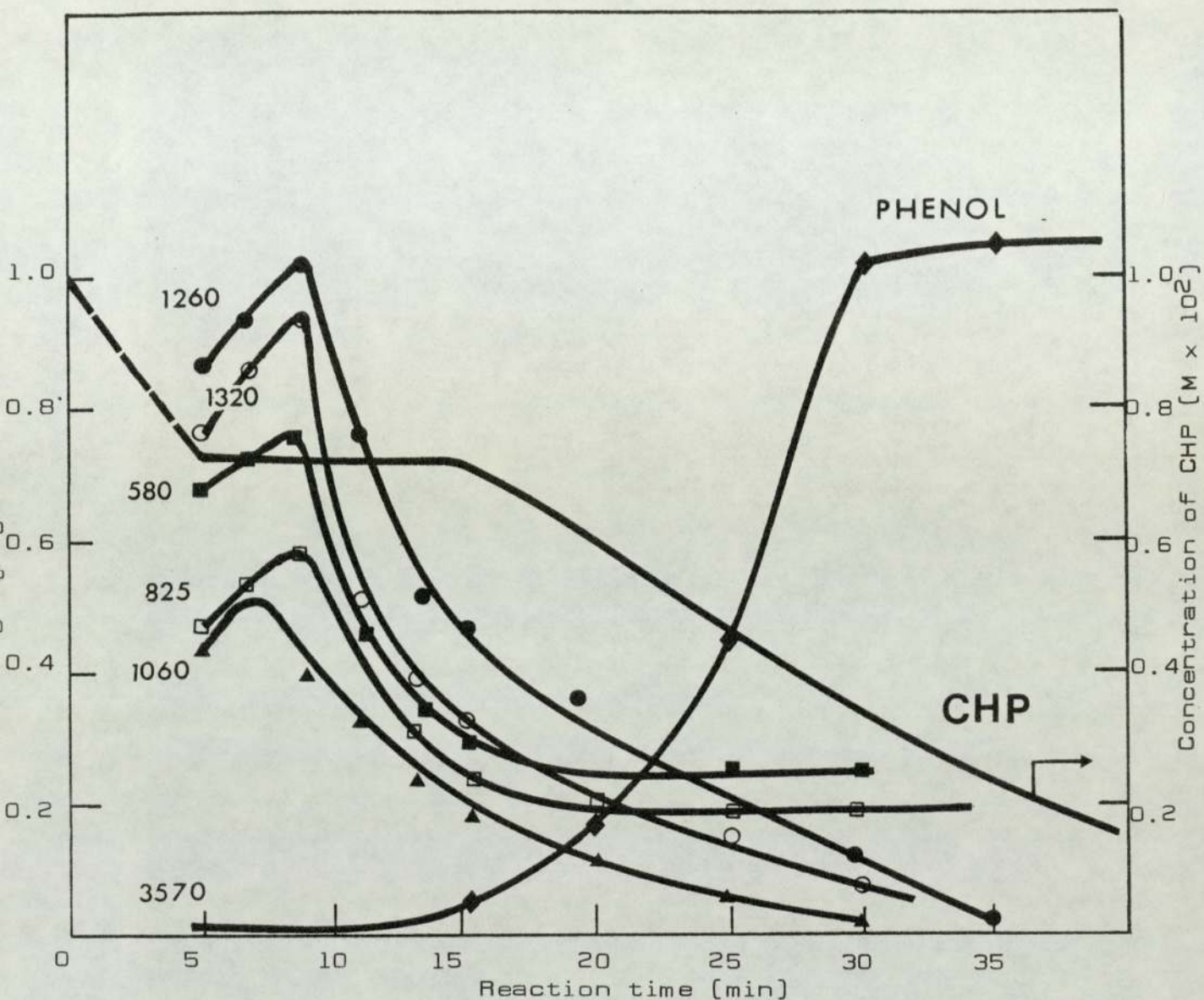


Fig.7.17

Kinetics of product formation as determined by following characteristic IR-absorptions for the reaction of CHP ($1 \times 10^{-2} \text{M}$) and NiDBP ($1 \times 10^{-4} \text{M}$) in chlorobenzene at 110° . Vibrational frequencies shown on curves refer to, O-SO₂- (1260, 1320 cm^{-1}), P-OH of P^S_{OH} (580, 825 cm^{-1}), >S=O (1060 cm^{-1}) and O-H of phenol (3570 cm^{-1}). Decomposition of the hydroperoxide in this reaction is also shown (CHP).

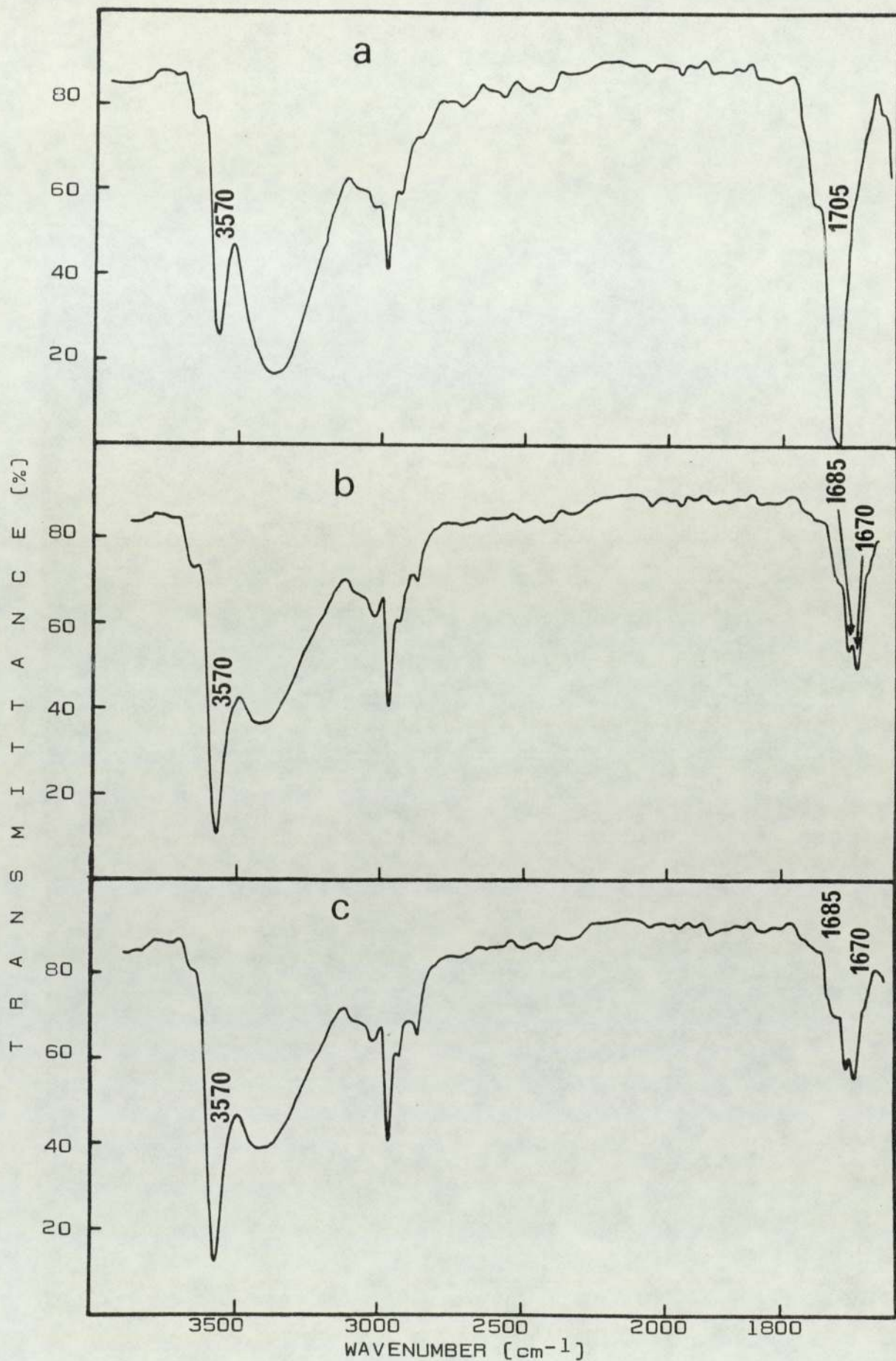


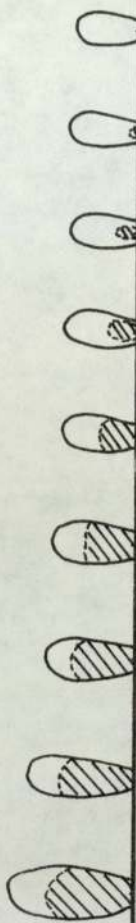
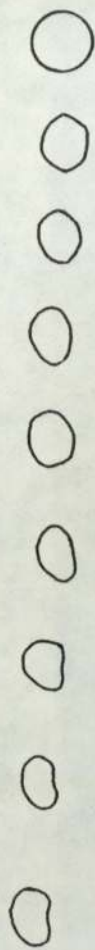
Fig.7.18 Infrared spectra of products formed from the reaction of CHP (5×10^{-1}) with [a] NiDBP ($2 \times 10^{-3}M$) at room temperature, [b] NiDBP ($2 \times 10^{-3}M$) in chlorobenzene at 110° and [c] NiDBC ($2 \times 10^{-3}M$) in chlorobenzene at 110° .

solvent front
 α -Me styrene
 DiPDiS

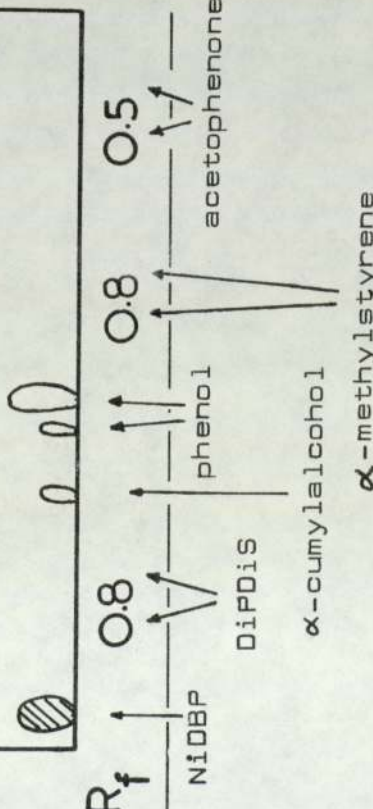
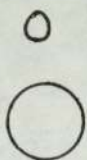
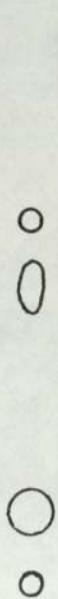
acetophenone

phenol
 NiDBP (shaded)

reaction time (min)



0.5 1 1.5 2.5 3 4 5 7 ∞



R_f 0.8 0.8 0.8 0.5

NiDBP DiPDiS α -cumylalcohol phenol acetophenone

α -methylstyrene

Figure 7.19 TLC run of authentic compounds in chloro-benzene

Figure 7.20 Products from the reaction of CHP (5×10^{-1} M) with NiDBP (1×10^{-2} M) at 110° in chlorobenzene

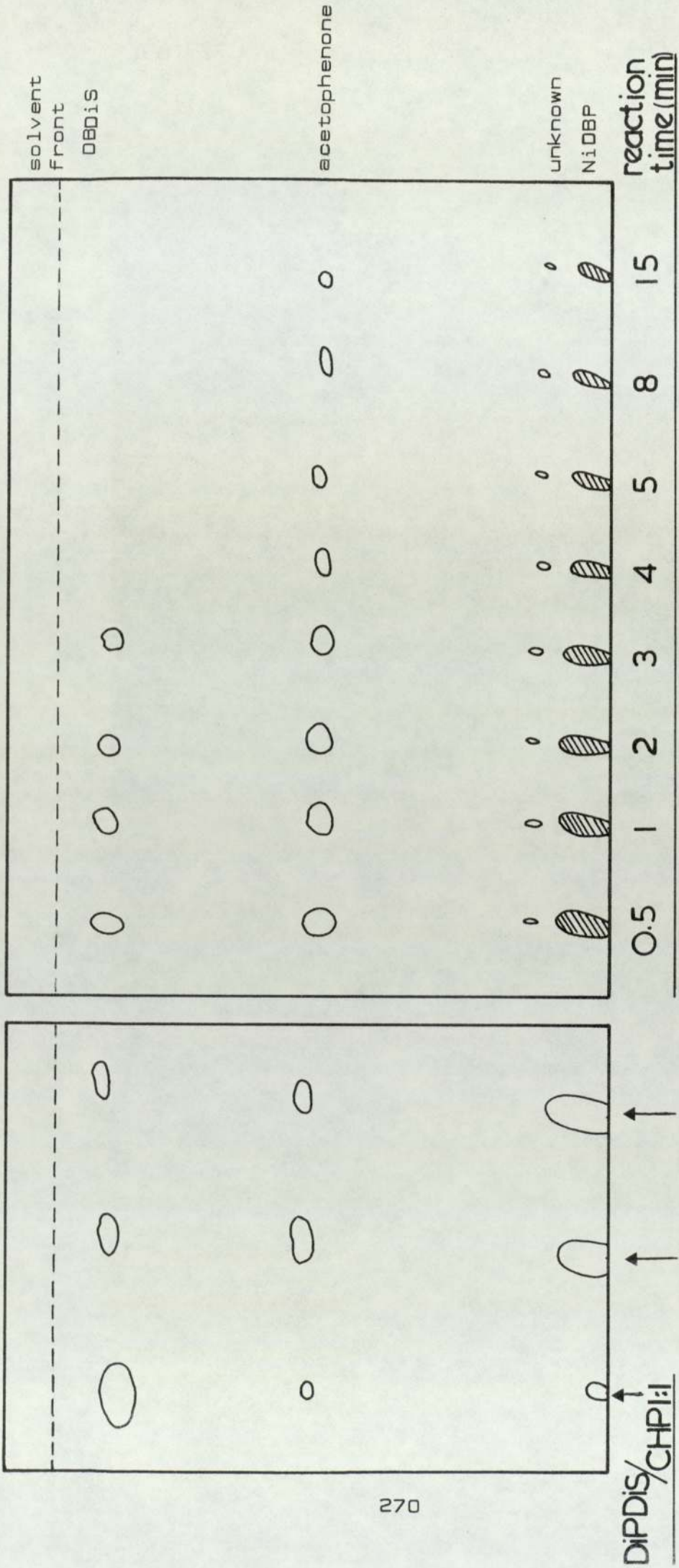


Figure 7.21 Products from the reaction of DiPDiS ($1 \times 10^{-2} M$) with CHP (1×10^{-2}) under N₂ and for NiDBP ($2 \times 10^{-3} M$) with CHP ($5 \times 10^{-1} M$) under N₂ and O₂ atmospheres.

Figure 7.22 Intermediate products from NiDBP ($1 \times 10^{-2} M$) induced decomposition of CHP ($1 \times 10^{-2} M$) at 110° under N₂ during the first fifteen minutes of the reaction.

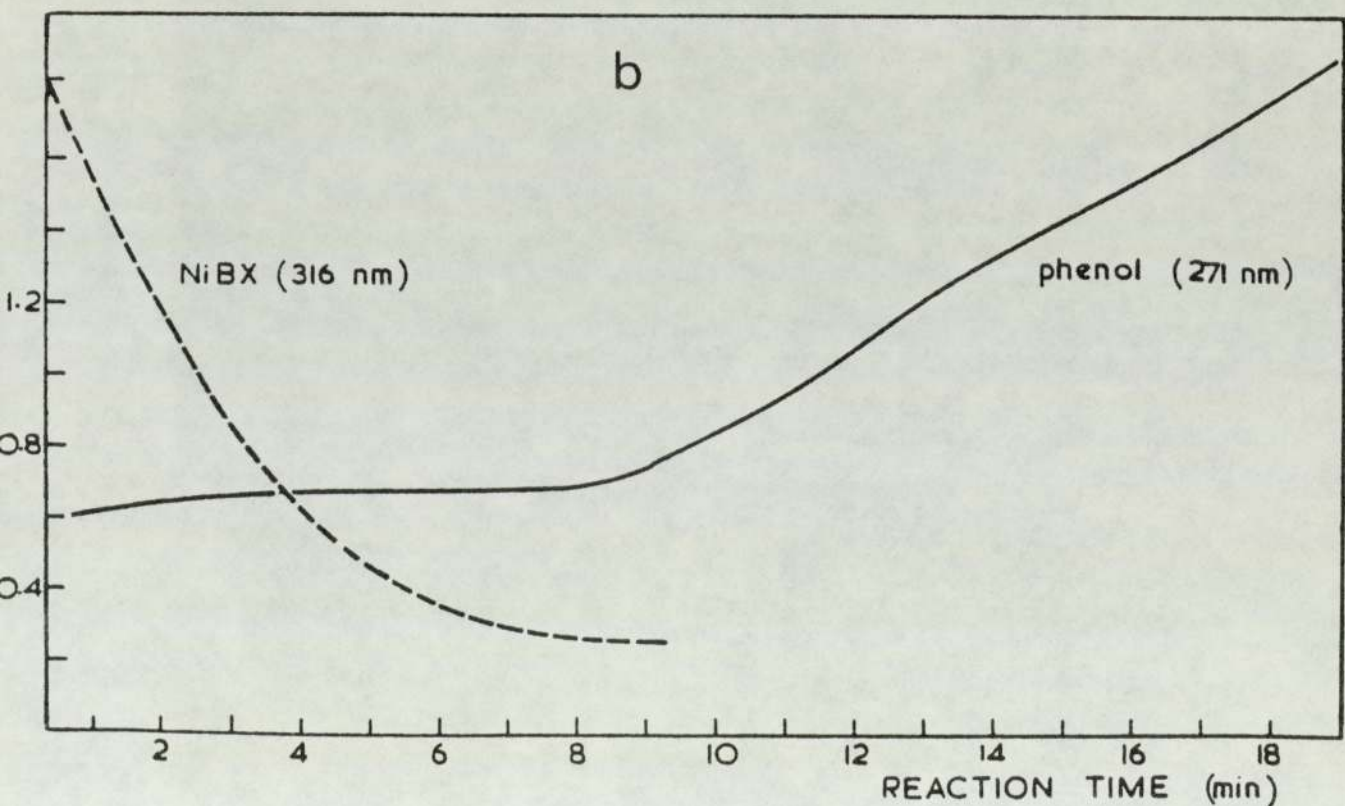
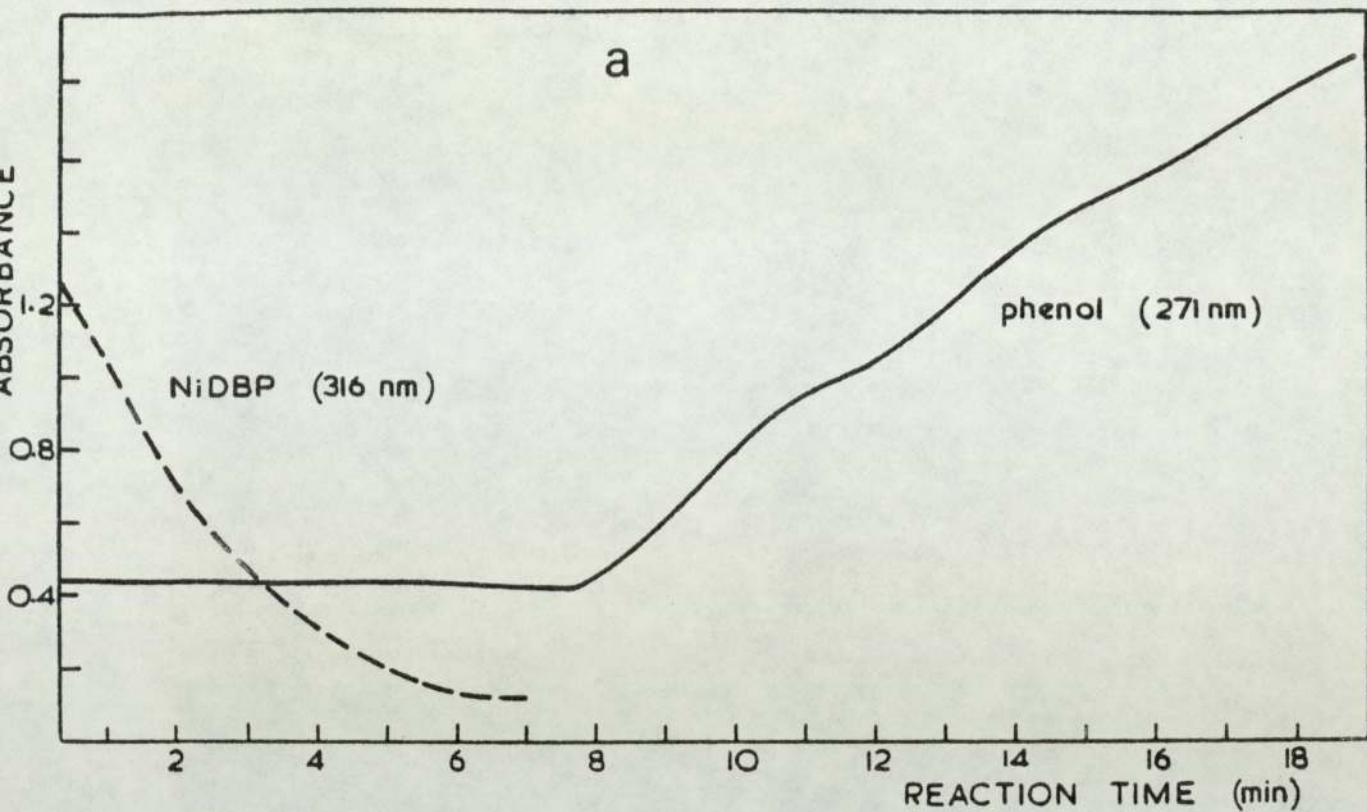


Fig. 7.23 Kinetics of disappearance of NiDBP [a] and NiBX [b], and appearance of phenol, during reaction of the nickel complex [$6 \times 10^{-4} \text{M}$] with CHP [$3 \times 10^{-2} \text{M}$] in dodecane at 70° .

C O N C L U S I O N S

1. Nickel complexes of dithiophosphoric and xanthic acids, NiDRP and NiRX, were found to be efficient UV-stabilisers for both LDPE and PP. For example, NiDRP (ca.0.1%) was shown to be superior to any known commercial single component stabiliser for PP.
2. NiDRP and NiRX were found to operate by virtually all the known mechanisms of antioxidant action in polyolefins. Further, it has been shown that none of the 'photophysical' processes, e.g. UV-absorption and screening, excited state quenching, effect of singlet oxygen, are capable of explaining the high activity associated with this class of stabilisers. The secondary role of 'photophysical' processes in effecting stabilisation has been suggested by other workers too.
3. Both hydroperoxide decomposition and free radical scavenging were found to make an important contribution to the stabilisation observed. This was verified under mild and severe processing conditions, where different levels of polymer hydroperoxide concentration would be expected in the absence of a stabiliser system.
4. Thiophosphoryl disulfide and xanthic acid disulfide [dixanthogen] have been shown to be very powerful thermal stabilisers for LDPE and PP. Although the nickel complexes of dithiophosphoric and xanthic acids were also found to impart extensive thermal stability

to the polyolefin matrix, their thermal antioxidant function is a consequence of their transformation products [the corresponding disulfides].

5. The photostabilising action of both the nickel complexes and their corresponding disulfides in LDPE and PP has been shown to be a function of processing conditions. In the case of the disulfide, increasing processing severity was marked by improved photostability of the polymer matrix; the opposite effect was found in the case of the nickel complexes.
6. The oxidation products [i.e. transformation products] of nickel dithiolates were found to be bound, mainly during the processing operation, to the polymer substrate. This was further verified from the similar thermal- and photo-oxidative behaviour observed for nickel dithiolate-stabilised PE films from which the metal complex was completely removed by solvent extraction to that of PE films stabilised by the corresponding disulfides.
7. The disulfides were found to possess excellent peroxidolytic ability and, to a certain extent, UV-stabiliser activity even though they do not meet the normally accepted requirement of a UV-stabiliser, i.e. UV-absorption in the region of the harmful solar UV-radiation. Furthermore, the antioxidant/photo-stabilising activity of the disulfide was found to increase the more severe the processing operation.

8. Effective protection of the disulfides, or their oxidation products, from UV-light can enhance further their stabilising effectiveness. In addition to the excellent thermal stabilisation they impart to polyolefins, disulfides compounded in PP and PE in the presence of HOBP, conferred a high level of UV-stability in these substrates.
9. NiDRP and NiRX (R=Butyl) appear to be ideal multi-purpose antioxidants with the additional advantage over the analogous complexes of dithiocarbamates of giving almost colourless films in both PE and PP substrates when used at the same molar concentrations. These complexes are easy to prepare from cheap starting materials.
10. Studies conducted on severely processed master-batches have indicated the suitability of NiDRP and its corresponding disulfide for adaptation for large-scale industrial operations and practice.
11. The mechanism of antioxidant action of these sulfur-containing compounds was verified from studies on model compounds. It has been shown that
 - a. NiDRP and NiRX operate by both hydroperoxide decomposition and free radical scavenging modes.
 - b. The nickel complexes themselves are mainly responsible for the free radical scavenging step while their transformation products (the derived disulfides and/or their oxidation products) are

mainly responsible for the catalytic non-radical decomposition of hydroperoxides.

- c. The relative importance of the radical process decreases with increasing hydroperoxide/anti-oxidant ratio. Thus at high ratios it was established that the contribution of radical processes toward the overall decomposition of hydroperoxides is small.

- d. Thiophosphoryl disulfide was found to decompose hydroperoxides catalytically to non-radical products at almost all hydroperoxide/disulfide molar ratios. The contribution of the free radical scavenging step was found to be quite small.

S U G G E S T I O N F O R

F U R T H E R W O R K

1. A systematic study on the antioxidant modes of action of sulfur-containing compounds in extruded polyolefin films. The preponderance of alkyl radicals under the operating conditions of an extruder can be utilised to test the radical scavenging mechanism proposed here for these compounds by study of melt flow index change in the presence of disulfides and their oxidation products.
2. The commercial UV-stabiliser, HOBP, was shown here to synergise the photo-stabiliser effectiveness of NiDRP and NiRX. In order to exploit the full potential of these synergistic combinations, further investigations are needed to arrive at optimum combination ratios for the appropriate processing conditions.
3. Incorporation of HOBP or hindered phenols (as part of the alkyl substituent groups) in the nickel complexes of dithiophosphoric and xanthic acids, and their corresponding disulfides, could provide a single component internally-synergised, antioxidant system. An advantage of this system is that the light stabiliser moiety, HOBP, present in this case as an integral part of an effective antioxidant system, is better protected against the deleterious effects of processing. Furthermore, the problem of the physical loss of phenolic stabilisers from the polymer may also be avoided.

4. It was shown that in the presence of DiPDiS and HOBP PE masterbatches exhibited excellent photo- and thermo-oxidative stabilities which were later shown to be due to a product of a transesterification reaction between HOBP and DiPDiS. It was further found that the problem of blooming of HOBP when prepared in an LDPE masterbatch [i.e. concentration 2.5%] had been surmounted. Reaction of DiPDiS, for example, with other commercially available phenolic antioxidants warrants further investigation.

5. Compatability and volatility of stabilisers during processing and subsequent in-service conditions of polymer articles have important consequences for their effectiveness and suitability in the longevity and performance of the host polymer material.

Although losses by means of chemical reactions and transformations of stabilisers used in this study account for much of the losses observed during the compounding of the polymer, a quantitative evaluation of the extent of stabiliser losses [by physical and chemical processes] from polymer films and from the neat stabiliser systems would provide valuable information in the design of a new stabiliser system.

6. The antioxidant function of the dithiolates used in this study was evaluated in polyethylene and polypropylene. Because of the good radical scavenging and hydroperoxide decomposing properties observed, extension of their use in

other polymers in which both these processes are important degradative routes is justified, e.g. PVC, ABS, and rubber.

7. Tests carried out in this study were concerned with chemical changes occurring during processing and subsequent heat ageing and UV-exposure of films.

A further evaluation of the antioxidant activity of the dithiolates is needed in which the mechanical properties of test specimens are investigated, and correlations made with these chemical findings.

Furthermore, outdoor weatherability tests of the dithiolate-stabilised polymer should be undertaken.

For practical purposes, a systematic study on the photo-oxidative stability of dithiolate-stabilised polyolefin articles under stress is required to enable an accurate prediction of their usable lifetime under similar service conditions.

8. The extent of binding of the antioxidant moieties during the processing of dithiolates in PE and PP is crucial to their role as stabilisers and to their effectiveness for long-term performance of the stabilised polymer. A quantitative study of the degree of binding achieved with the various sulfur-containing compounds used in this work will provide additional insight into their modes of antioxidant action. The exact nature of the bound moiety should be further examined to elucidate the mechanism of binding.

9. Since oxygen [or hydroperoxide] is an important factor which controls the effectiveness of disulfides in the stabilisation of LDPE films, an examination of the effect of added hydroperoxides during processing [e.g. masterbatches] is not inappropriate. The added hydroperoxide is expected to reduce the need for long processing time which would normally be required to regenerate a greater amount of the oxidised sulfur-centred radicals which are crucial for stabilisation. Furthermore, a synergist which is adversely effected by oxygen [or hydroperoxides] can be added later with minimum processing.
10. Synthesis of oxidation products of the different sulfur-containing compounds used in this study may provide unequivocal proof for the mechanism of action of those sulfur-containing stabilisers proposed on the basis of the present study.
11. The regenerative process proposed for PP and PE can be examined further. Chemical evidence of the amount of unsaturation present in PP and PE can substantiate further the mode of action proposed for the various sulfur-containing stabilisers examined here.

A P P E N D I X
P U B L I S H E D W O R K

MECHANISMS OF ANTIOXIDANT ACTION: TRANSFORMATIONS INVOLVED IN THE ANTIOXIDANT FUNCTION OF THE NICKEL DITHIOLATES

S. AL-MALAIKA and G. SCOTT

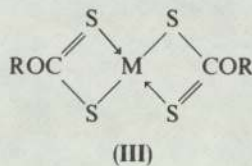
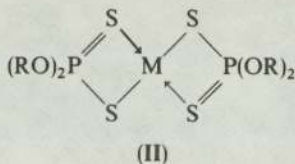
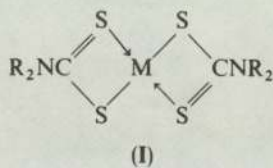
Department of Chemistry, University of Aston in Birmingham,
Gosta Green, Birmingham, B4 7ET, England

(Received 13 November 1979)

Abstract—The mechanism of the antioxidant function of the nickel *O,O*-dialkyl dithiophosphates is examined in relation to that of related nickel dithiolates. A common mechanistic pathway is identified and evidence is presented to suggest that two distinct catalytic processes are involved, the first involving homolytic peroxide breakdown and the second an ionic process. It is proposed that the initial stage of the reaction leads to the formation of the corresponding disulphides which then undergo further oxidation to sulphur acids which are responsible for the ionic catalytic decomposition of hydroperoxides and the dehydration of derived alcohols.

INTRODUCTION

Several classes of metal dithiolate complexes with powerful peroxide decomposing (PD) antioxidant properties are known; among the more important are the dithiocarbamates (I), the dithiophosphates (II) and the xanthates (III), all of which have found practical utility as antioxidants in a variety of polymers and hydrocarbon substrates [1].



It was established many years ago [2] that all three classes of compounds had a common mechanism of action which was shown to be the catalytic ionic decomposition of hydroperoxides by a product or products formed from them. The antioxidant stage was shown to be preceded by a radical generating pro-oxidant step the importance of which was

strongly dependent on the ratio of hydroperoxide to metal dithiolate.

Subsequent studies by Howard and co-workers [3,4] of the antioxidant action of the dithiophosphates cast doubt on the importance of heterolytic decomposition of hydroperoxides as the primary mechanism involved. These workers followed the very rapid homolytic decomposition of hydroperoxides by a stopped-flow technique over the temperature range 30–50° and concluded that this process was responsible for the antioxidant function of the transition metal dithiophosphates. Analogous investigations into the mechanism of the dithiocarbamates [3,4] has led to similar conclusions. There can be no doubt about the relevance of the radical generation stage to the overall mechanism of action of all the metal dithiolates but the question of its importance relative to the ionic peroxide decomposition under practical conditions remains to be answered. The purpose of this and subsequent communications is to show that the antioxidant behaviours of the three classes of nickel dithiolate (I–III) are essentially similar. The present study will examine the antioxidant mechanism of the dithiophosphates (II) in some detail.

EXPERIMENTAL

Materials

Nickel-*O,O*-dibutyl dithiophosphate (NiDBP), diisopropyl-dithiophosphoryl disulphide (DiPDiS, IV), and nickel butyl xanthate (NiBX) were prepared by the methods of Jorgenson [5], Mikeska [6] and Watt [7] respectively. Nickel dibutyl dithiocarbamate (NiDBC) was prepared by double decomposition of a 10% solution of the corresponding sodium salt (ex Robinson Brothers) with a saturated solution of the transition metal sulphate. Stabilized cumene hydroperoxide (CHP, ex BDH) was purified via its sodium salt by the method of Kharasch [8]. Puris grade chlorobenzene and dodecane (Koch-Light) were used without further purification.

TECHNIQUES

Thermal decomposition of CHP

In a specially designed reaction cell fitted with a condenser, chlorobenzene or dodecane was introduced and allowed to equilibrate for 5 min in a thermostatted oil bath ($\pm 0.5^\circ$). An amount of CHP was added and allowed a further 5 min to equilibrate under slow steady stream of N_2 which ensures purging and efficient mixing of the mixture. The additive was introduced quickly and sampling of the reaction mixture was commenced 5 min later. Iodometric titration was used for following the CHP decomposition in the presence and absence of the antioxidant. This procedure proved a satisfactory method of analysis of CHP. Hydroperoxide disappearance was additionally followed by monitoring the band at 3520 cm^{-1} by i.r. spectrophotometry. A satisfactory correlation with the results of iodometry emerged.

Kinetics of disappearance of NiDBP

Kinetic runs for the disappearance of NiDBP ($\lambda = 316\text{ nm}$) during the induced decomposition of CHP were carried out on a u.v./vis Unicam SP800 spectrophotometer with runs at 30 and 70° .

Product analysis

Products obtained from the thermal studies were analysed by GLC using Perkin-Elmer F30 chromatograph fitted with a flame ionization detector. Separation was best achieved by temperature programming and by use of a 2-m stainless-steel column packed with polyethylene glycol adipate on chromosorb W.

RESULTS

Comparison of nickel dithiolate complexes in the decomposition of cumene hydroperoxide

Figure 1 compares the behaviour of NiDBP, NiDBC and NiBX at equimolar concentrations in the catalytic decomposition of CHP at 110° . They all show the same general behaviour:

- (i) a rapid initial catalytic stage,
- (ii) a secondary induction period, leading into
- (iii) a slower first order catalytic reaction.

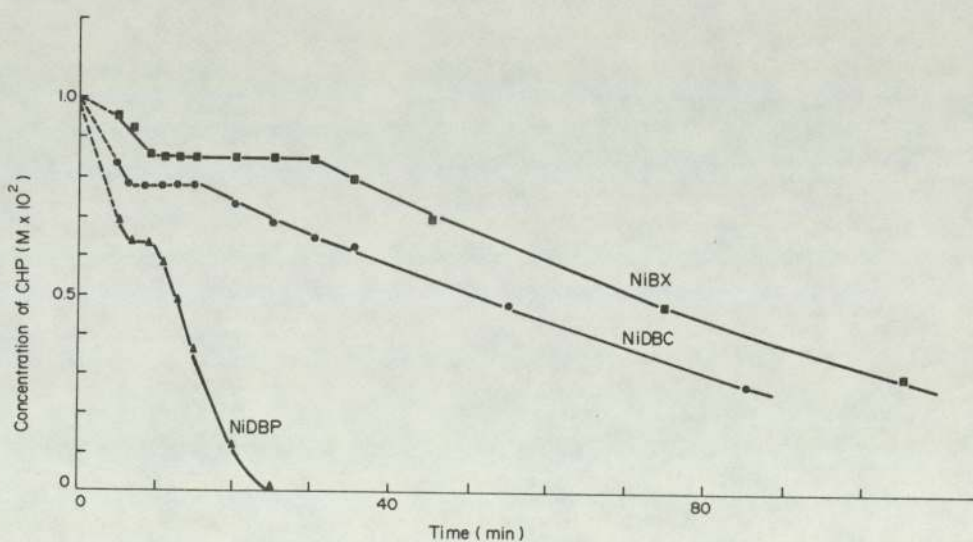


Fig. 1. Decomposition of CHP ($1 \times 10^{-2}\text{ M}$) in chlorobenzene at 110° in the presence of nickel dithiolates ($2 \times 10^{-4}\text{ M}$).

The first-order rate constants for the second catalytic stage are as follows:

$$\begin{aligned} \text{NiDBP, } &7.1 \times 10^{-2}\text{ sec}^{-1}; \\ \text{NiDBC, } &6.0 \times 10^{-3}\text{ sec}^{-1}; \\ \text{NiBX, } &6.1 \times 10^{-3}\text{ sec}^{-1}. \end{aligned}$$

It is clear from Fig. 1 that the secondary induction period reflects the formation of more stable products which are precursors of the second stage catalysts.

Reaction of NiDBP with CHP

Figure 2 compares the kinetics of the disappearance of CHP and NiDBP in chlorobenzene at 70° in the presence of a 125-fold excess of the former. It is clear that the metal complex was essentially destroyed before the second first-order catalytic stage commenced.

The effect of varying the concentration of NiDBP in the decomposition of a fixed concentration of CHP is shown in Fig. 3. At the highest molar concentration ($[\text{CHP}]/[\text{NiDBP}] = 500$), the decomposition does not achieve the second catalytic stage within the duration of the experiment and at the lowest ($[\text{CHP}]/[\text{NiDBP}] = 1$) the reaction occurs almost exclusively by the first stage catalysis. Intermediate ratios show the characteristic stepwise behaviour.

Autoxidation of dodecane in the presence of NiDBP

In order to follow the formation and decay of hydroperoxides under conditions approximating to those found during the processing of polyolefins, dodecane containing CHP ($1 \times 10^{-2}\text{ M}$) was oxidized at 150° both in the absence of additives (Fig. 4, curves 1 and 2) and in the presence of increasing concentrations of NiDBP (Fig. 4, curves 3-5). For curves 1, 3, 4, and 5 the reaction vessel was opened to the atmosphere only briefly and for the purpose of peroxide analysis. Curve 2 on the other hand represents peroxide analysis in the complete absence of O_2 . It is clear that the second stage catalytic process is very slow at the lowest $[\text{CHP}]/[\text{NiDBP}]$ molar ratio at which it can be

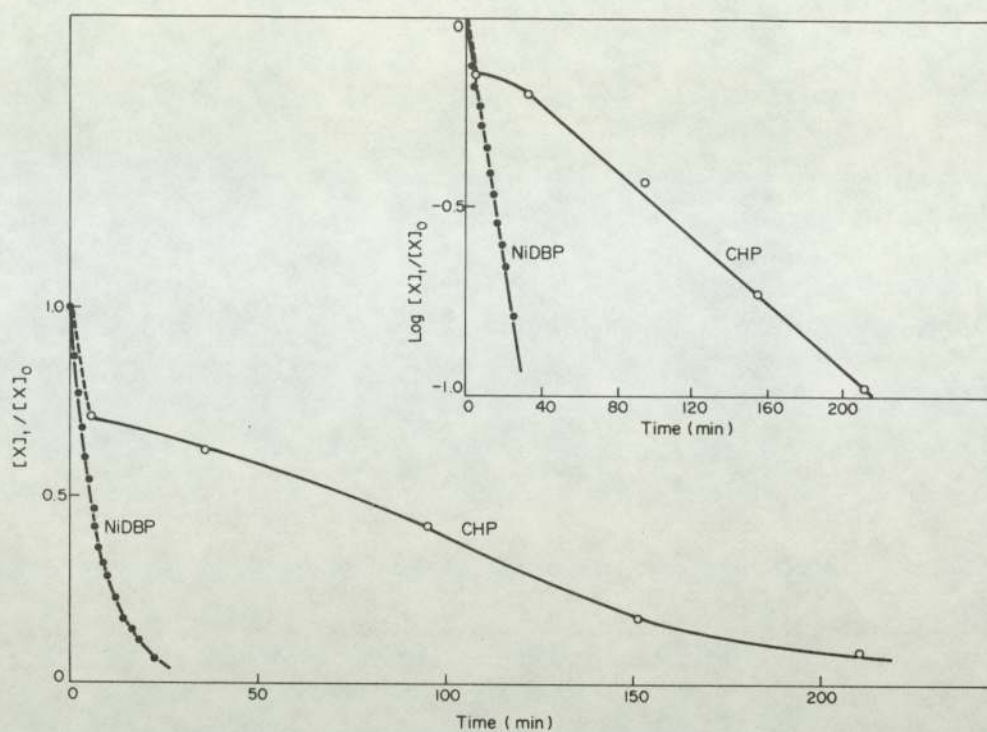


Fig. 2. Decomposition of CHP (1×10^{-2} M) in chlorobenzene at 70° in the presence of NiDBP (8×10^{-4} M) and the associated decay of the NiDBP u.v. absorbance. (The inset shows first order kinetic plots for the same reaction.)

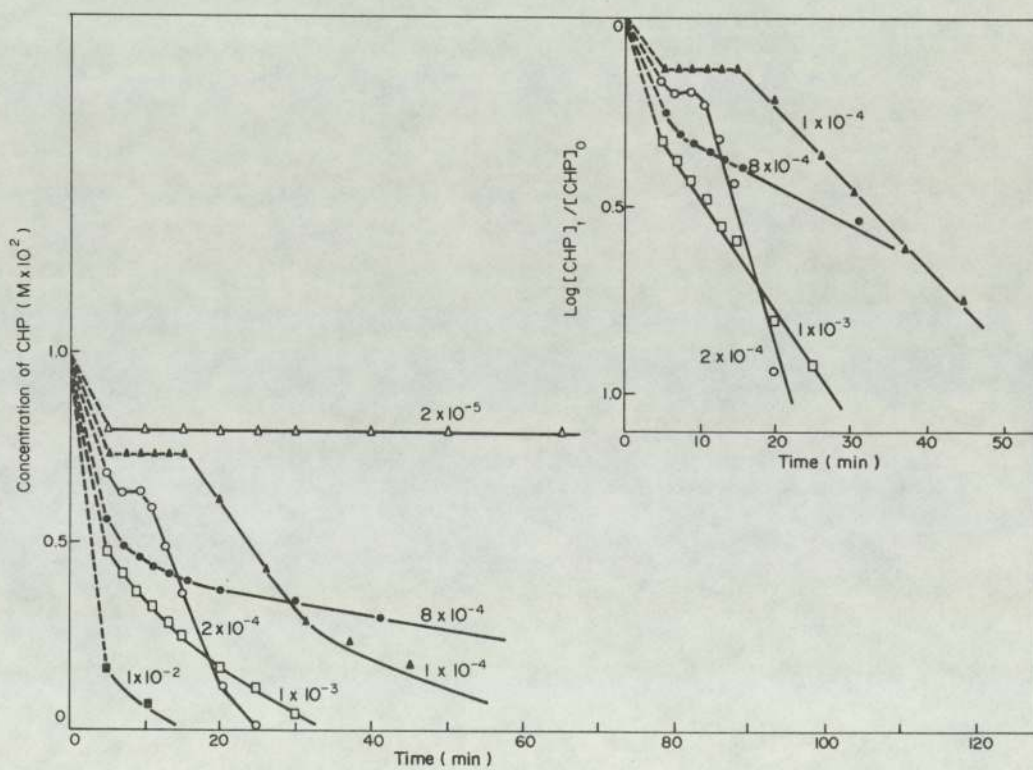


Fig. 3. Decomposition of CHP (1×10^{-2} M) in chlorobenzene at 110° in the presence of NiDBP at the molar concentrations shown. (The inset shows first order kinetic plots for the third stage of some of these reactions.)

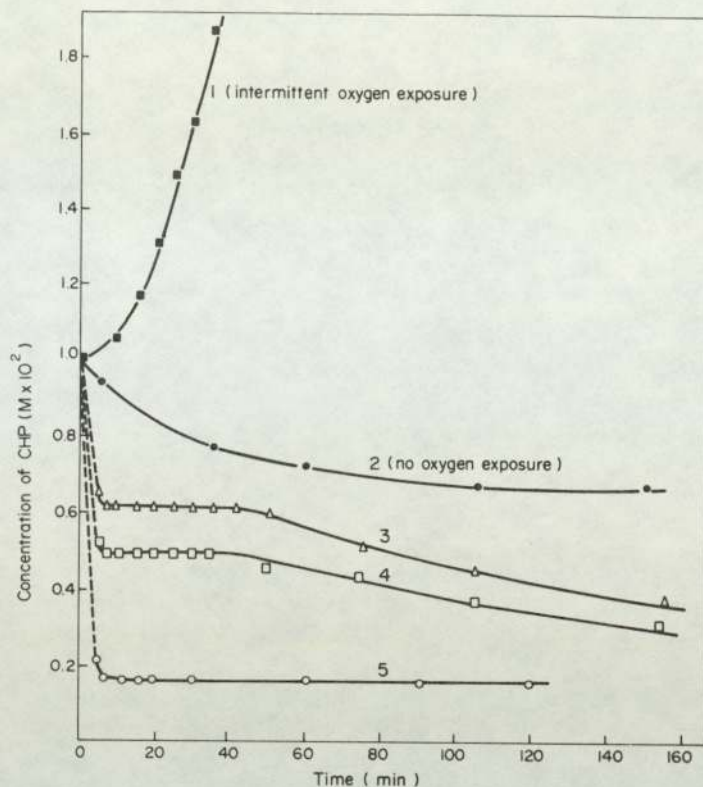


Fig. 4. Change in CHP concentration (1×10^{-2} M) in dodecane at 150° . 1, intermittent O_2 exposure, no additive; 2, no O_2 exposure, no additive; 3, NiDBP (1×10^{-4} M); 4, NiDBP (2×10^{-4} M); 5, NiDBP (10×10^{-4} M).

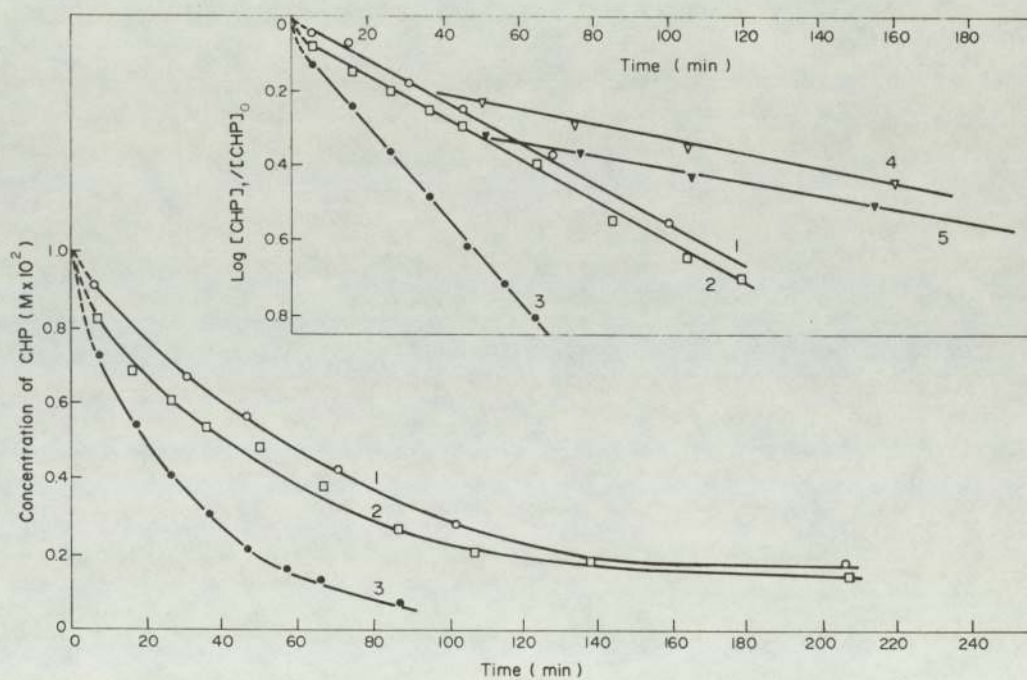


Fig. 5. Decomposition of CHP (1×10^{-2} M) in dodecane at 150° in the presence of DiPDiS at the molar concentrations indicated below. (Inset compares first order kinetics for the reactions of DiPDiS and NiDBP with CHP under identical conditions. The plots for NiDBP are those obtained from the third stage of the reaction.) 1, DiPDiS (1×10^{-4} M); 2, DiPDiS (2×10^{-4} M); 3, DiPDiS (10×10^{-4} M); 4, NiDBP (1×10^{-4} M); 5, NiDBP (2×10^{-4} M).

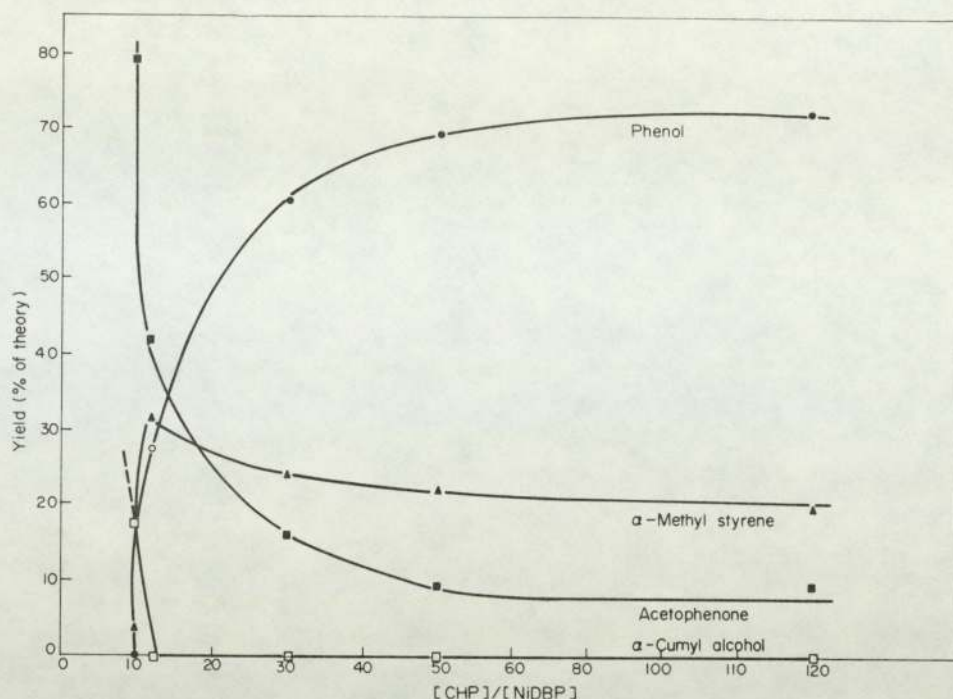


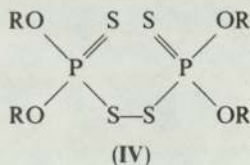
Fig. 6. Product yields after complete reaction of NiDBP with CHP at 110° in chlorobenzene at various molar ratios [CHP]/[NiDBP].

observed ($\approx 10:1$) but is practically very important at (50:1).

These results suggest the formation of a stable product from the metal dithiolate during its oxidation by the hydroperoxide in the rapid first stage catalytic process. This product was shown to be the corresponding disulphide (IV) by TLC examination of the products present during the induction period. Detailed discussion of the identification of this and other products will be discussed elsewhere [13].

Reaction of DiPDiS with CHP

In order to identify the second stage catalytic decomposition of CHP with the disulphide, di-isopropyl thiophosphoryl disulphide (DiPDiS, IV, R = isoPr) was investigated under the same conditions as NiDBP. The results (Fig. 5) show that the first catalytic stage is now missing and must be associated with the metal complex itself. First order kinetics are observed after a transitory faster reaction.



Products formed during the catalytic decomposition of CHP

It has previously been shown [2, 10] that the products formed from CHP are diagnostic of the processes occurring during the catalytic decomposition. Phenol and acetone indicate a primarily ionic process, whereas acetophenone is characteristic of a homolytic

process. α, α' -dimethyl benzyl alcohol (α -cumyl alcohol) may be formed in both a homolytic process and by stoichiometric reduction of the hydroperoxide. The formation of α -methyl styrene indicates the presence of an acid catalyst and is therefore generally associated with the ionic catalytic decomposition products phenol and acetone [10]. Figure 6 records the formation of these products for the CHP/NiDBP system at various molar ratios. It shows that, at [CHP]/[NiDBP] ratios of 10 and less, α -cumyl alcohol and acetophenone are the only products. At higher ratios, the ionic products predominate although some radical products are formed even at very high ratios. A similar investigation carried out with the disulphide shows (Fig. 7) that the main products at 10:1 ratios are derived from the ionic decomposition of CHP and even at a 1:1 ratio, 36% of phenol is formed. Above a 50:1 ratio the formation of free radical products remains constant at just under 20% of the total.

DISCUSSION

It is clear from these results that the decomposition of hydroperoxides by nickel dithiolates involves two quite different catalytic processes. The first, which gives rise to homolytic products, appears to correspond to that reported by Howard [3, 4] and is favoured by a low molar ratio of hydroperoxide to metal complex. The second, which gives rise to an ionic decomposition of hydroperoxide, occurs at higher hydroperoxide to metal dithiolate ratios and, as in the case of the zinc dithiophosphates, the catalyst appears to be derived from the intermediate disulphide (IV) [11, 12]. This process is entirely analogous

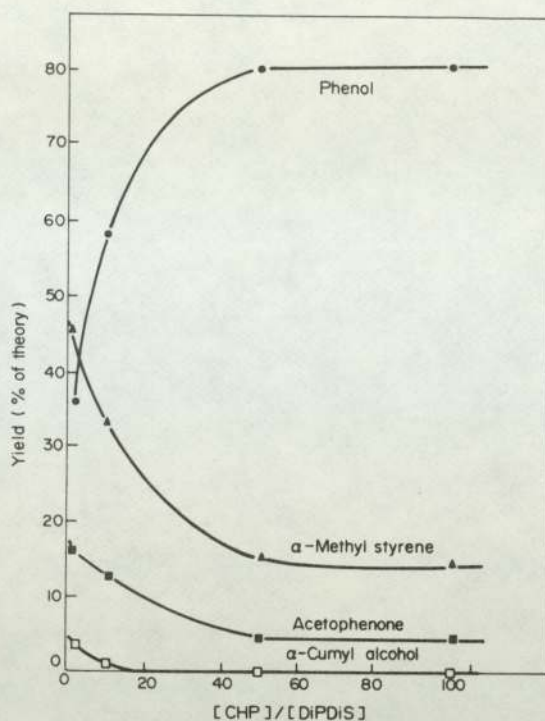


Fig. 7. Product yields after complete reaction DiPDiS with CHP at 110° in chlorobenzene at various molar ratios [CHP]/[DiPDiS].

to the formation of an ionic catalyst for hydroperoxide decomposition from mercaptobenzthiazole and its metal complexes through the intermediate disulphide [13] and is also consistent with the mechanism proposed earlier [2, 14] for the antioxidant function of the metal dithiocarbamates in a hydroperoxide initiated system.

The nature of the ionic catalyst or catalysts for peroxide decomposition formed from NiDBP and the thiophosphoryl disulphides is still under investigation. However, sulphur acids have been identified in the oxidation of the nickel dithiocarbamates [2] and of mercaptobenzthiazole disulphide [13] through the intermediate sulphinic and sulphonic acids. Furthermore, the product distribution for cumene hydroperoxide is strikingly similar to that observed with sulphur dioxide [10]. It seems likely then that sulphur acids are formed and contribute to the effects observed. The relative contribution of the free radical process decreases with decreasing concentration of NiDBP and becomes minimal above the stoichiometric ratio $[\text{CHP}]/[\text{NiDBP}] = 12$ which is the stoichiometry required for the oxidation of every sulphur in NiDBP to SO_3 . The nature of the sulphur acids will be discussed in a later communication [9].

NiDBC [2] and NiDBP [4] are mild retarders of α, α' -azo-bis-isobutyronitrile initiated autoxidations. Howard and co-workers [4] proposed that the nickel complexes are able to scavenge chain propagating alkyl peroxy radicals and the rapid interaction of these species was confirmed by low temperature ESR studies. It was also found that, when the decomposition of azocumene was carried out in an O_2 atmosphere and in the presence of the above complexes, the principal product was α -methyl styrene with smaller

amounts of acetophenone and α -cumyl alcohol. The presence of these products was interpreted in a scheme which involved initially cumyl peroxy radical formation, and deoxygenation by the nickel complexes, giving rise to the cumyloxy radical. The latter is the source of α -cumyl alcohol by hydrogen abstraction from the ligand. It was proposed that the nickel complex is itself oxidized to a Lewis acid which is strong enough to dehydrate α -cumyl alcohol [3, 4].

Surprisingly, in spite of this observation, Howard concluded that Lewis acid decomposition of hydroperoxides to non-radical products plays no part in the antioxidant function of the nickel complexes [3]. The present studies (Fig. 6) show that the two processes are cognate. At a molar ratio $[\text{CHP}]/[\text{NiDBP}] = 10$, the products formed from CHP are almost entirely those expected on the basis of a homolytic process, viz. acetophenone and α -cumyl alcohol with only a trace of α -methyl styrene and no phenol. At $[\text{CHP}]/[\text{NiDBP}] = 12$, no α -cumyl alcohol is formed, acetophenone formation is considerably reduced and the Lewis acid decomposition products, phenol and α -methyl styrene, become major products. Above this ratio, phenol and α -methyl styrene are the predominant products. The presence of a constant but low proportion of homolytic decomposition products at higher ratios indicates that the radical process makes a contribution at all ratios and this is consistent with the view that reducing agents based on sulphur (e.g. sulphinic acids, SO_2 etc) are involved as precursors to the Lewis acid formation since it has been shown that these form an effective redox initiating system with hydroperoxides [10, 15]. In practice, the radical generating process will only be important in the early stages of oxidation,

before the Lewis acids (SO_3 , H_2SO_4) have built up in the system. Once these are present they will determine the mode of peroxide decomposition. There is therefore not only a concentration dependent effect but also a time dependent effect involved in the action of the sulphur antioxidant [10, 3-16]; the fact that Howard's studies concentrated on the very early stage of the reactions between metal dithiolates and hydroperoxides doubtless contributes to his failure to observe the ionic hydroperoxide decomposition process which must be important to the long term behaviour of these antioxidants in the technological systems to which he refers [3]. The relative contribution of the two catalytic hydroperoxide decomposition processes to polymer stabilization will be discussed in subsequent publications.

REFERENCES

1. G. Scott, *Atmospheric Oxidation and Antioxidants*, pp. 216 et seq., 285, 290, 289 et seq., 345 et seq., 399, 406 et seq., 428 et seq., 443 et seq., 506 et seq. Elsevier, London (1965).
2. J. D. Holdsworth, G. Scott and D. Williams, *J. chem. Soc.* 4692 (1964).
3. J. A. Howard and J. H. B. Chenier, *Can. J. Chem.* **54**, 390 (1976).
4. J. A. Howard and J. H. B. Chenier, *Can. J. Chem.* **54**, 382 (1976).
5. C. K. Jorgensen, *J. Inorg. Nucl. Chem.* **24**, 1571 (1962).
6. L. A. Mikeska, U.S. Pat. 2, 471, 115 (19 September 1946).
7. G. W. Watt and B. J. McCormick, *J. Inorg. Nucl. Chem.* **27**, 898 (1965).
8. M. S. Kharasch, A. Fono and W. Nudenburg, *J. org. Chem.* **16**, 113 (1951).
9. S. Al-Malaika and G. Scott, To be published.
10. M. J. Husbands and G. Scott, *Eur. Polym. J.* **15**, 249 (1979).
11. Y. Ohkatsu, K. Kikkawa and T. Osa, *Bull. Chem. Soc. Jap.* **51**, 3606 (1978).
12. S. K. Ivanov and Y. Kateva, *Neftekhimiya* **18**, 417 (1978).
13. M. J. Husbands and G. Scott, *Eur. Polym. J.* **15**, 879 (1979).
14. R. P. R. Ranaweera and G. Scott, *Eur. Polym. J.* **12**, 825 (1976).
15. G. Armstrong, M. J. Husbands and G. Scott, *Eur. Polym. J.* **15**, 241 (1979).

MECHANISMS OF ANTI-OXIDANT ACTION:

THE ROLE OF NICKEL DITHIOLATES IN THE STABILIZATION OF LOW DENSITY POLYETHYLENE

S. AL-MALAIKA and G. SCOTT

Department of Chemistry, University of Aston in Birmingham,
Gosta Green, Birmingham, B4 7ET, England

(Received 7 December 1979)

Abstract—Nickel *O,O*-dialkyldithiophosphates and nickel xanthates stabilize low density polyethylene against both thermal and photo-oxidation. Under thermal oxidative conditions, the initial complexes are rapidly destroyed and the anti-oxidant function is associated with the further oxidation products formed via the corresponding disulphides. Their photostabilizing activity is related primarily to the photostability of the metal complexes themselves which act as light stable reservoirs for the anti-oxidant species.

INTRODUCTION

It has been shown [1–6] that the effectiveness of the nickel dialkyl dithiocarbamates (NiDRC) as u.v. stabilizers for polyolefins is primarily due to their ability to generate an ionic catalyst for the destruction of hydroperoxides. An associated requirement is the absorption of u.v. light in a non-destructive process, i.e. the metal complexes must be able to function as light stable reservoirs for the catalytic species [5, 6]. The nickel dithiophosphates and xanthates are known to exhibit a generally similar behaviour to the dithiocarbamates [7, 8] and recent studies in a model substrate have confirmed [9] the parallel anti-oxidant behaviour of all three classes of nickel dithiolates during thermal oxidation.

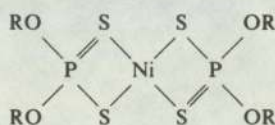
The purpose of the present study is to compare the behaviours of the dithiophosphates (NiDRP) and xanthates (NiRX) in polyethylene with that of the corresponding dithiocarbamates.

EXPERIMENTAL

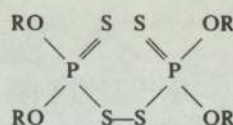
Materials

Unstabilized low density polyethylene (LDPE) was supplied by Imperial Chemical Industries Ltd as Alkathene WJG47, MFI = 2.

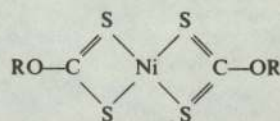
Nickel *O,O*-dialkyl dithiophosphates I (NiDRP), diisopropyl dithiophosphoryl disulphide II (DiPDiS) and nickel alkyl xanthates III (NiRX) were prepared by known procedures [11–13]. Alkyl xanthic disulphides (dixanthiogen, RX) were supplied by Robinson Brothers Ltd.



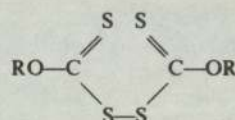
(I) R = nBu (NiDBP), R = iPr (NiDiPP)



(II) R = iPr (DiPDiS)



(III) R = nBu (NiBX), R = Et (NiEX)



(IV) R = iPr (iPX), R = Et (EX)

Toluene (BDH) was used without further purification.

Processing of LDPE

The additives (2.5×10^{-4} mol/100 g) were mixed with the polymer and processing conditions were simulated by use of the RAPRA torque rheometer. Processing was carried out at 150° for 30 min in an open chamber, except where indicated. The polymer was then compression moulded at 150° into sheets of thickness 0.008 in., as described previously [5].

Thermal ageing

The accelerated thermal oxidation of the compressed films was carried out in a Wallace oven at 110° in the presence of air. Each film sample was contained in a separate cell.

Irradiation

Films were irradiated in a u.v. cabinet in which 8 sunlamps (Westinghouse) and 24 actinic blue lamps were arranged in a symmetrical sequence.

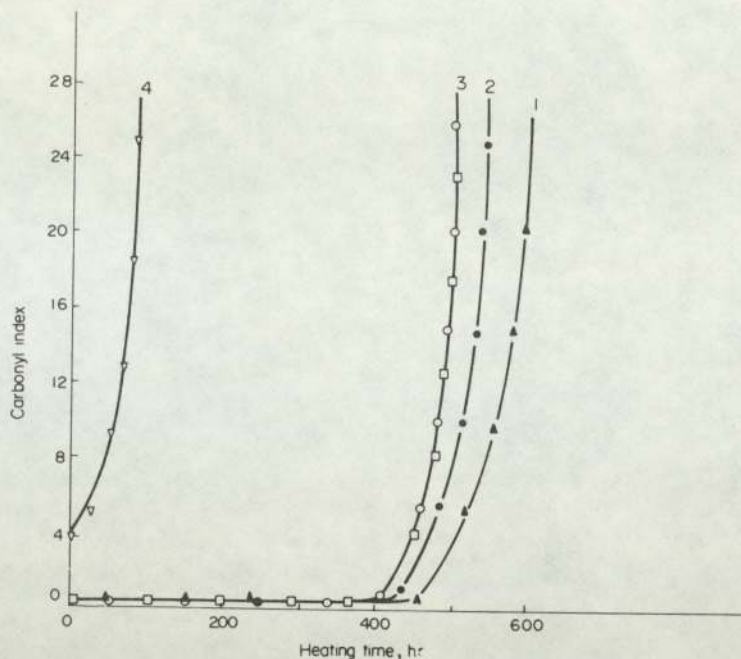


Fig. 1. Effect of thermal oxidation (at 110°) on LDPE films containing additives (2.5×10^{-4} mol/100 g). (1) NiDBP; (2) NiDiPP; (3) NiDiPP extracted before oven ageing (\square) and DiPDiS (\circ); (4) control (no additive).

Extraction of polymer films

Polymer films containing additives were extracted with toluene at $55 \pm 0.5^\circ$. The intensity of the u.v. absorption bands at 316 nm (dithiophosphate) and 320 nm (xanthate) were followed at intervals and were found to have decayed to zero within 10 hr and the spectra were identical to that of an unstabilized LDPE control.

RESULTS

Thermal anti-oxidant behaviour of nickel dithiolates and their derived disulphides

Films of LDPE containing nickel dithiophosphates (NiDRP) and nickel xanthates (NiRX) were examined as stabilizers for the thermal oxidation of LDPE at 110° (air oven). Comparison of Fig. 1 (curves 1 and 2) and Fig. 2 (curves 2 and 3) shows that they behave very similarly at the same molar concentration although the xanthates are somewhat more effective than the dithiophosphates.

Extraction of the stabilized films after processing under conditions which were shown effectively to remove the dithiolates (see Experimental section) had only a marginal effect on the thermal oxidative stability of the films (Fig. 1, curve 3 and Fig. 2, curve 4). Even more surprisingly, extraction of a NiRX stabilized film after 200 hr oven ageing, was shown by u.v. spectrophotometry to contain no nickel complex, was found to be slightly more stable than the unextracted film.

As has been shown elsewhere [9], the corresponding disulphides are the initial transformation products from the dithiophosphates and xanthates during their anti-oxidant function and typical examples (DiPDiS and iPX) were examined as thermal stabilizers under the same conditions. Their behaviour was only slightly inferior to that of the parent nickel complexes

(e.g. Fig. 1, cf. curves 2 and 3) and very similar to that of the extracted films. Separate experiments showed that variation of the alkyl substituent in the disulphides had a negligible effect on the anti-oxidant activity.

Photostabilizing effectiveness of the nickel dithiolates and derived disulphides

Figure 3, curve 1 shows that NiDiP is very effective u.v. stabilizer for LDPE which has been subjected to a severe processing operation (30 min in an open mixer). It shows the characteristic induction period which is typical of the metal dithiolates [5]. Extraction removes the induction period completely (Fig. 3, curve 3) but the polymer-bound residue behaves rather similarly to the corresponding disulphide (Fig. 3, curve 2) although it is not as effective. Extraction of the disulphide-containing film reduces its effectiveness to the same level as that of the extracted NiDiPP polymer film.

Figure 3 (inset) shows the effect of a less severe processing operation on the performance of the nickel complex (NiDiPP) and the derived disulphide (DiPDiS). Under these conditions, the disulphide is relatively ineffective whereas the nickel complex becomes somewhat more effective. This suggests that the primary function of the disulphide is to protect the polymer during processing whereas the nickel complex has an additional protective effect.

The behaviour of the nickel xanthates and xanthones was very similar although they were all less effective u.v. stabilizers on a molar basis (see Fig. 4). NiBX gave an induction period of 340 hr but NiEX gave no induction period (see Fig. 5). The activity of the disulphides in this case appeared to be limited to their ability to stabilize the polymer during processing. The

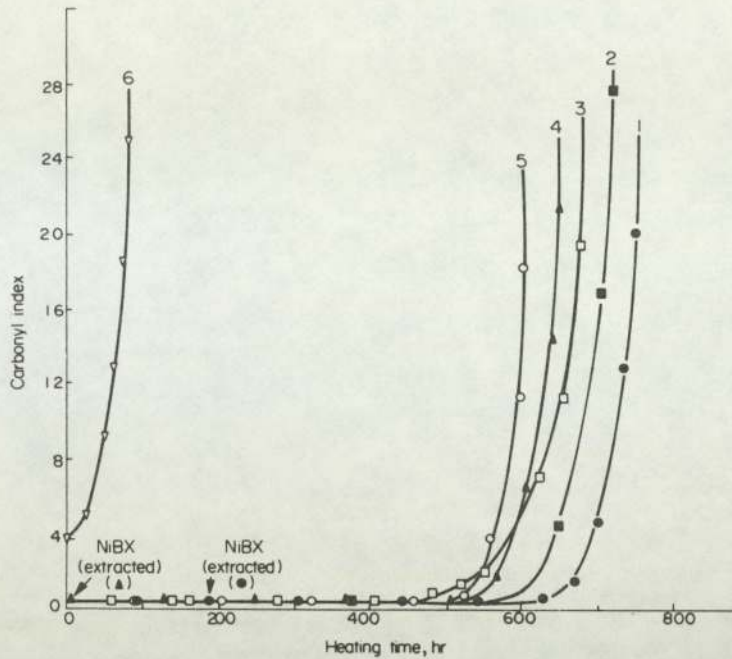


Fig. 2. Effect of thermal oxidation (at 110°) in the presence of air on LDPE films containing additives (2.5×10^{-4} mol/100 g). (1) NiBX extracted after the destruction of the complex (200 hr at 110°); (2) NiBX untreated; (3) NiEX untreated; (4) NiBX extracted prior to oven ageing; (5) iPX; (6) control (no additives).

post induction period rate was similar to that of the control.

Figure 5 shows that the u.v. stabilizing effect of the nickel dithiolates is related to their photostability in the polymer. As in the case of the nickel dithiocarbamates [5, 6], the induction period corresponds to the disappearance of the metal complex from the

polymer. However, it is clear from Figs 3 and 6 that the derived products, which become bound into the polymer during processing, have some photoretarding activity.

Figures 3 (inset) and 6 show that under mild conditions (30 min, closed mixer) the effect of thermally produced secondary products is very much reduced

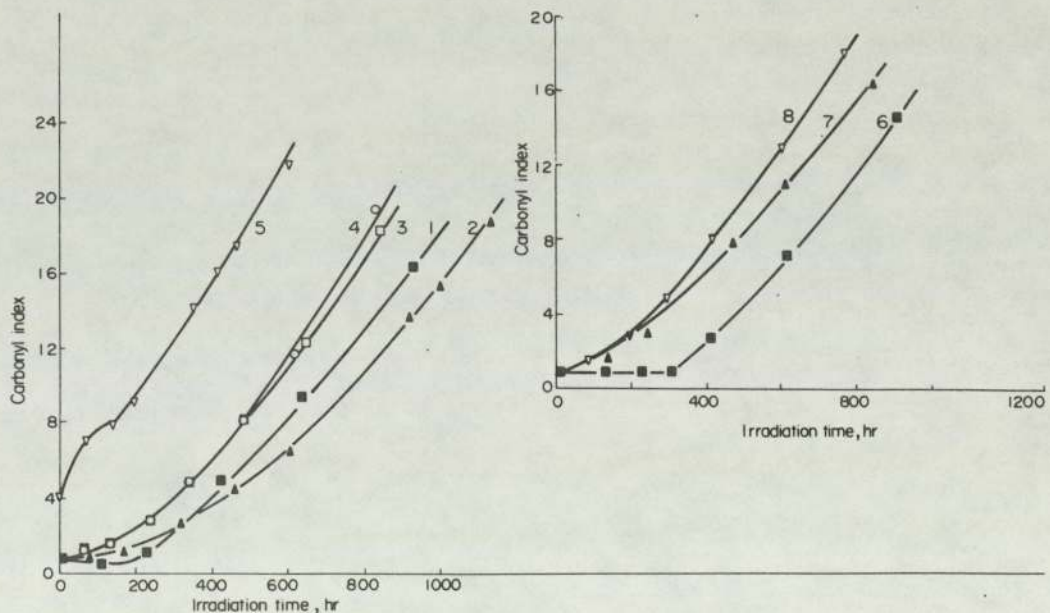


Fig. 3. Effect of additives on photo-oxidation of LDPE (2.5×10^{-4} mol/100 g). (1) NiDiPP; (2) DiPDiS; (3) NiDiPP (extracted); (4) DiPDiS (extracted); (5) control without additives (1-5 all processed at 150° in open mixer); (6) NiDiPP; (7) DiPDiS; (8) control without additives (6-8 all processed at $150^{\circ}/30$ min in closed mixer).

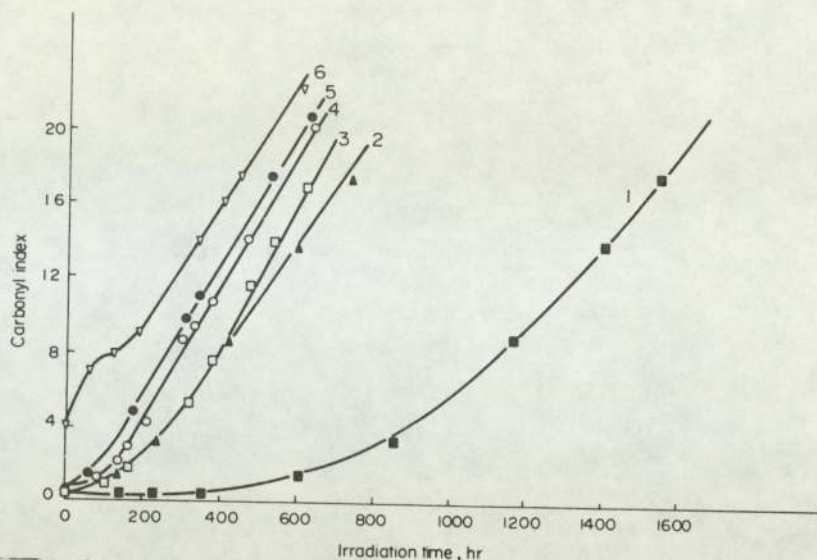


Fig. 4. Effect of additives on the photo-oxidation of LDPE processed at 150°/30 min in an open mixer (concentration of additives 2.5×10^{-4} mol/100 g). (1) NiBX; (2) NiEX; (3) EX; (4) iPX; (5) iPX (extracted); (6) control (no additives).

since the extracted film oxidizes at a rate similar to the control. The photostabilizing effect is in this case due almost entirely to the metal complex itself and the products derived from it during photo-oxidation.

DISCUSSION

Table 1 summarizes the anti-oxidant behaviour in LDPE of the metal dithiolates and their derived disulphides discussed above and relates this to the persistence of the additives in the polymer during thermal and photo-oxidation.

Previous studies have shown [1-4, 7, 13] that products formed from metal thiolates are effective thermal anti-oxidants rather than the metal com-

plexes themselves. In model systems, the corresponding disulphides are the first products to be formed and are precursors of a variety of oxyacids of sulphur [7, 9, 13] which are effective catalysts for the ionic decomposition of hydroperoxides. It is clear from Figs 1-3 and Table 1 that the behaviour of the nickel dithiolates under processing conditions is more complex since anti-oxidant residues, formed by thermal oxidative destruction of the initially added complex, become chemically bound to the polymer giving rise to powerful thermal anti-oxidant activity and more limited u.v. stabilizing activity in the fabricated polymer. The former effect appears to be independent of the presence of the starting metal dithiolate.

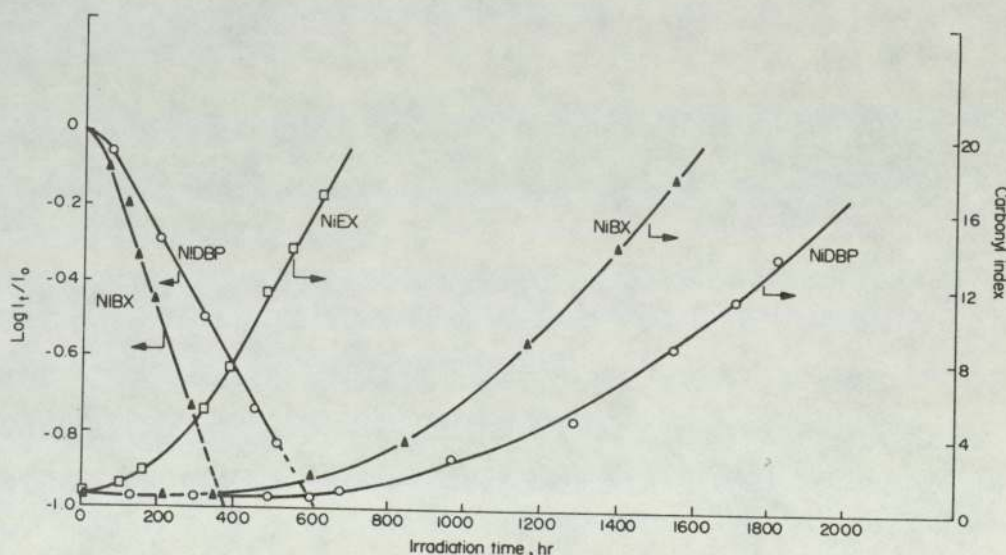


Fig. 5. Kinetics of the disappearance of NiEX, NiBX (320 nm) and NiDBP (316 nm) in LDPE during photo-oxidation compared to the changes of carbonyl index under the same conditions (concentration of additives 2.5×10^{-4} mol/100 g).

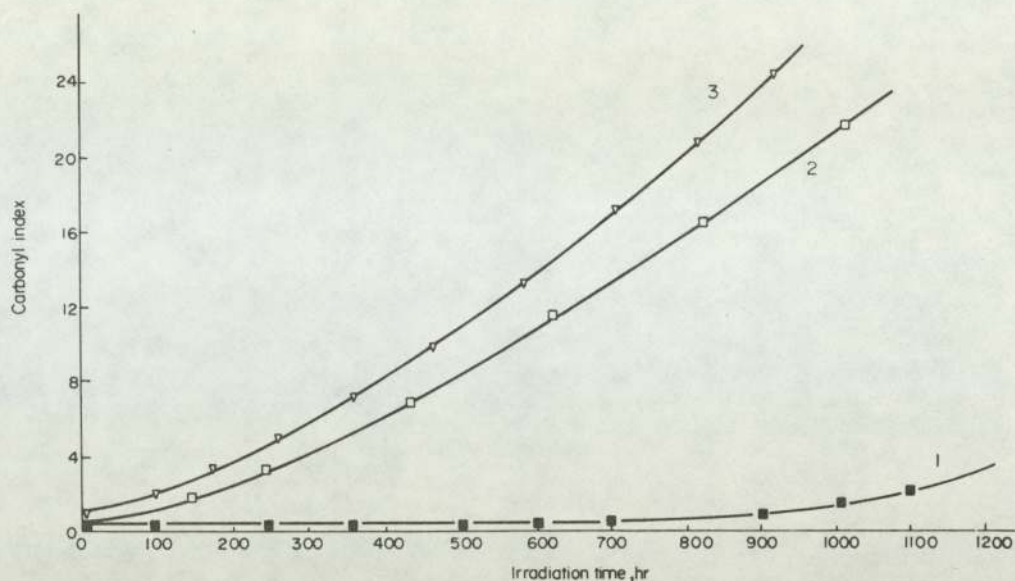


Fig. 6. Effect of NiDBP (extracted and unextracted) on the photo-oxidation of LDPE (processed at 150°C/30 min in a closed mixer; concentration 2.5×10^{-4} mol/100 g). (1) NiDBP; (2) NiDBP (extracted); (3) control (no additives).

The much weaker photostabilizing activity of the bound anti-oxidant appears to be associated with the absence of an induction period. It is effectively synergized by the presence of unchanged nickel dithiolates.

The initial metal complexes rather than their transformation products therefore appear to be primarily responsible for the induction periods observed (see Figs 3-5). It has been suggested previously

Table 1. Effects of metal dithiolates on the thermal and photo-oxidation of LDPE

Anti-oxidant§	u.v. Exposure		Thermal oxidation at 110°	
	IP (hr)	Additive disappearance (hr)†	IP (hr)	Additive disappearance (hr)
NiDBP	600	600	450	200
NiDiPP	200	200	420	80
NiDiPP (ext)*	0	0	400	0
DiPDiS	400	—	400	—
NiBX	340	345	600	200
NiBX (ext)*	0	0	500	0
NiBX (ext)†	—	—	630	200
NiEX	350	20	450	20
iPX	0	—	510	—

* Extracted after processing and before thermal oxidation.

† Extracted after thermal ageing for 200 hr (NiBX destroyed).

‡ By disappearance of metal ligand absorption at 316 nm (NiDRP); 320 nm (NiRX).

§ In LDPE at 2.5×10^{-4} mol/100 g processed at 30 min in open mixer.

Table 2. Effect of processing on nickel xanthate concentration

Anti-oxidant	Concentration originally added to LDPE (mol/100 g)	Concentration remaining after processing (mol/100 g)*
NiBX	2.5×10^{-4}	1.6×10^{-4}
NiEX	2.5×10^{-4}	0.3×10^{-4}

* 30 min at 150° in open mixer.

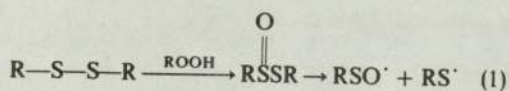
[5, 6, 15, 16] that stability under photo-oxidative conditions is a primary requirement of the metal complex u.v. stabilizers and it has been shown [5, 6] that they exert an auto-protective effect which permits the controlled release of the effective anti-oxidant from the complex over a long period. This principle clearly operates in the case of the dithiophosphates and xanthates but comparison of Figs 3 and 5 indicates that, unlike the case of the dithiocarbamates [5], the processing severity of the polymer also affects the persistence of NiDBP in the polymer. The nickel xanthates are even more susceptible to loss during processing. Table 1 and Figs 4 and 5 show that NiEX is considerably less effective than NiBX under both thermal and photo-oxidative conditions. However, Table 2 shows that a substantial part of the NiEX originally present must have been converted (through the disulphide) to the effective thermal anti-oxidant since only 12% of the original metal complex was still present after processing. Table 1 shows that this disappeared within 20 hr of thermal oxidation, compared with the thermal oxidative induction period of 450 hr.

The mechanism by which the anti-oxidant residues become bound to the polymer are not entirely clear but, since almost identical effects can be achieved by mixing the polymer with the corresponding disulphides under the same conditions (see Figs 3 and 6), it seems likely that the latter are intermediates. Moreover, the fact that the extent of binding increases markedly with an increase in the amount of air present suggests that a radical process is involved, facilitated by the hydroperoxides present in the system. The most likely chemical

reaction (1) involves oxidation of the disulphide to the corresponding unstable thiolsulphinat, a reaction believed to be involved in the pro-oxidant function of disulphides [17]. Further studies are in progress on the mechanism of bound anti-oxidant formation.

REFERENCES

1. R. P. R. Ranaweera and G. Scott, *J. Polym. Sci., Polym. Lett. Ed.* **13**, 71 (1975).
2. R. P. R. Ranaweera and G. Scott, *Eur. Polym. J.* **12**, 591 (1976).
3. R. P. R. Ranaweera and G. Scott, *Eur. Polym. J.* **12**, 825 (1976).
4. G. Scott, *J. Polym. Sci., Symp. No.* 357 (1976).
5. K. B. Chakraborty and G. Scott, *Eur. Polym. J.* **13**, 1007 (1977).
6. K. B. Chakraborty and G. Scott, *Polym. Degrad. Stab.* **1**, 37 (1979).
7. J. D. Holdsworth, G. Scott and D. Williams, *J. Chem. Soc.* 4692 (1964).
8. G. Scott, *Atmospheric Oxidation and Antioxidants*, p. 192 *et seq.* Elsevier, London (1965).
9. S. Al-Malaika and G. Scott, *Eur. Polym. J.* In press.
10. G. K. Jorgenson, *J. inorg. nucl. Chem.* **24**, 1571 (1962).
11. L. A. Mikeska, U.S. Pat. 2,471,115 (19 Sept 1946).
12. G. W. Watt and B. J. McCormick, *J. inorg. nucl. Chem.* **27**, 898 (1965).
13. M. J. Husbands and G. Scott, *Eur. Polym. J.* **15**, 879 (1979).
14. M. J. Husbands and G. Scott, *Eur. Polym. J.* **15**, 249 (1979).
15. G. Scott, *Macromolec. Chem.* **8**, 319 (1973).
16. G. Scott, In *Developments in Polymer Degradation* (Edited by N. Grassie), Vol. 1, p. 205. Applied Science Publishers (1977).
17. G. Scott, In *Mechanisms of Reaction of Sulphur Compounds* (Edited by N. Kharasch), Vol. 4, p. 99 (1969).



R E F E R E N C E S

1. Scott, G., in 'Atmospheric Oxidation and Antioxidants', Elsevier, London and New York, 1965, ch. 3.
a) ch. 3, b) p. 203 et seq., c) p.507, d)p.131, e)p.192 et seq.
2. Rabek, J.F., in 'Comprehensive Chemical Kinetics', eds. Bamford, C.H., and Tipper, C.F., Elsevier, London and New York, 1976, vol. 14, ch. 4.
3. Bolland, J.L., Quart. Rev., [London], 3, 1 [1949].
4. Kaplan, M.L., and Trozzolo, A.M., in 'Singlet Oxygen', eds. Wasserman, H.H., and Murray, R.W., Academic Press, New York, [1979], vol. 40, ch. 11.
5. Scott, G., Pure and Appl. Chem., 52, 365 [1980].
6. Scott, G., S. Afr. J. Chem., 32 [4], 137 [1979].
7. Scott, G., Chem. Brit., 9 [6], 267 [1973].
8. Hutson, G.V., and Scott, G., Chem. Ind., 725 [1972].
9. Carlsson, D.J., and Wiles, D.M., Macromolecules, 4, 174 [1971].
10. Geuskens, G., in 'Comprehensive Chemical Kinetics', eds. Bamford, C.H., and Tipper, C.F., Elsevier, London and New York, 1976, Vol. 14, ch. 3.
11. Mellor, D., Moir, A., and Scott, G., Europ. Polym. J., 9, 219 [1973]
12. Scott, G., Polym. Plast. Technol. Eng. 11 [1], 1 [1978].

13. Aspler, J., Carlsson, D.J., and Wiles, D.M., *Macromolec.*, 9, 691 [1976].
14. Scott, G., in 'Singlet Oxygen', eds. Ranby, B., and Rabek, J.F., Wiley, London [1978], ch. 23.
15. Ranby, B., and Rabek, J.F., in 'Photodegradation, Photo-oxidation and Photostabilisation of Polymers', Wiley, London, [1975], [a] ch. 8, [b] ch. 4, [c] p.132
16. Wiles, D.M., in 'Singlet Oxygen', eds. Ranby, B., and Rabek, J.F., Wiley, London, [1978], ch. 34.
17. Chakraborty, K.B., and Scott, G., *Polym. Letters*, 18, 98 [1977].
18. Carlsson, D.J., and Wiles, D.M., *J. Macrom. Sci., Rev. Macrom. Chem.*, C14 [1], 65 [1976].
19. Chakraborty, K.B., and Scott, G., *Europ. Polym. J.*, 13, 731 [1977].
20. Scott, G., *Amer. Chem. Soc., Symp. Series*, 25, 340 [1976]
21. Cicchetti, D., *Adv. Polym. Sci.*, 7, 70 [1970].
22. Carlsson, D.J., and Wiles, D.M., *J. Macrom. Sci., Rev. Macrom. Chem.*, C14 [2], 155 [1976].
23. Scott, G., *J. Polym. Sci., Symp.*, 57, 357 [1976].
24. Amin. M.U., and Scott, G., and Tillekeratne, L.M.K., *Europ. Polym. J.*, 11, 85 [1975].

25. Carlsson, D.J., Garton, A., and Wiles, D.M., in 'Developments in Polymer Stabilisation-1', ed. Scott, G., App. Sci., London [1979], ch. 7.
26. Scott, G., Europ. Polym. J., Supplement, 189 [1969].
27. Howard, J.A., in 'Free Radicals', ed. Kochi, J.K., Wiley-Interscience, New York, [1973], vol. 2, ch. 12.
28. Husbands, M.J., and Scott, G., Europ. Polym. J., 15, 249 [1979].
29. Armstrong, C., Husbands, M.J., and Scott, G., Europ. Polym. J., 15, 241 [1979].
30. Ingham, F.A.A., Stuckey, J.E., and Scott, G., Europ. Polym. J., 11, 783 [1975].
31. Ranaweera, R.P.R., and Scott, G., Chem. Ind., 774 [1974]
32. Holdsworth, J.D., Scott, G., and Williams, D., J. Chem. Soc., 4692 [1964].
33. Pimblott, J.G., Stuckey, J.E., and Scott, G., J. App. Polym. Sci., 19, 865 [1975].
34. Al-Malaika, S., and Scott, G., Europ. Polym. J., 16, 503, [1980].
35. Luston, J., in 'Developments in Polymer Stabilisation-2', ed., Scott, G., App. Sci., [1980], p. 187.
36. McKeller, J.F., and Allen, N.S., in 'Photochemistry of Man-Made Polymers', App. Sci., London, [1978], [a] p. 219, [b] p. 229.

37. Sheena, H.H., Private Communication.
38. Chakraborty, K.B., and Scott, G., *Europ. Polym. J.*, 15, 35 [1979].
39. Burn, A.J., *Adv. Chem. Ser.*, 75, 323 [1968].
40. Howard, J.A., and Chenier, J.H.B., *Can. J. Chem.*, 54, 382 [1976].
41. Ivanov, S.K., and Kateva, Y.D., *Dokl. Bolg. Akad. Nauk.* 21, 681 [1968].
42. Colclough, T., and Cuneen, J.I., *J. Chem. Soc.*, 4790 [1964].
43. Howard, J.A., Ohkatsu, Y., Chenier, J.H.B., and Ingold, K.U., *Can. J. Chem.*, 51, 1543 [1973].
44. Ranaweera, R.P.R., and Scott, G., *Europ. Polym. J.*, 12, 591 [1976].
45. Chakraborty, K.B., and Scott, G., *Polym. Degrad. and Stals.*, 1, 37 [1979].
46. Chakraborty, K.B., and Scott, G., *Europ. Polym. J.*, 13, 1007 [1977].
47. Husbands, M.J., and Scott, G., *Europ. Polym. J.*, 15, 879 [1979].
48. Burn, A.J., *Tetrahedron* 22, 2153 [1966].
49. Sanin, P.I., Blagovidov, I.F., Vipper, A.B., Kuliev, A.M., Krein, S.E., Ramaiya, K.S., Shor, G.I., Sher, V.V., and Zaslaukii, Yu.S., *Proc. 8th World Petroleum Congress* 5, 91 [1971].

50. Ohkatsu, Y., Kikkawa, K., Osa, T., *Bul. Chem. Soc. Jap.*, 51, [12], 3606 [1978].
51. Chadwick, D.H., and Watt, R.S., in 'Phosphorous and its Compounds' ed. Wazer, J.R.V., Interscience publisher, New York [1961], vol. II, p. 1264.
52. Reid, E.E., in 'Organic Chemistry of Bivalent Sulfur', chemical publisher, New York, [1958], vol. I, p. 305.
53. US. Patent 3,044,981, Farbenfabr Bayer 29.12.1959.
54. US. Patent 2,884,405.
55. Fr. Patent 1,314,410 Hercules Powder, 5.10.1961.
56. Reid, E.E., in 'Organic Chem. of Bivalent Sulfur', chemical publisher, New York, [1958], vol. IV
[a] p. 155, [b] p. 141, [c] p. 152, [d] p. 168,
[e] p. 182-184.
57. Karasch, M.S., Fono, A., and Nudenberg, W., *J. Org. Chem.*, 16, 113 [1951].
58. Vogel, A.I., in 'Practical Organic Chemistry', third edition, Longmans, London, 1966, p. 499.
59. Watt, G.W., and McCormick, B.J., *J. Inorg. Nucl. Chem.*, 27, 898 [1965].
60. Kowala, C., and Swan, J.M., *Aus. J. Chem.*, 11, 233 [1970].
61. Ikeda, T., and Hagihara, H., *Acta cryst.*, 21, 919 [1966].

62. Jørgensen, C.K., J. Inorg. Nucl. Chem., 24, 1571 [1962].
63. Livingstone, S.E., and Mihkelson, A.E., Inorg. Chem., 9, [11], 2545 [1970].
64. Pimblott, J.G., PhD Thesis, University of Aston [1973].
65. Mikeska, L.A., U.S. Pat. 2.471.115 [19 Sept. 1946].
66. Norman, G.R., LeSuer, W.M., and Mastin, T.W., J. Am. Chem. Soc., 74, 161 [1952].
67. Paul, K.T., RAPRA Bulletin, 2, 29 [1972].
68. Capron, E., and Crowder, J.R., J. Oil Col. Chem. Assoc., 58, 9, [1975].
69. Amin., M.U., PhD Thesis, University of Aston, 1973.
70. Willard, H.H., Mervitt, L.L., Dean, J.A., in 'Instrumental Methods of Analysis' D.Van. Nostrand Company, New York, Fifth edition, 1974, p. 170.
71. Operating Instructions for Melt Indexer Serial No. 985, Davenport Ltd., London.
72. Mair, R.D., and Graupner, J., Anal. Chem., 36, 194 [1964].
73. Wagner, C.D., Smith, R.H., and Peters, E.D., Anal. Chem., 19, 976 [1947].
74. Hiatt, R., in 'Organic Peroxides', ed., Swern, D., Wiley, New York, 1971, vol. II, Ch. 1.

75. Kosolapoff, G.M., in 'Organophosphorous Compounds', Wiley, New York [1958], p. 236.
76. Corbridge, D.E.C., in 'Phosphorous, an Outline of its Chemistry, Biochemistry and Technology', Elsevier, Amsterdam [1978], ch. 7.
77. Bacon, W.E., and LeSuer, W.M., J. Am. Chem. Soc., 76, 670 [1954].
78. Ailman, D.E., and Magee, R.J., in 'Organic Phosphorous Compounds', ed. Kosolapoff, G.M., and Maier, L., Wiley, New York [1975], vol. 7, ch. 19, p. 523.
79. Jørgensen in 'Inorganic Complexes', Academic Press, New York [1963], ch. 7, p. 138.
80. Livingstone, S.E., Quart. Rev., 19, 386 [1965].
81. Coucouvanis, D., Prog. Inorg. Chem., 11, 233 [1970].
[a] 303 et. seq., [b] 260.
82. Holah, D.J., and Murphy, C.N., Can. J. Chem., 49, 2726 [1972].
83. Warden, B.G., Billig, E., and Gray, H.B., Inorg. Chem., 5, 78 [1966].
84. Rockett, J., App. Spectroscopy 16 [2], 39 [1962].
85. McIvor, P.A., and Hubley, C.E., Can. J. Chem., 37, 869 [1959].
86. Dickert, J.J., and Rowe, C.N., J. Org. Chem., 32, 647 [1967].

87. De Puy, C.H., and King, R.W., Chem. Rev., 60, 431 [1960].
88. Billingham, N.C., in 'The Weathering of Plastics and Rubbers', P.E.11 [1976].
89. Shankaranarayana, M.L., and Patel, C.C., [a] Acta. Chem. Scan., 19, 1113 [1965], [b] Can. J. Chem., 39, 2590 [1961].
90. Raizman, P., and Thompson, Q.E., in 'The Analytical Chem. of Sulfur and its Compounds', ed. Karchmer, J.H., Wiley, New York [1972], part II, ch. 10.
91. Little, L.H., Poling, G.W., Leja, J., J. Can. Chem., 39, 745 [1961].
92. Baldinus, J.G., in 'Treatise on Analytical Chemistry', eds. Kolthoff, I.M., and Elving, P.J., Wiley-Interscience, New York [1976], vol. 15, part II, Sec. B-2, p.18.
93. Chamberlain, C.S., and Drago, R.S., Inorg. Chim. Acta, 32, 75 [1979].
94. Purcell, K.F., and Kotz, J.C., in 'Inorganic Chemistry', Holt-Saunders [1977], p. 373.
95. Scott, G., Sheena, H.H., and Harriman, A.M., Europ. Polym. J., 14, 1071 [1978].
96. Luango, J.P., J. Polym. Sci., XLII, 139 [1960].
97. Aggarwell and Sweeting, Chem. Rev., 57, 665 [1957].
98. Baum, B.J., J. App. Poly. Sci., 2, 281 [1959].

99. Rugg, F.M., Smith, J.J., and Bacon, R.C., *J. Poly. Sci.*, 13, 535 [1954].
100. Carlsson, D.J., and Wiles, D.M., *Macromolec.*, 2 [6], 587, 597 [1969].
101. Wood, D.L., and Loungo, J.P., *Modern Plastics*, 38, 132 [1961].
102. Cross, L.H., Richard, R.B., and Willis, H.A., *Dis. Farad. Soc.*, 9, 235 [1950].
103. Hanneman, W.W., and Porter, R.S., *Amer. Chem. Soc.*, [Div. Pet. Chem.] 1964, Philadelphia.
104. Feng, I.M., *Wear*, 3, 309 [1960].
105. Adams, J.H., *J. Polym. Sci., Part A1*, 8, 1077 [1970].
106. Ranaweera, R.P.R., and Scott, G., *J. Polym. Sci., Polym. Lett. Ed.* 13, 71 [1975].
107. Ranaweera, R.P.R., and Scott, G., *Europ. Polym. J.*, 12, 825 [1976].
108. Hawkins, W.L., in *Degradation and Stabilisation of Polymers Symposium, Belgium [1974]*, p. 59.
109. Evans, B.W., and Scott, G., *Europ. Polym. J.*, 10, 453 [1974].
110. Neilson, L.E., *J. App. Phys.*, 25, 1209 [1954].
111. Amin, M.U., and Scott, G., *Europ. Polym. J.*, 10, 1019 [1974].

112. Chew, C.H., Jan, L.M., and Scott, G., *Europ. Polym. J.*, 13, 361 [1977].
113. Hartley, G.H., and Guilett, J.E., *Macromolecules*, 1, 165 [1968].
114. Golemba, F.J., and Guillet, J.E., *Macromolecules*, 5, 63 [1972].
115. Hawkens, W.L., and Sautter, H., *J. Polym. Sci.*, part A, I, 3499 [1963].
116. Hawkens, W.L., and Sautter, H., *Chem. Ind.*, 20, [1962].
117. Chenier, J.H.B., Howard, J.A., and Tait, J.C., *Can. J. Chem.*, 56 [2], 157 [1978].
118. Burn, A.J., Cecil, R., and Young, V.U., *J. Inst. Petr.*, 57, 319 [1971].
119. Kennerly, G.W., and Patterson, W.L., *Ind. Eng. Chem.*, 48, 1917 [1956].
120. Shopov, D., and Ivanov, S.K., *Neftekhimya*, 5, 410 [1965].
121. Cyanamid Plastics Additives, *Technical Bull.*, D.42.
122. Scott, G., *Macromolec. Chem.*, 8, 319 [1973].
123. Hutson, G.V., and Scott, G., *Europ. Polym. J.*, 10, 45 [1974].
124. Bateman, L., Cain, M.E., Colclough, T., and Cuneen, J.I., *J. Chem. Soc.*, 3570 [1962].
125. Barnard, D., Bateman, L., Cuneen, J.I., and Smith, J.F., *Chemistry and Physics of Rubber-like Substances*, ed. Bateman, L., Maclaren, London [1963], p. 593.

126. Huyser, E.S., in 'Methods in free radical Chemistry', Marcel Dekker, N.Y. [1969], vol. 2, ch.1.
127. Trozzolo, A.M., in 'Polymer Stabilisation', ed. Hawkins, W.L., Wiley Inters., N.Y., [1972].
128. Calvert, P.D., and Billingham, N.C., J.App. Polym.Sci., 24, 357 [1979].
129. Luongo, J.P., J.App.Polym.Sci., 3, 302 [1960].
130. Shelton, J.R., in 'Polymer Stabilisation' ed. Hawkins, W.L., Wiley, N.Y. [1972], ch.2.
131. Palazatta, M.C., Pignolet, L.M., Inorg.Chem., 15,1982 [1976]
132. Tamres, M., and Strong, R.L., in 'Molecular Association' ed. Foster, R., Academic Press [1979], vol.2, ch.5,p.405.
133. Howard, J.A., and Chenier, J.H.B., Can.J.Chem., 54, 390 [1976]
134. Humphris, K.J., and Scott, G., J.Chem.Soc. Perk.II, 831 [1973].
135. Laver, H.S., in 'Developments in Polymer Stabilisation-1', ed. Scott, G., App.Sci., [1979], ch.5.
136. Barnard, D., Bateman, L., Cole, E.R., and Cuneen, J.I., Chem.Ind., 918 [1958].